Biomolecular interactions and cellular effects of steroidal and metallosupramolecular metallodrugs

UNIVERSITY OF BIRMINGHAM

Carlos Sanchez Cano

A thesis submitted in partial fulfilment of the requirements for the degree of Doctor of Philosophy in Chemistry

University of Birmingham, School of Chemistry
June 2009

This thesis is dedicated

to the ones that gave life

to me

Acknowledgements

I would like to start expressing my gratitude to the Analytical department of the School of Chemistry for the technical support received during the last three-four years. In particular to Graham Burns, not only for his help with chromatographic separations, but for his friendship, the many countryside pubs and West Bromwich Albion.

I should thank as well all the people in level six, level four and level three in the School of Chemistry, for the nights and many laughs in the Staff House. From all of them, I would like to thank especially the bloody Italian community, thanks for the food, the extra language and for Luca's grandmother (which should be protected by the UNESCO).

Many people have been important for me during the last years in Jerez, Granada, Madrid, Warwick and Birmingham. To all of you thanks for everything, you know who you are. However, a few names should be mentioned, starting with Bhaven, Benedicte, Jean Louis and Susana who gave me shelter when I was homeless. Roberto and Gisela, who shared with me many years of friendship and "papas a lo pobre" in Manchester. The Harborne Rugby Club, for three years of scrums, rucks, lineouts, friendship and beer and finally Lucia, for many, many things.

This thesis would have not been possible without Prof. Kevin Chipman, Dr. Chris Bunce and Dr. Nicholas Hodges and their groups. They allowed me to use their facilities on level four of the School of Biosciences and their help and suggestions were responsible of part of the biological work presented herein.

To all the Hannon group, past and present, all important in my development as scientist and as a person. I especially owe the steroid synthesis group (Martin Huxley, Michael Browning and lately my mad project student Jenna Willcox).

A few people were very important in my formation as a scientist. Between them, I would like to thank Dr. Adoración Gómez Quiroga and Prof. Carmen Navarro-Ranninger from the Universidad Autonoma de Madrid and Prof. Allison Rodger from Warwick University, for the opportunity given and the help and support provided. I am especially grateful to Dr. Purificación Sánchez Sánchez from the Universidad de Granada (who started my passion for research) and to my PhD supervisor Prof. Michael

J. Hannon (always supportive, helpful and full of ideas); without them I would not think or work as I do and I would not be the scientist that I am either.

And last but not least, to my family, especially my brother David and my parents; there are too many reasons to thank you and not a single one to complain about you.

List of papers published from this Thesis

1) Dinuclear Ruthenium(II) triple-stranded helicates: luminiscent supramolecular cylinders that bind and coil DNA and exhibit activity against cancer cell lines. G. I. Pascu, A. C. G. Hotze, C. Sanchez Cano, B. M. Kariuki, M. J. Hannon, *Angew. Chem., Intl. Ed.*, 2007, **46**, 4374.

2) A supramolecular triple-stranded iron cylinder with unprecedented DNA binding action is a potent cytostatic and apoptotic agent without exhibiting genotoxicity. A. C. G. Hotze, N. J. Hodges, R. E. Hayden, C. Sanchez-Cano, C. Paines, N. Male, M. Tse, C. M. Bunce, J. K. Chipman and M. J. Hannon., *Chemistry and Biology*, 2008, **15**, 1258.

3) An Androgenic Steroid Delivery Vector that Imparts Activity to a Non-Conventional Platinum(II) Metallo-drug. M. Huxley, C. Sanchez-Cano, M. J. Browning, C. Navarro-Ranninger, A. G. Quiroga, A. Rodger and M. J. Hannon. *Manuscript to be submitted to Chem. Eur. J.*

4) Conjugation of Testosterone Modifies the Interaction of Inactive Platinum(II) Complexes with DNA Causing Significant Bending and Unwinding of the Helix. M. Huxley, C. Sanchez-Cano, M. J. Browning, C. Navarro-Ranninger, A. G. Quiroga, A. Rodger and M. J. Hannon. *Manuscript to be submitted to Chem. Eur. J.*

5) Novel and emerging approaches for the delivery of metallodrugs (Review). C. Sanchez-Cano, M. J. Hannon. *Manuscript to be submitted to Dalton Trans Special Issue in Metallodrugs, Late June.*

6) Non-Covalent Metallo-Drugs coupled to sex hormone steroids. C. Sanchez-Cano, M. J. Hannon. *Manuscript to be submitted to Dalton Trans Special Issue in Metallodrugs, Late June*.

Abbreviations

5’-GMP	Guanosine 5’-monophosphate
9EG	9-Methylguanine
AKR	Aldo-keto reductase
AR	Androgen Receptor
AR+	Androgen Receptor Positive
AR–	Androgen Receptor Alpha Negative
AV	Annexin-V
CaPs	Calcium phosphates
CD	Circular Dichroism
CDDP	cis-diamminedichloroplatinum(II)
ct-DNA	Calf Thymus Deoxyribonucleic Acid
CTR1	Copper transporter protein
D_2O	Deuterium oxide
DACH	Diaminocyclohexane
DAPI	4’,6-diamidino-2-phenylindole
DCM	Dichloromethane
DMF	Dimethylformamide
DMEM	Dulbecco’s modified Eagle's medium
DMSO	Dimethylsulphoxide
DNA	Deoxyribonucleicacid
ESI-MS	Electrospray Ionisation Mass Spectrometry
Et_3N	Triethylamine
EDTA	Ethylenediaminetetraacetic acid
EB	Ethidium bromide
EE	17α-Ethynylestradiol
EGF	Epithelial growing factor
EGFR	Epithelial growing factor receptor
EPR	Enhance permeability and retention
ER	Estrogen Receptor
ERα	Estrogen Receptor Alpha
ERβ	Estrogen Receptor Beta
ER+	Estrogen Receptor Positive

ER–	Estrogen Receptor Alpha Negative
ET	17α-Ethynyltestosterone
Et_2O	Diethylether
EtOH	Ethanol
FA	Folic acid
FBS	Foetal bovine serum
FDA	Food and drug administration (United States)
Fig	Figure
FR	Folate receptor
GSH	Glutathione
HA	Hydroxyapatite
HEPES	4-(2-hydroxyethyl)-1-piperazineethanesulfonic acid
HMG	High Mobility Group
HPLC	High performance liquid chromatography
HSA	Human Serum Albumin
HSD	Hydroxysteroid dehydrogenase
ICD	Induced Circular Dichroism
ICP-MS	Inductively coupled plasma mass spectrometry
ILD	Induced Linear Dichroism
LD	Linear Dichroism
MeOH	Methanol
MLCT	Metal to ligand charge transfer
MTT	3-(4,5-Dimethylthiazol-2-yl)-2,5-diphenyltetrazolium bromide
NADPH	Reduced nicotinamide adenine dinucleotide phosphate
NER	Nucleotide excision repair
NMR	Nuclear Magnetic Resonance
PAMAM	Poly(amidoamine)
PBS	Phosphate buffered saline
PHPMA	Poly(N-(2-hydroxypropyl)-methacrylamide)
PI	Propidium iodide
PNA	Peptide nucleic acid
ppm	Parts Per Million
PQ	phenanthrenequinone
PR	Progesterone receptor

PSMA	Prostate specific membrane antigen aptamer
Pyr	Pyridine
Quin	Quinoline
RBA	Relative Binding Affinity
RNA	Ribonucleicacid
RPMI	Roswell Park Memorial Institute medium
SWNHs	Single-walled nanohorns
SWNTs	Sigled-walled nanotubes
TAE	Tris acetate EDTA
TFA	Trifluoroacetic acid
THF	Tetrahydrofuran
tpy	2,2′,2″-terpyridine
Tris	tris(hydroxymethyl)aminomethane
TWJ	Three way junction
UV/Vis	Ultra-Violet/Visible
ZnPc	Zinc phthalocyanine

Abstract

The work described herein concerns the effect on the anticancer activity and the ability to reach their possible intracellular targets of certain steroidal metallodrugs and metallosupramolecular cylinders. Chapter 1 surveys the background to the project, surveying different DNA-binding modes, explaining their importance in the anticancer properties of metallodrugs and showing an overview of the different strategies used for enhanced delivery of these metallodrugs.

In Chapter 2 the synthesis of new steroidal DNA covalent-binding platinum(II) complexes together with techniques to purify previously synthesised steroidal complexes are presented. Their cytotoxicity, cellular uptake and biomolecular interaction are investigated, showing that the coupling of the steroid confers activity to otherwise inactive complexes, modifying their DNA binding mode and cellular uptake and distribution.

Chapter 3 explores the coupling of similar steroidal delivery vectors to non-covalent metallodrugs, presenting simple synthetic pathways to create such complexes in a single step. Their anticancer activity and DNA-binding affinity are investigated: surprisingly showing that this coupling has negative effects.

In Chapter 4 the cytoxicity and cellular behaviour of metallosupramolecular cylinders are studied. It is shown that these complexes can cross the cellular membrane, concentrating in the nuclei where they can interact with cellular DNA.

Contents

Chapter 1: Introduction

DNA is the most important molecule in the cell. Its contents encode all the genetic data (in most organisms) which is ultimately responsible for most of the functions, actions and physical traits of the organism. The genetic information is processed through transcription into RNA, which is then used to synthesise specific amino-acidic sequences, leading to desired proteins. Alternatively the RNA itself may have regulative functions of other genes or proteins. This means that through regulation of DNA, the whole cellular activity can be controlled. Changes in the DNA sequence or defective genetic information can produce protein actions that are the origin of many diseases. To avoid this, cells have processes that lead to programmed death in case of important changes in the genomic DNA. Some organisms make use of this dependence on DNA and turn it to their own advantage with defensive or pathogenic intentions. Good examples of this are the viruses; they can introduce their own genetic material into the cellular genomic DNA to control the whole cell and reproduce within the infected organism. Other examples are the productions of antibiotics, toxins or other compounds that act through a direct interaction with the target organism DNA providing an advantage to the organism that synthesises them. For these reasons, cellular DNA is interesting as a medicinal target with the potential of control diseases, parasites or viruses.

1.1 Modes of DNA interaction

It has been demonstrated that synthetic molecules can target DNA using four different binding modes: Major and minor groove binding, intercalation, and base covalent binding (Fig. 1.1)[1]. Recently two new modes of ligand-DNA interaction have been described; phosphate binding and junction binding (Fig. 1.1)[1-3]. Most of these modes have been observed in nature and synthetic molecules have been created to imitate the natural products. The major groove has been successfully targeted with synthetic peptides or oligonucleotides containing Zinc fingers[4] or forming triple stranded DNA[5-6] respectively. These oligonucleotides form the triplex DNA through the formation of Hoogsteen or reverse Hoogsteen base pairing, which confers certain sequence-specificity, making them interesting for gene regulation[5-7]. Peptide nucleic

acids (PNAs) have been synthesised as well with the same aim of the oligonucleotides. These molecules replace the sugar backbone of DNA/RNA by a neutral polymeric chain of aminoacids, removing the negative charge of the oligonucleotides that will reduce their binding to anionic double helical DNA[8]. Recently, metallosupramolecular cylinders able to target the DNA double helix in the major groove (Fig. 1.2 A) have been reported. They are the first truly synthetic agents to target only the major groove[1].

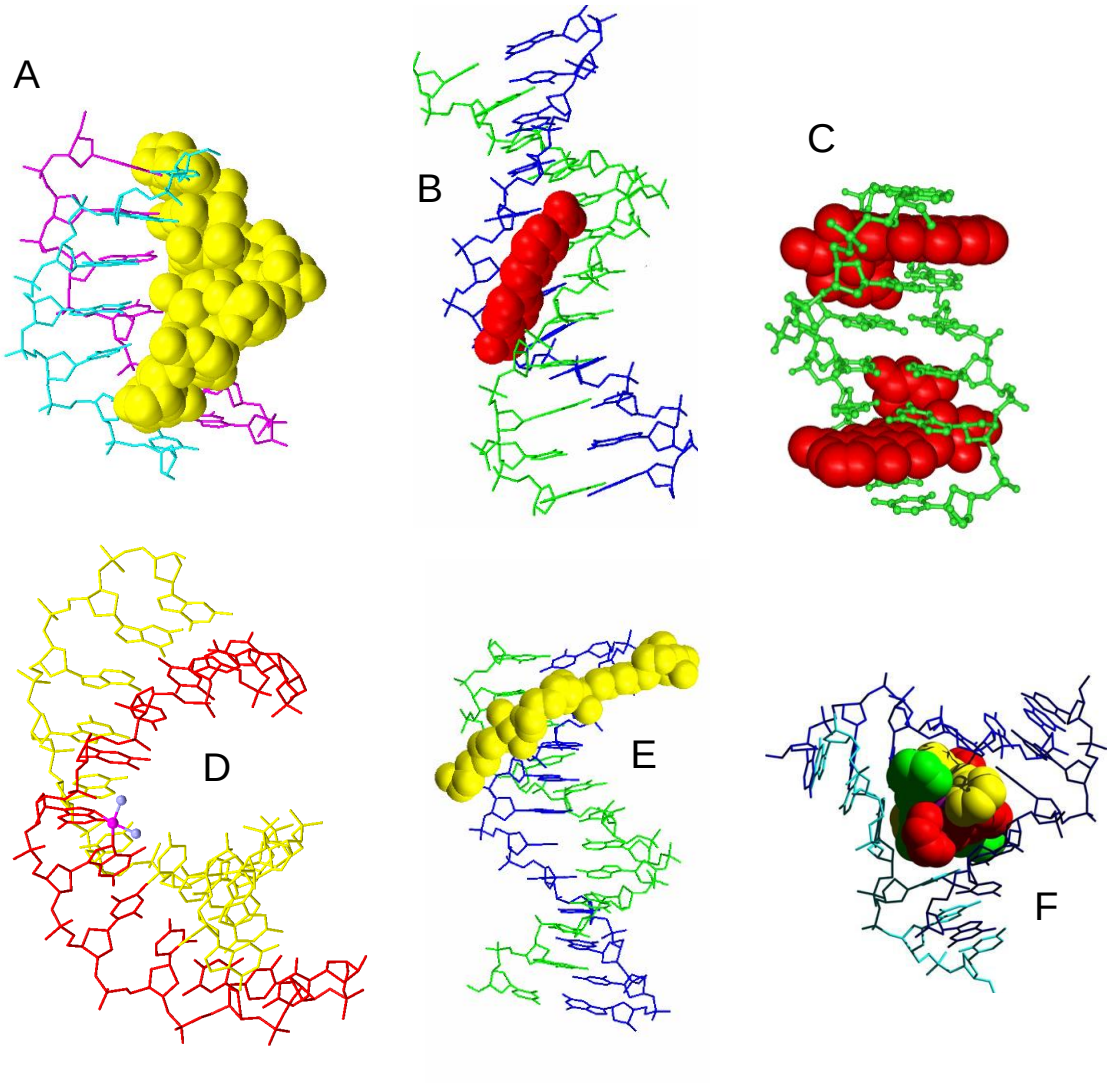

Figure 1.1. Synthetic molecules targeting the major groove (A; synthetic oligonucleotide; PDB ref. 149D), minor groove (B; DAPI, Fig 1.2; 1D30), intercalate between DNA bases (C; Doxorubicin, Fig. 1.2; 1D12), binding to bases (D; cisplatin, Fig. 1.5; 1AIO) phospate backbone (E; TriplatinNC, Fig. 1.7; 2DYW) and three way junction (F; iron supramolecular helicate Fig 1.8; 2ETO).

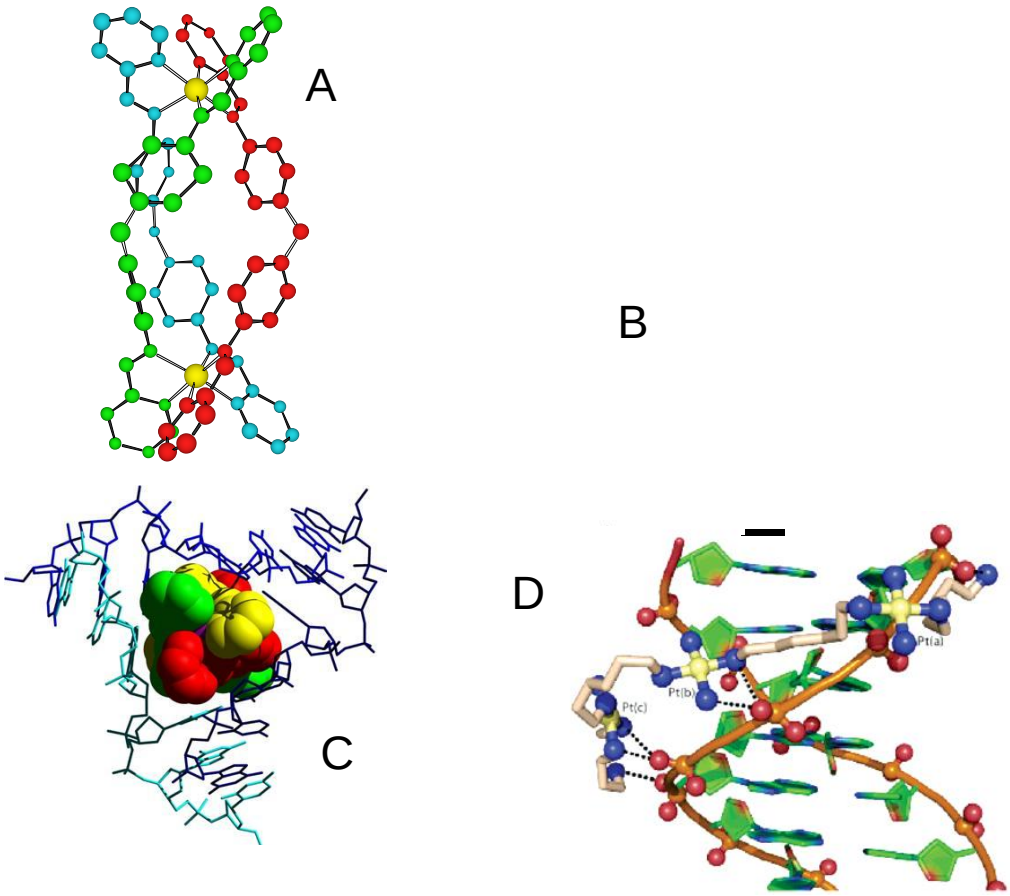

Figure 1.2. Metallodrugs that bind in the major groove (A) or intercalate between DNA bases (B); non-covalent DNA Three Way Junction binding (C, taken from Olesky et al[2]) and Phospate binding (D, TriplatinNC, taken from Komeda et al[3]).

The DNA double helix minor groove, on the other hand, can be targeted with organic synthetic molecules (Fig. 1.3 B,C)[1]. Such agents are usually small arc shaped cationic structures with selectivity towards AT regions (due to the narrower size of the minor groove when compared with GC sequences, making them fit tighter), such as diarylamides (DAPI, berenil and pentamidine) and bis-benzimidazoles (Hoechst family)[1]. They are used as anticancer, antiprotozoal, antiviral and antibacterial agents,[9] and some of them show interesting fluorescent abilities (increased when bound to DNA), and are widely used as imaging molecules and DNA stains[1]. Another example is Distamycin A, a natural antibiotic used commercially against bacterial and viral infections. As the previous synthetic examples it is a cationic long molecule with methylpyrroles that bind specifically in AT rich regions[10]. Dervan's group have modified the basic structure with different pyrrole/imidazole sequences that allow the recognition of different DNA sequences *via* the minor groove[10].The resulting molecules

are the pre-eminent example of sequence specific synthetic DNA binding agents (Fig. 1.3C).

Figure 1.3. Synthetic molecules targeting the major groove (A), minor groove (B, C), intercalate between DNA bases (D), binding to bases (E).

A third way of binding is intercalation. This involves the introduction of planar aromatic molecules between the bases[1] (Fig. 1.3D) and was first proposed in the 1960s[11]. Intercalation can happen from either major and minor grooves, opening the gap between stacked base pairs and producing unwinding of the DNA double helix. Intercalators have a maximum loading of a molecule per 2 gaps[12]; this is due to the fact that the backbone is not flexible enough to have molecules intercalated in adjacent gaps. An example of a molecule with intercalative properties is ethidium bromide, a carcinogenic compound used in normal molecular biology and biochemistry techniques that increases its fluorescent properties when intercalated between the bases of the DNA[13]. An example of a clinically used intercalator is the antibiotic doxorubicin and its family (antrhacycline antibiotics), a group of planar organic molecules that have been widely used as anticancer drugs since 1960s[14].

Finally, the last of the conventional modes of DNA binding is covalent binding to the nucleobases, mainly to the N7 atoms of G or A bases[1]. These covalent bonds produce modifications in the structure of the DNA leading to lesions in the genetic code that not always can be repaired, finishing usually in programmed cellular death. Nitrogen mustards such as melphalan (Fig. 1.3E), platinum complexes such as cisplatin[15], nitrosoureas and cross linking agents such as mitomycin C[16], are in clinical use as anticancer agents.

Figure 1.4. Hydrogen bonds with the DNA phosphate backbone observed in the arginine fork (A) and with Farrell's TriplatinNC (B).

All of these modes of interaction with DNA have been known since the 1960s and in 40 years no substantial new ways of DNA binding have been described. This has changed recently and in the last 5 years two new modes of DNA binding have been described: binding to DNA junctions (especially three way junctions)[2] and binding to the phosphate backbone of the DNA[3]. Phosphate binding has been observed in the nature previously: Proteins can bind this region through hydrogen bonds from cationic residues, especially arginine, which forms the known arginine forks (Fig. 1.4 A). Alkali metals of the groups I and II can bind to DNA in this area as well[1]. Recently Farrell synthesised a non-natural compound that could bind to the DNA phosphate backbone in similar way to the arginine residues[3]. The synthesised compound is a cationic trinuclear Pt complex, without Pt-Cl groups that would allow covalent binding to the DNA (Fig. 1.2, TriplatinNC). The positive charge, absence of leaving groups and presence of several amino groups allow the complex to bind to the phosphate groups of the backbone through hydrogen bonds (Fig. 1.4 B), forming similar structures to arginine forks. Single crystal X-Ray diffraction of DNA and ligand reveals that the complex can

both track along the backbone of a single strand or stretch across the minor groove making contacts with the phosphate backbones on each strand[3].

The second new DNA binding mode occurs through the recognition of DNA junctions. These structures are formed by RNAs or DNAs in different situations, the common structures being the connective points of three or four double stranded chains. Some of these can be observed in different structural types of RNA, replication forks (a kind of three way junction) or during the recombination process (the four way or Holliday junction). Until recently, compounds aimed at these structures were just bifunctional agents that target two of the B-DNA arms involved in the junction. Thus bis-intercalators and bis-minor groove binders were synthesised and showed the ability to recognize these structures, but still bind to the DNA in their usual way[1]. Recently, the Hannon group described the structure of a cationic metallosupramolecular complex that could bind in the internal cavity of a three way junction (Fig. 1.2)[2]. This dimetallic triple-stranded complex has a cylindrical shape and similar size to Zinc fingers and is able to target the major groove of the DNA double helix producing dramatic coiling[17]. Single crystal X-Ray diffraction of the complex with a palindromic DNA sequence showed that the cylindrical compound could recognise as well the structure of a three way junction (TWJ). The compound was perfectly inserted in the cavity created by the TWJ structure, without alterations to the DNA structure or the complex. The fit was so perfect that the two internal aromatic phenyls of each strand of the complex stack with the two bases of one of the strands of the TWJ. The three pyridine rings of the end of the cylinder that protrude into the TWJ bind in the minor grooves of the three strands of the structure in a similar way to the minor groove binders described before[2]. This recognition was unprecedented and of high interest since opens the possibility to target replication or transcription forks.

1.2 Metallic complexes as anticancer drugs

The popular image of a medicine corresponds to organic molecules with complicated structures. These molecules would be cleverly designed, aiming at incredibly specific targets and would provide great activity and low side effects. Reality is different and inorganic formulated drugs (especially coordination complexes of the metallic transition elements) represent a major part of the pharmaceutical industry[18-19]. The best example

of this is cisplatin, a platinum (II) square planar coordination complex that presents two ammine groups and two chloride atoms in cis configuration bound to the metallic centre (Fig. 1.5)[15]. This complex was first synthesised by Peyrone in 1844[20], but was not until the 1960s that Rosenberg discovered its antibacterial[21] and cytotoxic[22] abilities. Cisplatin was accepted as a clinical anti-cancer drug in 1978 and since then has been used broadly alone or in combination against different cancers presenting a business of two billion US dollar per year[23-24].

Figure 1.5. Structure of cisplatin (A), carboplatin (B), oxaliplatin (C), nedaplatin (D).

It is commonly accepted that cisplatin interacts not only with DNA but also with plasma proteins[25], enzymes[26], serum albumin[27], and with sulphur containing molecules such as glutathione, the latter taking part in a deactivation processes[28]. It can also interact with lipids and intermembrane proteins, while it is trying to enter into the cell[29]. The cellular uptake process was believed for a long time to occur by passive diffusion[30-34], but recent works suggest other possible routes: some copper transporters can regulate the amount of platinum inside the cell[35]. However, DNA is the target that leads to cisplatin activity[23, 36].

Cisplatin is not thought to be the active agent once the drug is inside the body and partial or complete hydrolysis in the intracellular environment is thought responsible for activation[37]. This hydrolysis affords cationic compounds that interact with DNA, mainly through bonding to the N^7 of purine bases, with Guanine preferred over Adenine (90% of all Pt-DNA bonds). Binding to N^1 of Adenine or N^3 of Cytosine is possible as well, but not so common. Cisplatin-DNA interactions appear mainly as bifunctional adducts[38], being the intrastrand 1,2 GpG the most common (formed in 65% of the occasions). Intrastrand 1,2 ApG cross links can be detected as well on 25% of the

lesions, with a 5% of 1,3 GpXpG[39]. Finally, small amount of interstrand adducts (mainly GG) and monofunctional adducts can be detected[40]. As might be expected, the various bonding arrangements found in Pt-DNA adducts result in different distortions to the DNA helix. The major intrastrand 1,2 GpG lesion is located in the major groove, and produce the DNA double strand to unwind by 13º[41]. It also bends (kinks), the DNA by 45º towards the site of platination[42]. This bent DNA is recognized by nuclear HMG proteins[39, 43], binding to the DNA and protecting the lesion from DNA repair [44]. If enough of these adducts are produced without repair (normally through nucleotide excision repair), the cell will die through apoptotic process.

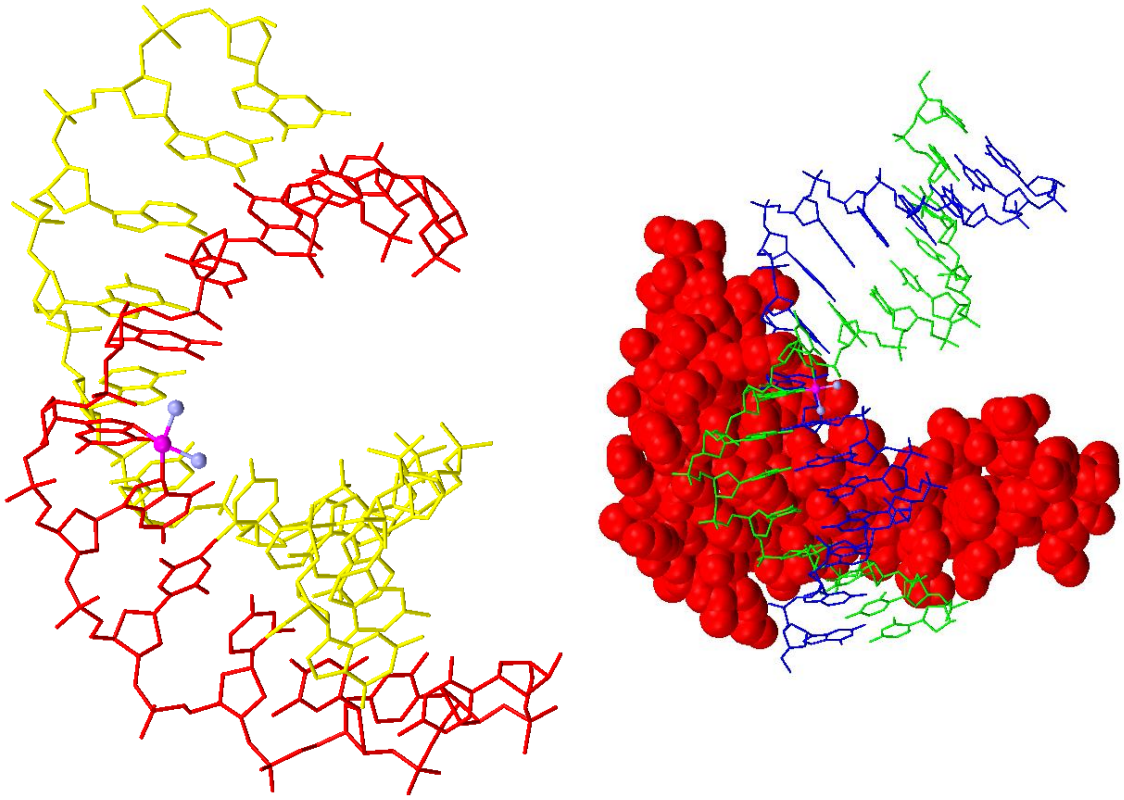

Figure 1.6. XRay structure of cisplatin DNA interaction (left; PDB ref. 1AIO), and being recognised by HMG proteins (right; 1CKT).

The trans isomer of cisplatin, by contrast, does not show any activity against carcinogenic cells. This could be due to the non formation of bifunctional 1-2 GpG intrastrand adducts: transplatin only forms 1,3 GpXpG intrastrand crosslinks. These adducts are quite unstable and evolve to 1,1' GC interstrand adducts[45], unwinding the

DNA double helix by 9º and not being recognised by HMG domain proteins. Another possibility for this low activity could be the higher life time of the mono-functional adducts and the low formation of bi-functional adducts compared with cisplatin[46]. DNA adducts and structural modifications different to cisplatin's could explain the inactive nature observed for trans platinum compounds. This shows the importance of DNA binding in the cellular behaviour of platinum complexes. For that reason it was postulated that for a platinum drug to be active, it needed to present two good leaving groups in cis geometry.

However, this process is not selective: cisplatin interacts with non-cancerous cells and other bio-molecules (such us proteins) producing secondary effects that limit the dose that can be administered. In addition, some tumours are resistant towards the drug and others can develop resistance after the treatment[15]. For that reason a second generation of complexes was developed and three of such compounds are already on the market (Carboplatin, Oxaliplatin and Nedaplatin) (Fig. 1.5)[23]. These new complexes allowed the solution of some of the problems previously described: respectively lower side effects, broader activity and the ability to overcome some types of resistance, lower neuro and nefrotoxicity. Carboplatin (Fig. 1.5B) has a cyclobutane,1-1,dicarboxylate as leaving group instead of the chlorides of cisplatin. This increases the stability of the complex, showing lower interaction with non-wanted molecules[15], leading to lower secondary effects and cytotoxicity. For that reason carboplatin is administered to patients with other weaknesses or illness. However, no activity is observed when cisplatin resistant tumours are treated with this derivative[36]. Oxaliplatin (Fig. 1.5C), on the other hand, shows a different activity spectrum to cisplatin. It is quite effective against tumours that develop resistance as result of the treatment with cisplatin[47]. The mechanism of action is the same as cisplatin, but it seems not to be recognised by the HMG proteins as result of the bulkiness of its DNA adduct (the DACH ligand remains on the lesion rather than two ammonias)[48]. None of these drugs have addressed all of the problems, probably due to their similarity to cisplatin in their structure and thus their mode of action.

All second generation complexes bind to DNA in a similar way to cisplatin, providing similar activity. Complexes that bind differently from cisplatin to the DNA can lead to activity through different mechanisms that could circumvent cisplatin problems. For that reason, further generations of compounds have been explored,

searching for different interactions with the cellular DNA. This class of agents is broad and includes many "non-conventional" structures such trans geometries[38, 49-51], polymetallic[52-54], monofunctional[55-57] or platinum (IV) complexes (targeting oral administration)[15]. None of these has yet arrived on the market, although some have entered clinical trials.

Complexes with trans geometry can be activated by modification of the coordination sphere. Three main types of compounds can be observed here: trans platinum complexes activated by bulky aromatic substituents, by aliphatic amino groups and finally by iminoethers (Fig. 1.7A-E)[38, 58]. All of them show different DNA binding abilities and produce different distortions to the DNA structure compared with transplatin and cisplatin [38, 58]. When one or both amino groups are substituted by bulky aromatic rings, the new compounds show activities at least one order of magnitude better than transplatin. The complexes are as cytotoxic as their cis isomers and cisplatin, presenting good activity against cisplatin and oxaliplatin resistant cell lines[38, 58]. They show higher cellular uptake, slower reaction binding rates to glutathione and twice as many interstrand adducts compared with transplatin. These interstrand adducts are formed quicker than for transplatin and present a similar structure to the ones observed in cisplatin, being 1,2' GG instead of 1,1' GC (as observed for transplatin). The presence of the aromatic ring changes the DNA unwinding structure/ability relationship, 17º for the trans against 13º of cisplatin, 9º of transplatin and 4º of their cis derivatives. It is interesting to note that complexes with a single aromatic in the coordinative sphere also show *in vivo* anti-leukeamic activity, not observed for the bisubstituted compounds, may be due to the high number of monofunctional adducts observed for this complexes. These adducts produce local conformational distortions in the DNA very similar to the ones produced by the 1,2 GpG intrastrand cisplatin adducts (perhaps due to a partial intercalation of the aromatic ring between the adjacent bases), and are recognized by HMG proteins and cisplatin-specific antibodies. The poor solubility problem presented for these complexes was solved changing the chloride leaving groups by acetate groups. This change makes them the trans equivalent of carboplatin, providing them with high water solubility, but maintaining the same activity as the original compounds[59].

Figure 1.7. Examples of non-conventional platinum complexes: planar aromatic trans complexes (A), aliphatic amines trans complexes (B), piperidine/piperazine-aliphatic amine trans complexes (C), iminoether trans complexes (D), multimetallic BBR3464 (E) and platinum(IV) Satraplatin (F).

A second example of trans activation can be observed when the N donor amino groups are substituted by one or two aliphatic amines (Fig. 1.7B, C). These complexes show similar activity to cisplatin in sensitive cell lines and higher against cisplatin resistant[38, 58]. The improved activity in resistant cell lines again can be due to a particularly high percentage of monofunctional and interstrand adducts, with this adduct found in the form of 1,2' GG crosslinks. This leads to higher efficiencies than cisplatin and transplatin in blocking DNA *in vitro* synthesis and lower levels of repair of the lesions observed[38, 58]. These two modes for activate trans geometries are mixed when one of the amines or ammonia is substituted by a positively charged non planar piperidine or piperazine molecule (Fig. 1.7C). The toxicity of these new complexes decreases compared with the original compounds, but they present better response towards cisplatin resistance mechanisms[58]. These cationic complexes show a high percentage of interstrand crosslinks, but lower than previous compounds, and extremely high double stranded DNA unwinding abilities, showing around 30º compared to 13º of cisplatin and 17º showed by the trans aromatic complexes[60]. Cis derivatives, in contrast,

unwind the DNA double helix by 13º (the same as cisplatin) and present normal cisplatin like interstrand adducts percentages, showing lower toxicities compared to the trans complexes[61].

The third way to activate trans geometries is through the use of N donor iminoether groups (Fig. 1.7D)[38, 58]. Contrary to the previous examples, the main DNA adduct is not an interstrand crosslink, rather a higher percentage of monofunctional adducts are formed with preference for sequences pyrimidine-Guanine-pyrimidine (py-G-py). Even though, they show *in vitro* anticancer activities similar to cisplatin (with a better response towards resistance mechanisms) and present *in vivo* activity (having interesting lipophilic properties that make possible potential oral administration). These monofunctinal lesions unwind the DNA double helix 6º[38, 58], as seen in previous non-active monofunctional complexes[62] (against 13º for cisplatin and higher values for aromatic trans complexes). However, they do not denature the DNA double helix as transplatin or other monofunctionally binding complexes, and they force a 21º DNA bend towards the minor groove (against the 45º towards the major groove of cisplatin). Not being recognised by HMG domain proteins, they can be removed by nuclear excision repair (NER); but formation of protein-DNA crosslinks inhibits both the DNA synthesis and NER systems[58].

Interestingly, monofunctional adducts caused by biologically inactive[63-64] $[Pt(NH_3)_3Cl]Cl$ and [Pt(dien)Cl]Cl cause relatively few DNA structural changes. They bind monofunctionally to N7 of guanine, producing 6º of unwinding to the double helix without visible bending of the DNA[62]. When bulkier amines are attached to the platinum[55], monofunctional adducts are still formed without any trace of bifunctional adducts[56, 65] (although some of this have been observed with triammines with 2-diazapyrenium[66-67]). They still produce minor distortions to DNA compared to cisplatin[68], unwinding the double helix to a similar extent to non-bulky amines[57] without visible bending of the structure[69]. This ability to distort DNA may be co-related to why such complexes possess poor cytotoxicity. Unlike cisplatin they don't seem to undergo hydrolysis before binding to guanine[70], and show low sensitivity to the excision repair mechanism[66]. However, triammines do inhibit DNA replication, with an increased effectivity when bulky substituents are introduced[56]. As with cisplatin, trans isomers seem to produce less effect on the DNA[71], being less active than the cis isomers.

These are not the only compounds specifically designed to yield adducts different to the ones produced by cisplatin, with the idea that different DNA interaction would lead to broader anti-cancer activity; multimetallic complexes have been studied as well. Of particular note are Farrell's trans platinum multimetallic complexes[52], especially BBR3464 (which underwent phase II clinical trials; Fig. 1.7E), that show increased intracellular accumulation, and dramatic *in vivo* and *in vitro* activity against cisplatin sensitive and resistant tumours[72]. These compounds could produce a whole series of different DNA adducts, including 1,2 , 1,3 and 1,5 intrastrand and 1,2' , 1,4' and 1,6' interstrand crosslinks adducts. None of the intrastrand lesions are recognised by HMG proteins and can be repaired by nuclear excision repair proteins (NER proteins) more easily than cisplatin 1,2 GpG adducts. However, a high level (20%) of interstrand crosslinks are detected (against 3% of cisplatin) that unwind by 14º the double helix of DNA and are able to span 6-8 bases the DNA[73]. These interstrand crosslinks are not recognised by HMG proteins, and the 1,4' adduct is particularly interesting, as it cannot be repaired by NER proteins[74].

Finally, using octahedral platinum(IV) centres (Fig. 1.7F), two more ligands can be added to the metallic centre, this can lead to higher lipophilicities and water solubilities. Compounds in this oxidation state are more inert, lowering the reactivity with biomolecules leading to fewer side effects[75]. These two factors (improved solubility/lipophilicity and higher inertness) made them the perfect molecules to attempt oral administration. They show high stability in the gastro-intestinal track and are incorporated into the blood stream[76]. Once inside the organism they are reduced by proteins like GSH or even Fe(II) containing proteins[77] (heme groups), producing platinum(II) derivatives, which are believed to be the DNA interacting active species[78]. Currently the major challenge of these compounds is to minimize the possible plasmatic reduction (3 s $t_{1/2}$ in blood for tetraplatin[78] and 6.3 min for satraplatin[75]), which could lead to unwanted secondary effects and to the loss of platinum(IV) potential advantages.

Biological activities have been discovered for complexes of other metals, giving the possibility to attack different targets that maybe would resolve the problems created by platinum drugs[18-19]. The most effective of these are ruthenium complexes of which two are currently in clinical trials; the ruthenium (III) derivatives KP1019[79] and NAMI-A[80-81] (Fig. 1.8). The first of these, KP1019, uses the iron transporting proteins Ferritin and Albumin to be transported through the blood and into the cells, where it interacts (in

some form) with DNA, showing activity against colon carcinoma and a variety of human primary tumours. NAMI-A seems to act in a totally different way since it doesn't show any activity towards primary tumours. However, it has very interesting antiangiogenetic and antiinvasive properties, making it particularly active against metastasic stages of cancer. Complexes with similar (primary or anti-metastatic) activities have been developed with the use of arenes and ruthenium (II) as the metallic centre[82-85]. Other metals like iron[86-88], titanium[89-92] or gallium[93-94] have been studied as well, with complexes of the last two also entering clinical trials.

Figure 1.8. Structures of NAMI-A (A) and KP1019 (B).

All of these drugs were designed with a view to obtaining activity through covalent binding of the metallic centre to its target (DNA). Non-covalent interactions with DNA and other macromolecules are observed in the nature, and are of great importance. Examples of this can be seen in the fields of recognition[95] or antibiotics[14], and it is also of potential interest for the development of new medicines. Two major ways of non-covalent DNA binding have been known for the last forty years; groove binding (major and minor) and intercalation[1]. Two more has been added recently; junction[2] and phosphate binding[3]. Metallodrugs binding to DNA through all four ways has been developed (Fig. 1.2), and indeed the last two modes have been discovered through the use of coordination complexes (Fig. 1.2C, D)[1]. Although promising results have been observed, the use of this kind of compounds as anticarcinogenic drugs is still under its first steps.

1.3 Delivery strategies for metallodrugs

Although important breakthroughs in tumour active metallodrugs have taken place in the last 20 years, some of the problems formerly presented by cisplatin are common to almost all of the new compounds and remain unsolved. A different way of tackling the problem is the use of delivery systems[96] and here two main paths have been followed: the use of systems that deliver the selected drug slowly, usually relying for targeting on the EPR (enhanced permeability and retention) effect[97] (caused by the increased production of permeability mediators and angiogenesis, together with the decrease of the lymphatic drainage in tumour tissues); or the chemical modification of the drug targeting a direct feature of the selected tumour[96], stopping the action in healthy cells. Herein we present an overview of the strategies used for the delivery and selective administration of existing anticancer metallodrugs.

1.3.1 Delivery through covalent modification

Since cisplatin's discovery, chemists have been trying to improve its abilities or solve its problems through covalent modification of its structure[15, 23, 38, 96, 98]. Side effects or resistance have been partially solved with new chemically formulated drugs and the same has been explored targeting or delivery[96, 98]. A variety of different ideas have been explored ranging from binding to biomolecules, to the use of prodrug techniques. An example of a biomolecule strategy was the attachment of the drug to a cysteine binding molecule (Fig. 1.9)[99]. The aim was to bind to blood transport proteins and thereby localize it using the EPR effect. Formulations of this complex achieved 90% binding with human serum albumine (HSA) in 15 minutes of reaction. *In vitro* cell tests showed a 5-8 fold decrease in activity against lung carcinoma; however, the agents presented improved activity when treating *in vivo* tumours in mice. A similar tethering-to-HSA strategy has also been used for ruthenium organometallic complexes[100]. This gave a 20 fold increase of the activity in ovarian cell lines compared with the parent complex[100].

Figure 1.9. Example of Pt(II) complex with cysteine binding domain.

As we will see in this chapter, carriers can be directed toward specific organs or receptors by attaching biomolecules that target them[101-104]. Metallodrugs have been targeted against liver or bones and estrogen or folate receptors using similar ideas[96]. Galactose or bile acid molecules have been use to target platinum drugs to the liver, taking advantage of physiological properties (galactose receptors are expressed highly in liver and bile acids are synthesised and effectively recycled and reused by the same organ). Natural[105] and synthetic oestrogenic molecules[106] have been attached to platinum or organometallic drugs and imaging systems to target oestrogen receptor (Fig. 1.10A). Endocytotic delivery has been sought by attaching folic acid molecules to platinum drugs[107]. This acid displays high affinity for Folate Receptors (FR) that introduces the drug inside the cell through an endocytotic process. Moreover FR is expressed highly in human cancer cells, especially in ovarian and endometrial cancers and is absent in most of normal cells[108]. The ostoetropic (bone seeking) abilities presented by bisphosphonate molecules have been used to target bone tumours and ossifying metastases. Platinum molecules were attached to bisphosphonates (Fig. 1.10B), acting as leaving groups. These molecules have interesting cytotoxicity values and *in vivo* experiments showed strong inhibition of primary tumours and prolonged survival[96].

Figure 1.10. Examples of oestrogen receptor directed Pt(II) estradiol derivative (A), and bone directed Pt(II) complex (B).

A way of reducing side effects of platinum drugs would be to better target them to the nuclear DNA. To explore this metallodrugs have been bound to molecules with high binding affinity for DNA or that are known to localize in the nuclei[98]. Oligonucleotides or peptide nucleic acid (PNA) have been attached to platinum (II) and (IV) compounds and have shown some ability to overcome cisplatin resistance (perhaps by dual, and more specific, binding) and sequence specific inhibition of specific oncogens[98]. A level

of sequence specificity could also be achieved with the use of minor groove binders. Sequence selective chains of pyrolles and imidazoles can target the platinum complex towards certain sequences (Fig. 1.11)[109-110]. Intercalators posses high binding affinity towards DNA and have also been explored. Some complexes including intercalative ligands show impressive cytotoxic abilities and act in different ways to cisplatin[111-113], making such agents interesting against cisplatin resistant cell lines. Some intercalators show fluorescence properties and this has been used for cellular tracking of the complex[114-115]. Such nuclear targeting is less attractive than tissue targeting but might nevertheless prove useful.

Figure 1.11. Example of nuclear DNA directed Pt (II) complex.

Prodrugs have also been explored. A prodrug is an inert compound that can be turned into an active drug upon selective modification at a given site, thereby delivering the active complex only at the desired target. Different strategies have been used for the activation of metallo-prodrugs but probably the most successful to date is the use of compounds that can undergo reduction. Platinum (IV) is a chemical form of platinum that present much lower activity than platinum (II). However, these platinum (IV) compounds can undergo intra or extracellular reduction releasing active platinum (II) species[23]. Platinum (IV) complexes have, also, octahedral coordination sphere, giving the possibility to attach extra ligands that could increase the water solubility, making possible the oral administration. Different platinum (IV) complexes have entered clinical trials[23], the most effective to date being Satraplatin (Fig. 1.12A). Satraplatin usually is administered orally and reached phase III trials although it appears to have been unsuccessful in the final stage and has not (at this time) been approved by the FDA[116]. Complexes that are modified under low pH conditions (Fig. 1.12B)[96] or can be photoactivated (Fig. 1.12C)[117] have been studied as well. Carcinogenic cells present lower pH than its normal counterparts, as a result of the hypoxia produced by the low irrigation. For this reason platinum (II) complexes have been synthesised and considered for their pH dependent reactivity and cytotoxicity[96]. Local effects can also

be obtained using inactive drugs that are modified and activated by external irradiation with light of certain wavelength[117]. Some initial studies have looked at molecules that could be cleaved by specific enzymes. Sugars and esters have been attached to platinum molecules aiming at cleavage bye β-glucuronidases or esterases[98]. Although to date the cleavage seems to be aimed at altering the cellular permeability of such complexes rather than the inherent activity of the platinum unit.

Figure 1.12. Examples of Platinum (IV) complex (Satraplatin, A), pH activated Pt(II) prodrug (B), photoactivated Pt(IV) prodrug (C), and enzymatically activated Pt(II) prodrug (D).

1.3.2 Ceramic materials

The usual method of cisplatin chemotherapy is through intravenous administration as a short-term infusion. This method yields a big concentration of complex in the injection area in the short initial time and the drug is then removed quickly to the rest of the organism. This leads to high side effects both in the treated organ and in the rest of the organism. An early attempt to control this release was the surgical implantation of solid material close to the tumour that would release slowly the drug for a long period reducing the side effects[118-119]. Different materials have been used in this role[120-121], but due to their similarity with bone structures Calcium Phosphates (CaPs) were extensively studied[118, 119, 122-123]. First formulations consisted of packed solids, hydroxyapatite ceramic or solid phase cement that included the drugs in solid state[121-122]. When these systems were used it was shown that implantation close to the tumour could inhibit its growth and decrease the side effects produced by cisplatin[123]. Passage into the tumour was a complex event, a function of solubilization of the drug, adsorption to the CaPs ceramic and diffusion gradients in the organism[124].

More recently crystals of CaPs have attracted attention due to their physical and chemical properties, high surface interaction properties and their biocompatibility[125]. Examples using hydroxyapatite or tricalcium phosphate ceramics showed that these systems could be used to deliver Steroids[126], proteins[127], hormones[128], anticancer drugs[119, 122, 129] and other molecules[130-132]. Carbonated hydroxyapatite (HA) crystals were especially interesting due to their similarities to the crystals found in bones. The compounds were adsorbed in the crystals instead of being included as solids. This adsorption depended on the physical and chemical characteristic of the HA crystals such as the chemical composition, the structure and porosity, the surface area or the size[124, 128, 133-134]. Initial studies loading cisplatin in HA crystals showed that the adsorption and release of the drug was dependent on temperature, chloride concentration in the medium and crystallinity of the HA[124, 135]. This last factor indicated that lower crystallinity lead towards higher adsorption and slower release. Initial *in vitro* tests showed cytotoxicity in these systems[135].

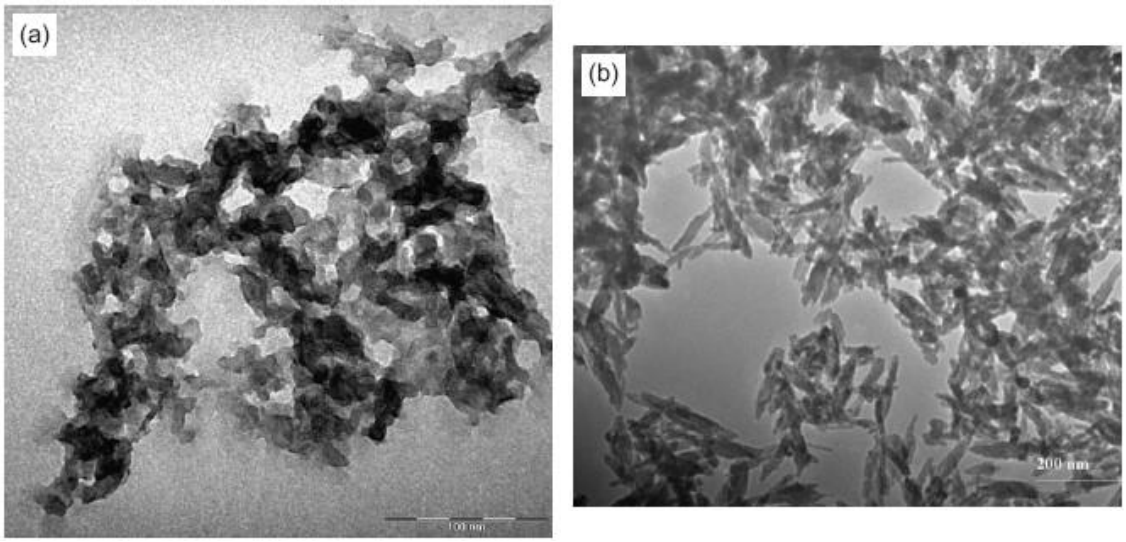

Figure 1.13. TEM images of synthetic plate (A) or needle shaped (B) HA crystals. Taken from Palazzo et al[136].

Later studies demostrated that shape of the HA crystals is important as well. In 2007 Natile *et al* showed that cisplatin molecules and bisphosphonate platinum derivatives could be loaded into the porous structures of bone like plate or needle shaped HA crystals (Fig. 1.13)[136]. The different crystalline structures showed similar Ca/P bulk ratios, but different surface area and Ca/P surface ratio (higher for plate shaped). Cisplatin was adsorbed better on needle shaped crystals, where the lower amount of Calcium in the surface allowed easier loading of the positively charged aquated cisplatin

molecules. The bisphosphonate derivative did not show any preference, presenting similar adsorption in both structures. However, release of the platinum agent was slower from the plate shaped crystals. By contrast cisplatin release was the same for both shaped HA crystals.

1.3.3 Carbon Nanotubes

Carbon nanotubes have been recently started to be explored for delivery of drugs due to their unique physical, chemical and physiological properties[136]. They have proved to be able to transport a wide range of molecules across membranes and into living cells[137-140]. In addition, their structural stability may prolong the circulation time and the bioavailability of the loaded molecules. Ajima et al in 2005[141] used single-walled carbon nanohorns (SWNHs) for the delivery of cisplatin. These are a kind of single-walled nanotube (SWNTs) that do not exist alone, but instead several hundred assemble to form a spherical structure between 80 and 100 nm, presenting an adequate size for delivery through EPR. SWNHs were loaded with cisplatin through a selective precipitation process using DMF, showing a Pt/C ratio of 1/100 and incorporating around 15% of the cisplatin. The complex appeared unaltered and the system presented a low release rate retaining 40% of the complex withing the nanotubes after 48 hours and 20% after 14 days. The formulation kept activity similar to cisplatin in a period of time of 48 hours. When the selective precipitation was made from water, the amount of complex incorporated increased to 46%[142]. Over 48 hours 100% was released. Finally systems generated in this way showed better *in vitro* and *in vivo* antitumour activity compared with cisplatin, maintaining the activity in mice for long times (25 days). Similar techniques have also been used for the drug Zinc phthalocyanine (ZnPc) with good results showing the flexibility of this kind of system. Encapsulated drug lead to the almost complete disappearance of tumours in mice when irradiated at 670 nm[143], this effect was not observed when ZnPc or the SWNHs were administered alone.

More recently SWNTs were functionalized with Platinum (IV) molecules by Lippard through covalent tethering (Fig. 1.14). The SWNTs were expected to internalize the drug and release the platinum payload once inside the cell[144]. An average of 65 molecules of platinum was attached to each SWNT and they were shown to enter the cell through an endocytotic process, introducing higher levels of platinum in the cell than the untethered complex or cisplatin. They showed high toxicity in testicular cancer

improving 25 fold the activity of the parent complex (and 2.5 fold greater than cisplatin). These structures were further functionalized by adding folic acid (FA) to the platinum (IV) unit after preparation[101]. This was hoped to target the SWNTs towards FR+ cell lines and indeed proved to increase the selectivity. Toxicity was increased in these cell lines compared to FR- lines, giving 9 fold greater activity compared with cisplatin.

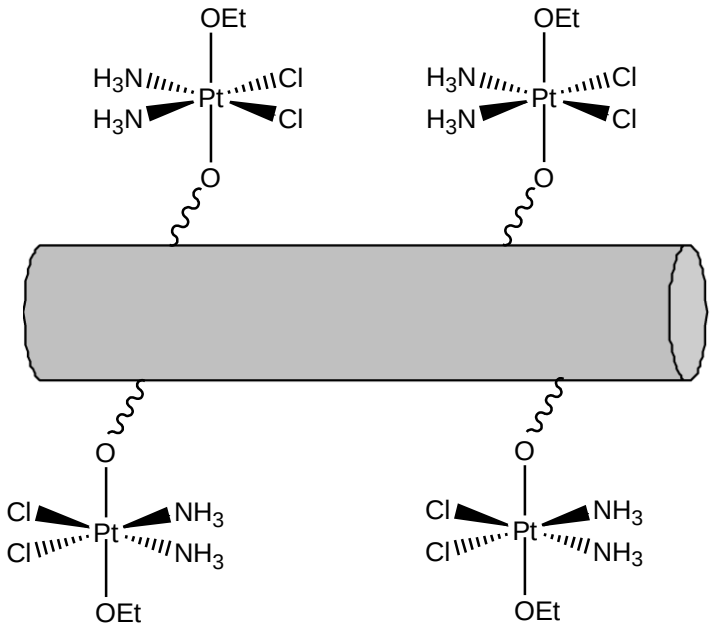

Figure 1.14. SWNTs-Pt(IV) tethered conjugated.

Platinum (II) conjugates of SWNTs have been synthesised as well[102]. These conjugates have been targeted with an epithelial growing factor (EGF) towards its receptor (EGFR). The studies showed that the constructs entered the cell through EGFR directed endocytosis, as proven by the lack of uptake when EGF was not attached or the EGFR was knocked out. This uptake was observed in both *in vivo* and *in vitro* systems and the SWNTs were detected close to the nuclei. Increases in the cytotoxicity compared with cisplatin and the untargeted Pt-SWNTs were observed, proving that activity was EGFR directed. Similar results were obtained for tumour growth in mice, with lower growth and higher accumulation observed in the tumour when targeted. No data about the way the platinum moiety is released have been provided but nevertheless this was the first example of selective tumour targeting of SWNTs *in vivo*.

1.3.4 Liposomes and nanocapsules

The use of liposomes as delivery vectors involves the inclusion of the drug inside a lipidic bilayer biodegradable particle. It is especially useful if low solubility and poor stability are an issue and the liposomes have the advantage that they can be targeted by the EPR effect[96]. Formulations of cisplatin in liposomes failed initially, with only low amounts of the drug encapsulated due to its low lipophilicity[145]. These liposomes had a low cisplatin to lipid ratio, and showed low DNA platination and activity[146]. Two different strategies have been used to improve the encapsulation ratio. The first was the use of lipophilic derivatives of cisplatin that would help the increase of complex inside the bilayer. An example of this is Aroplatin, a formulation of a mixture of at least 18 compounds with different length chain alkyl ammines that recently have reported positive results from phase II trials[147]. A second attempt modified the composition of the liposome itself (using mixtures of dipalmitoyl phosphatidyl glycerol, soy phosphatidyl choline, cholesterol, and methoxy-polyethyleneglycol-distearoyl phosphatidylethanolamine) obtaining high encapsulation efficacy[148]. Lipoplatin, as the formulation between this lipidic mixture and cisplatin is called, is expected to enter phase III of clinical trials and formulations with carboplatin are ready to start clinical trials[96].

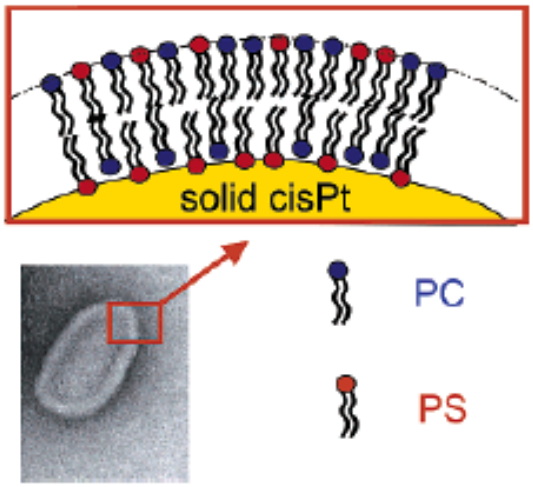

Figure 1.15. Example of molecular organization of cisplatin nanocapsules taken from Chupin et al[150].

A new technique for the introduction of cisplatin in liposomes has also been developed, providing interesting results[149]. Following a procedure of hydratation, thaw freezing and centrifugation, bean shape particles with a lipidic bilayer were created (Fig. 1.15). These particles increased the drug to lipid ratio by two or three orders of

magnitude compared with previous examples, and activity against ovarian cell lines were up to thousand fold better compared with cisplatin. Inside these nanocapsules, solid particles without water were detected. In principle it was thought that these particles were created by solid cisplatin covered by positively charged aquated species that would attract the negatively charged lipids. However, further studies showed that, while 90% of the particles were formed by precipitated cisplatin, the remaining 10% was formed by chlorobridged cisplatin molecules[150]. Increase of toxicity was thought to be due to protection from inactivation and increase uptake compared with normal cisplatin.

The possibility of using the same technique with different drugs has been proven and lanthanides and different platinum based complexes have been introduced[149]. The results with carboplatin in particular were interesting[151]. Encapsulation strongly improved its cytotoxicity towards a panel of human cancer cell lines, showing IC_{50}s up to three orders of magnitude lower than those of the free drug. When uptake was studied, similar results were found for cells treated with solutions of 20 nM of the nanocapsules and 1 μM of the free platinum drug. This improved uptake did not however explain all the increase in cytotoxicity, indicating that the increased activity was not due solely to improved uptake by cells.

1.3.5 Nanoparticles

The use of polymeric nanoparticles as sequential release vector for antitumour drugs is a well established method[152-154]. It allows protection of the loaded compound from the exterior environment, increasing the blood circulation time of the active dose before reaching its target. This not only protects the drug from body fluids, but the body will also be isolated from undesired chemical consequences of the drug, allowing minimisation of dose-dependent side effects. Encapsulation of cisplatin in nanoparticles presents a challenge because of its physico-chemical properties. Cisplatin is insoluble in organic solvents, and partially soluble in water. Only low loading ratios of cisplatin are achieved[154] within the hydrophobic interiors of such polymer nanoparticles and the partial solubility makes difficult to obtain cisplatin polymer nanoparticle systems that maintain the adequate concentration for long time periods[156]. Tests have shown accumulation in unwanted (non-target) organs[157] and low cytotoxicity compared with the free drug[158]. A strategy to incorporate platinum (IV) units with coordinated groups

that increase their hydrophobicity and organic solubility has been recently explored (Fig. 1.16A)[103]. This increased the internalisation of the platinum moiety in the nanoparticle, arriving at a maximum loading of around 20% of the provided drug. Controlled release of the complex was achieved for a period of 60 hours, releasing the unmodified loaded compound. Nanoparticles loaded with this complex showed IC_{50} values one order of magnitude lower than the parent compound and presenting better activity than cisplatin.

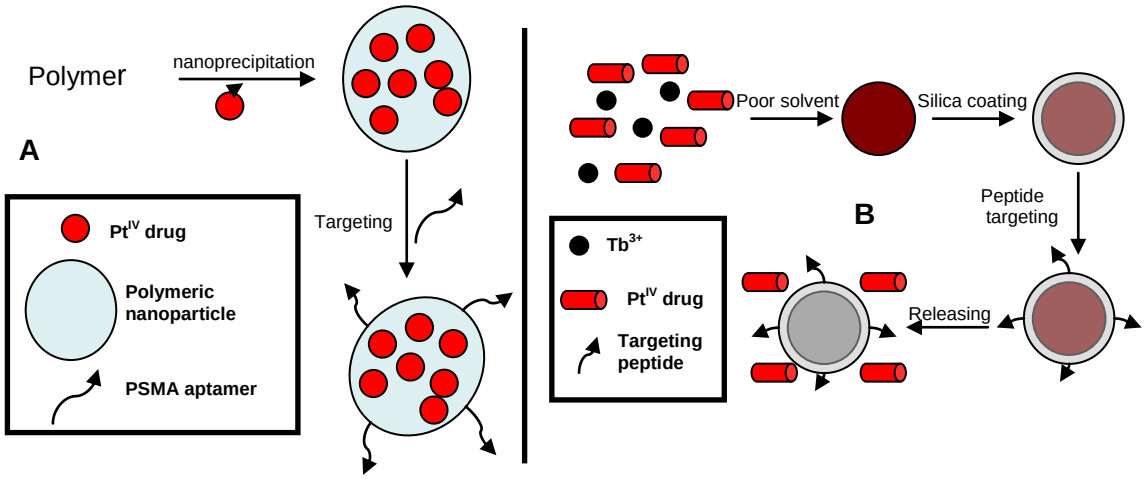

Figure 1.16. Synthesis of encapsulated Pt (IV) nanoparticles (A, Dhar et al[103]) and Pt(IV)/Tb^{3+} nanoparticles (B, Rieter et al[104]).

The particles could be targeted towards prostate cancer by conjugation of the prostate specific membrane antigen aptamer (PSMA) and this did not modify the loading or releasing pattern of the platinum agent. Cytotoxicity in PSMA- cell lines was not affected by the targeting, but a four fold increase of toxicity in PSMA+ cell lines were as observed, yielding overall toxicities around 80 times better than the parent prodrug. This selectivity towards PSMA + cell lines was produced by a receptor mediated endocytosis that allowed the introduction of the targeted nanoparticles in times as short as 2 hours and gave rise to 1,2 GpG intrastrand crosslinks in those cells after 12 hours.

A different way to circumvent the identified problems has been explored by Rieter et all (Fig. 1.16B)[104]. Instead of using polymeric nanoparticles with a hydrophobic interior, they formed the nanoparticle from precipitation of the same platinum moiety. Nanoparticles of platinum (IV) and Tb^{3+} ions were precipitated, giving a 2-3 Tb^{3+}-Pt (IV) ratio. These systems released half of the payload drug in times as short as 1 hour. However, if they were coated with amorphous silica shells, this half-release time was

increased to 5.5 or 9 hours, depending of the size of the coating (2 nm or 7 nm respectively). Cytotoxicity was similar to cisplatin for breast cancer, but the compound was inactive against integrin expressing colon carcinomas. Upon conjugation of peptides with high binding affinity towards integrin the toxicity was increased in the colon cancers to slightly better activity than cisplatin.

Non-platinum metallodrugs had also been targeted using the same techniques. Organometallic ferrocenyl tamoxifen derivatives were loaded into polymeric nanoparticles with the aim of increase their bioavailability and to reduce the removal from the physiological medium[158]. Cell results showed that loaded compounds retained their ability to stop the ER mediated transcription. However, encapsulation of the compounds increased the number of apoptotic cells observed compared with the free complexes. Similar strategies have also been used for the delivery of MRI and fluorescent imaging agents[160].

1.3.6 Biomolecules

The previous examples for protection and release are based on systems with non-physiological carriers. Recently, a strategy which uses proteins with internal cavities as delivery vectors has been developed. It is based in the use of apoferritin, the unloaded state of the natural iron (II) storage protein Ferritin[161]. It presents an inner cage formed by the assembly of its 24 protein subunits that leave 8 hydrophilic channels. Ferritin can be internalized by some tumour tissues through endocytosis directed by membrane-specific receptors[162-163]. Gadolinium III[164], metal ions[165] or nanoparticles of iron salts[166] have been internalised in the apoferritin cavity, and this strategy has been used to deliver anticancer drugs to the brain[167]. In order to introduce a platinum drug inside the protein cage two procedures were used (Fig. 1.17)[168]. In the first one, molecules of cisplatin or carboplatin were added in solution together with apoferritin. The pH was dropped to 2 in order to dissociate the protein, opening the cage. The process was then reversed to make the apoferritine associate again entrapping the drugs. Both cisplatin and carboplatin were succesfully internalized, although only low amounts of them were included: only 2 molecules of cisplatin or 3 of carboplatin per ferritin

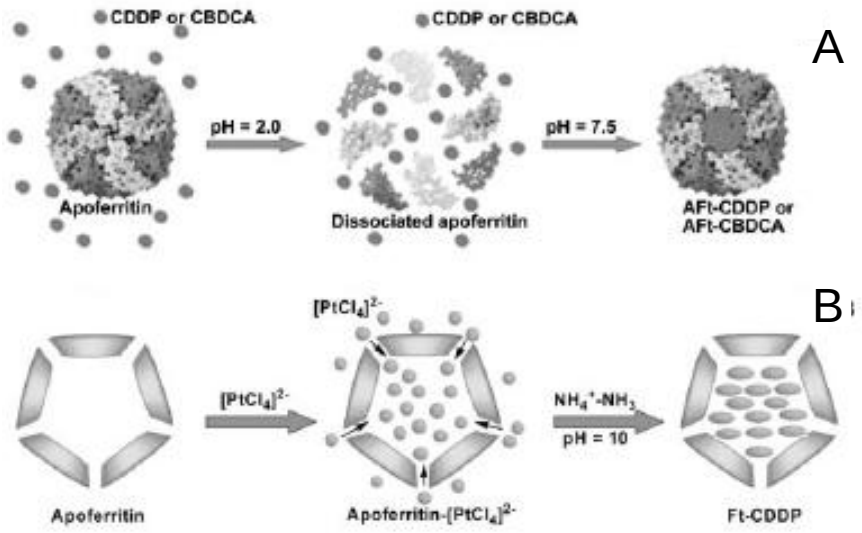

Figure 1.17. Cisplatin or carboplatin loaded apoferritin through unfolding-refolding method (A) or *in situ* generation method (B). Taken from Yang et al[168].

In the second method apoferritin in its natural conformation was treated with anionic $[PtCl_4]^{2-}$ salts (K_2PtCl_4). Being negatively charged, these platinum molecules entered into the internal cavity. The mixture was then treated with ammonium groups forming neutral diammonium dichloride platinum (II) complexes. Thirty such compounds were detected per cavity, a big increase compared with the 2 or 3 internalized molecules in the first method. This is significant even if only 15 of them correspond to cisplatin (mixed with transplatin). Preliminary studies against rat cell lines showed that both systems presented increased toxic abilities compared with the apoferritin control. Proteins loaded following the second procedure showed higher toxicity than the ones loaded under the first procedure. No comparison with cisplatin or carboplatin was presented since no data about release of the payload was available.

1.3.7 Small molecular carriers

Encapsulation, as seen previously, is commonly used by many of the delivery systems, and often involves several drug molecules in a single delivery unit[142, 149, 103, 168]. Lately a new strategy for encapsulation has been developed, including a single drug molecule in each delivery device. Platinum molecules were encapsulated in macrocycles with the intention of delivery into cell lines first in 2004[169]. A dinuclear platinum molecule was included in a cucurbi[7]til macrocycle without showing any significant effect in the cytotoxicity. Cucurbit[n]urils are small barrel shaped macrocycles with an internal hydrophobic cavity and hydrophilic exterior and can host

different molecules[170]. Later studies showed that they could also be used as delivery vectors for a wide range of platinum compounds (Fig. 1.18), showing mixed effects depending on the compound[171]. The size of the cavity and the binding affinity was important on the cytoxicity. In oxaliplatin-derived intercalators, small changes of macrocycle size could decrease activity or give small improvements (up to 2.5 fold)[172]. Unfortunately binding affinity could not be measured, making impossible to fully understand the interactions between macrocycles and drugs.

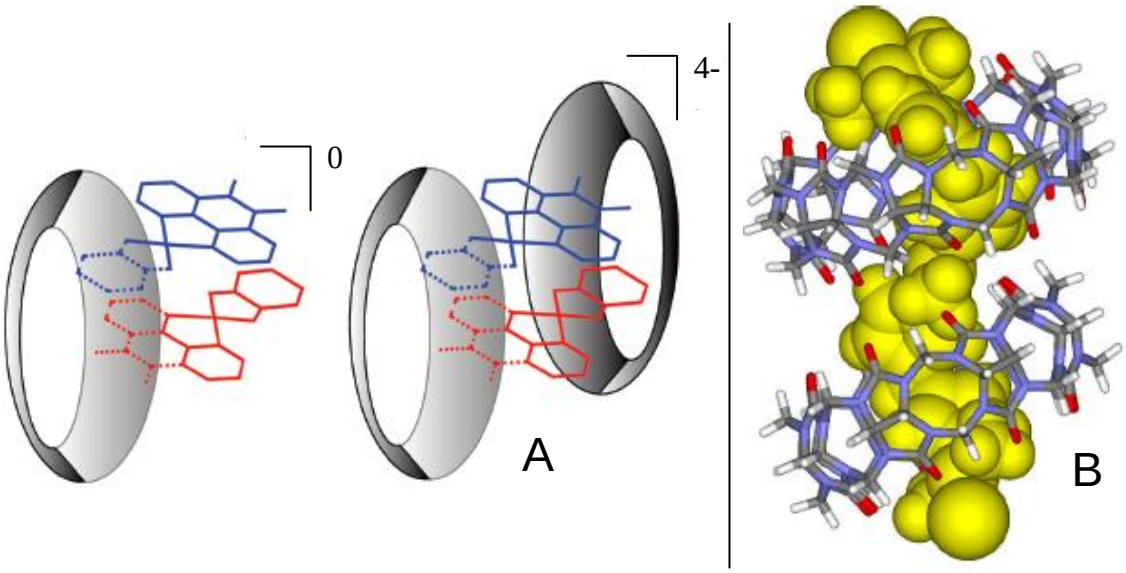

Figure 1.18. Representation of oxaliplatin derivatives intercalators encapsulated in calyx(4)arene macrocycles (A, taken from Benghuzzi et al[131]) and molecular representation of triplatin encapsulated in two cucurbit[8]uril macrocycles (B, taken from Wheathe et al[171]).

The decrease in the activity seen for some of the compounds could be a result of the protective effects that the macrocycles have on their encapsulated molecules. The reaction ratio with mononucleotides decreased upon encapsulation, and the number of DNA-Pt adducts also decreased[171]. On the other hand, glutathione deactivation was drastically reduced, showing that encapsulation could protect these molecules from intracellular degradation[173]. Finally when the complexes were tested in mice, data showed the tolerated dose doubled compared with non-macrocycle treated drugs[171].

The same technique has been used with different macrocycles such as calyx(4)arenes (Fig. 1.18A) and β-cyclodextrins[174]. When the oxaliplatin-derived intercalators used before were encapsulated in these macrocycles they increased their stability to glutathione three fold. Cytotoxicity (as also seen with cucurbit[n]uril) was not modified.

These macrocycles could find use as delivery vectors especially against cisplatin resistant cell lines with increased expression of Glutathione.

1.3.8 Polymers

The previous examples mainly deal encapsulation of the drug inside the carrier[142, 149, 103, 168, 171]. Another approach is to use polymeric molecules that bind covalently to the platinum instead of encapsulating it[175]. This is an alternative way to protect the complexes from degradation, giving as well the opportunity for a chemically controlled release. As a polymeric system, accumulation at cancer cells is expected by the EPR effect. There are various ways to interpret this basic design, the most important being the Platinum-Polymer complexes, the Platinum-Dendrimer complexes and the Micellar-Platinum systems[175].

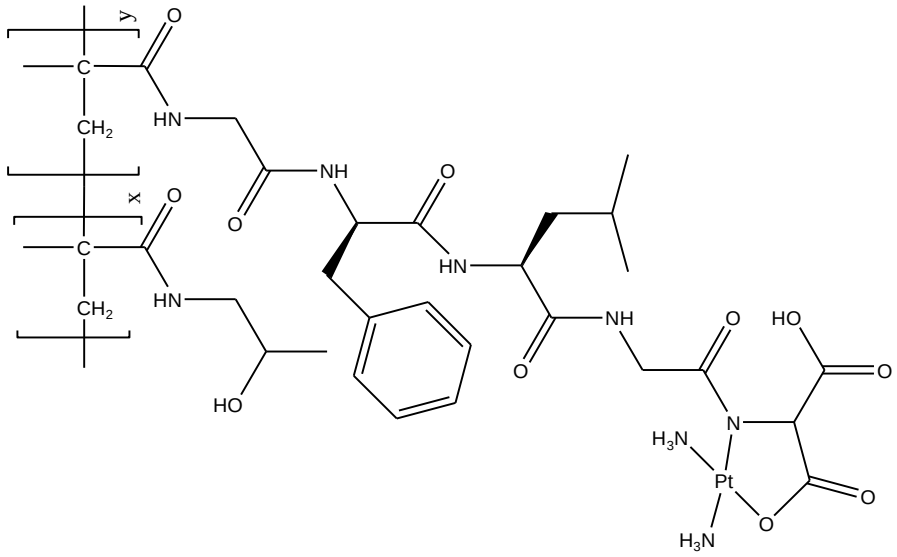

Figure 1.19. Structure of platinum-polymer AP5280.

The first and maybe the most simple of these are the Platinum-Polymer complexes. Different polymers can be used, from poly(aminoacids) to more complicated poly(amidoamine) (PAMAM) or poly (N-(2-hydroxypropyl)-methacrylamide) (PHPMA) polymers. They allow the presence of linking groups that can be cleavaged under desired conditions, providing a certain level of specificity[175]. Different examples are described in the literature, but by far the most successful are the ones using PHPMA[176]. Two of such complexes, AP5280[177] and AP5346[178], are in clinical trials. Both contain pH sensitive peptide side chains where the platinum molecule would bind and a molecule of cisplatin or oxaliplatin respectively bound to it. AP5280 (Fig. 1.19)

entered phase I trials but presented dose limiting side effects of vomiting and nausea[177]. AP5346 on the other hand advanced through phase I. A phase II study in patients with recurrent ovarian cancer has recently been completed under the commercial name of Prolindac[TM. 179].

Dendrimers are highly branched polymers with multiple end groups. Examples like PAMAM are commercially available and have been studied as delivery vectors for several drugs[180]. PAMAM with carboxylic end groups showed high platinum loading, but as well the possibility of formation of crosslinks[181]. PAMAM dendrimers have high plasma stability, and are expected to accumulate in the tumours by the EPR effect. Low release of the platinum payloads in plasma-like conditions was observed, with less than 1% of the charge released in 72 hours. However, these compounds present between 250 and 550 times less systemic toxicities compared with cisplatin, with activities that reduced by 40% the mass of the tumours[181].

Micellar systems are aggregates of surfactant molecules in solution, formed above the critical micelle concentration. They are generally used to increase the aqueous solubility of hydrophobic complexes[182]. As described in 1.3 the main problem to use such formulations with platinum drugs is their intrinsic hydrophobic/hydrophilic properties[167]. This has been addressed by the use of diblock polymers that could bind to cisplatin and then self assemble into micellar structures. As for previous examples of polymers, the payload liberation was dependent of the concentration of ionic chloride. Several examples show high tumour accumulation and similar or slightly improved cytotoxic properties compared with cisplatin. In addition some present lower nephrotoxicity than the parent drug[183].

1.4 Final Remarks

As we have seen delivery vectors can have a big impact on the effects of drug release or targeting. Some of them can increase cellular uptake, increasing the activity, protect the compounds against extra and intracellular deactivation, or help to overcome resistance. Some can localize drugs in selected tumours through the EPR effect, through physiological properties or through targeting to specific biomolecules. They can also increase the circulation time of the drug in the blood or control the release of the drugs

allowing longer times of treatment and lower side effects due to the low concentrations. Together this body of work represents an extremely exciting way to overcome known metallodrug problems, allowing better administration strategies and decreasing the unwanted secondary effects. However, the focus has been only at a small subset of known active metallo-drug designs (principally cisplatin and derivatives). Non-conventional metallodrugs are also an important tool to overcome some of the drawbacks presented by cisplatin, mainly because of the different actions at the molecular level. The combination of these delivery strategies with interesting non-platinum or non-conventional complexes could lead to new and successful strategies in the fight against cancer.

Three different points will be addressed in this thesis. First we will study how the introduction of a delivery vector through covalent modification can affect the activity and behaviour of the metallodrug in the cell. To do this, previously synthesised active non-conventional estradiol- and testosterone-functionalized platinum(II) monofunctional complexes (targeting oestrogen or androgen receptors) will be compared with the equivalent inactive non-steroidal complexes. In order to know where the activity of such complexes came from, toxicity of the free steroidal ligands and effect of addition of free steroids to non-steroidal complexes will be studied. Cellular uptake, DNA interaction and protein interaction will be studied as well, to see how the presence of the steroid can alter their cellular and macromolecular binding behaviour. Finally we will explore possible synthetic routes that could allow the standardization of the coupling of steroids to existent metallodrugs.

In the second chapter the coupling of these steroidal delivery vectors to non-covalent metallodrugs will be explored. New non-conventional metallo-intercalators will be designed and synthesised from well known and simply synthesised metallodrugs and commercially available steroids. We will study their anticancer activity, testing them against different cancers with different steroidal dependence and comparing them with both steroidal and non-steroidal control complexes. Again, the cellular uptake and interaction with macromolecules (especially with DNA) of these new complexes will be studied, searching for a possible explanation for the origin of their cellular behaviour. This should allow us to compare the results of the coupling of a steroidal delivery vector in the behaviour of covalent and non-covalent DNA metallo-binders.

Finally in the third and last chapter we will investigate the anticancer activity of supramolecular dimetallic cylinders previously synthesised in our laboratory. These agents present the interesting ability to bind to the DNA in the major groove or in the internal cavity of a three way junction, and preliminary experiments show certain anticancer activity in levels close to carboplatin. Studies of the dependence of this activity to the structure of the cylinders (using complexes with small and big structural modification and with different metals inside the structure) and cellular distribution will be undertaken; to know if they can reach the nuclei and interact with the genomic DNA, possible target of their activity.

1.5 References

1 M. J. Hannon, *Chem. Soc. Rev.*, 2007, **36**, 280.

2 A. Oleksy, A.G. Blanco, R. Boer, I. Usón, J. Aymami, A. Rodger, M.J. Hannon and M. Coll, *Angew. Chem., Intl. Ed.*, 2006, **45**, 1227.

3 S. Komeda, T. Moulaei, K. K. Woods, M. Chimuka, N. P. Farrell, L. D. Williams, *J. Am. Chem. Soc*., 2006, **128**, 16092.

4 D. Jantz, B. T. Amann, G. J. Gatto, J. M. Berg, *Chem. Rev.*, 2004, **104**, 789.

5 T. Da Ros, G. spalluto, M. Prato, T. Saison-Behmoaras, A. Boutorine, B. Cacciari, *Curr. Med. Chem.*, 2005, **12**, 71.

6 N. T. Thuong, C. Helene, *Angew. Chem. Int. Ed. Engl.*, 1993, **32**, 666.

7 D. Praseuth, A. L. Guieysse, C. Helene, *Biochim. Biophys. Acta-Gene Struct. Express.*, 1999, **1489**, 181.

8 P. E. Nielsen, *Curr. Med. Chem.*, 2001, **8**, 545.

9 L. Betts, J. A. Josey, J. M. Veal, S. R. Jordan, *Science*, 1995, **270**, 1838.

10 P. B. Dervan, *Bioorg. Med. Chem.*, 2001, **9**, 2215.

11 L. S. Lerner, *J. Mol. Biol.*, 1961, **3**, 18.

12 D. M. Crothers, *Biopolymers*, 1968, **6**, 575.

13 J. C. Peberdy, J. Malina, S. Khalid, M. J. Hannon, A. Rodger, *J. Inorg. Biochem.,* 2007, **101**, 1937.

14 R. Martínez, L. Chacón-García, *Curr. Med. Chem.*, 2005, **12**, 127.

15 B. Lippert, Cisplatin, Chemistry and Biochemistry of A Leading Anti-Cancer Drug, Wiley-VCH, Weinheim, 1999.

16 M. Tomasz, *Chemistry and Biology*, 1995, **2**, 575.

17 M. J. Hannon, V. Moreno, M. J. Prieto, E. Molderheim, E. Sletten, I. Meistermann, C. J. Isaac, K. J. Sanders, A. Rodger, *Angew. Chem. Int. Ed.*, 2001, **40**, 879.

18 Z. Guo, P.J. Sadler, *Angew. Chem. Intl. Ed.*, 1999, **38**, 1512.

19 T. Storr, K.H. Thompson, C. Orvig. *Chem. Soc. Rev.*, 2006, **35**, 534.

20 M. Peyrone, *Ann. Chem. Pharm*., 1844, **51**, 1.

21 B. Rosenberg, L. Van Camp, T. Krigas, *Nature*, 1965, **205**, 698.

22 B. Rosenberg, L. Van Camp, E. B. Grimley, A. J. Thompson, *J. Biol. Chem.*, 1967, **242**, 1347.

23 M.J. Hannon, *Pure and Applied Chemistry*, 2007, **79**, 2243.

24 P. J. Dyson, G. Sava, *Dalton Trans.*, 2006, 1929.

25 S. J. Banister, L. A. Sternson, A. J. Repta, G. W. James, *Clin. Chem.*, 1977, **23**, 2258.

26 J. L. Aull, R. L. Allen, A. R. Bapat, H. H. Daron, M. E. Friedman, J. F. Wilson, *Biochim. Biophys. Acta*, 1979, **571**, 352.

27 A. I. Ivanov, J. Christodoulou, J. A. Parkinson, K. J. Barnham, A. Tucker, J. Woodrow, P. J. Sadler, *J. Biol. Chem.*, 1998, **273**, 14721.

28 A. Eastman, C*hem-Biol. Interact.*, 1987, **61**, 241.

29 G. Speelmans, R. Staffhorst, K. Versluis, J. Reedijk, B. deKruijff, *Biochemistry*, 1997, **36**, 10545.

30 G. R. Gale, C. R. Morris, L. M. Atkins, A. B. Smith, *Cancer Res.*, 1973, **33**, 813.

31 R. A. Hromas, J. A. North, C. P. Burns, *Cancer Lett.*, 1987, **36**, 197.

32 S. P. Binks, M. Dobrota, *Biochem. Pharmacol.*, 1990, **40**, 1329.

33 S. C. Mann, P. A. Andrews, S. B. Howell, *Cancer Chemoth. Pharm.*, 1990, **25**, 236.

34 L. R. Kelland, P. Mistry, G. Abel, S. Y. Loh, C. F. Oneill, B. A. Murrer, K. R. Harrap, *Cancer Res.*, 1992, **52**, 3857.

35 S. Ishida, J. Lee, D. J. Thiele, I. Herskowitz, *Proc. Natl. Acad. Sci.*, 2002, **99**, 14298.

36 E. R. Jamieson, S. J. Lippard, *Chem. Rev.*, 1999, **99**, 2467.

37 S. E. Miller, D. A. House, *Inorg. Chim. Acta*, 1989, **166**, 189.

38 G. Natile, M. Coluccia, *Coordin. Chem. Rev.*, 2001, **216**, 383.

39 U. M. Ohndorf, M. A. Rould, Q. He, C. O. Pabo and S. J. Lippard, *Nature*, 1999, **399**, 708.

40 A. Eastman, *Biochemistry*, 1986, **25**, 3912.

41 S. F. Bellon, J. H. Colleman, S. J. Lippard, *Biochemistry*, 1991, **30**, 8026.

42 P. M. Takahara, A. C. Rosenzweig, C. A. Frederick, S. J. Lippard., *Nature*, 1995, **377**, 649.

43 J. -S. Hoffmann, D. Locker, G. Villani and M. Leng, *J. Mol. Biol.*, 1997, **270**, 539.

44 L. Li, X. Liu, A. B. Glassman, M. J. Keating, M. Stros, W. Plunkett and L.Y. Yang, *Cancer Res.*, 1997, **57**, 1487.

45 U. Bierbach and N. Farrell, *Inorg. Chem.*, 1997, **36**, 3657.

46 D. P. Bancroft, C. A. Lepre and S. J. Lippard, *J. Am. Chem. Soc.*, 1990, **112**, 6860.

47 O. Rixe, W. Ortuzar, M. Alvarez, R. Parker, E. Reed, K. Paull, T. Fojo, *Biochem. Pharmacol.*, 1996, **52**, 1855.

48 E. Raymond, S. Faivre, S. Chaney, J. Woynarowski, E. Cvitkovic, *Mol. Cancer Ther.*, 2002, **1**, 227.

49 N. Farrell, T. T. B. Ha, J. -P. Souchard, F. L. Wimmer, S. Cros, N.P. Johnson, *J. Med. Chem.*, 1989, **32**, 2240.

50 E. I. Montero, S. Diaz, A. M. Gonzalez-Vadillo, J. M. Perez, C. Alonso, C. Navarro-Ranninger, *J. Med. Chem.*, 1999, **42**, 4264.

51 M. Coluccia, A. Nassi, F. Loseto, A. Boccarelli, M.A. Mariggio , D. Giordano, F. P. Intini, P. A. Caputo, G. Natile, *J. Med. Chem.*, 1993, **36**, 510.

52 N. Farrell, *Met. Ions Biol. Syst.*, 2004, **41**, 252.

53 M. B. Kloster, J. C. Hannis, D. C. Muddiman, N. Farrell, *Biochemistry*, 1999, **38**, 14731.

54 D. Jodrell, T. Evans, W. Steward, D. Cameron, J. Prendiville, C. Aschele, C. Noberasco, M. Lind, J. Carmichael, N. Dobbs, *Eur. J. Cancer*, 2004, **40**, 1872.

55 L. S. Hollis, A. R. Amundsen, E. W. Stern, *J. Med. Chem.*, 1989, **32**, 128.

56 L. S. Hollis, W. I. Sundquist, J. N. Burstyn, W. J. Heiger-Bernays, S. F. Bellon, K. J. Ahmed, A. R. Amundsen, E. W. Stern, S. J. Lippard, *Cancer Res.*, 1991, **51**, 1866.

57 K. S. Lovejoy, R. C. Todd, S. Zhang, M. S. McCormick, J. A. D'Aquino, J. T. Reardon, A. Sancar, K. M. Giacomini, S. J. Lippard, *Proc. Natl. Acad. Sci.*, 2008, **105**, 8902.

58 M. Coluccia, G. Natile, *Anti-Cancer Agents in Medicinal Chemistry*, 2007, **7**, 111.

59 E. S. Ma, W. D. Bates, A. Edmunds, L. R. Kelland, T. Fojo, N. Farrell, *J. Med. Chem.*, 2005, **48**, 5651.

60 Y. Najajreh, Y. Ardeli-Tzaraf, J. Kasparkova, P. Heringova, D. Prilutski, L. Balter, S. Jawbry, E. Khazanov, J. Manuel Perez, Y. Barenholz, V. Brabec, D. Gibson, *J. Med. Chem.*, 2006, **49**, 4674.

61 J. Kasparkova, V. Marini, Y. Najajreh, D. Gibson, V. Brabec, *Biochemistry*, 2003, **42**, 6321.

62 V. Bursova, J. Kasparkova, C. Hofr, V. Brabec, *Biophys. J.*, 2005, **88**, 1207.

63 M. J. Cleare, J. D. Hoeschele, *Bioinorg. Chem.*, 1973, **2**, 187.

64 J. P. Macquet, J. L. Butour, *J. Natl. Cancer Inst.*, 1983, **70**, 899.

65 E. L. M. Lempers, M. J. Bloemink, H, Brouwer, Y, Kidani, J. Reedijk, *J. Inorg. Biochem.*, 1990, **40**, 23.

66 F. Gaucheron, J. M. Malinge, A. J. Blacker, J. M. Lehn, M. Leng, *Proc. Natl. Acad. Sci.*, 1991, **88**, 3516.

67 D. Payet, F. Guacheron, M. Sip, M. Leng, *Nucleic Acid Res.*, 1993, **21**, 5846.

68 Y. Ma, C. S. Day, U. Bierbach, *J. Inorg. Biochem.*, 2005, **99**, 2013.

69 T. Peleg-Shulman, J. Katzhendler, D. Gibson, *J. Inorg. Biochem.*, 2000, **81**, 313.

70 V. X. Jin, S. I. Tan, J. D. Ranford, *Inorg. Chim. Acta*, 2005, **358**, 677.

71 C. Bauer, T. Peleg-Shulman, D. Gibson, A. H.-J. Wang, *Eur. J. Biochem.*, 1998, **256**, 253.

72 N. Farrell, *Platinum-Based Drugs in Cancer Therapy* (Eds.: L. R. Kelland, N. Farrell), Humana Press Inc., Totowa, 2000, 321.

73 V. Brabec, J. Kasparkova, O. Vrana, O. Novakova, J. W. Cox, Y. Qu, N. Farrell, *Biochemistry*, 1999, **38**, 6781.

74 J. Kasparkova, J. Zehnulova, N. Farrell, V. Brabec, *J. Biol. Chem.*, 2002, **277**, 48076.

75 M. D. Hall, H. R. Mellor, R. Callaghan, T. W. Hambley, *J. Med. Chem.*, 2007, **50**, 3403.

76 C. M. Giandomenico, M. J. Abrams, B. A. Murrer, J. F. Vollano, M. I. Rheinheimer, S. B. Wyer, G. E. Bossard and J. D. Higgins III, *Inorg. Chem.* 1995, **34**, 1015.

77 J. L. Carr, M. D. Tingle, M. J. McKeage, *Cancer Chemother. Pharmacol.*, 2006, **57**, 483.

78 H. D. Hall, T. W. Hambley, *Coord. Chem. Re*v., 2002, **232**, 49.

79 C. G. Hartinger, S. Zorbas-Selfried, M. A. Jakupee, B. Kynast, H. Zorbas, B. K. Keppler, *J. Inorg. Biochem.*, 2006, **100**, 891.

80 E. Alessio, G. Mestroni, A. Bergamo, G. Sava, *Curr. Topics Med. Chem.*, 2004, **4**, 1525.

81 E. Alessio, G. Mestroni, A. Bergamo, G. Sava, *Met. Ions Biol. Syst.*, 2004, **42**, 323.

82 Y. K. Yan, M. Melchart, A. Habtemariam, P. J. Sadler, *Chem. Commun.*, 2005, 4764.

83 V. Brabec, O. Novakova, *Drug Resist. Updates*, 2006, **9**, 111.

84 O. Novakova, J. Kasparkova, V. Bursova, C. Hofr, M. Vojtiskova, H. Chen, P. J. Sadler, V. Brabec, *Chem. Biol.*, 2005, **12**, 121.

85 W. H. Ang, P. J. Dyson, *Eur. J. Inorg. Chem.*, **2008**, 4003.

86 G. Jaouen, *Bioorganometallics: Biomolecules, Labelling, Medicine*, Wiley VCH, Weinheim **2005**.

87 A. Vessiéres, S. Top, W. Beck, E. Hillard, G. Jaouen, *Dalton Trans.*, 2006, 529.

88 C. Boit, *Curr. Med. Chem. Anti-Infect. Agents*, 2004, **3**, 135.

89 M. M. Harding, G. Mokdsi, *Curr. Med. Chem.*, 2000, **7**, 1289.

90 O. Oberschmidt, A. R. Hanauske, C. Pampillon, N. J. Sweeney, K. Strohfeldt, M. Tacke, *Anti-Cancer Drugs*, 2007, **18**, 317.

91 O. R. Allen, L. Croll, A. L. Gott, R. J. Knox, P. C. McGowan, *Organometallics*, 2004, **23**, 288.

92 G. D. Potter, M. C. Baird, M. Chan, S. P. Cole, *Inorg. Chem. Commun.*, 2006, **9**, 1114.

93 A. V. Rudnev, L. S. Foteeva, C. Kowol, R. Berger, M. A. Jakupec, V. B. Arion, A. R. Timerbaev, B. K. Keppler, *J. Inorg. Biochem.*, 2006, **100**, 1819.

94 M. A. Jakupec, B. K. Keppler, *Current Topics Med. Chem.*, 2004, **4**, 1575.

95 C. Branden, J. Tooze, *Introduction to Protein Structure*, Garland Publishing Inc., 1991.

96 M. Galanski, B.K. Keppler, *Anti-Cancer Agents in Medicinal Chemistry*, 2007, **7**, 55.

97 Y. Matsamura, H. Maeda, *Cancer Res.*, 1986, **46**, 6387.

98 S. van Zutphen, J. Reedijk, *Coord. Chem. Rev.*, 2005, **249**, 2845.

99 A. Warnecke, I. Fichtner, d. Garmann, U. Jaehde, F. Kratz, *Bioconjugated Chem.*, 2004, **15**, 1349.

100 W. H. Ang, E. Daldini, L. Juillerat-Jeanneret, P. J. Dyson, *Inorg. Chem.*, 2007, **46**, 9048.

101 S. Dhar, L. Zhuang, J. Thomale, H. Dai, S. J. Lippard, *J. Am. Chem. Soc.*, 2008, **130**, 11467.

102 A. A. Bhirde, V. Patel, J. Gavard, G. Zhang, A. A. Sousa, A. Masedunskas, R. D. Leapman, R. Weigert, J. S. Gutkind, J. F. Rusling, *ACS Nano*, 2009, **3**, 307.

103 S. Dhar, F. X. Gu, R. Langer, O. C. Farokhzad, S. J. Lippard, *Proc. Natl. Acad. Sci.*, 2008, **105**, 17356.

104 W. J. Rieter, K. M. Pott, K. M. L. Taylor, W. Lin, *J. Am. Chem. Soc.*, 2008, **130**, 11584.

105 A. Jackson, J. Davis, R. J. Pither, A. Rodger, M. J. Hannon, *Inorg. Chem.*, 2001, **40**, 3964.

106 S. Top, E.B. Kaloun, A. Vessieres, G. Leclercq, I. Laios, M. Ourevitch, C. Deuschel, M.J. McGlinchey, G. Jaouen, *ChemBioChem.*, 2003, **4**, 754.

107 O. Aronov, A. T. Horowitz, A. Gabizon, D. Gibson, *Bioconjugate Chem.*, 2003, **14**, 563.

108 J. Sudimack, R. J. Lee, *Adv. Drug Deliv. Rev.*, 2000, **41**, 147.

109 D. Jaramillo, N. J. Wheate, S. F. Ralph, W. A. Howard, Yi. Tor, J. R. Aldrich-Wright, *Inorg. Chem.*, 2005, **45**, 6004.

110 N. J. Wheate, R. I. Taleb, A. M. Krause-Heuer, R. L. Cook, S. Wang, V. J. Higgins, J. R. Aldrich-Wright, *Dalton Trans.*, **2007**, 5055.

111 H. H. Lee, B. D. Palmer, B. C. Baguley, M. Chin, W. D. McFadyen, G. Wickham, D. Thorsbournepalmer, L. P. G. Wakelin, W. A. Denny, *J. Med. Chem.*, 1992, **35**, 2983.

112 J. R. Choudhury, R. Guddneppanavar, G. Saluta, G. L. Kucera, U. Bierbach, *J. Med. Chem.*, 2008, **51**, 3069.

113 S. Kemp, N. J. Wheate, D. P. Buck, M. Nikac, J. G. Collins, J. R. Aldrich-Wright, *J. Inorg. Biochem.*, 2007, **101**, 1049.

114 B. A. J. Jansen, P. Wielaard, G. V. Kalayda, M. Ferrari, C, Molenaar, H. J. Tanke, J. Brouwer, J. Reedijk, *J. Biol. Inorg. Chem.*, 2004, **9**, 403.

115 P. Marques-Gallego, H. den Dulk, J. Brouwer, H. Kooijman, A. L. Spek, O. Roubeau, S. J. Teat, J. Reedijk, *Inorg. Chem.*, 2008, **47**, 11171.

116 H. Choy, C. Park, M. Yao, *Clin .Cancer Res.*, 2008, **14**, 1633.

117 P. J. Bednarski, F. S. Mackay, P. J. Sadler, *Anti-Cancer Agents in Medicinal Chemistry*, 2007, **7**, 75.

118 A. Lebugle, A. Rodrigues, P. Bonnevialle, J. J. Voigt, P. Canal, F. Rodriguez , *Biomaterials*, 2002, **23**, 3517.

119 A. Uchida, Y. Shinto, N. Araki, K. Ono, *J. Orthop. Res.*, 1992, **10**, 440.

120 N. Margiotta, R. Ostuni, D. Teoli, M. Morpurgo, N. Realdon, B. Palazzo, G. Natile, *Dalton Trans.*, 2007, 3131.

121 G. Palumbo, L. Avigliano, G. Strukul, F. Pinna, D. Del Principe, I. D'Angelo, M. Annicchiarico-Petruzzelli, B. Locardi, N. Rosato, *J. Mater. Sci.*, 1997, **8**, 417.

122 Y. Tahara, Y. Ishii, *J. Orthop. Sci.*, 2001, **6**, 556.

123 S. Miura, Y.Mii, Y. Miyauchi, H. Ohgushi, T. Morishita, K. Hohnoki, M. Aoki, S. Tamai, Y. Konishi, *Jpn. J. Clin. Oncol.*, 1995, **25**, 61.

124 A. Barroug, M. J. Glimcher, *J. Orthop. Res.*, 2002, **20**, 274.

125 C. Rey, H.-M. Kim, L. Gerstenfeld, M. J. Glimcher, *J. Bone. Miner. Res.*, 1995, **10**, 1577.

126 H. A. Benghuzzi, B. G. England, P. R. Bajpai, *Biomed. Sci. Instrum.*, 1992, **28**, 129.

127 P. K. Bajpai, H. A. Benghuzzi, *J. Biomed. Mater. Res.*, 1988, **22**, 1245.

128 J. Guicheux, G. Grimandi, M. Trecant, A. Faivre, S. Takahashi, G. Daculsi, *J. Biomed. Mater. Res.*, 1997, **34**, 165.

129 M. Itokazu, T. Sugiyama, T. Ohno, E. Eada, Y. Katagiri, *J. Biomed. Mater. Res.*, 1998, **39**, 536.

130 L. Ahrams, P. K. Bajpai, *Biomed. Sci. Instrum.*, 1993, **30**, 169.

131 H. A. Benghuzzi, R. M. Barbaro, P. K. Bajpai, *Biomed. Sci. Instrum.*, 1990, **26**, 151.

132 C. Hamanishi, K. Kitamoto, S. Tanaka, M. Otusuka, Y. Doi, T. Kitahashi, *J. Biomed. Mater. Res.*, 1996, **33**, 139.

133 A. Barroug, E. Lernous, J. Lemaitre, P. G. Rouxhet, *J. Colloid. Interf. Sci.*, 1998, **208**, 147.

134 V. C. Honnorat-Benabbou, A. Lebugle, B. Sallek, D. Lagarrigue, *J. Mater. Sci.*, 2001, **12**, 107.

135 A. Barroug, L. T. Kuhn, L. C. Gerstenfeld, M. J. Glimcher, *J. Orthop. Res*., 2004, ***22***, 703.

136 B. Palazzo, M. Iafisco, M. Laforgia, N. Margiotta, G. Natile, C. L. Bianchi , D. Walsh, S. Mann, N. Roveri, *Adv. Funct. Mater.*, 2007, **17**, 2180.

137 S. Iijima, *Nature*, 1991, **354**, 56.

138 N. W. S. Kam, T. C. Jessop, P. A. Wender, H. Dai, *J. Am. Chem. Soc.*, 2004, **126**, 6850.

139 N. W. S. Kam, Z. Liu, H. Dai, *J. Am. Chem. Soc.*, 2005, **127**, 12492.

140 Z. Liu, W. Cai, L. He, N. Nakayama, K. Chen, X. Sun, X. Chen, H. Dai, *Nat. Nanotechnol.*, 2007, **2**, 47.

141 K. Ajima, M. Yudasaka, T. Murakami, A. Maigne, K. Shiba, S. Iijima, *Mol. Pharm.*, 2005, **2**, 475.

142 K. Ajima, T. Murakami, Y. Mizoguchi, K. Tsuchida, T. Ichihashi, S. Iijima, M. Yudasaka, *ACS Nano*, 2008, **2**, 2057.

143 M. Zhang, T. Murakami, K. Ajima, K. Tsuchida, A. S. D. Sandanayaka, O. Ito, S. Iijima, M. Yudasaka, *Proc. Natl. Acad. Sci.*, 2008, **105**, 14733.

144 R. P. Feazell, N. Nakayama-Ratchford, H. Dai, S. J. Lippard, *J. Am. Chem. Soc.*, 2007, **129**, 8438.

145 M. S. Newman, G. T. Colbern, P. K. Working, C. Engbers, M. A. Amantea, *Cancer Chemother. Pharmacol.*, 1999, **43**, 1.

146 J. M. Meerum Terwogt, G. Groenewegen, D. Pluim, M. Maliepaard, M. M. Tibben, A. Huisman, W. W. ten Bokkel Huinink, M. Schot, H. Welbank, E. E. Voest, J. H. Beijnen, J. H. M. Schellens, *Cancer Chemother. Pharmacol.*, 2002, **49**, 201.

147 C. Lu, R. Perez-Soler, B. Piperdi, G. L. Walsh, S. G. Swisher, W. R. Smythe, H. J. Shin, Y. J. Ro, L. Feng, M. Truong, A. Yalamanchili, G. Lopez-Berestein, W. K. Hong, A. R. Khokhar, D. M. Shin, *J. Clin. Oncol.*, 2005, **23**, 3495.

148 G. P. Stathopoulos, T. Boulikas, M. Vougiouka, G. Deliconstantinos, S. Rigatos, E. Darli, V. Viliotoy, J. G. Stathopoulos, *Oncology Rep.*, 2005, **13**, 589.

149 K. N. Burger R. W. Staffhorst, H. C. de Vijlder,M. J. Velinova, P. H. Bomans, P. M. Frederik, B. de Kruijff, *Nat. Med.*, 2002, **8**, 81.

150 V. Chupin, A. I. de Kroon, B. de Kruijff, *J. Am. Chem. Soc.*, 2004, **126**, 13816.

151 I. H. L. Hamelers, E. van Loenen, R. W. H. M. Staffhorst, B. de Kruijff, A. I. P. M. de Kroon, *Mol. Cancer. Ther.*, 2006, **5**, 2007.

152 M. Ferrari, *Nat. Rev. Cancer*, 2005, **5**, 161.

153 L. Zhang, F. X. Gu, J. M. Chan, A. Z. Wang, R. S. Langer, O. C. Farokhzad, *Clin. Pharmacol. Ther.*, 2007, **83**, 761.

154 D. Peer, J. M. Karp, S. Hong, O. C. Farokhzad, M. Rimona, R. Langer, *Nat. Nanotechnol.*, 2007, **2**,751.

155 K. Avgoustakisa , A. Beletsia, Z. Panagia, P. Klepetsanisa, A. G. Karydasb, D. S. Ithakissios, *J. Controlled Release*, 2002, **79**,123.

156 J. Fujiyama , Y. Nakase, K. Osaki, C. Sakakura, H. Yamagishi , A Hagiwara, *J. Controlled Release* , 2003, **89**, 397.

157 S. Stolnik, C. R. Heald, J. Neal, M. C. Garnett, S. S. Davis, L. Illum, S. C. Purkis, R. J. Barlow, P. R. Gellert, *J. Drug Targeting*, 2001, **9**, 361.

158 D. Moreno, C. Tros de Ilarduya, E. Bandres, M. Bunuales, M. Azcona, J. Garcia-Foncillas, M. J. Garrido, *Eur. J. Pharm. Biopharm.*, 2008, **68**, 503.

159 A. Nguyen, V. Marsaud, C. Bouclier, S. Top, A. Vessieres, P. Pigeon, R. Gref, P. Legrand, G. Jaouen, J.-M. Renoir, *Int. J. Pharm.*, 2008, **347**, 128.

160 W. J. M. Mulder, G. J. Strijkers, G. A. F. van Tilborg, A. W. Griffioen, K. Nicolay, *NMR Biomed.*, 2006, **19**, 142.

161 J. M. Dominguez-Vera, *J. Inorg. Biochem.*, 2004, **98**, 469.

162 S. Fargion, P. Arosio, A. L. Fracanzoni, V. Cislaghi, S. Levi, A. Cozzi, A. Piperno, A. G. Firelli, *Blood*, 1988, **71**, 753..

163 P. C. Adams, L. W. Powell, J. W. Halliday, *Hepatology*, 1988, **8**, 719.

164 S. Aime, L. Frullano, S. G. Crich, *Angew. Chem. Int. Ed.*, 2002, **41**, 1017.

165 T. Ueno, M. Suzuki, T. Goto, T. Matsumoto, K. Nagayama, Y. Watanabe, *Angew. Chem. Int. Ed.*, 2004, **43**, 2527.

166 J. Polanams, A. D. Ray, R. K. Watt, *Inorg. Chem.*, 2005, **44**, 3203.

167 S. W. Hulet, S. Powers, J. R. Connor, *J. Neurol. Sci.*, 1999, **165**, 48.

168 Z. Yang, X. Wang, H. Diao, J. Zhang, H. Li, H. Sung, Z. Guo, *Chem. Commun.*, **2007**, 3453.

169 N. J. Wheate, A. I. Day, R. J. Blanch, A. P. Arnold, C. Cullinane, J. G. Collins, *Chem. Commun.*, **2004** , 1424.

170 J. Lagona, P. Mukhopadhyay, S. Chakrabarti, L. Isaacs, *Angew. Chem. Int. Ed.*, 2005, **44**, 4844.

171 N. J. Wheathe, *J. Inorg. Biochem.*, 2008, **102**, 2060.

172 S. Kemp, N. J. Wheate, S. Wang, J. G. Collins, S. F. Ralph, A. I. Day, V. J. Higgins, J. R. Aldrich-Wright, *J. Biol. Inorg. Chem.*, 2007, **12**, 969.

173 S. Kemp, N. J. Wheate, M. P. Pisani, J. R. Aldrich-Wright, *J. Med. Chem.*, 2008, **51**, 2787.

174 A. M. Krause-Heuer, N. J. Wheate, M. J. Tilby, D. G. Pearson, C. J. Ottley, J. R. Aldrich-Wright, *Inorg. Chem.*, 2008, **47**, 6880.

175 K. J. Haxton, H. M. Burt, *J. Pharm. Sci.*, in press, DOI: 10.1002/jps.21611.

176 E. Gianasi, M. Wasil, E. G. Evagorou, A. Keddle, G. Wilson, R. Duncan, *Eur. J. Cancer*, 1999, **35**, 994.

177 J. M. Rademaker-Lakhai, C. Terret, S. B. Howell, C. M. Baud, R. F. de Boer, D. Pluim, J. H. Beijnen, J. H. M. Schellens, J. P. Droz, *Clin. Cancer Res.*, 2004, **10**, 3386.

178 M. Campone, J. M. Rademaker-Lakhai, J. Bennouna, S. B. Howell, D. P. Nowotnik, J. H. Beijnen, J. H. M. Schellens, *Cancer Chemother. Pharmacol.*, 2007, **60**, 523.

179 For details on ProLindac development see http://www.accesspharma.com or http://www.accesspharma.com/pdf/prolindac%20poster%20214.pdf .

180 D. A. Tomalia, L. A. Reyna, S. Svenson, *Biochem. Soc. Trans.*, 2007, **35**, 61.

181 N. Malik, E. G. Evagorou, R. Duncan, *Anticancer. Drugs*, 1999, **10**, 767.

182 G. Riess, *Prog. Polym. Sci.*, 2003, **28**, 1107.

183 Y. Geng, D. E. Discher, *J. Am. Chem. Soc.*, 2005, **127**,12780.

Chapter 2: Steroidal covalent metallodrugs

2.1 Introduction

Platinum metallo-drugs are among the most effective clinical agents for the treatment of cancer and three such agents (cisplatin, carboplatin and oxaliplatin) are in widespread use. These agents are believed to act by binding to DNA, with the three structurally-related drugs having similar molecular-level actions[1-6]. Clinical challenges include circumventing acquired resistance to cisplatin and widening the spectrum of cancers which can be treated; this requires chemists to explore new metallo-drugs which are distinct from the traditional cisplatin structure and which will have different molecular-level interactions. Other challenges include minimizing the side-effects which arise because of the action of the drugs in other sites in the body and with other bio-molecules such as proteins. More effective targeting of the drugs to specific organs or tumour types is thus desirable, as is maximising the delivery of the cytotoxic agent into the cell and on to the (nuclear) DNA. In the search of a "magic bullet" (a drug that is aimed precisely at a disease site and that would not harm healthy tissues) the use of carriers that would take the drug to the target and release it there has been explored. Ideally, this delivery-vector needs to take the drug into physical contact with its physiological target only in the desired anatomical location of the body. It should be retained at the site of action for a long enough period of time and not be removed from circulation too rapidly[7]. Different bio-molecules have been used in the last years as delivery vectors with varying degree of success[8-10]. Sex hormones such as oestrogens and testosterone are interesting because of their importance in reproductive system cancers[11-13].

Breast cancer is a major cause of cancer death for women in the western world and cisplatin is not useful against it. It is known that 60-75% of breast cancer tumours over-express oestrogen receptors (ER)[14]. For that reason, rhenium and ^{99m}technetium units for imaging have been attached to oestrogen-based ligands[15-16] to enhance delivery, aiming for selective uptake in cells displaying elevated levels of the oestrogen receptor (ER). Steroid mimics have been attempted as well, by replacing part of the steroidal skeleton with rhenium (V), but this type of approach led to unstable complexes[17]. It has been suggested that an organometallic substrate (or any other type of ER targeted complex),

would need to posses a binding affinity of at least 1% relative to oestrogen towards the ER for selective uptake of the substrate into cells to occur[18]. Cytotoxic metallo-drugs have also been conjugated to steroids or synthetic oestrogens (Fig. 2.1). Jaouen et al synthesized a series of organo-metallic ferrocene-functionalized tamoxifens and hydroxy-tamoxifens[19], showing similar activity to tamoxifen in ERα+ cell lines, but increased activity in ERβ+ (compared to tamoxifen). However, when oxaliplatin-like molecules were attached to tamoxifen no effect on the activity of the free synthetic oestrogen was observed[20]. Three-substituted oestrogen-based platinum(II) complexes have been reported as well, showing cytotoxic activity in MCF-7 tumour cells comparable to cisplatin[21-22]. Unfortunately these compounds posses extremely low relative binding affinity (RBA) towards the ER due to removal of the OH in 3 position, which is important for the recognition by the receptor.

Figure 2.1. A. Conjugate of the anti-oestrogen tamoxifen with platinum(II). B. Structure of 3-substituted oestrogen conjugate with potentially cytotoxic platinum(II).

Recently Osella synthesised 17α-substituted oestrogens with bidentate ligands based on ethylenediammine-type chelates (Fig. 2.2 A). Malonate-platinum(II) moeities were coordinated to the ligands to provide better water solubility[23]. Unfortunately stability problems and low RBAs meant they were not suitable for cell tests. In an attempt to solve this problem oestrogens were functionalised with chelates linked through benzyl spacers[24]. The platinum(II) complexes showed an estimated RBA of aproximately 2%. However cell tests in ER+ and hormone independent cell lines did not show growth inhibition at treated concentrations (while cisplatin showed almost 50% growth inhibition). Berube used a different strategy. He synthesised a series of oestrogens coupled to platinum units through the 16 position (Fig. 2.2 B). The resulting complexes showed high cytotoxicity and indeed a higher RBA than estradiol, but they didn't show

any specificity towards ER+ cell lines[25-26]. Lippard has explored steroidal platinum(IV) compounds (Fig. 2.2 C) after discovering oestrogen sensitises cancer cells to platinum(II) cytotoxic agents[27]. In this approach the steroid is released from the metal prior to DNA binding; again these complexes showed high toxicity but not specificity[28]. Non-conventional drugs have been attached as well: Hannon *et al* attached a monofunctional platinum-terpyridine derivative (Fig. 2.2 D), that showed the capacity to bind to DNA and proteins at the same time[29].

Figure 2.2. Recent examples of steroids coordinated to platinum drugs.

2.1.1 Steroid coupled platinum(II) triammines

All these previous examples have three things in common: an active metallodrug has been coupled to the carrier; estradiol or a synthetic oestrogen has been used with the goal of targeting the ER; and a relatively complicated synthesis is required. Previously no steroidal metal complexes have targeted the androgen receptor (AR) with the aim of localising cytotoxic drugs[30]. The androgen receptor (AR) is the predominant sex-steroid nuclear receptor in malignant tissue and found over-expressed in ~80 % of breast[31-33],

74-90 % of ovarian[34-36] and substantially all prostate tumours[37-39]. Recently, colleagues in our group (Martin Huxley and Michael J. Browning) developed a simple procedure to attach non-conventional metallodrugs to steroids[40-42]. Using simple coupling reactions between commercially available steroids and arylhalides estradiol and testosterone derived ligands were created and coordinated to triammine cationic platinum(II) monofunctional centres (Fig. 2.2E, Fig 2.3)[40-41]. This allowed the creation of a small library of steroidal complexes, both estradiol and testosterone, in just two simple steps.

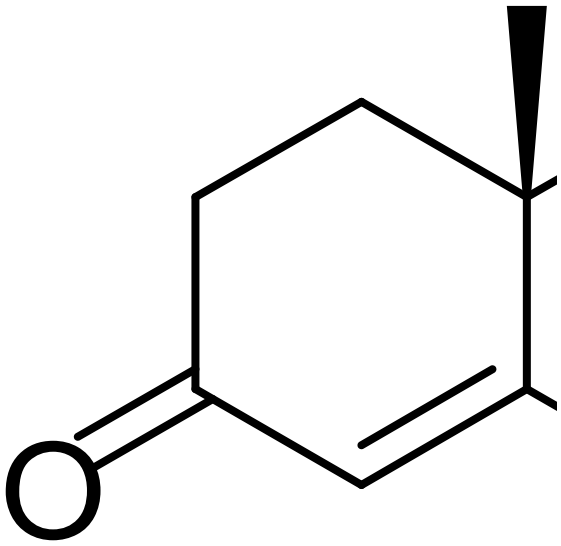

Figure 2.3. Steroid linked non-conventional cationic platinum(II) complexes previously synthesised. EE and ET indicate estradiol (EE) or testosterone (ET) derived ligands and complexes.

The anti-cancer properties of the testosterone coupled pyridine, quinoline and isoquinoline derivatives were tested[40, 42]. The complexes were subject to *in vitro* testing in two cancer cell lines, ovarian line SK-OV-3 (AR-), and breast line T-47D (AR+). The results (Fig. 2.4), showed that non-steroidal complexes were inactive or presented very low activity[43-45], whilst the steroidal platinum(II) conjugates all show between 2 and 12-fold improved toxicity[40,42]. It was also remarkable that the cis-complexes all displayed a 2-3 fold higher activity compared with trans isomers, indicating geometry as well as the

steroidal linkage influences cytotoxicity. The origin of this cytotoxicity cannot be ascribed solely to the platinum moiety (IC_{50} values of 115 μM and 197 μM for SK-O-V3 and T-47D). There appears to exist a synergistic effect; upon conjugation of an testosterone-based ligand to an inactive non-conventional cationic platinum(II) centre a potent new compound is created. At the moment, no data have been provided of the estradiol analogues' toxicities.

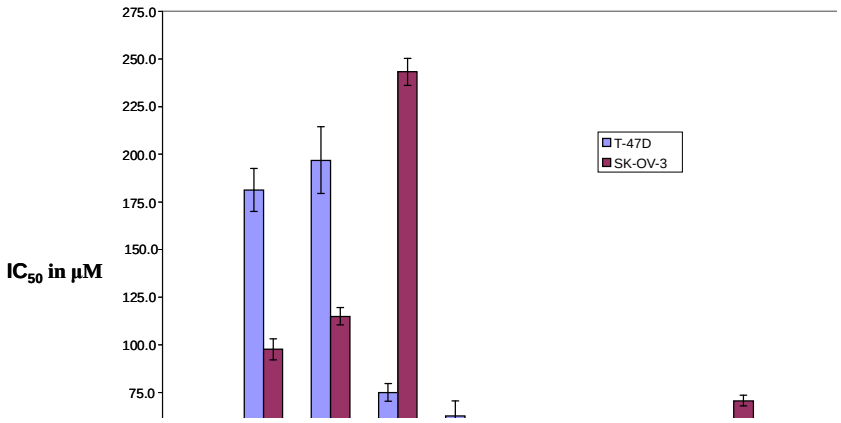

Figure 2.4. IC_{50} values of testostene coupled and non-steroidal platinum(II) compounds in the tumor cells lines T-47D and SK-OV-3.

As presented in previous chapter (Chapter 1.2) platinum complex activity is related with the mode of binding to DNA and the distortions produced to the double helix. Non-conventional platinum drugs have been created, designed to yield adducts different to the ones produced by cisplatin, with the idea that different DNA interaction would lead to broader anti-cancer activity. Steroid delivery has been used before to try to improve activity of Pt drugs against breast cancer by targeting the Estrogen Receptor (ER)[23-28]. However, none of the studies has explored how the presence of the steroid affects the DNA binding of the Pt unit, simply reporting cytotoxicity data. From our own laboratories, a monofunctional platinum-terpyridine estrogen derivative was prepared and shown to be able to bind to DNA and proteins at the same time; however no detailed information about the interactions was obtained[29]. Studies with our library

of compounds showed that the presence of a steroid, attached to an aromatic ring of a non-conventional and inactive platinum(II) complex has a significant and dramatic effect on the interaction of monofunctional complexes with DNA[40-41, 46]. The presence of the steroid increases the ability of the compounds to bend and unwind the DNA greatly (Table 2.1)[40,46]. This is remarkable, compared with small unwinding abilities and no bending shown by inactive monofunctional complexes (Section 1.2).

	Unwinding Angle		*Unwinding Angle*
trans-[Pt(2ET)Cl(NH$_3$)$_2$]$^+$	19º	**trans-[Pt(1EE)Cl(NH$_3$)$_2$]$^+$**	11º
trans-[Pt(3ET)Cl(NH$_3$)$_2$]$^+$	11º	**trans-[Pt(2EE)Cl(NH$_3$)$_2$]$^+$**	8.5º
trans-[Pt(4ET)Cl(NH$_3$)$_2$]$^+$	15º	**trans-[Pt(7EE)Cl(NH$_3$)$_2$]$^+$**	10.5º
trans-[Pt(6ET)Cl(NH$_3$)$_2$]$^+$	19º	**trans-[Pt(4EE)Cl(NH$_3$)$_2$]$^+$**	>32º
trans-[Pt(5ET)Cl(NH$_3$)$_2$]$^+$	4º	**trans-[Pt(6EE)Cl(NH$_3$)$_2$]$^+$**	13º
cis-[Pt(2ET)Cl(NH$_3$)$_2$]$^+$	21º	**trans-[Pt(5EE)Cl(NH$_3$)$_2$]$^+$**	13º
cis-[Pt(6ET)Cl(NH$_3$)$_2$]$^+$	19º	**cis-[Pt(3EE)Cl(NH$_3$)$_2$]$^+$**	19º
cis-[Pt(5ET)Cl(NH$_3$)$_2$]$^+$	21º	**cis-[Pt(6EE)Cl(NH$_3$)$_2$]$^+$**	13º
trans-[Pt(Py)Cl(NH$_3$)$_2$]$^+$	6.5º	**cis-[Pt(5EE)Cl(NH$_3$)$_2$]$^+$**	15º
cis-[Pt(Py)Cl(NH$_3$)$_2$]$^+$	6.5º	**transplatin**	9º
trans-[Pt(QUI)Cl(NH$_3$)$_2$]$^+$	8.5º	**cisplatin**	13º

Table 2.1. Unwinding angles of steroidal pyridine and quinoline derivatives in pBR322[40-41].

Even though the initial results are promising, a few problems about the synthesis and anticancer activity of these compounds still need to be addressed. During the synthetic process, it was not possible to obtain some potential complexes of the library and others were produced only in low yields. This low amount of complex obtained was mainly due to inefficiency of the purification process required to remove impurities and secondary products (which involved multiple recrystalizations and the use of activated charcoal). Also, although initial cytotoxicity data showed that conjugation of testosterone introduced activity to previously inactive platinum(II) centres, no cytotoxicity data was obtained for corresponding estradiol derivatives, the possible dependence to the steroidal induced cellular effects was not studied and no information about response to resistance mechanism was provided. Cellular uptake experiments were needed to understand the delivery abilities of the used steroidal vectors and further studies of macromolecular interaction were needed to understand the difference in toxicity between cis and trans isomers. All of these problems will be addressed herein, together with a synthetic attempt to standardize the coupling of metallodrugs to steroids.

2.2 Synthesis and purification new monofunctional Pt(II) steroidal-complexes

Building on these previous studies we now present the synthesis of three new steroidal pyridine complexes (which had not previously been synthesised) and two interesting additional products. Also, we describe a simple and quick method to purify this kind of compounds, which allows us to increase the final yield. Importantly we are then able to differentiate between the cis and trans isomers through normal NMR techniques.

2.2.1 Synthesis of new compounds

Synthesis of trans-[Pt(1ET)Cl(NH_3)$_2$](NO_3):

When transplatin was stripped of one of its chloride ions and reacted with one equivalent of 1ET (added dropwise at -18ºC) trans-[Pt(1ET)Cl(NH_3)$_2$]$^+$ was produced. Purification following the method outlined below (Section 2.2.2), afforded the compound in 49% yield. The white solid was analysed by mass spectrometry, showing the expected peak at 654 m/z ([Pt(1ET)Cl(NH_3)$_2$]$^+$) and elemental analysis proved its purity. The ^{1}H NMR spectrum (Fig. 2.5) shows the characteristic testosterone steroid, with an unmodified singlet at 5.7 ppm integrating for a proton that corresponds to H_4. The two singlet peaks at 1.3 and 1.0 ppm (integration of three each) corresponding to the two methyl groups, Me_{19} and Me_{18} respectively. The absence of other peaks is further confirmation of the purity of the complex. The pyridine unit gives rise to four signals at 8.9, 8.0, 7.7 and 7.5 ppm (doublet of doublets, doublet of doublets of doublets, doublet and doublet of doublets of doublets), indicating $H_{6'}$, $H_{4'}$, $H_{3'}$ and $H_{5'}$ respectively, all with integration of one. Assignment was achieved by comparison with similar compounds. A peak corresponding to NH_3 with an integration of six is observed at 4 ppm. This single peak confirms the trans nature of the complex (see Section 2.2.2).

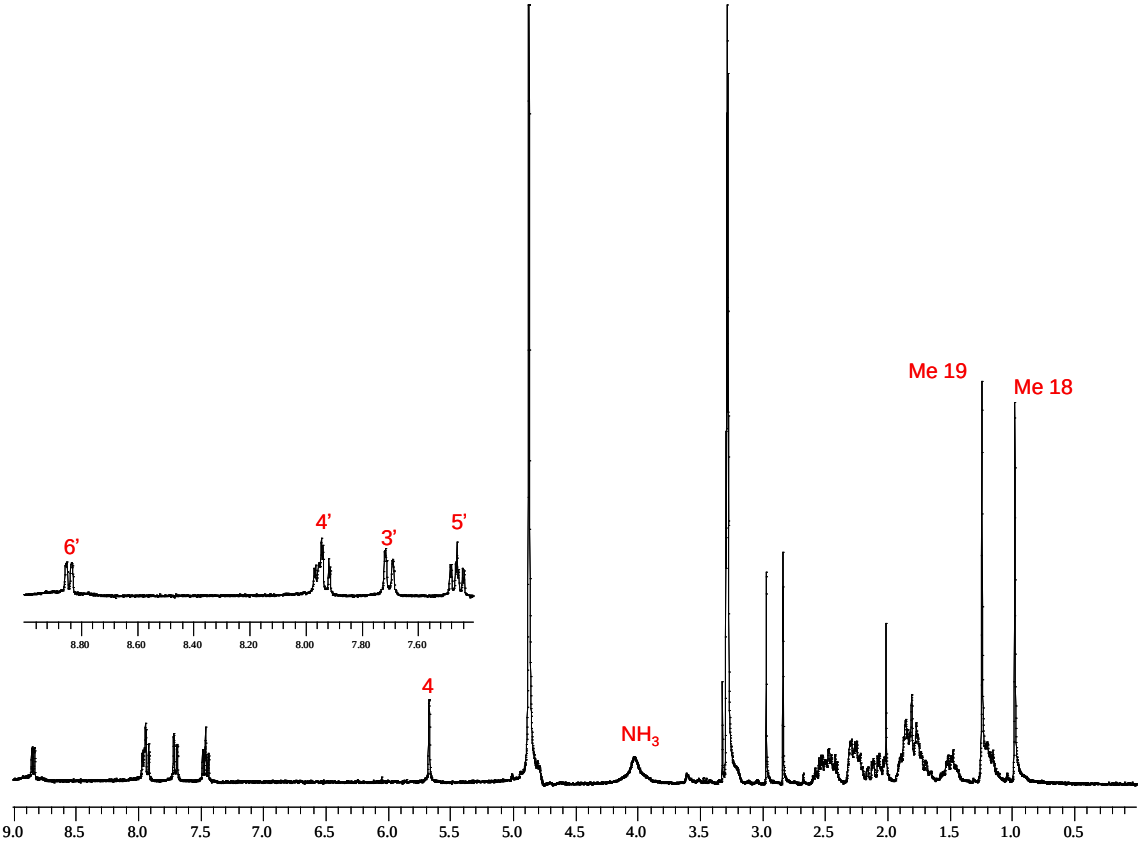

Figure 2.5. ^{1}H-NMR of trans-[Pt(1ET)Cl$(NH_3)_2$]$^{+}$ in deuterated methanol.

Synthesis of cis-[Pt(1ET)Cl$(NH_3)_2$](NO_3):

When the same reaction was done with cisplatin instead of transplatin, the result was a brown-black solid that was not the expected product. However, if the addition of the ligand (1ET) was performed under Argon bubbling, the desired cis version of previous complex was obtained. As for the trans isomer, the ESI-MS of the white powder showed a peak at 654 m/z (corresponds to [Pt(1ET)Cl$(NH_3)_2$]$^{+}$) indicating the binding of the platinum centre to the ligand. The yield was half that of the trans version, probably as a result of the sensitivity of the synthesis and the need for the inert atmosphere. The ^{1}H NMR spectrum (Fig. 2.6) shows four signals at 8.8, 7.9, 7.6 and 7.4 ppm (doublet of doublets, doublet of doublets of doublets, doublet and doublet of doublets of doublets),

indicating $H_{6'}$, $H_{4'}$, $H_{3'}$ and $H_{5'}$ (assignment under the known and distinctive coupling patterns on a pyridine ring). As expected, chemical shifts are different to those presented by trans complex. Also different are the methyl signals at 1.2 and 1.0 ppm corresponding to the two methyl groups, Me_{19} and Me_{18} respectively. The peak at 5.7 ppm corresponding to H_4 does not change shift, consistent with its remote location from the metal centre. Evidence of the cis form of the complex is provided by the two ammine signals observed at 4.5 and 4.1 ppm (integration of 3 protons each). This spectrum provides evidence for the formation of cis-$[Pt(1ET)Cl(NH_3)_2]^+$.

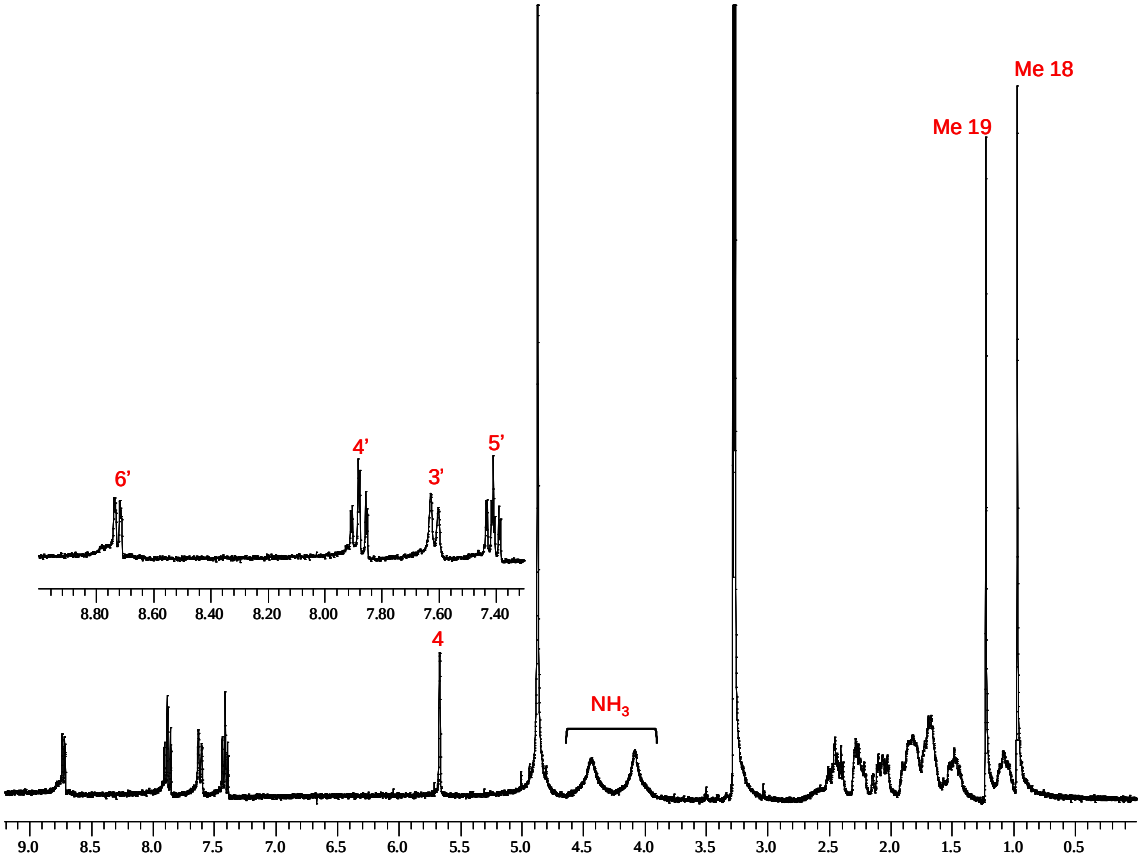

Figure 2.6. ^{1}H-NMR of cis-$[Pt(1ET)Cl(NH_3)_2]^+$ in deuterated methanol.

Synthesis of cis-[Pt(2EE)Cl(NH_3)$_2$](NO_3):

Reacting 2EE and cisplatin also gave a brown-black compound, but similarly, if the addition of the ligand was done under Argon bubbling, cis-[Pt(2EE)Cl(NH_3)$_2$]$^+$ was obtained. ESI-MS of the white powder reveal a peak at 638 m/z and elemental analysis (after purified as described in Chapter 2.2.2) indicated the expected stoichiometry. Again the yield was 1.5 fold lower than the trans version. The ^{1}H NMR spectrum (Fig. 2.7) shows four signals at 8.8, 8.7, 8.0 and 7.5 ppm (doublet, doublet of doublets, doublet of triplets and doublet of doublets), indicating $H_{2'}$, $H_{6'}$, $H_{4'}$ and $H_{5'}$ of the pyridine respectively, all with an integration of one. Assignment again used the known pyridine splitting patterns. The presence of a single methyl signal at 0.9 ppm, corresponding to Me_{18}, gives a further indication of the purity of the compounds. Estradiol protons H_1, H_2 and H_4 can be observed at 7.1, 6.6 and 6.5 ppm respectively (doublet, doublet of doublets and doublet). Evidence of the cis form of the complex is provided by the two ammine signals observed at 4.6 and 4.2 ppm (integration of 3 protons each). This spectrum provides evidence for the formation of cis-[Pt(2EE)Cl(NH_3)$_2$]$^+$.

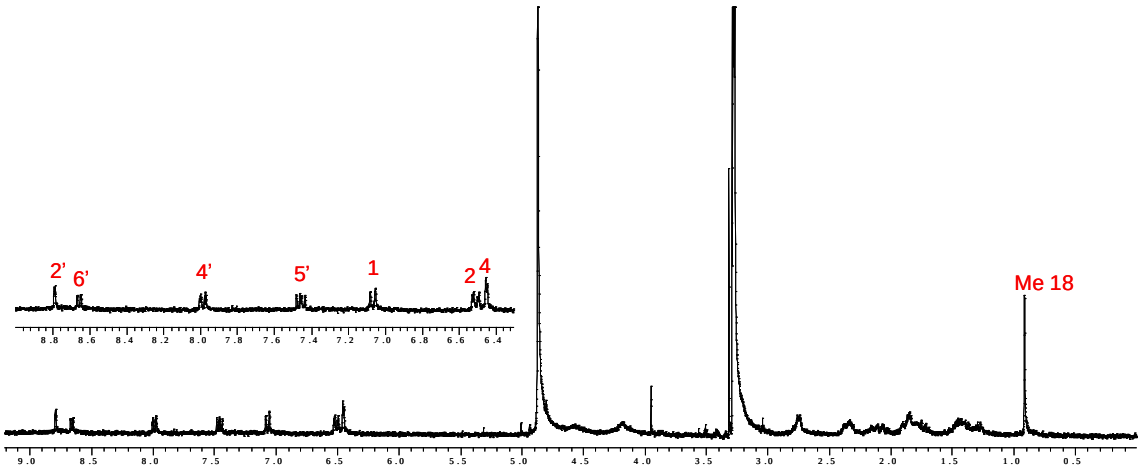

Figure 2.7. ^{1}H-NMR of cis-[Pt(2EE)Cl(NH_3)$_2$]$^+$ in deuterated methanol.

Before purification a crude solution of the product in DMF was left in the fridge. After 24 hours, translucent crystals appeared. These crystals were explored by single crystal X-Ray Diffraction, and revealed two estradiol molecules attached through two triple bonds (Fig. 2.8). This is an expected side product (Glaser reaction)[47] of the synthesis of the ligands, and was present as result of a poor purification of the ligand (2EE). However, further purification of the ligands was not necessary synthetically because the side product does not react with platinum and is very readily purified from the complexes.

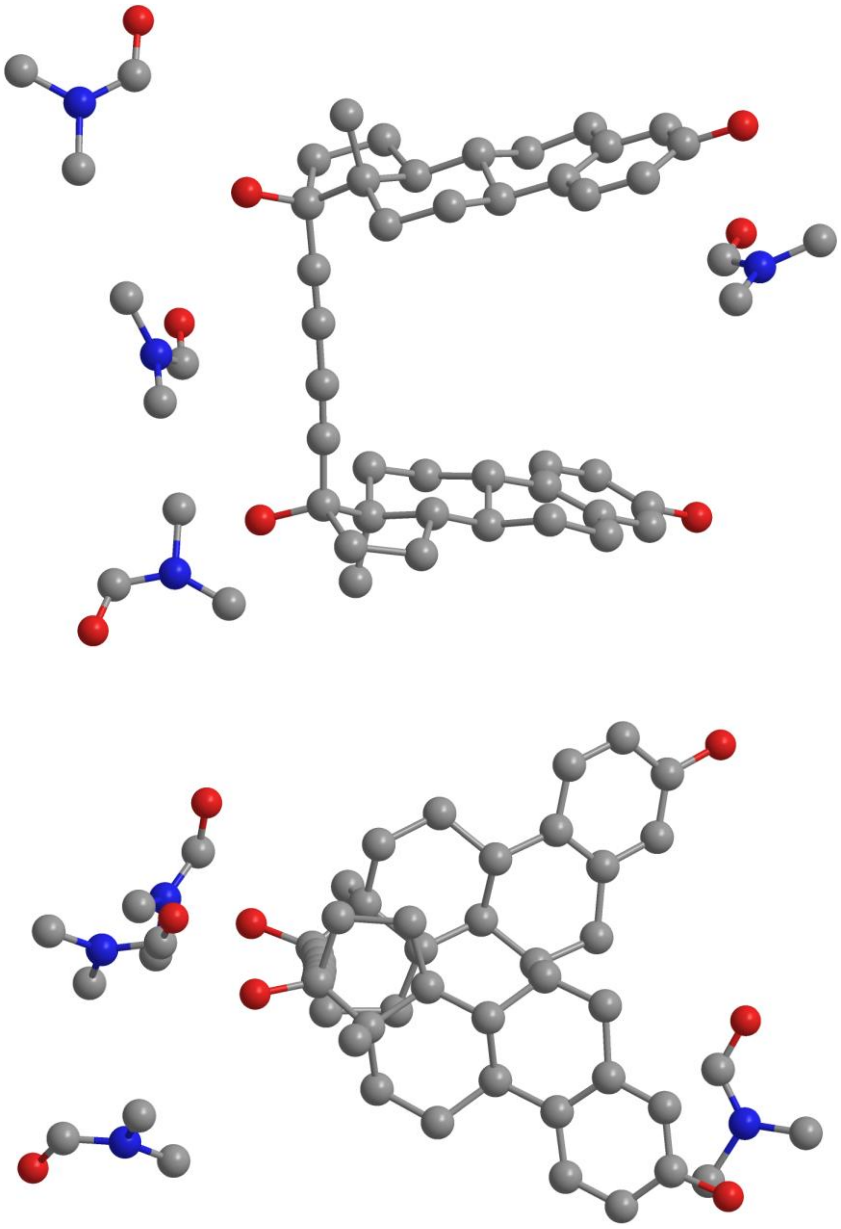

Figure 2.8. X-Ray diffraction crystal structure of the Glaser coupling product of 17α-ethynyl-estradiol.

When a normal Glaser reaction[47] was done with 17α-ethynylestradiol, the same compound was obtained in really good yield (70%), showing simplicity of preparation and purification. This type of compound could be interesting because similar bis-estradiol compounds have been presented in the literature targeted at the ER in breast cancer[48]. Compounds with two molecules of bile acid have been used as well as gene transfer vehicles[49]. However, both those types of dimeric steroid compounds required long and difficult synthesis and purification. This new product can be synthesised and purified easily by a normal Glaser reaction in a single step from commercially available reagents.

2.2.2 Purification of monofunctional Pt(II) steroidal-complexes

Aside from these three new Pt complexes which co-workers in the group had been unable to prepare, a series of these compound types had been prepared[40-42]. However, two factors had been a problem; the first one is the purification, and the second one is the overall yield. The many steps of purification (such us recrystalizations and reaction with activated charcoal) make the final yield of the reaction go down to between 10-30%. Especially dramatic is the case of cis-$[Pt(2ET)Cl(NH_3)_2]^+$, (the most active of the testosterones) that showed a yield of just 12%[40, 42].

To address this problem, the use of HPLC separation techniques were explored, allowing us to discriminate between the single substituted and di-substituted complexes. First attempts of purification, under isocratic techniques and gradient techniques without the use of TFA (not used at first as steroidal compound show certain sensitivity to acidic mediums under high temperatures), were not successful. However, separation can be achieved using a water:methanol (0-100%) gradient during 40 minutes, with the use of TFA (0.05%) to sharpen the peaks. This could be applied to all these types of compounds and allowed us to standardise the purification into a simple and single step process. This has been a dramatic improvement compared to the previous purifications, which were different for each compound and involved different number of steps. Moreover the compounds were obtained in higher purity by this new method

Following this procedure, the compounds can be achieved with yields improved 2 or 3 fold times (from 12% to 44% for cis-$[Pt(2ET)Cl(NH_3)_2]^+$) and with purities higher than 95% (assessed by HPLC, Fig. 2.9). Different methods are not needed for the different steroids, since both testosterone and estradiol can be purified following the

same procedure, nor for the isomer, or molecule linked to the steroid (pyridine, quinoline, aniline, etc.)

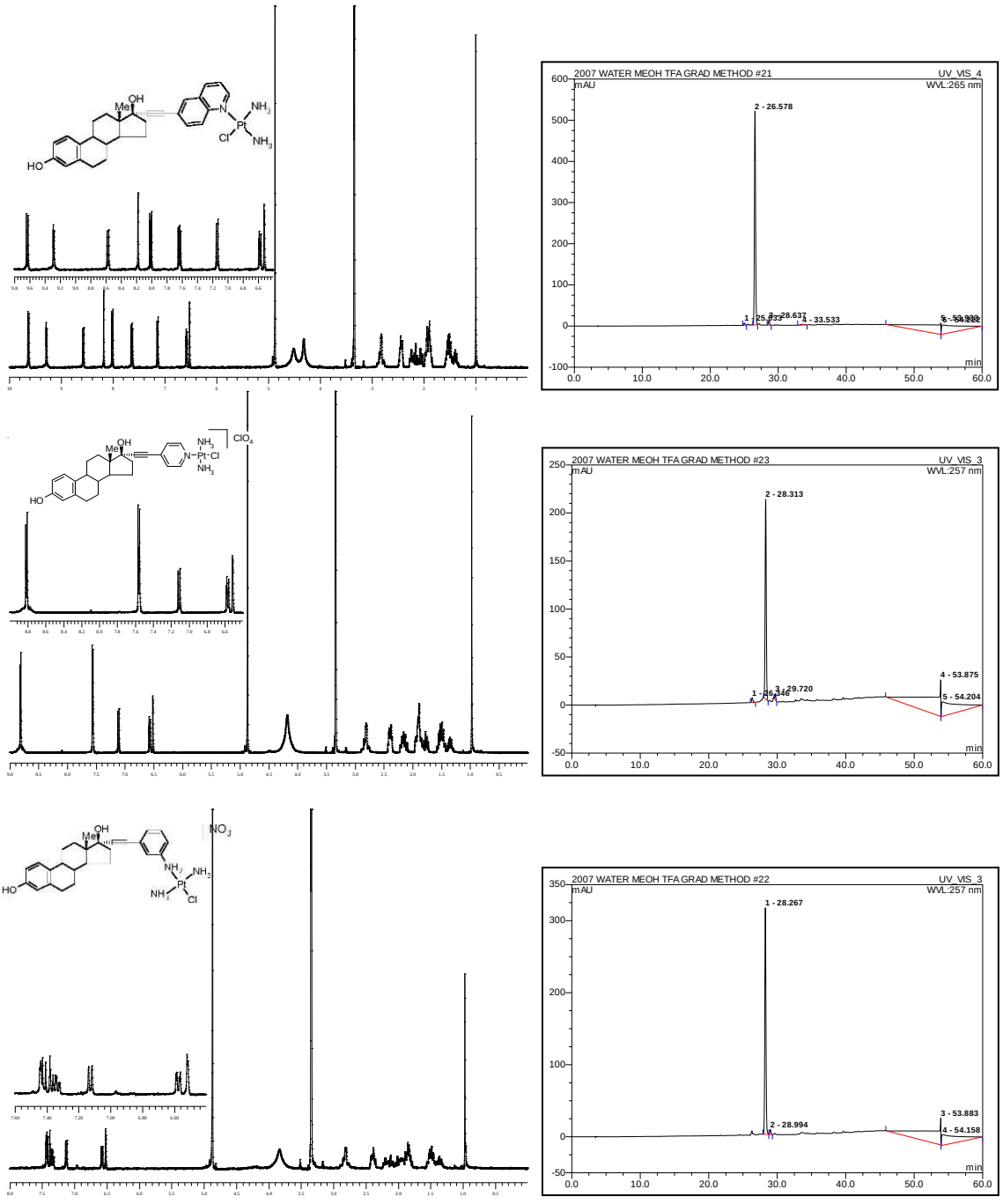

Figure 2.9. Examples of purification of different complexes following the HPLC method described before. cis-$[Pt(6EE)Cl(NH_3)_2]^+$ (top), trans-$[Pt(3EE)Cl(NH_3)_2]^+$ (middle) and trans-$[Pt(7EE)Cl(NH_3)_2]^+$ (bottom).

After the purification with HPLC, all the residual solvents were removed. In these pure dried samples the ammino groups could be detected by ^{1}H-NMR. Spectra of different isomers show that cis isomers have two different ammino peaks integrating each for 3 protons, while in trans isomers there is only one peak integrating for 6 protons (Fig. 2.10). This is due to the different chemical enviroment of cis isomers against the identical one to

which the trans ones are exposed. In the spectra of the compounds previously prepared and purified by other techniques the ammines were frequently extremely broad and unresolved, perhaps due to binding to residual solvents.

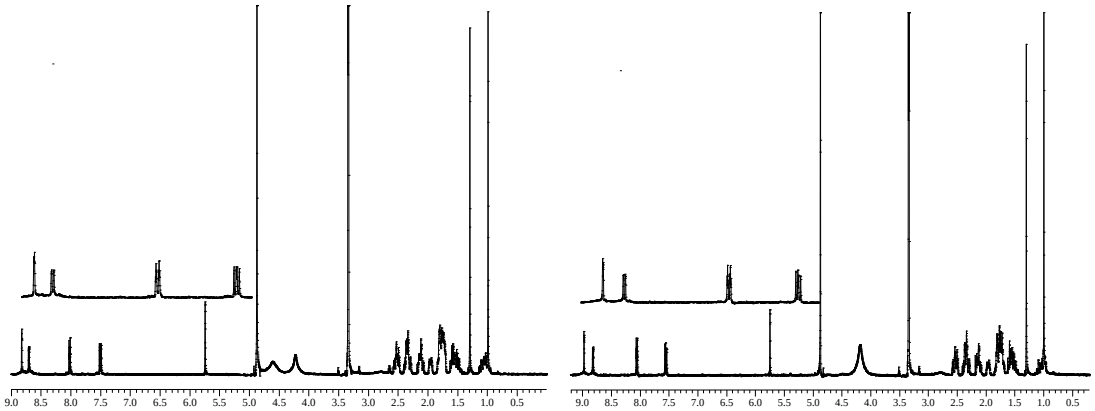

cis-$[Pt(2ET)Cl(NH_3)_2]^+$ trans-$[Pt(2ET)Cl(NH_3)_2]^+$

Figure 2.10. ^{1}H-NMR differenciation between cis and trans isomers.

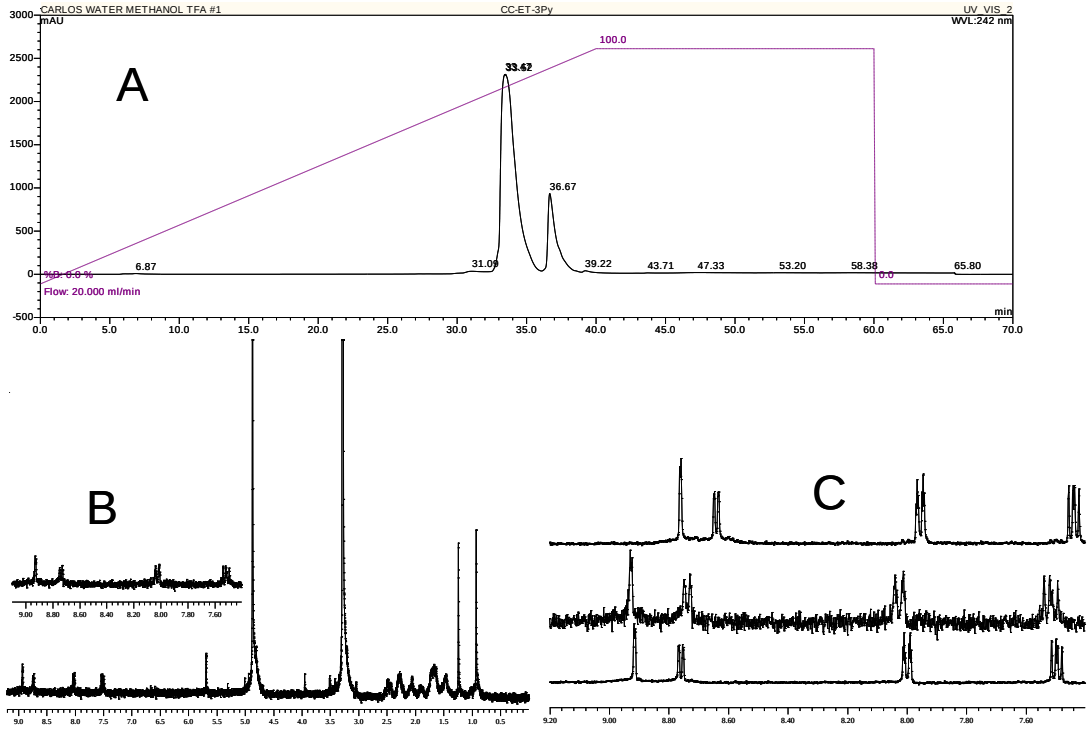

Figure 2.11. A) HPLC chromatograph of cis-$[Pt(2ET)Cl(NH_3)_2]^+$ and the bisubstituted $[Pt(2ET)_2(NH_3)_2]^{2+}$ "impurity" B)^{1}H-NMR of bisubstituted $[Pt(2ET)_2(NH_3)_2]^{2+}$ in deuterated methanol. C) ^{1}H-NMR of $[Pt(2ET)_2(NH_3)_2]^{2+}$ (middle), compared with cis-$[Pt(2ET)Cl(NH_3)_2]^+$ (top) and trans-$[Pt(2ET)Cl(NH_3)_2]^+$ (bottom) in deuterated methanol.

The final advantage of this method is the possibility to isolate the disubstituted complexes. This usually represent between 5-10% of the final product. If the starting reaction is on a sufficiently large scale, enough compound can be obtained, and

characterization can be achieved (Fig. 2.11). An example of this is the disubstituted version of the 2ET $[Pt(2ET)_2(NH_3)_2]^{2+}$, obtained in the purification of the cis-$[Pt(2ET)Cl(NH_3)_2]^{+}$. Determining the geometry is complicated, since the two ammino groups of both cis and trans isomers present identical chemical environment. In the future, this kind of compound and also the Glaser coupling reaction product, could be interesting to be tested to see the effect of the metallic centre in disteroidal compounds.

2.3 Toxicity of steroid derivatives

As seen in Section 2.1.1 (Fig. 2.4) initial cytotoxicity data showed exciting activities for our testosterone linked monofunctional platinum(II) centres. No cytotoxicity data was obtained for estradiol derivatives and dependence to the steroidal induced cellular effects, response to resistance mechanism and cellular uptake were not studied. New information in these areas is presented in this section.

2.3.1 Toxicity of Estradiol derivatives

In order to check if the synergic effect observed for testosterone linked compounds is also present when the steroid used is estradiol, the activity of a series of pyridine and quinoline like estradiol linked triammine platinum(II) complexes has been tested. Different cell lines with different ER and AR status have been used (Table 2.2); SK-OV-3, A2780, A2780cr (ovarian carcinoma), T-47D, MDA-MB-231 (breast carcinoma) and HBL-100† (breast epithelium†). SK-OV-3 is in addition a cisplatin resistant cell line. The activity was measured after treatment for 72h with the studied complexes. The steroidal-Terpyridine derivatives $[Pt(EET)Cl]^{+}$ and $[Pt(ETT)Cl]^{+}$ (Fig. 2.2 D)[29, 50] were tested as well as non-steroidal complexes and cisplatin (as controls).

Cell line	ERα	ERβ	AR
HBL-100	-	+	-
T-47 D	+	+	+
SK-OV-3	+	+	-
MDA-MB-231	-	+	-
A2780	-	+	-
A2780cr	-	+	-

Table 2.2. Steroid receptor status among cell lines used.

† Although recently doubt has been cast on the provenance and veracity of HBL-100 as a breast cancer cell line (Lacroix, M. (2008). Int. J. Cancer 122, 1–4.) the results that we obtained in this line are included for completeness and allow comparison with the many other previous studies in that cell line.

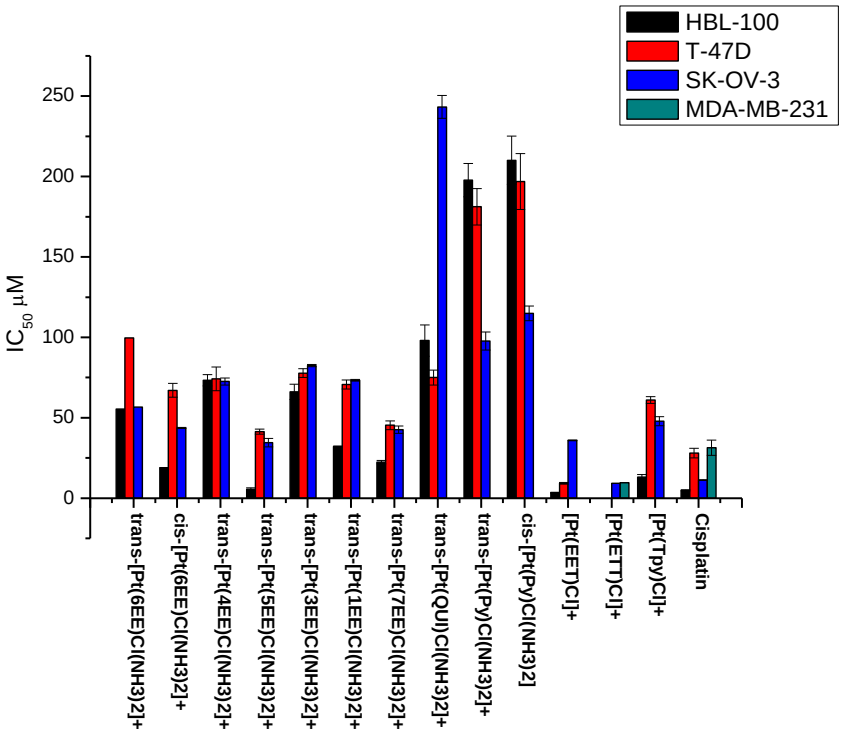

Figure 2.12. IC_{50} values of estradiol-coupled and non-steroidal platinum(II) compounds.

The non-steroidal complexes present low activity, with values over 100 µM, considered as non active. The estradiol linked complexes, as hoped, show higher activity than the non-steroidal analogues (Fig. 2.12). However, this activity is not remarkably high, and is generally lower than for the testosterone (androgenic) complexes (also very active). In general, most of the complexes show lower activity than cisplatin in every cell line. The only exceptions are trans-$[Pt(5EE)Cl(NH_3)_2]^+$ and the steroidal-terpyridine derivatives (both $[Pt(EET)Cl]^+$ and $[Pt(ETT)Cl]^+$)[29, 50]. Trans-$[Pt(5EE)Cl(NH_3)_2]^+$ show similar activity to cisplatin only in HBL-100, but the steroidal terpyridine compounds present cisplatin-like growth inhibition abilities in SK-OV-3 and better in HBL-100, T-47D and MDA-MB-231 (IC_{50} 3 times lower than cisplatin for the last two). The non-steroidal $[Pt(Tpy)Cl]^+$ derivative shows good activity by itself, as reported by Lowe[51], but nevertheless, coupling to the steroid does introduce an improvement in the activity.

It is interesting to see that the lower IC_{50} values for almost all the compounds, including cisplatin and the non-steroidal references, were obtained in HBL-100. This is

at first sight confusing since this cell line show ERα – status, while the other two are ERα +. However if we compare the values in each cell line to those of cisplatin in that cell line, we see that the higher ratios are present in T-47D, and that SK-OV-3 shows always higher or similar values than HBL-100 (except for trans-$[Pt(5EE)Cl(NH_3)_2]^+$, where HBL-100 present the higher ratios). So the lower IC_{50} in HBL-100 could be merely an inherent higher sensitivity of this cell line to platinum drugs. In general we can say that when compared ratiometrically to cisplatin (Table 2.3), the compounds are more active in ERα + cell lines than in ERα – ones.

	SK-OV-3 (ERα+)	HBL-100 (ERα-)	T-47D (ERα+)
trans-$[Pt(6EE)Cl(NH_3)_2]^+$	0.20	0.09	0.28
cis-$[Pt(6EE)Cl(NH_3)_2]^+$	0.26	0.26	0.42
trans-$[Pt(4EE)Cl(NH_3)_2]^+$	0.15	0.07	0.38
trans-$[Pt(5EE)Cl(NH_3)_2]^+$	0.32	0.86	0.68
trans-$[Pt(5EE)Cl(NH_3)_2]^+$	0.14	0.07	0.36
trans-$[Pt(1EE)Cl(NH_3)_2]^+$	0.15	0.15	0.40
$[Pt(EET)Cl]^+$	0,31	1.45	3.06
$[Pt(Tpy)Cl]^+$	0.23	0.37	0.46

Table2. 3. Cisplatin/Complexes IC_{50} ratio in the different cell lines.

2.3.2 Effect of added estradiol to non-steroidal complexes

In 2000, Lippard[27] showed that co-administration of estradiol and/or progesterone, with platinum complexes increased their toxicity by 2 or 4 fold in hormone dependent cell lines (ER+ or PR+). It was suggested that these hormones increase the production of HMG proteins, possibly upon binding to its receptors. One of the questions that we have with our compounds is if the improved activity is coming from the steroid domain linkage, or is just as a result of this hormonal effect. To study this possibility we explored the effect of co-administering the non steroidal controls trans-$[Pt(QUI)Cl(NH_3)_2]^+$ and $[Pt(Tpy)Cl]^+$ with 10^{-7} M of 17α-ethynylestradiol (as used by Lippard).

	SK-OV-3	HBL-100	T-47D
trans-$[Pt(QUI)Cl(NH_3)_2]$	243.3 ± 7.1	98 ± 9.7	75 ± 4.6
trans-$[Pt(QUI)Cl(NH_3)_2]$*	125	10	53.7
trans-$[Pt(4EE)Cl(NH_3)_2]$	74.52 ± 2.14	73.33 ± 3.51	74.23 ± 7.4
trans-$[Pt(6EE)Cl(NH_3)_2]$	56.58	55.45	99.68
trans-$[Pt(4ET)Cl(NH_3)_2]$&	49.9 ± 1.8	24 ± 1.2	51.4 ± 1.9
trans-$[Pt(6ET)Cl(NH_3)_2]$&	45.4 ± 3.5	26.3 ± 2.8	38.6 ± 2.4
$[Pt(Tpy)Cl]^+$	22.46 ± 2.27	13.02 ± 1.65	60.96 ± 2.12
$[Pt(Tpy)Cl]^+$*	13	10	30
$[Pt(EET)Cl]^+$	18.59 ± 2.18	3.35 ± 0.35	9.25 ± 0.59

Table 2.4. Effect of the addition of estradiol to non-steroidal complexes in their IC_{50} values (μM). *= addition of estradiol; &= data from Martin Huxley[40].

Table 2.4 shows the results of this experiment, and comparison with the steroid coupled complexes. Both treated complexes, as expected, show more or less a 2 fold increase of the activity in SK-OV-3 and T-47D (considered ER+). However, in HBL-100, where no action was expected (considered ER-) the improvement is much bigger for trans-$[Pt(QUI)Cl(NH_3)_2]^+$, almost 10 times, but only 1.3 times for $[Pt(Tpy)Cl]^+$. In general, this increase in the growth inhibition abilities is not strong enough to reach the activities of the steroidal linked derivatives; the only exceptions are found for trans-$[Pt(QUI)Cl(NH_3)_2]^+$ in HBL-100 (addition of estradiol produced an unexpectedly high effect), and $[Pt(Tpy)Cl]^+$ in SK-OV-3 (due to small differences between initial cytotoxicities of the complexes). We could say that the increased anticancer activity observed for covalently coupled steroidal platinum(II) complexes is not solely due to the possible steroidal effects produced by the ligand in hormone dependent cell lines.

2.3.3 Activity of free ligands

Steroids are a family of compounds found naturally in all sort of organisms and posses a spectrum of biological activity. Recently a series of natural steroidal alkaloids with a structure similar to our quinoline derivatives has been isolated from marine sponges. These compounds show anti-angiogenic capacities, showing anti-proliferative activity against HUVEC cells (Human umbilical vein endothelial cells)[52] (Fig. 2.13).

Figure 2.13. Structures of cortistatins obtained from the marine sponge *Corticium Simplex*

It is noteworthy that our platinum complexes formed with quinolines and isoquinolines steroidal derivatives showed good activity in cancer cell lines, being some of the best of the series (especially complexes of 6EE and 6ET). Moreover a platinum complex of the 5EE derivative showed similar activity to cisplatin in HBL-100. For this reason it was important investigate the possibility that the activity could come from the ligand instead of from the synergy between the components. Four free ligands were tested in the same cell lines to check their activity. 2ET, 4ET, 5EE and 6ET were

chosen to cover the different steroids (estradiol and testosterone) and structures (pyridine and quinoline in different positions).

	SK-OV-3	HBL-100	T-47D
2ET	>200	>170	>200
trans-[Pt(2ET)Cl(NH$_3$)$_2$]$^{+}$[&]	39.1 ± 1.7	27.3 ± 1.9	62.8 ± 7.8
cis-[Pt(2ET)Cl(NH$_3$)$_2$]$^{+}$[&]	15.7 ± 0.4	7.4 ± 0.9	15.9 ± 0.5
4ET	21.1		48.6
trans-[Pt(4EE)Cl(NH$_3$)$_2$]$^{+}$	74.52 ± 2.14	73.33 ± 3.51	74.23 ± 7.4
trans-[Pt(4ET)Cl(NH$_3$)$_2$]$^{+}$[&]	49.9 ± 1.8	24 ± 1.2	51.4 ± 1.9
5EE	35	9	40
trans-[Pt(5EE)Cl(NH$_3$)$_2$]$^{+}$	34.53 ± 2.6	5.63 ± 0.72	41.39 ± 1.59
trans-[Pt(5ET)Cl(NH$_3$)$_2$]$^{+}$[&]	70.7± 2.7	28 ± 1.8	51.4 ± 1.9
cis-[Pt(5ET)Cl(NH$_3$)$_2$]$^{+}$[&]	26.3 ± 0.3	27.7 ± 1	32.8 ± 0.7
6ET	30.6		38.7
trans-[Pt(6EE)Cl(NH$_3$)$_2$]$^{+}$	56.58	55.45	99.68
cis-[Pt(6EE)Cl(NH$_3$)$_2$]$^{+}$	43.5 ± 0.4	18.7 ± 0.5	67.1 ± 4.3
trans-[Pt(6ET)Cl(NH$_3$)$_2$]$^{+}$[&]	45.4 ± 3.5	26.3 ± 2.8	38.6 ± 2.4
cis-[Pt(6ET)Cl(NH$_3$)$_2$]$^{+}$[&]	16.4 ± 0.7	12.4 ± 1.4	14.4 ± 1

Table 2.5. Activity of free ligands and comparison with complexes formed with these ligands. [&]= data from Martin Huxley[40].

Results are shown in Table 2.5 together with the data for some of their Pt complexes. As we observe, 2ET is not active at all, with IC_{50} normally over 200 μM. This indicates that the activity of its platinum(II) complexes must come from the platinum conjugate. In contrast, 4ET, 5EE and 6ET ligands show a similar activity to the platinum complexes (in most cases better). The only cell line in which the free estradiol ligand shows a lower cytotoxicity is in HBL-100 (5EE), which maybe due to its sensitivity to platinum and ERα – status. We cannot consider that the activity of the (quinoline based) complexes came from the introduction of the metal centre. For this reason experiments undertaken after this point used only the pyridine derivatives, since we cannot prove that our aim of enhancing and locating the activity of a metal centre is achieved with the quinoline and isoquinoline derivatives.

2.3.4 Toxicity of Testosterone derivatives

Testosterone can be metabolized to estradiol by aromatases. Moreover, AR has proven to have an important regulatory role of ERα (ER = estrogen receptor) in breast cancer[53]. Both T-47D and SK-OV-3 are ERα and ERβ positives, so it was interesting to observe the cytotoxicity capacities in other (ER-) tumour cells. Breast cell line MDA-MB-231 (AR-, ERα- and ERβ +) and ovarian cell line A2780 (AR-, ERα- and ERβ +) were chosen. In order to see how well our compounds are able to overcome resistance mechanisms, the cisplatin resistant strain of A2780 was selected as well. Major resistance mechanisms found in A2780cisR are reduced uptake of platinum(II) drugs

and elevated levels of the tri-peptide glutathione whose cysteine residue detoxifies platinum(II) drugs via rapid binding[54]. cis-$[Pt(2ET)Cl(NH_3)_2]^+$, being the most potent complex with no inherent ligand activity, was chosen for further studies, alongside its trans isomer and the non-steroidal analogous complexes (Table. 2.6). The steroidal-complexes again show better activity than the non-steroidal analogues, but, interestingly, trans-$[Pt(2ET)Cl(NH_3)_2]^+$ shows the same cisplatin-like levels of activity as its cis isomer in the MDA-MB-231 cell line. Even more interesting both isomers show certain selectivity: apparently, the trans derivative is more efficient when the are not present in the cell, while the cis isomer shows better activities in the presence of ERα receptors. This could indicate different interactions with the receptors, or different effects upon binding to them.

For A2780, cis-$[Pt(2ET)Cl(NH_3)_2]^+$ is again more active than the trans isomer but no dramatically more so its the non-steroidal analogue. However, the platinum resistance mechanisms do not affect the steroidal complex to the same extent as the non-steroidal. Indeed the activity of cis-$[Pt(2ET)Cl(NH_3)_2]^+$ remains at a potent level. This could suggest that steroidal complexes, as expected, are transported better into the cell.

Table 2.6. IC_{50} values (μM) of cis and trans-$[Pt(2ET)Cl(NH_3)_2]^+$ and their non-steroidal controls.

	MDA-MB-231	SK-OV-3	T-47D	A2780	A2780cisR	Rx[a]
trans-$[Pt(Py)Cl(NH_3)_2]^+$	334 ± 54	98 ± 6	181 ± 11	72 ± 7	157 ± 2	*2.2 ± 0.2*
cis-$[Pt(Py)Cl(NH_3)_2]^+$	186 ± 14	115 ± 5	197 ± 17	25.0 ± 1.2	105 ± 3	*4.2 ± 0.2*
trans-$[Pt(2ET)Cl(NH_3)_2]^+$	27.3 ± 4.7	39.1 ± 2[&]	63 ± 8[&]	35.3 ± 4.2	88 ± 2	*2.5 ± 0.3*
cis-$[Pt(2ET)Cl(NH_3)_2]^+$	29.2 ± 8.1	15.7 ± 0.5[&]	15.9 ± 0.5[&]	17.4 ± 3.1	33.3 ± 4.3	*1.9 ± 0.4*
Cisplatin	31.3 ± 4.7	6.0 ± 1.3	32.0 ± 4.8	3.0 ± 0.5	12.8 ± 1.4	*4.3 ± 0.8*

[a]Rx is increase in IC50 observed for a compound when tested in the cisplatin-resistant A2780cisR compared to A2780. [&]= data from Martin Huxley.

2.3.5 Cellular uptake

In order to explore the uptake, MDA-MB-231, T-47D and SK-OV-3 cells were treated with platinum drugs and uptake determined using Induced Coupled Plasmon Mass Spectrometry (ICP-MS). A short time of exposure (3h) and a single concentration for all compounds (30 μM)[55] was chosen in order to determine speed and efficiency of all, under the same conditions. The short time period negates any issues related to the different effects of the compounds on cell division or death. Again cis-$[Pt(2ET)Cl(NH_3)_2]^+$, as the most interesting compound, and its trans isomer was chosen, and non-steroidal analogues and cisplatin were used as controls. Whole cell, cytoplasm

and nucleic fractions were obtained from the same experiment to observe distribution through the cell. In Figure 2.14 we can see the results. Surprisingly, linkage of a testosterone lowers the delivery in whole cells through all three cell lines (at least at this time point). There is a co-relation between cellular uptake and cytotoxicity for the non-steroidal complexes, but not for the testosterone derivatives (Appendix B). However, when the cytoplasm and nuclear fractions are studied we notice that similar levels of platinum are observed for both steroidal and non-steroidal complexes, suggesting that a lot of the non-steroidal complexes get stuck into the membrane, while all, or almost all of the steroidal ones cross into the cytoplasm. So it appears that addition of a lipophilic biomolecule does help the cationic complexes to cross through the cellular membrane, as expected. Distribution inside the cell is also different: almost all of the steroidal complexes are in the cytoplasm at this time point, while distribution in the non-steroidal complexes is similar between cytoplasm and nuclei. This may be because of slower transport of steroidal complexes to the nuclei or for a possible interaction with cytoplasmatic proteins. A more effective delivery across the cellular membrane is visible then in steroidal complexes, however, nuclear or cytoplasm delivery seems not to be related to cytotoxic values through the cell lines studied.

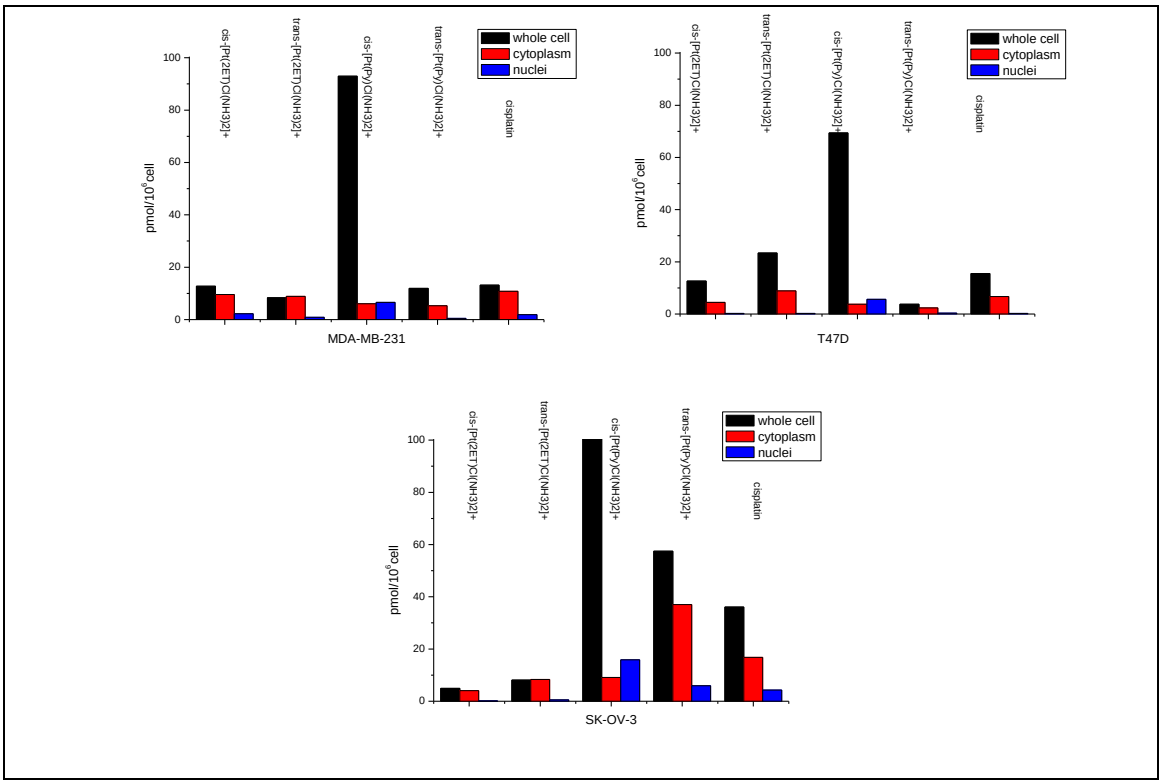

Figure 2.14. pmols of Pt in T-47D, SK-OV-3 and MDA-MB-231 after 3 hours of treatment with 30 μM of cis and trans-$[Pt(2ET)Cl(NH_3)_2]^+$, cis and trans-$[Pt(Py)Cl(NH_3)_2]^+$ and cisplatin.

2.4 Interaction with macromolecules

It is known that the presence of the bulky steroid has a dramatic effect on the structure of DNA: previous experiments (Section 2.1.1) showed that when these complexes interact with ct-DNA they bend it and unwind the double helix. The observed bending and unwinding are much bigger for steroidal complexes than for the non-steroidal analogues. Due to the co-relation between DNA mode of binding and anticancer activity (Section 1.2) it is possible that these differences in DNA distortions are the origin of the steroidal complexes' toxicity. A few questions are still left to be addressed about the interaction of our complexes with macromolecules. Previous experiments (Section 2.1.1) were not able to explain the difference in activity between cis and trans isomers and they did not provide information about how the presence of the metallic unit affected the interaction with proteins that usually bind steroids. Finally, since steroids can interact with DNA and have importance in cellular response toward platinum complexes, an important question is how the presence of free oestrogen and androgenic molecules affects the interaction of the non-steroidal complexes with DNA (although previously (Section 2.3.2) we showed that the simultaneous action of steroids and non-steroidal platinum(II) complexes is not the origin of the additional cytotoxicity).

Herein we will explore further the behaviour of conjugates of testosterone and otherwise inactive platinum(II) complexes in aqueous solution, with nucleobases, DNA and proteins using a variety of techniques, such as ESI-MS, NMR, gel electrophoresis and CD.

2.4.1 Effect of free steroid in DNA unwinding

Gel electrophoresis of negative-supercoiled and open-circle plasmid DNA can be used to assess unwinding of the DNA helix caused by platinum complexes[56-57]. Plasmid DNA produces two bands on agarose gels, a band of negatively-supercoiled DNA (SC) and another of open-circle DNA (OC). Upon binding of the complexes a retardation of the negatively-supercoiled band and an acceleration of the open-circle band are observed. These changes in migration speed would be consistent with bending/kinking of the DNA helix by the Pt centre leading to positive supercoiling of the plasmid which causes uncoiling of the negatively-supercoiled band and positive supercoiling of the open-circle band. Given enough complex binding to DNA these two bands co-migrate.

Using that point, unwinding angles can be quantified by applying the formula $\phi = -18\sigma / r_{(c)}$,[58] where, ϕ=unwinding angle, σ=superhelicity constant and r(c) = ratio (base:complex bound) where supercoiled and relaxed DNA co-migrate. Plasmid pBR322 was chosen, and using cisplatin, known to unwind the DNA by 13°[56], σ was determined to be -0.059. Complexes were incubated in different concentrations (between 30:1 to 2:1 base:complex ratio) with the plasmid for 24h, in the presence or absece of steroids (estradiol and testosterone; ratio steroid:complex 1:1). Mixing complexes with pBR322 resulted in changes to the migration of the plasmid bands, indicating all bind to DNA (as expected), and unwinding angles were calculated (Table 2.7).

Table 2.7. Unwinding angles of non-steroidal complex with and without ethisterone(EE) and 17α-ethynyl-estradiol (ET) in pBR322.

	Unwinding Angle	*Addition of EE*	*Addition of ET*
trans-[Pt(Py)Cl(NH_3)$_2$]$^+$	6.5º	6.5º	6.5º
trans-[Pt(QUI)Cl(NH_3)$_2$]$^+$	8.5º	8.5º	8.5º
cis-[Pt(Py)Cl(NH_3)$_2$]$^+$	6.5º	6.5º	6.5º
EE	0º	0º	0º
ET	0º	0º	0º

Addition of the steroid did not cause any effect on the close circular plasmid pBR322, and no additional effect was observed when the steroids were added to the non-steroidal complexes (Table 2.7). This explain that the dramatic DNA unwinding abilities previously observed for the steroid conjugated platinum(II) complexes (Table 2.1) are probably the result of the conjugation of the steroid to the platinum moiety, instead of combination of the effects produced by the non-conjugated units.

2.4.2 Studies with mononucleotides models

No significant differences are detected in the DNA distortions produced by cis and trans isomers that could explain the lower anticancer activity of the trans complexes. In order to further study how the different isomers bind to DNA, the interactions with model nucleobases such as 9-ethylguanine (9EG) and guanosine 5'monophosphate were studied (Fig 2.15). NMR and ESI-MS were used to investigate the interaction.

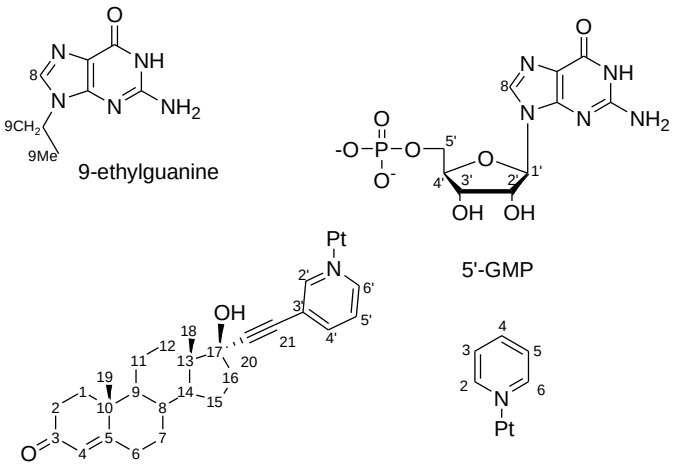

Figure 2.15. The structure of a steroidal, a non-steroidal platinum(II) complex, 5'-GMP and 9EG.

ESI-MS studies:

An initial study by a colleague had shown that adducts with bound nucleobases could be detected by ESI-MS. In addition a deprotonated hydrolytic product was also observed[40].

Those studies were performed in TAE buffer, a system without the presence of Cl^- anions that can affect the hydrolysis of the complexes and lately their DNA binding. However, since some Cl^-, around 4mM[59], is present inside the cell, here we chose to study how presence of Cl^- affects DNA binding. Cis and trans-$[Pt(2ET)Cl(NH_3)_2]^+$ and cis and trans-$[Pt(Py)Cl(NH_3)_2]^+$ were treated with 5'-GMP for 72 h, in presence of chloride in sodium cacodylate buffer (pH 6.8). Sodium cacodylate is an arsenic derived buffer used for DNA interaction studies that have a small amount of Cl^- ions (around one fith of the concentration of the buffer for pH used). ESI mass spectra confirm that mono-functional adducts are formed for all the complexes. No deprotonated hydrolysis products are observed for cis isomers, while it is the main peak for trans isomers.

Table 2.8. ESI-MS peaks found for the reaction of the studied complexes and mononucleotides 5'-GMP and 9-EG.

	+ 5' GMP in TAE (Martin Huxley)[40]		+ 5' GMP in sodium cacodylate		+ 9-EG in sodium cacodylate	
	$[Pt(NH_3)_2(L)(5'\text{-}GMP)]^+$	$[Pt(NH_3)_2(L)(OH_2)]^+\text{-}(H^+)$	$[Pt(NH_3)_2(L)(5'\text{-}GMP)]^+$	$[Pt(NH_3)_2(L)(OH_2)]^+\text{-}(H^+)$	$[Pt(NH_3)_2(L)(9\text{-}EG)]^+$	$[Pt(NH_3)_2(L)(OH_2)]^+\text{-}(H^+)$
trans-$[Pt(2ET)Cl(NH_3)_2]^+$	+	+	+	+	+	+
cis-$[Pt(2ET)Cl(NH_3)_2]^+$	+	+	+	-	+	-
trans-$[Pt(Py)Cl(NH_3)_2]^+$	+	+	+	+	+	+
cis-$[Pt(Py)Cl(NH_3)_2]^+$	+	+	+	-	+	-

The same experiment was repeated with 9-EG to observe possible effect of the phosphate and sugar ring and showed similar results to 5'-GMP (Table 2.8).

NMR studies:

To understand these MS results better, the same compounds were also investigated by NMR, adding 5'-GMP in presence of sodium cacodylate buffer. Fig. 2.16 shows representative spectra for cis and trans-$[Pt(2ET)Cl(NH_3)_2]^+$ with GMP at 0 and 24h.

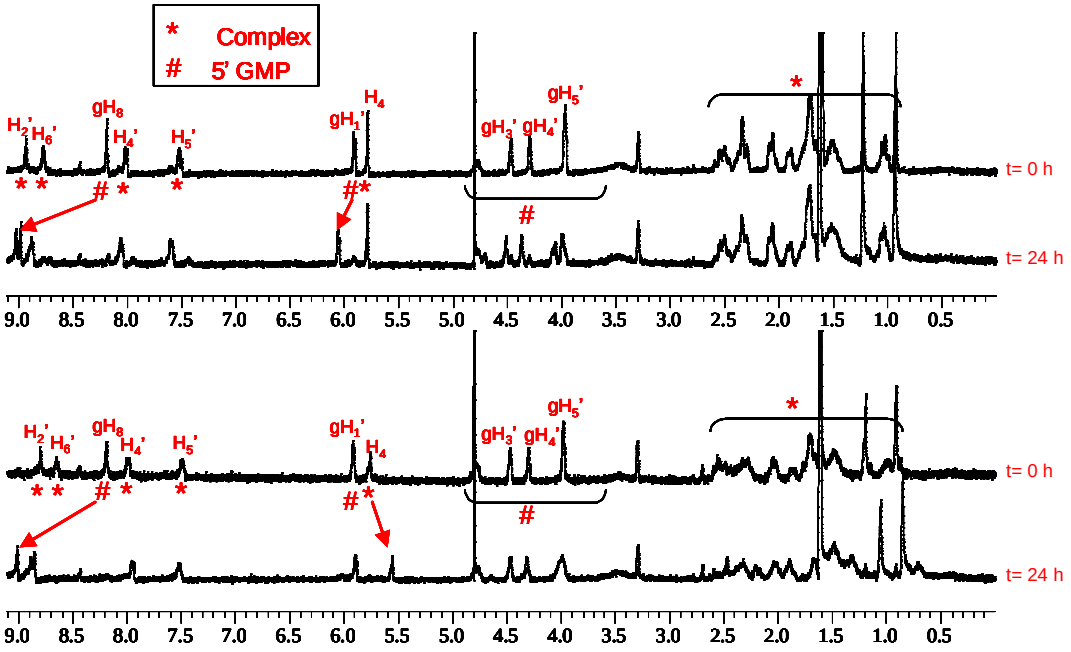

Figure 2.16. ^1H NMR spectra for cis-$[Pt(2ET)Cl(NH_3)_2]^+$ (bottom) and trans-$[Pt(2ET)Cl(NH_3)_2]^+$ (top) with 5'-GMP in 1mM sodium cacodylate buffer in D_2O (pH 6.8) and 1:1 nucleotide:complex ratio.

Changes to resonances of 5'-GMP and those of pyridine protons are clearly observed in both sets of spectra. The dramatic shift of the gH_8 proton of 5'-GMP in Figure 2.16 (both complexes) is strongly indicative of platinum binding to the N^7 of the guanine ring[60] and the reaction is complete after 24 hours (as no unbound gH_8 is visible anymore). The binding to the trans-$[Pt(2ET)Cl(NH_3)_2]^+$ results in shifting of the gH_1', gH_3' and gH_4' to lower field and splitting of the resonance ascribed to gH_5' indicating the furanose ring is affected (Table 2.9) (gH_2' was not detected as result of their similar chemical shift to water). For cis-$[Pt(2ET)Cl(NH_3)_2]^+$ the sugar ring protons show no effect for gH_3' and gH_4' and only minor effects on gH_1' (upfield 0.03ppm) and gH_5' (same chemical shift but broad). The shifts of the aromatic proton resonances of the pyridine ring support 5'-GMP binding with complexes, with all signals of trans-$[Pt(2ET)Cl(NH_3)_2]^+$ moving between 0.09 and 0.06 downfield. cis-$[Pt(2ET)Cl(NH_3)_2]^+$, meanwhile, shows a similar effect for H_2' (0.05ppm) and H_5' (0.03ppm), but H_4' moves 0.04ppm upfield, and more dramatically H_6' moves downfield by 0.23ppm (probably because of proximity of GMP). Finally, to our surprise, upfield shifts are clearly

observed for H_4 (a proton with a really stable chemical shift compared with other steroidal or aromatic protons of the ligands) and Me_{18} and Me_{19} of the testosterone skeleton for cis-$[Pt(2ET)Cl(NH_3)_2]^+$ but not trans-$[Pt(2ET)Cl(NH_3)_2]^+$. The 3-position of ethynyltestosterone on pyridine and the cis geometry around the platinum(II) centre appear to bring the steroidal skeleton close to 5'-GMP. The non-steroidal complexes behave in a similar way and their NMR spectra can be seen in Figs 2.17 and 2.18.

Table 2.9. Chemical shifts of more important protons of studied complexes in presence of 5'-GMP, 9-EG, alone and hydrolytic products.

	H_4	Me_{18}	Me_{19}	H_2'	H_4'	H_5'	H_6'	$pyH_{2/6}$	$pyH_{3/5}$	pyH_4	gH_8	gH_1'	gH_3'	gH_4'	gH_5'	$9H_8$	$9CH_2$	9Me
GMP											8.18	5.92	4.47	4.30	3.97			
9EG																7.75	3.99	1.32
2ET-cis	5.79	0.9	1.21	8.79	8	7.5	8.65											
2ET-cis hydrolysis	5.79	0.9	1.21	8.79	8	7.5	8.65											
2ET-cis GMP	5.59	0.85	1.05	8.85	7.96	7.53	8.88				9.01	5.89	4.47	4.30	4broad			
2ET-cis 9EG	5.69	0.88	1.15	8.73	7.98	7.5	8.71									8.22	3.98	1.25
2ET-trans	5.79	0.94	1.23	8.94	8.01	7.53	8.77											
2ET-trans hydrolysis	5.79	0.94	1.23	8.86	7.94	7.44	8.71											
2ET-trans GMP	5.79	0.94	1.24	9.02	8.07	7.6	8.88				8.97	6.05	4.51	4.36	4.00/4.06			
2ET-trans 9EG	5.79	0.94	1.23	9	8.09	7.6	8.84									8.30	4.10	1.38
Py-cis								8.7	7.53	7.99								
Py-cis hydrolysis								8.7	7.53	7.99								
Py-cis GMP								8.76	7.41	7.89	8.98	5.96	4.47	4.34	4/4.02			
Py-cis 9EG								8.67	7.49	7.99						8.20	3.99	1.26
Py-trans								8.82	7.54	8								
Py-trans hydrolysis								8.76	7.46	7.92								
Py-trans GMP								8.9	7.62	8.05	8.96	6.07	4.51	4.37	4/4.06			
Py-trans 9EG								8.89	7.61	8.06						8.30	4.11	1.39

Cis and trans-$[Pt(Py)Cl(NH_3)_2]^+$ bind to N^7 of 5'-GMP as shown by downfield shift of gH_8. For trans-$[Pt(Py)Cl(NH_3)_2]^+$ (Fig. 2.17) downfield shifts between 0.06 and 0.08 ppm are observed for all the pyridine proton resonances (almost exactly as observed for trans-$[Pt(2ET)Cl(NH_3)_2]^+$). Furanose ring protons gH_1', gH_3', gH_4' and gH_5' (showing split of the signal) move downfield as well (similar to the shifts produced by trans-$[Pt(2ET)Cl(NH_3)_2]^+$). The similar chemical shifts displacements observed in the nucleotide sugar ring and the complexes pyridine upon binding to 5'-GMP of trans isomers could indicate that the interaction responsible of the modification of the furanose ring does not depend of the presence of the steroid.

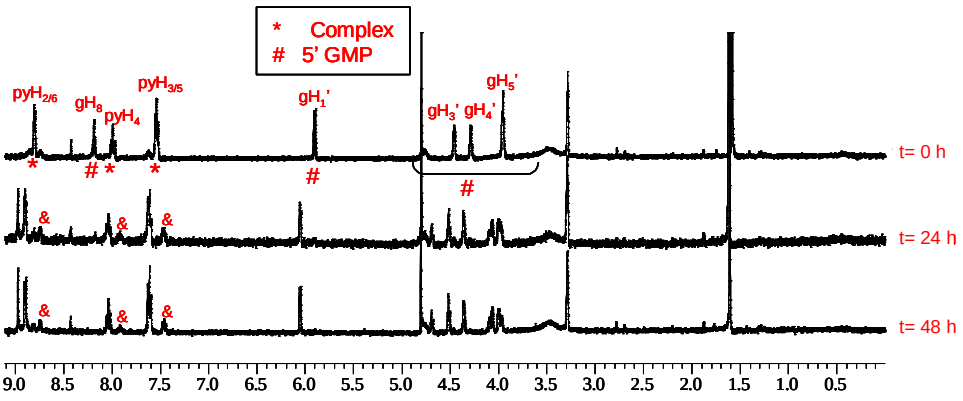

Figure 2.17. ^1H NMR spectra for trans-$[Pt(Py)Cl(NH_3)_2]^+$ with 5'-GMP in 1mM sodium cacodylate buffer in D_2O (pH 6.8) and 1:1 nucleotide:complex ratio. &, this set of peaks will be addressed below in this section.

This is partially reinforced by the fact that, for cis-$[Pt(Py)Cl(NH_3)_2]^+$, the furanose gH_3' and gH_5' show a similar effect to cis-$[Pt(2ET)Cl(NH_3)_2]^+$ (no effect), although the other two protons (gH_1' and gH_4') show downfield shifts of around 0.05 ppm, like the trans compounds (Fig. 2.18). Cis-$[Pt(Py)Cl(NH_3)_2]^+$ pyridine protons pyH_4 and $pyH_{3/5}$ move upfield (around 0.1ppm), meanwhile $pyH_{2/6}$ is downfield shifted around the same amount. This is not observed for trans complexes or for the cis steroidal derivative. However, a similar upfield effect can be observed in the steroidal skeleton of cis-$[Pt(2ET)Cl(NH_3)_2]^+$ and can be indicative that the cis symmetry induces the pyridine (or the steroid in case of our testosterone coupled complex) to be closer to the 5'-GMP (probably to the nucleobase due to the lack of modification of the furanose ring protons).

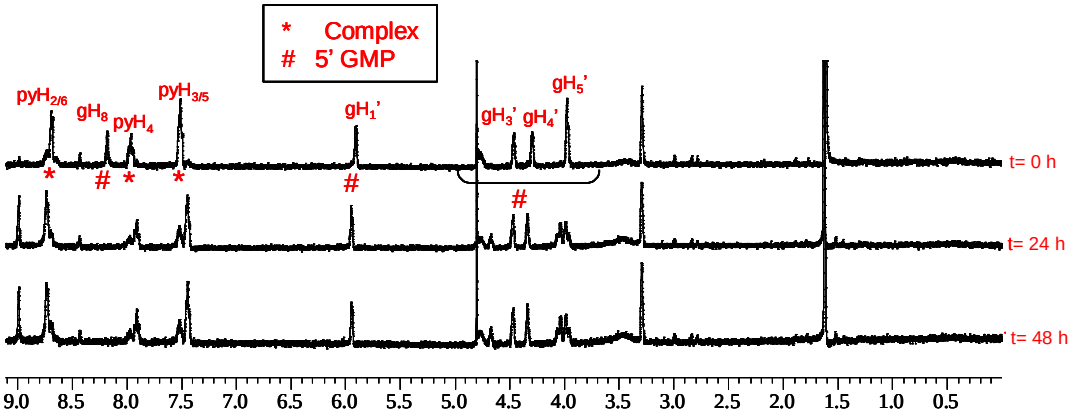

Figure 2.18. ^1H NMR spectra for cis-$[Pt(Py)Cl(NH_3)_2]^+$ with 5'-GMP in 1mM sodium cacodylate buffer in D_2O (pH 6.8) and 1:1 nucleotide:complex ratio.

To further prove the former hypothesis while excluding any interference of the phosphate and furanose group, the complexes were also mixed with 9-EG and the reaction followed by ^1H NMR (Figs. 2.19 to 2.22). Mixing with 9-EG resulted in the downfield shift of the $9H_8$' resonance from 7.75 ppm to 8.20 ppm (cis isomers, Figs. 2.20 and 2.21) and 8.30 ppm (trans isomers, Figs. 2.19 and 2.22); indicating again platinum binding directly via N^7. Differences in the spectra of the cis and trans complexes indicate the binding arrangements are very different, as found when using 5'-GMP. The spectra of trans isomers (both trans-$[Pt(2ET)Cl(NH_3)_2]^+$ (Fig. 2.22) and trans-$[Pt(Py)Cl(NH_3)_2]^+$ (Fig. 2.19)) and 9-EG, show the same downfield shift of pyridine resonances in similar values observed for 5'-GMP (around 0.1 ppm) and the downfield alterations for the methyl and methylene groups of the 9-EG. However, cis isomers (both cis-$[Pt(2ET)Cl(NH_3)_2]^+$ (Fig. 2.21) and cis-$[Pt(Py)Cl(NH_3)_2]^+$ (Fig. 2.20))

show upfield alterations for 9Me methyl group and no modifications for the methylene group $9CH_2$. This confirms that the interaction of the studied complexes with the sugar ring probably occurs through the pyridine ring (for both cis and trans complexes) and is more related with the spatial position of that ring in the complex than with the presence or not of steroid. Also, both cis-$[Pt(Py)Cl(NH_3)_2]^+$ and cis-$[Pt(2ET)Cl(NH_3)_2]^+$ show upfield shifts for their pyridine resonances (cis-$[Pt(Py)Cl(NH_3)_2]^+$) or steroid skeleton (cis-$[Pt(2ET)Cl(NH_3)_2]^+$) when bound to 9EG. This behaviour in absence of the phosphate and furanose ring tells us that these displacements of the chemical shifts of the steroidal skeleton for cis-$[Pt(2ET)Cl(NH_3)_2]^+$ can be caused by a possible stack with the nucleobase of the mononucleotide.

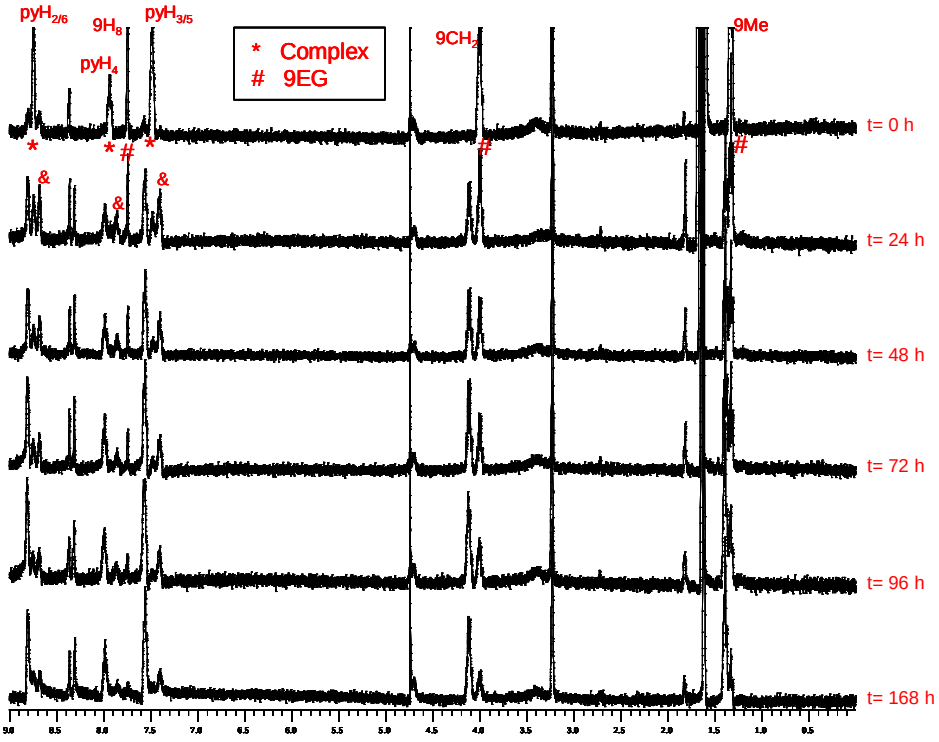

Figure 2.19. ^1H NMR spectra for trans-$[Pt(Py)Cl(NH_3)_2]^+$ and 9-EG in 1mM sodium cacodylate buffer in D_2O (pH 6.8) and 1:1 nucleotide:complex ratio. &, this set of peaks will be addressed below in this section.

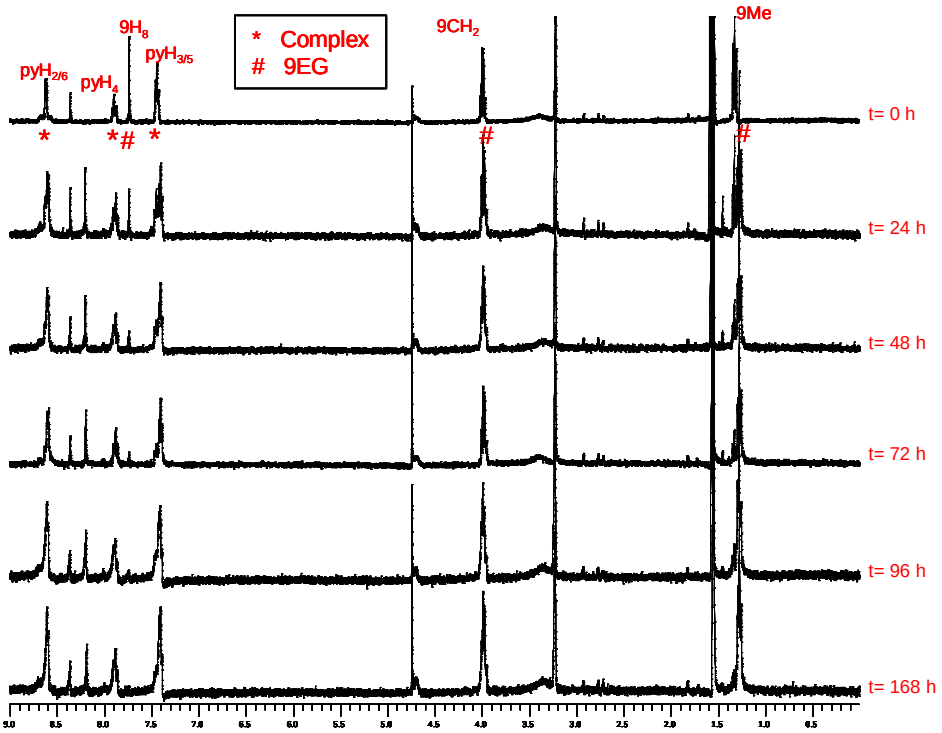

Figure 2.20. ^{1}H NMR spectra for cis-[Pt(Py)Cl(NH_3)$_2$]$^{+}$ with 9-EG in 1mM sodium cacodylate buffer in D_2O (pH 6.8) and 1:1 nucleotide:complex ratio.

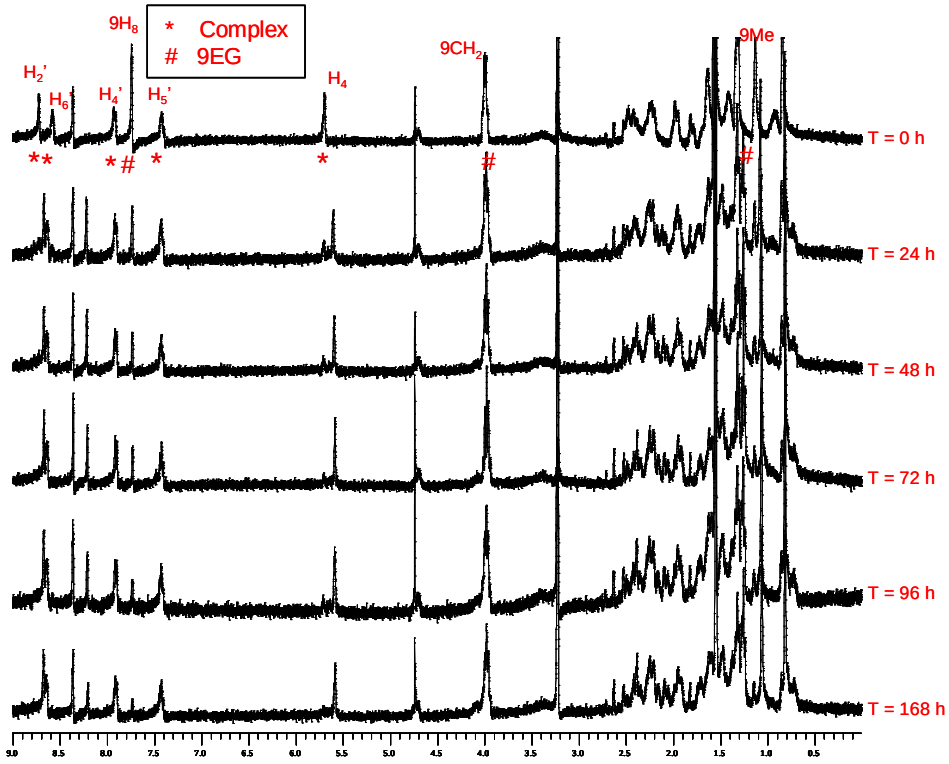

Figure 2.21. ^{1}H NMR spectra for cis-[Pt(2ET)Cl(NH_3)$_2$]$^{+}$ with 9-EG in 1mM sodium cacodylate buffer in D_2O (pH 6.8) and 1:1 nucleotide:complex ratio.

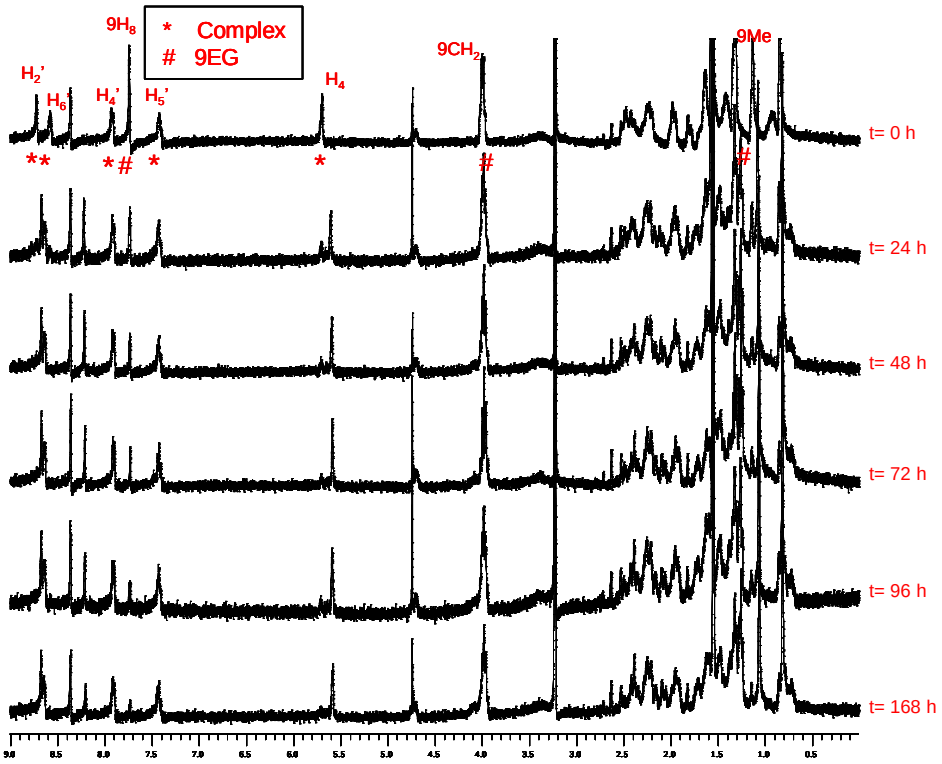

Figure 2.22. ^{1}H NMR spectra trans-[Pt(2ET)Cl$(NH_3)_2$]$^{+}$ (bottom left) with 9-EG in 1mM sodium cacodylate buffer in D_2O (pH 6.8) and 1:1 nucleotide:complex ratio. &, this set of peaks will be address below in this section.

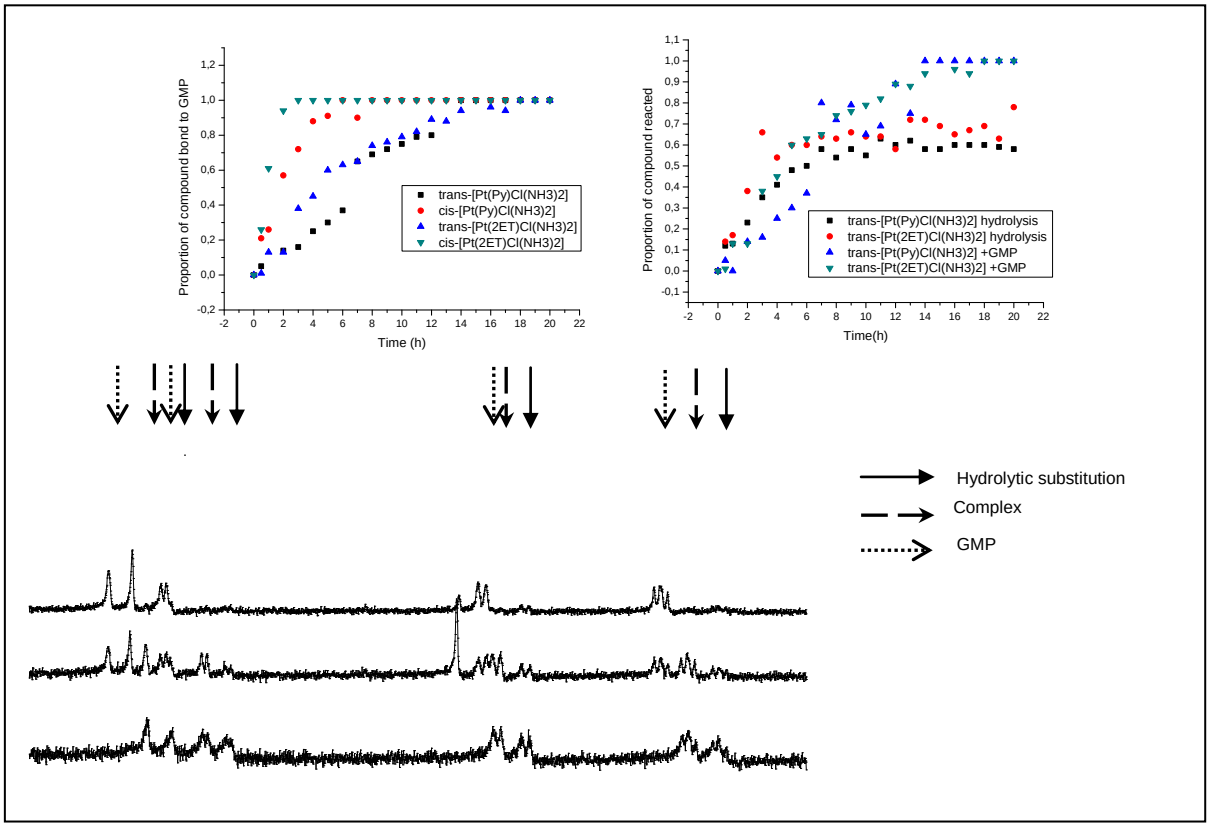

Figure 2.23. A) Rate of appearance of 5'-GMP adducts (left) and comparison of hydrolysis and 5'-GMP appearance for trans isomers (right). B) ^{1}H NMR spectra of trans-[Pt(2ET)Cl$(NH_3)_2$]$^{+}$ (lower), trans-[Pt(2ET)Cl$(NH_3)_2$]$^{+}$ in sodium cacodilate after 5 hours (second), trans-[Pt(2ET)Cl$(NH_3)_2$]$^{+}$ in sodium cacodilate with 5'-GMP after 5 hours (third), and trans-[Pt(2ET)Cl$(NH_3)_2$]$^{+}$ in sodium cacodilate with 5'-GMP after 24 hours (upper)

When the reaction between the complexes and 5'-GMP is followed in time, we see that interaction between cis-$[Pt(2ET)Cl(NH_3)_2]^+$ and 5'-GMP is substantially complete in 3 hours, whilst the reaction between trans-$[Pt(2ET)Cl(NH_3)_2]^+$ and 5'-GMP requires around 18 hours. Similar results are observed for the non-steroidal analogues. However, binding is a bit slower, indicating that the steroid may have some effect on the kinetics (graph Fig. 2.23). It is interesting to note that during this experiment only a single set of new resonances is detected for the cis isomers, while two new products are seen for the trans ones (Fig. 2.23, and peaks marked as $^{\&}$ previously in this section).

Because ESI shows hydrolysis for the trans isomers and not for cis isomers, the same experiment was repeated without mononucleotide (just in buffer), to detect if this second set of signals is hydrolysis. The NMR of the cis compounds (Figs. 2.25 and 2.27) are not modified, while the trans ones (Figs. 2.24 and 2.26) show a different set of signals that coincide with previous ones. Thus confirming then that cis isomers do not show hydrolysis while the trans complexes do. The lack of hydrolysis products for the cis geometry complexes might suggest that this geometry hinders substitution reactions. Moreover, NH_3 and pyridine ligands, in cis and trans-$[Pt(2ET)Cl(NH_3)_2]^+$, respectively have very similar ability to labilise the chloride ligand trans to them and the noticeably shorter reaction time of cis-$[Pt(2ET)Cl(NH_3)_2]^+$ compared to trans-$[Pt(2ET)Cl(NH_3)_2]^+$ with 5'-GMP is unlikely to arise from that effect. The fact that the kinetics of the hydrolysis in trans complexes is almost identical to the kinetics of binding to 5'-GMP (Fig. 2.23), can be taken as trans and cis isomers have different mechanism of binding to DNA, with the trans first undergoing hydrolysis and the cis reacting directly with the nucleobase.

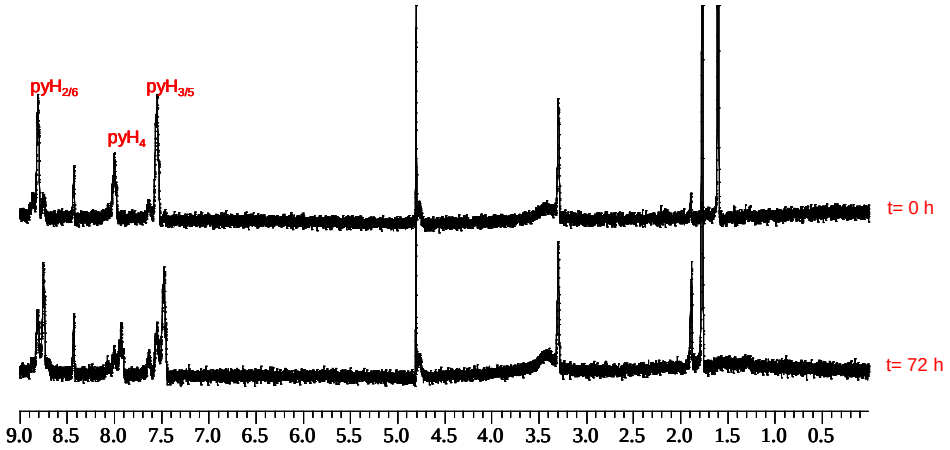

Figure 2.24. ^1H NMR spectra for trans-$[Pt(Py)Cl(NH_3)_2]^+$ hydrolysis in 1mM sodium cacodylate buffer in D_2O (pH 6.8) and 1:1 nucleotide:complex ratio.

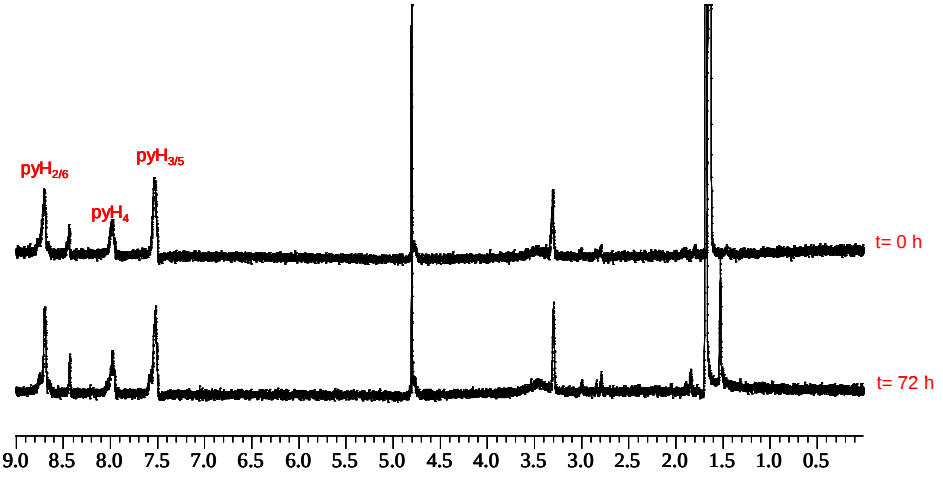

Figure 2.25. ^{1}H NMR spectra for cis-[Pt(Py)Cl(NH_3)$_2$]$^{+}$ hydrolysis in 1mM sodium cacodylate buffer in D_2O (pH 6.8) and 1:1 nucleotide:complex ratio.

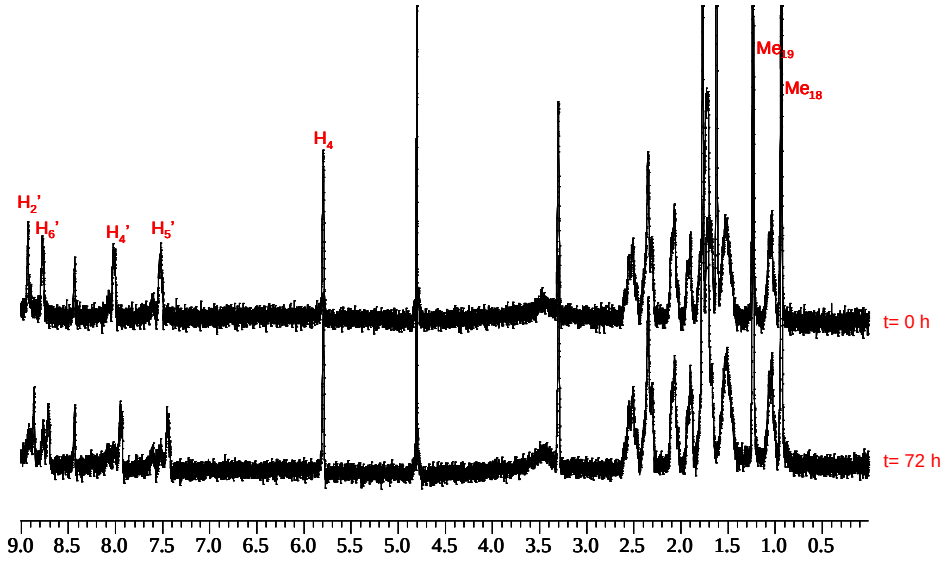

Figure 2.26. ^{1}H NMR spectra trans-[Pt(2ET)Cl(NH_3)$_2$]$^{+}$ hydrolysis in 1mM sodium cacodylate buffer in D_2O (pH 6.8) and 1:1 nucleotide:complex ratio.

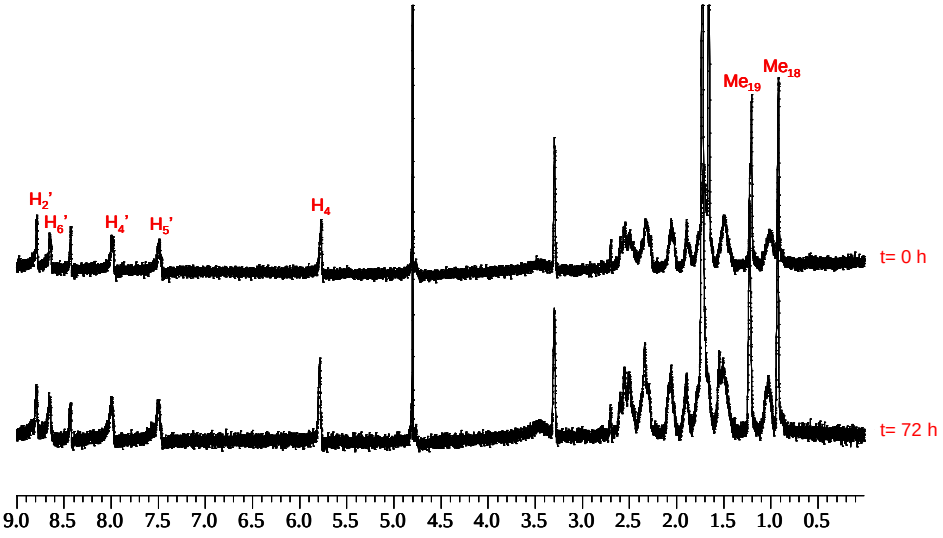

Figure 2.27. ^{1}H NMR spectra for cis-[Pt(2ET)Cl(NH_3)$_2$]$^{+}$ hydrolysis in 1mM sodium cacodylate buffer in D_2O (pH 6.8) and 1:1 nucleotide:complex ratio.

In summary, all the compounds bind to nucleobases, but the manner of the reaction and effects on the sugar ring seems to be more related to the geometric isomer than to the presence or absence of the steroid. The speed of the binding is also principally dependent on the isomer, although the steroid does have some effect, enhancing the rate of reaction. The cis conformation brings the steroidal ligand and nucleobase closer together as expected and demonstrated by the steroidal skeleton alterations created by the mononucleotides. The retention of these modifications without the presence of sugar ring seems to indicate a possible interaction with the guanine rings. The ability to bind to nucleobases is a good predictor that these complexes will bind to DNA and this was explored next.

2.4.3 Studies with DNA

Circular Dichroism:

CD measures the difference of absorption in left and right circularly polarised light, and when performed using macromolecules can be used to report changes in the conformation of the macromolecule itself, and to prove information on its interaction with small molecules, particularly by confering induced CD (ICD) signals in the spectroscopy of the small molecule[61]. When a titration of ct-DNA with our complexes was recorded by CD, the first thing observed was that the B-DNA conformation is retained with non-steroidal complexes. B-DNA is marked by a characteristic positive CD band centred at 275 nm, and a negative band at 250 nm, with the zero being around 260 nm (Fig. 2.28).

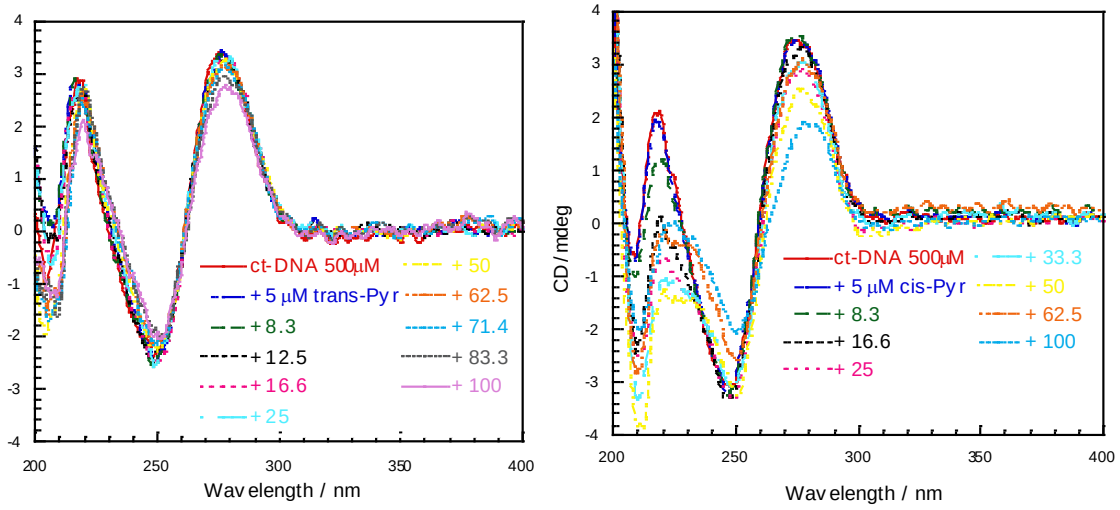

Figure 2.28. ct-DNA CD titration with cis-$[Pt(Py)Cl(NH_3)_2]^+$ (right) and trans-$[Pt(Py)Cl(NH_3)_2]^+$ (left). (Michael Browning)[41].

When ct-DNA is titrated with the steroidal complexes dramatic alterations in the 200-300 nm region compared with non-steroidal compounds are observed. These modifications are different for cis and trans geometries, showing again the possibility of different DNA interacting modes (Fig. 2.29). However, the testosterone molecule coupled to the metallic centres make the complexes chiral, therefore they have their own CD spectrum. For that reason the titration spectra would be a combination of ct-DNA and the complexes CD absorbance, making impossible to obtain any DNA conformational information.

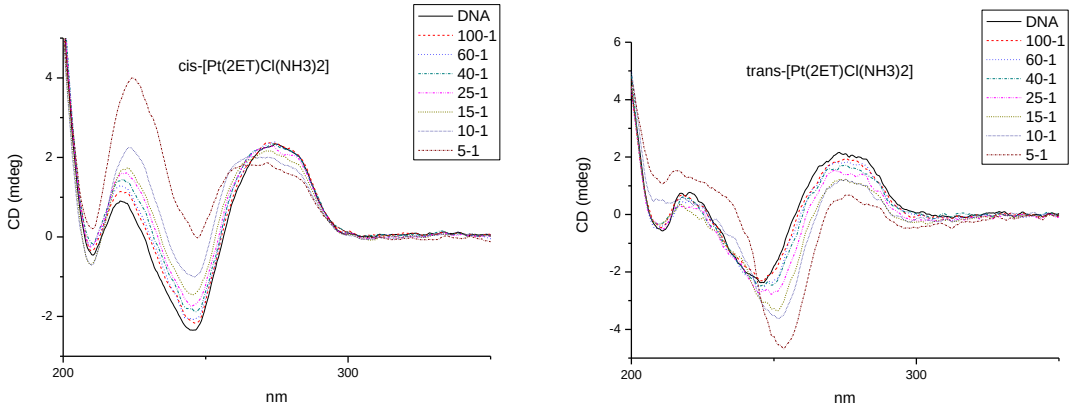

Figure 2.29. ct-DNA CD titration with cis and trans-$[Pt(2ET)Cl(NH_3)_2]^+$.

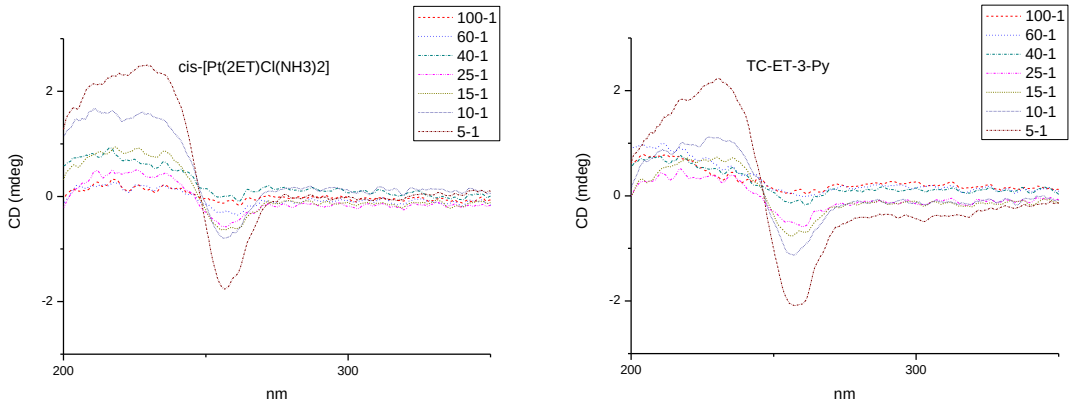

Figure 2.30. CD titration with cis and trans-$[Pt(2ET)Cl(NH_3)_2]^+$.

When the CD spectra of both cis and trans-$[Pt(2ET)Cl(NH_3)_2]^+$ are measured under the same conditions and concentrations of the different titration points Fig.2.30 is produced. As expected, both complexes show similar CD absorbance, due to the fact that the chirality is introduced by the ethisterone molecule, common to both of them. Subtracting this set of spectra from the initial ct-DNA tritation, information about DNA conformation modifications could perhaps be obtained. Fig. 2.31 shows the corrected

DNA titration, where DNA binding modes for both complexes can still be observed. However, major modifications of the ct-DNA spectrum are observed where cis and trans-$[Pt(2ET)Cl(NH_3)_2]^+$ present CD absorbance bands, so no conformational information is available.

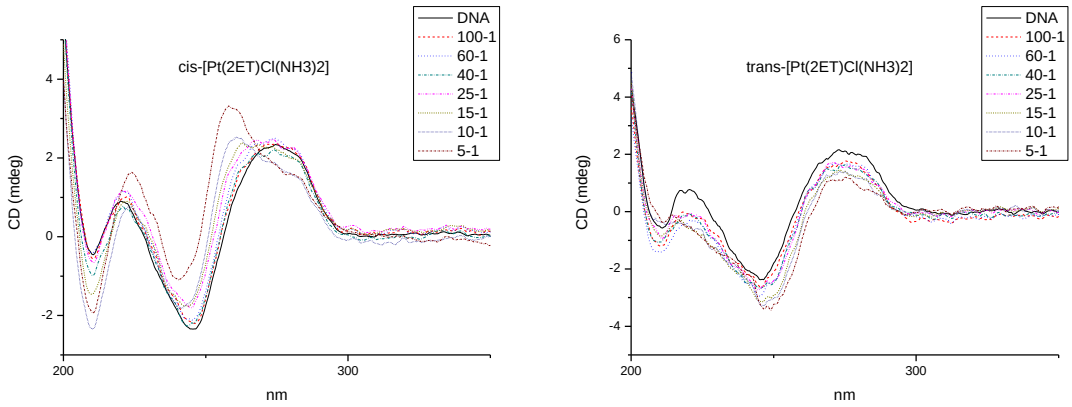

Figure 2.31. Corrected ct-DNA CD titration with cis and trans-$[Pt(2ET)Cl(NH_3)_2]^+$.

The induced CD (ICD) signals produced in the titration (subtracting from the original spectrum all the chiral components) are different for cis and trans-$[Pt(2ET)Cl(NH_3)_2]^+$ (Fig. 2.32). It is noticeable as well the fact that both ICD show similar mirror image patterns with different intensities (the cis isomer shows higher intensity than the trans). This fact could indicate a possible difference in the steroid orientation towards the DNA, induced upon binding of cis or trans isomers (as steroid position in the complex is different). Higher ICD intensities could indicate as well that the cis geometry bring the testosterone closer to the DNA, as suggested in 2.4.1. These differences in the DNA binding mode between cis and trans isomers (presented here and in section 2.4.1) could be the reason of the difference in activity observed between the two geometries (togheter with the substantial differences in rates of binding and hydrolysis).

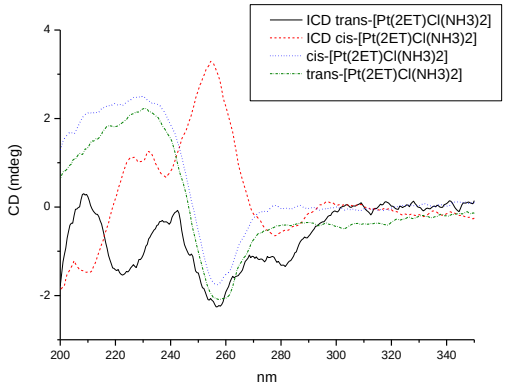

Figure 2.32. ICD of ct-DNA CD titration with cis and trans-$[Pt(2ET)Cl(NH_3)_2]^+$.

2.4.4 Studies with proteins

Steroids are biomolecules with an important role in the organism, showing different actions around the body[62-64]. Most of them are due to their interaction with proteins, controlling their transport around the body[65], metabolism[66] or activity[67] (through their own nuclear receptors). One of the most important groups of proteins in steroids regulation are the AKRs (aldo-Keto reductases), a family of cytosolic NADPH dependent proteins that reduce aldehydes and ketones to their correspondent primary and secondary alcohols. There are 13 human subfamilies of them, with different substrates and function[68]. Of particular interest to us is the subfamily of AKR1C that catalyze the reduction of ketosteroids to hydroxysteroids in both 3 (3β-HSD and 3α-HSD action) and 17 positions (17α-HSD)[69] (Fig. 2.33), and which are able to regulate the occupancy of steroid receptors in determinated tissues[69]. This is done upon the direct regulation of the amount of steroids available in the cell, transforming them into products with lower receptor affinities (sometimes even 5 orders of magnitude lower[70]), that can lead to the final elimination of the steroids. They are also known to be important in the role of androgens in prostate cancer[71]. Four different forms of this subfamily have been detected, with different targets and tissue distribution (Table 2.10).

Figure 2.33. Possible tranformations catalyzed by AKRs in estradiol and testosterone.

	Activity	Receptor regulated
AKR1C1	20α-HSD, 3β-HSD, 3α-HSD	PR, ERβ
AKR 1C2	3α-HSD	AR
AKR1C3	17α-HSD, 3α-HSD	AR, ERα
AKR1C4	3α-HSD	Hepatic clearance of steroids

Table 2.10. Activities of AKRs and Receptors regulated.

In modifying the structure of steroids (adding the Pt complexes) there is a risk of the modified molecules loosing their capacity to interact with their natural receptors. It is known that steroidal complexes can interact with Human serum albumin[29], and with their receptors with different efficiencies[23-28]. However, what has not been studied is how such compounds might interact with AKRs regulatory proteins that can transform them inside the cell, or even help with excretion. Indeed potential metabolism of steroidal metal complexes has not been considered previously. For that reason it is of interest to see how our complexes interact with this kind of proteins. Herein, two different kinds of experiments are investigated (AKRs provided by Dr. Chris Bunce group, School of Biosciences, University of Birmingham); first we check by HPLC whether our complex can be reduced by these proteins. Second, we undertake enzymatic studies in order to determinate their abilities as inhibitor and substrate for AKRs.

HPLC experiments:

Our first experiment was to measure the disappearance of complex and appearance of metabolite in a reaction at room temperature. This would tell us if the complex were metabolized, if so into how many products (and maybe which products) and how rapidly. The different species were detected with the same HPLC method used to purify the complexes (Water:Methanol (0-100%) gradient for 40 minutes, with the use of TFA; retention time around 30 minutes). The experiment was undertaken for cis-$[Pt(2ET)Cl(NH_3)_2]^+$ since it was the most active complex, and for the four AKR1Cs. Recombinant enzyme was treated with cis-$[Pt(2ET)Cl(NH_3)_2]^+$ and NADPH. The final volume was taken to 2 ml with KH_2PO_4 Buffer. The order of addition was Buffer, enzyme, substrate and NADPH. Samples were taken and injected into HPLC every hour for 24 hours and followed at 254 nm. As controls, the same experiment was repeated with AKR1C3 for ethisterone and 9,10-phenanthrenequinone.

At time 0 h two main peaks appear in the chromatograph; NADPH (around 9.7 min) and cis-$[Pt(2ET)Cl(NH_3)_2]^+$ (30.1 min). For all four AKRs after a few hours these peaks start to decrease in magnitude and two new peaks appear both running around 2 minutes faster in the chromatograph (7.5 and 28.6 min) (Fig. 2.34 and 2.35). When the two peaks around 30 minutes (28.6 and 30.1 min) were collected and analysed by ESI-MS, the second one (at 30.1 min) corresponds to the expected starting material (our complex). The one at 28.6 min. shows a similar mass, rather than the expected reduced species; this can be due to reoxidation of the compound once separated (although trifuoroacetic acid can act as an oxidant in presence of metals[72], or maybe occurs as a result of too strong ESI-MS ionization). However, the different retention time marks the increased polarity of the product, suggestive of a reduction.

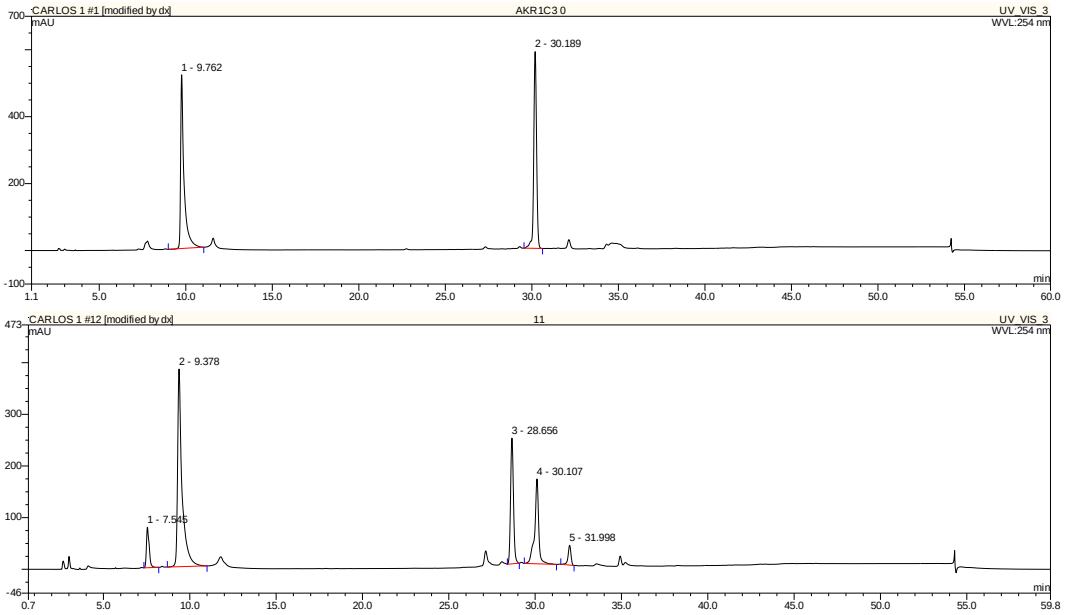

Figure 2.34. HPLC chromatographs of cis-$[Pt(2ET)Cl(NH_3)_2]^+$ with AKR1C3 at t = 0 (top) and t = 1 h (bottom).

This indicated that the complex was a possible substrate for all of the AKR1Cs studied. When appearance of metabolite and disappearance of substrate (our complex) were plotted against time (Fig. 2.36) we could see that the four enzymes produced the main metabolite at almost the same rate (AKR1C3 a bit slower). 50% of the transformation (metabolite produced) is complete in around 13 hours, except for AKR1C3 where only 45% of the substrate transformation is reached even at 22 hours. This is interesting since AKR1C3 regulates the access of steroids to AR and ERα. However, if we observe the rate of disappearance of starting material, this is somewhat different from what we would expect. As expected, for most of the AKR1Cs a

"stationary phase" is reached between 11 and 13 hours. However, this only occurs for AKR1C2 (responsible of regulation of AR) when 50% of the starting material has disappeared. Meanwhile, for both AKR1C1 and 3 the "stationary phase" is reached when between 40 and 30% of starting material is remaining, indicating possible presence of secondary products. For AKR1C4 this is not observed, probably due to technical errors.

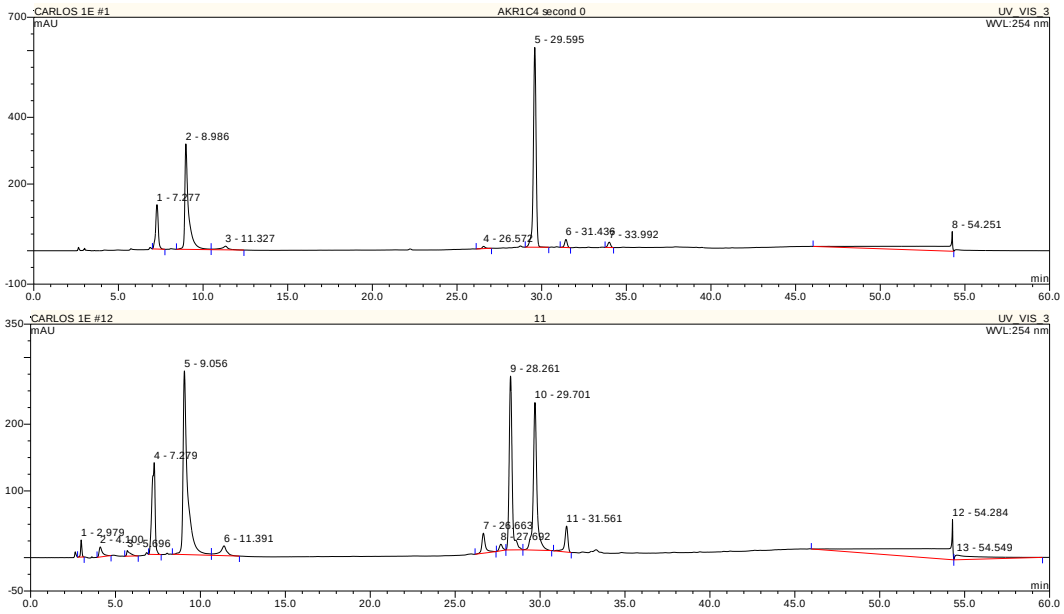

Figure 2.35. HPLC chromatographs of cis-$[Pt(2ET)Cl(NH_3)_2]^+$ with AKR1C4 at t = 0 (top) and t = 1 h (bottom).

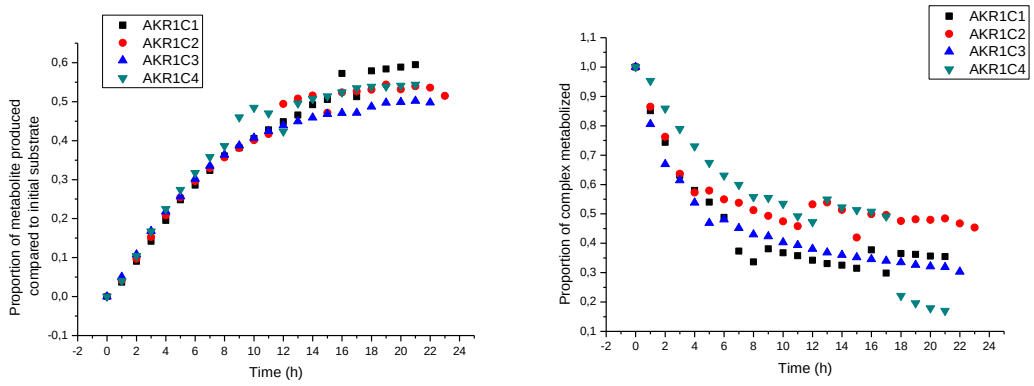

Figure 2.36. Rate of appearance of AKR1C metabolic product (left) and disappearance of cis-$[Pt(2ET)Cl(NH_3)_2]^+$ (right).

Two controls were used, to check the effect of the presence of the metallic centre; a good substrate phenanthrenequinone, and ethisterone (as a simple androgen, to see the direct effect of the metallic centre). Even at room temperature, both phenanthrenequinone and ethisterone proved to be much better substrates, disappearing totally in 1 h. Remarkably, the change in the retention time showed by the metabolized

ethisterone (travel 1.7 min. faster) is similar to the one observed when cis-$[Pt(2ET)Cl(NH_3)_2]^+$ is used (travel 1.5 min faster), confirming the transformation of our complex and indicating that an analogous product is obtained (Fig. 2.37). This experiment proves that the introduction of the metallic centre causes a major decrease in the rate at which normal steroidal metabolic proteins modify the complex. While these initial results are informative they were conducted at room temperature.

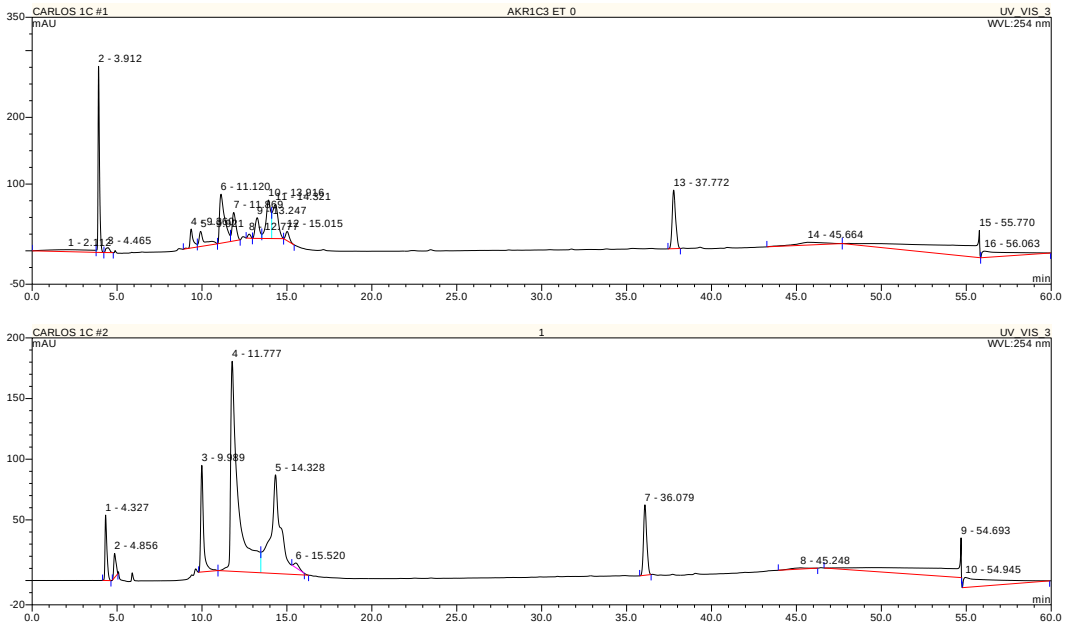

Figure 2.37. HPLC chromatographs of ethisterone with AKR1C3 at t = 0 (top) and t = 1 h (bottom).

Enzymatic experiments:

In order to understand more about the interaction of cis-$[Pt(2ET)Cl(NH_3)_2]^+$ with these proteins further experiments were conducted under physiological conditions. Our compound is toxic, making difficult to understand fully the interaction with proteins using data from cellular assays. For that reason an *in vitro* experiment using similar conditions to the physiologically found was considered our best option. This would give an idea about how they interact under similar conditions to the ones found in the cell, and would be closer to reality than the HPLC experiments. The four AKR1Cs used previously, were treated with different concentrations of cis-$[Pt(2ET)Cl(NH_3)_2]^+$ (from 40 µM to 0.313 µM), and the rate of disappearance of NADPH noted (UV absorbance at 340 nm). Reactions were done at 35ºC in phosphate buffer. In the first attempt, no turnover was observed over a 5 minutes time for any of the enzymes, indicating that the compound was a poor substrate for them. In order to improve activity, we repeated the experiment using four times the concentration of enzymes. This time turnover was

observed (Fig. 2.38), but it was quite slow, confirming that the compound was a poor substrate for the enzymes. However, K_m values (Table 2.11; Michaelis-Menten constant, obtained from the Michaelis-Menten kinetic equation $v_0=(v_{max}[S])/(K_m+[S])$ defined as the concentration of substrate [S] at which the v_0 is half of v_{max} and is indicative of the affinity of the active centre of the enzyme for the substrate) indicate that the presence of the metallic centres do not affect their affinity towards the AKR1Cs enzymes, showing rate constant values in the range of naturally occurring strong androgens (5α-dihydrotestosterone)[73]. However, the transformation rate of cis-$[Pt(2ET)Cl(NH_3)_2]^+$ per unit of enzyme (k_{cat}; Table 2.11; catalytic rate constant, defined as the amount of substrate [S] transformed per unit of enzyme and time; $k_{cat}=(v_{max}/[E]_0)$) was between 20 and 30 times lower than for 9.10-phenanthrenequinone and 4 times lower than for 5α-dihydrotestosterone[73]. These results indicate that even if it is possible for the complexes to be turned over by AKR1Cs in the cells, this process is quite slow. For that reason it is quite unlikely that the cytotoxicity of our complexes is significantly directed by the action of AKR1Cs inside the cells. It is, however, interesting to note that the enzymes showing best activity are AKR1C2 and AKR1C3, enzymes responsible of the control of access to AR by androgens.

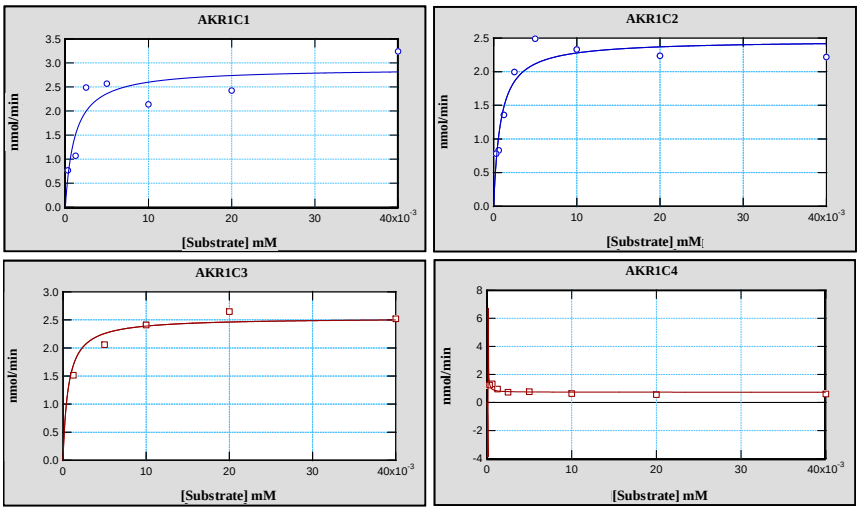

Figure 2.38. Rate of comsumption of NADPH (nmol/min) compared with concentration of cis-$[Pt(2ET)Cl(NH_3)_2]^+$ for AKR1Cs.

	cis-[Pt(2ET)Cl(NH$_3$)$_2$]		*9,10-phenanthrenequinone*	
	Km (μM)	kcat (min^{-1})	Km (μM)	kcat (min^{-1})
AKR1C1	1.12 ± 0.60	1.46 ± 0.16	2.48 ± 0.54	21.0 ± 1.59
AKR1C2	0.83 ± 0.22	1.60 ± 0.09	2.37 ± 0.46	38.1 ± 2.58
AKR1C3	0.62 ± 0.18	1.65 ± 0.08	1.59 ± 0.28	18.8 ± 1.46
AKR1C4	-	-	2.44 ± 0.54	18.9 ± 1.47

Table 2.11. Km (μM) and Kcat of cis-$[Pt(2ET)Cl(NH_3)_2]^+$ with AKR1Cs, calculated using the "Enzymics" program (Softzymics, Princetown, NJ, USA).

If a compound is a poor substrate, but still can be metabolized by the protein (as seen by HPLC) it could still be effective as an AKR inhibitor. To study this possibility an experiment was performed in which a good substrate (9,10-phenanthrenequinone) was provided in different concentrations (from 20 to 0.313 µM) and turnover in a time period of 5 minutes measured in the presence of different concentrations of our compound (from 0 to 0.1 mM). The experiment was repeated for the four AKR1Cs, and results can be seen in Figure 2.39. Immediately we can see that all four enzymes are inhibited (through an uncompetitive inhibitory mode) by our steroidal platinum complex. However this inhibition is mild and we need to go to high concentrations of our compound to see dramatic effect in the activity (around 100 µM). They present high K_i (Table 2.12), needing high concentrations to stop the activity by 50% compared with other inhibitors[108]. It is interesting to note that the highest inhibition is in AKR1C4 (estimated 50% of activity inhibition at around 30 µM) which is present in the liver and is responsible of hepatic clearance.

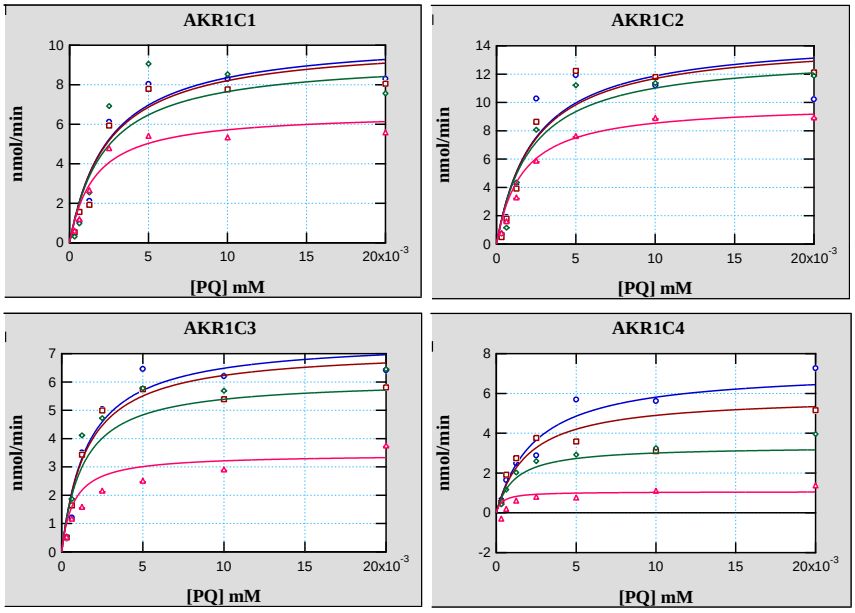

Figure 2.39. Rate of consumption of NADPH (nmol/min) compared with concentration of PQ for AKR1Cs under different concentrations of cis-$[Pt(2ET)Cl(NH_3)_2]^+$ (0 (blue), 4 (brown), 20 (green) and 100 µM (red)).

	Ki
AKR1C1	174 ± 66.7
AKR1C2	207 ± 78.5
AKR1C3	84.8 ± 19.3
AKR1C4	17.2 ± 3.8

Table 2.12. Ki inhibitory constants (µM) of the compound, calculated using the "Enzymics" program (Softzymics, Princetown, NJ, USA).

The experiment was repeated, pretreating the enzymes for 24 hour with our complex. After that time, 9,10-phenanthrenequinone and NADPH were added, and the turnover measured. The results are presented in Figure 2.40. We can observe that the inhibition increased after 24 hours pre-treatment with cis-$[Pt(2ET)Cl(NH_3)_2]^+$, with the K_i decreasing around an order of magnitude (Table 2.13), except for AKR1C4 that seems to suffer degradation under the conditions used (as the drop of activity without complex suggest, maybe as result of a covalent binding of the complex with the enzyme). The mode of this inhibition is unchanged for AKR1C2 and 3 (Uncompetitive), while change for AKR1C1 (competitive), suggesting that the complex inhibit through binding to the active site. It is interesting to note that inhibition almost stops the activity of AKR1C3 at 0.1 mM concentration, this being the most strongly inhibited with an estimated 50% of activity inhibition at around 5 µM. Due to the affinity towards the enzyme showed by cis-$[Pt(2ET)Cl(NH_3)_2]^+$, this effect is probably more related to the occupation of the enzymatic active centre during the pre-treatment by complex than to covalent modifications of the protein.

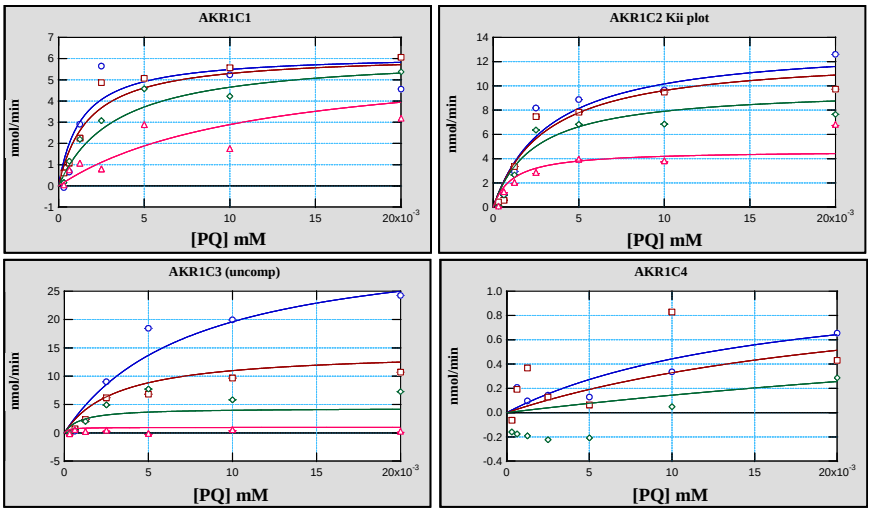

Figure 2.40. Rate of consumption of NADPH (nmol/min) compared with concentration of PQ for AKR1Cs under different concentrations of cis-$[Pt(2ET)Cl(NH_3)_2]^+$ after 24 hours pre-treatment (0 (blue), 4 (brown), 20 (green) and 100 µM (red)).

	Ki
AKR1C1 on	13 ± 5.3
AKR1C2 on	52.7 ± 13.5
AKR1C3 on	2.9 ± 0.7
AKR1C4 on	-

Table 2.13. Ki inhibitory constants (µM) after pre-treatment with the compound for 24 hours, calculated using the "Enzymics" program (Softzymics, Princetown, NJ, USA).

The different experiments undertaken demonstrate that our compound has the ability to be a substrate for AKR1C enzymes (reaction that can be followed by HPLC, but not for AKRC4), but it is neither a good substrate nor a good inhibitor. Conjugation of the platinum centre to the steroidal molecule, does maintain the affinity of the enzyme active centre towards the complex, but affects heavily the transformation rate (action of the enzyme) of the substrate (steroidal moiety). This indicates that our compound can be metabolised by proteins inside the cell, but the slow rate of transformation make us think that cis-$[Pt(2ET)Cl(NH_3)_2]^+$ does not act as an AKR-activated prodrug.

2.5 Synthesis of additional new steroidal compounds

As we have seen before, steroids can be used to target breast cancer (sections 2.1, 2.2 and 2.3), and possibly prostate cancer. The syntheses of these complexes normally follow two main steps; one in which the organic ligand is created, and a second one in which the metal centre is attached. These ligands are created specifically for each compound following sometimes difficult synthetic routes. Our intention is to create a simple method to attach different molecules to steroids using the same simple procedure used for our monofunctional complexes (section 2.1), developing schemes for the standardization of the attachment to steroids.

Following previous work made in our laboratory[16,29,40-42], we knew that all the designs should contain two elements: a steroidal domain and a linker that allows attachment to the platinum(II). This linker would present a simple reactive centre that would allow us to attach different chelators, or metallic binding domains to the steroid (Fig. 2.42). We chose to explore a benzaldehyde as linker. To attach this moiety to the steroid, Sonogashira coupling[75] was chosen as a synthetic route (Fig. 2.41), due to the commercial availability of inexpensive bromo-aromatic derivatives and 17α-ethynyltestosterone and estradiol.

A Sonogashira coupling is a palladium catalysed reaction between an acetylinic group and a halo-aromatic. A copper(I) salt (often CuI) is used to reduce Pd(II) to catalytically active Pd(0) in situ. As a result, the reaction requires inert conditions as copper(I) salts can catalyse homo-coupling of the acetylinic groups in a Glaser coupling[47]. Removal of the acetylinic proton is conducted in basic medium. The

proposed catalytic cycle for the Sonogashira reaction is presented in Figure 2.41 and in addition to the product, a protonated base is the major byproduct of the reaction. The catalytic cycle involves reduction of Pd(II) to Pd(0) by Cu(I), insertion of the catalyst into an aromatic-bromo bond and the formation of a palladium-carbon bond after the deprotonation of acetylsteroid by a base. The protonated base precipitates out from solution and a 1,2-insertion reaction at the Pd centre completes the reaction to form the desired product.

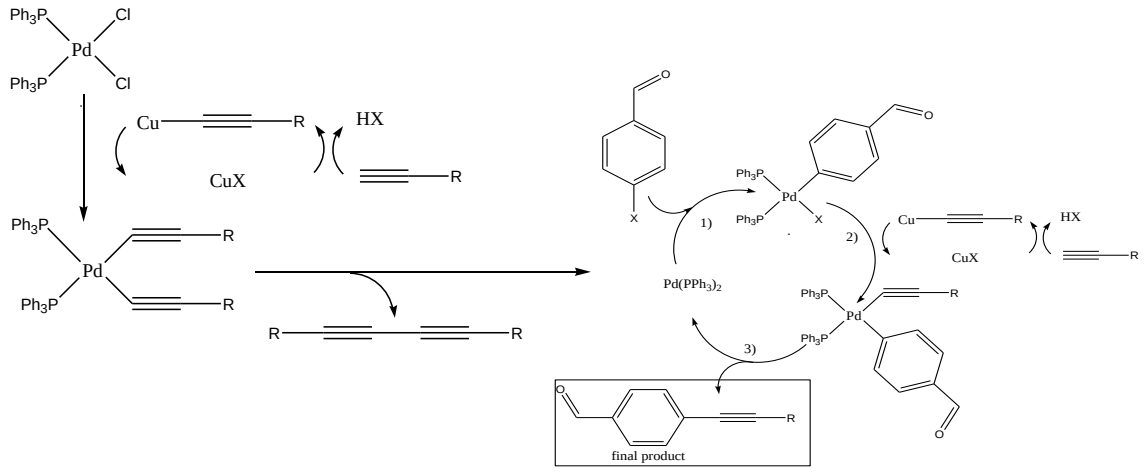

Figure 2.41. Sonogashira coupling Reactive cicles

Figure 2.42. Scheme of intended synthesis

Following attachment of the benzaldehyde, picolinamine and thiosemicarbazones complexes were synthesised. Both are active units in the absence of the steroid[76-78] and

would be good examples for the attachment of other molecules. Also, we present herein the synthesis of new Ru (III) complexes of the previously synthesised EET and ETT ligands[29, 50].

2.5.1 Synthesis of multiple chelators

Synthesis of steroidal linker to chelators (ETBza)

The Sonogashira cross-coupling reaction between ethisterone and 4-bromobenzaldehyde afforded the product 17α-benzaldehyde-4-ylethynyl-testosterone as a yellow solid in good yield (73%). The product was insoluble in water, but soluble in most common organic solvents. Purification of the crude product involved a flash silica column using ethanol:dicloromethane (3%) as eluent.

The product was analysed by mass spectroscopy giving peaks consistent with the proposed structure (m/z 417.4 $[H(ETBza)]^+$). In the ^1H NMR spectrum (Fig. 2.43) both steroidal skeleton (from 0-6 ppm) and benzaldehyde (from 7-11 ppm) are present in a 1:1 ratio and the loss of the acetylene resonance ca. 2.55 ppm indicates a reaction at that centre. The α,β-unsaturated carbonyl proton of the A ring of the testosterone and the methyl resonances appear at 5.92, 1.38 and 1.14 ppm respectively, hardly shifted when compared to ethisterone (as would be expected due to the distance form the aromatic ring). The aromatic protons of the benzaldehyde moiety appear as two doublets at 7.98 and 7.75 ppm. The increase in the gap between these resonances compared to the free 4-brombenzaldehyde is due to the attachment to the testosterone. Finally, the α-carbonyl proton of the benzaldehyde can be assigned at 10.17 ppm. In the next steps, this proton will be an important marker indicating whether the condensations have worked or not. This structure is the starting point for the next ligands: thiosemicarbazone (ETTsc) and picolinamine (ETPcl).

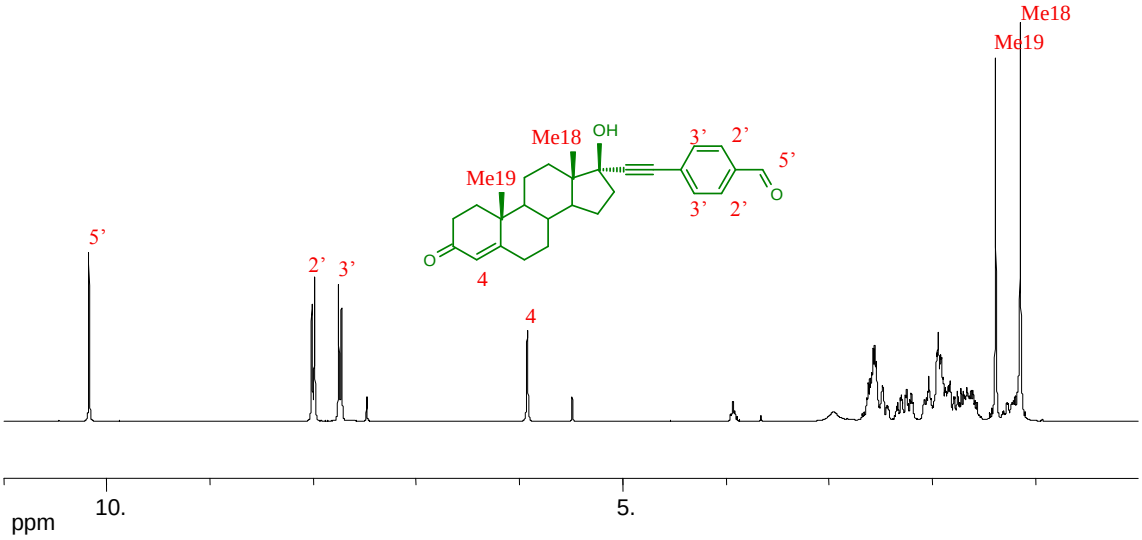

Figure 2.43. ^{1}H-NMR of ETBza in deuterated chloroform.

Synthesis of steroidal thiosemicarbazone (ETTsc)

The steroidal benzaldehyde linker was condensed with a thiosemicarbazide, giving a thiosemicarbazone, affording ETTsc in good yield (72%) (Fig. 2.44). After synthesis, the product was purified on a flash silica column using the same conditions as for ETBza. The product showed insolubility in water, again, and a reduced solubility in organic solvents compared with ETBza.

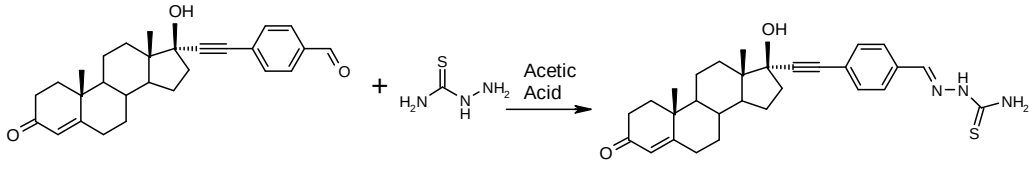

Figure 2.44. Synthetic procedure for ETTsc.

The product was analysed by elemental analysis and mass spectrometry, showing the expected result with the desired structure. The ^{1}H NMR spectrum (Fig. 2.45 shows the disappearance of the α-carbonilic proton from ETBza, and the appearance of the iminic

proton of the thiosemicarbazone at 8.17 ppm as result of the condensation. The labile protons of the NH of the thiosemicarbazone are visible as well at 10.58, 7.92, 7.58 ppm. Finally a small opening in the gap between aromatic protons is seen as result of the condensation, the two doublets being found at 7.78 and 7.44 ppm. The α,β-unsaturated carbonyl proton and methyl resonances appear with little shifting compared to ETBza (as would be expected due to the distance from the aromatic ring again).

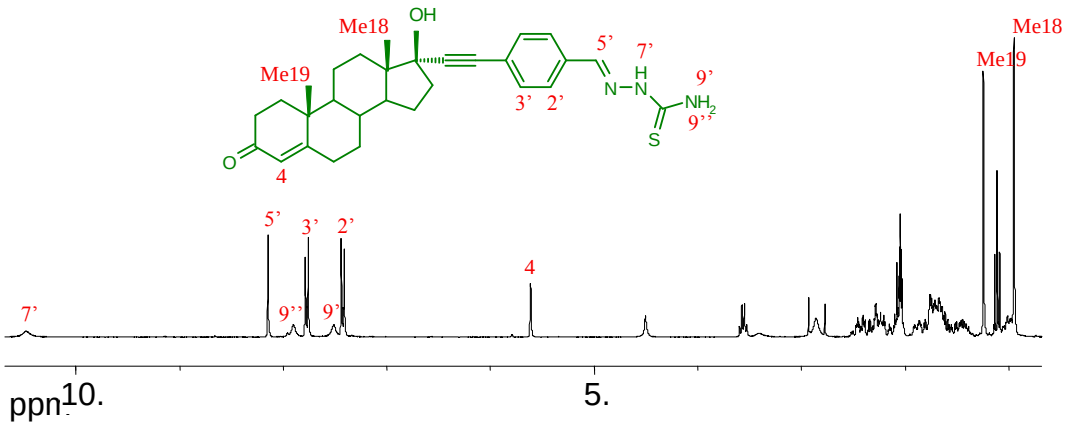

Figure 2.45. ^{1}H-NMR of ETTsc in deuterated acetone.

Synthesis of steroidal picolinamine (ETPcl)

ETPcl was synthesised through the condensation of the ethisterone coupled benzaldehyde (ETBza) and a 2-picolinamine, followed by an *in situ* reduction (Fig. 2.46), as described by Yajima *et al*[79] for non-steroidal analogues. The crude product was soluble in similar range of solvents to ETBza, containing a mixture of ETPcl with ETBza (as shown by ESI-MS). Numerous purification attempts of the crude product were unsuccessful.

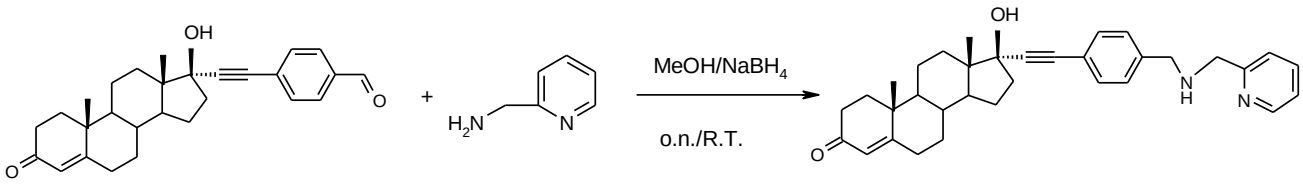

Figure 2.46. Synthetic procedure for ETPcl.

In the ^{1}H NMR (Fig. 2.47) as a result of the similar chemical shift of the products it is impossible to fully assign the peaks. However, the α-carbonilic proton is still visible due to the absence of signals in this area, confirming the presence of the starting material. Since the aldehyde ligand ETBza will have low reactivity to palladium and platinum salts, we proceeded without further purification.

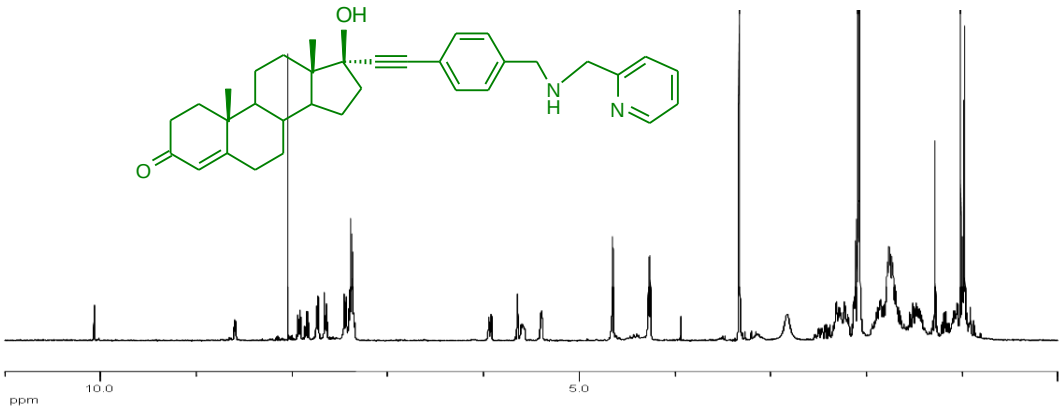

Figure 2.47. ^{1}H-NMR of ETPcl in deuterated chloroform.

Steroidal thiosemicarbazones complexes

A set of neutral Pt(II) and Pd(II) compounds have been prepared, using the ETTsc and ETPcl bidentate ligands. All these complexes show low solubility, being soluble only in DMF and DMSO. Attempts to increase solubility by ligand exchange of one or two chlorides co-ligands with different monoanionic or neutral substituents failed.

Synthesis of [Pt(ETTsc)Cl_2].

The desired product was formed relatively easily by reaction of potassium tetrachloroplatinate with ETTsc in the minimum amount of ethanol. Unfortunately the low solubility of the resulting yellow-orange solid, (only soluble in DMF and DMSO), prevented a further purification. The mass spectrum shows a peak at m/z=756 whose isotopic distribution pattern matches that of [Pt(ETTsc)Cl_2H]$^+$. The ^{1}H NMR spectrum (Fig. 2.48) shows the benzene ring system, shifted to low field, as result of the Pt(II) coordination.

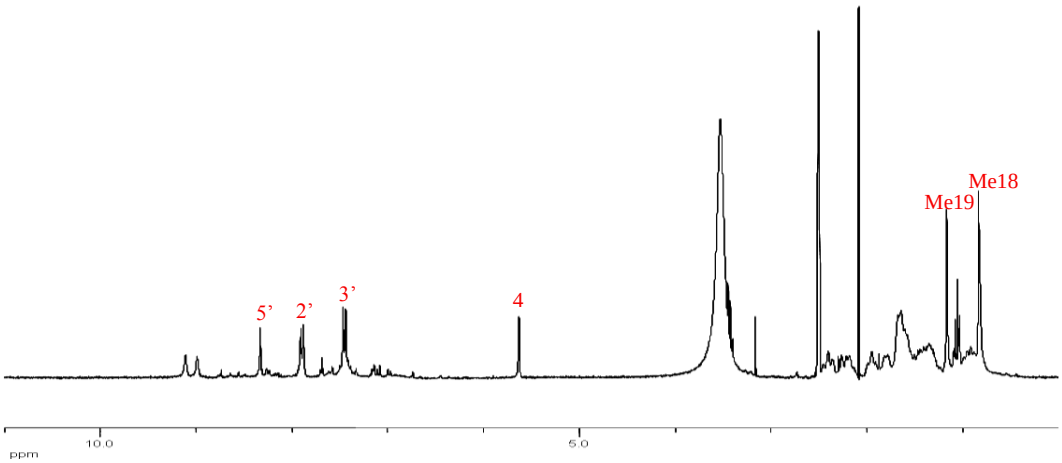

Figure 2.48. ^{1}H-NMR of [Pt(ETTsc)Cl_2] in deuterated DMSO.

Synthesis of [Pd(ETTsc)Cl_2].

With a similar procedure from the previous complex, but using potassium tetrachloropalladate instead of the platinum salt, a bright orange solid was obtained. Mass spectrometry analysis shows a main peak at 666 m/z, corresponding with the expected complex [Pd(ETTsc)Cl_2], but shows as well a secondary peak at 1084 m/z, that correspond to [Pd(ETTsc)$_2$]. The ^{1}H NMR (Fig. 2.49) shows a main product, probably the expected [Pd(ETTsc)Cl_2], and impurity of 20-30%, probably [Pd(ETTsc)$_2$].

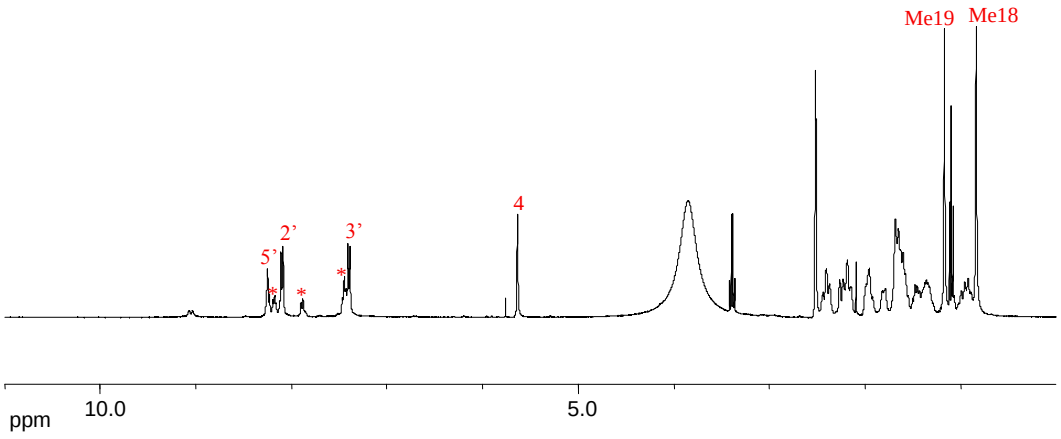

Figure 2.49. 1H-NMR of [Pd(ETTsc)Cl_2] in deuterated DMSO. * bisubstituted complex

Experiments using the more labile palladium (II) salt bis-benzonitrile palladium (II) dichloride, gave a different result. The mass spectrum shows a major peak corresponding to [Pd(ETTsc)$_2$] and a really minor [Pd(ETTsc)Cl_2]. ^{1}H NMR (Fig. 2.50) show and almost clear set of signals, corresponding to the minor product from the other synthesis. Small resonances are visible at shifts previously assigned to [Pd(ETTsc)Cl_2].

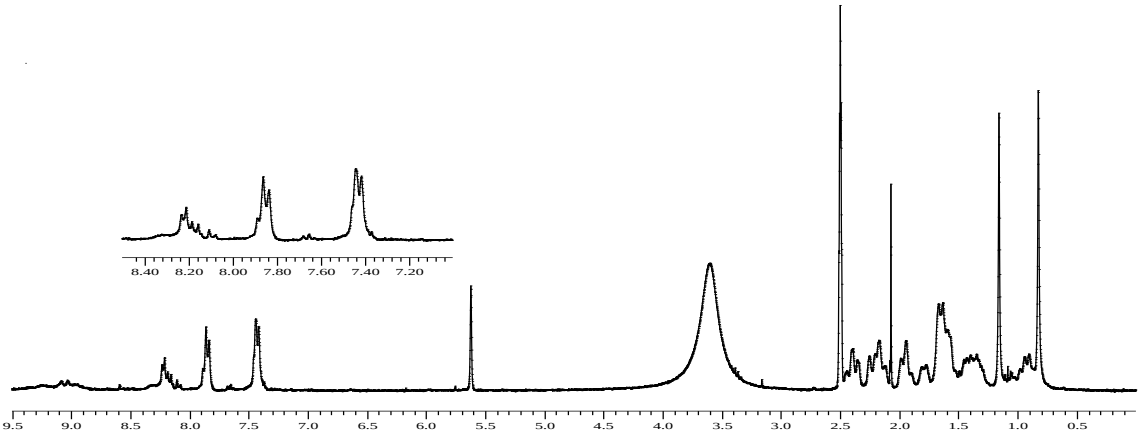

Figure 2.50. ^{1}H-NMR of [Pd(ETTsc)$_2$] in deuterated DMSO.

The low solubility of both compounds, only soluble in DMF and DMSO, has this far made imposible to purify any of them.

Steroidal picolinammine complexes

Synthesis of [Pd(ETPcl)Cl$_2$].

This palladium complex has been synthesised from ETPcl, reacting with potassium tetrachloropalladate in the minimum amount of methanol. A yellow solid was obtained, only soluble in DMSO and DMF. Analysis in mass spectrometry gives a peak of m/z=685 ([Pd(ETPcl)Cl$_2$]H$^+$). The ^{1}H NMR (Fig. 2.51) show a clear set of signals for the benzene ring at 7.56 and 7.34 ppm. Four pyridinic protons appear at 8.65, 7.97, 7.51 and 7.43 ppm. The α,β-unsaturated carbonyl proton and methyl resonances appear with little shifting again, as result of the long distance from the Pd(II) nucleus. On the other hand around 4 ppm, in the region where the resonance for the methylene protons should appear, a complex set of signals is observed. Integration of this region did not allow a definitive assignment of the signals without further NMR experiments.

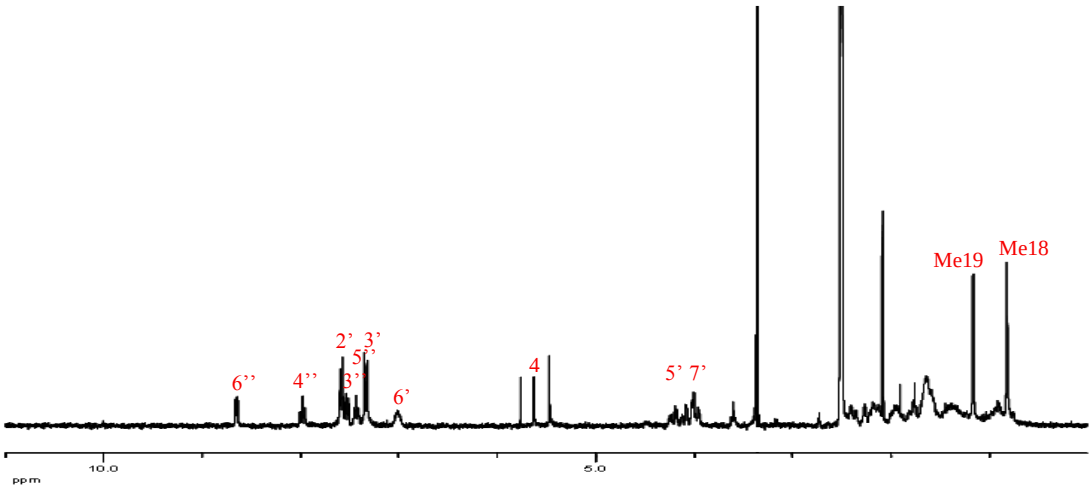

Figure 2.51. ^{1}H-NMR of [Pd(ETPcl)Cl_2] in deuterated DMSO.

The synthesis of Pt(II) analogue using different salts, such as potassium tetrachloroplatinate and bis(benzonitrile) platinum(II) dichloride, was unsuccessful.

2.1.2 Synthesis of new steroidal terpyridine complexes

[Ru(EET)Cl_3]

Using two steroidal terpyridine ligands previously designed in our group [29, 50] we now prepared some Ru(III) chloro derivatives. [Ru(tpy)Cl_3] compound is reported to be active against cancer cell lines and this presents an interesting unit for conjugation[80-81]. Synthesis of the metal complex was straightforward and under normal procedures used for non-steroidal complexes, the compounds were obtained. Reacting EET with Ru(III)Cl_3 led to the desired compound. Purification was simple: since the complex is neutral and soluble only in DMSO or DMF, only continuous washes with different solvents were needed to remove the impurities. Mass spectrometry and elemental

analysis confirm the 1:1 stechiometry. Impurities removed by washing include the bis-ligand Ru(II) complex (previously synthesised by Phil Barker)[50], that can be isolated by washes of the crude product with ethanol.

As this is a neutral and paramagnetic complex, characterization was more difficult than for previous complexes, however ESI-MS show a major peak corresponding to the $[Ru(EET)Cl_2]^+$. Finally paramagnetic ^{1}H-NMR (Fig. 2.52) shows 5 paramagnetic signals at 7.12, -3.25, -8.05, -9 and -35.4 ppm, corresponding to the five protons close to the Ru(III) centre, $H_{3''}$, $H_{4'}$, $H_{5'}$, $H_{3'}$ and $H_{6'}$ respectively (assigned by comparison with non-steroidal complexes[82]). Most of these signals are not visible under normal NMR conditions. However, protons belonging to the steroidal skeleton appear both under paramagnetic and normal conditions, as a result of the distance to the metallic centre. Protons H_1, H_2 and H_4 can be detected at the normal 7 to 6.3 ppm (6.95, 6.46, 6.38 ppm) and the methyl group at 1.11 ppm. The NMR confirms the removal of impurities after the washes.

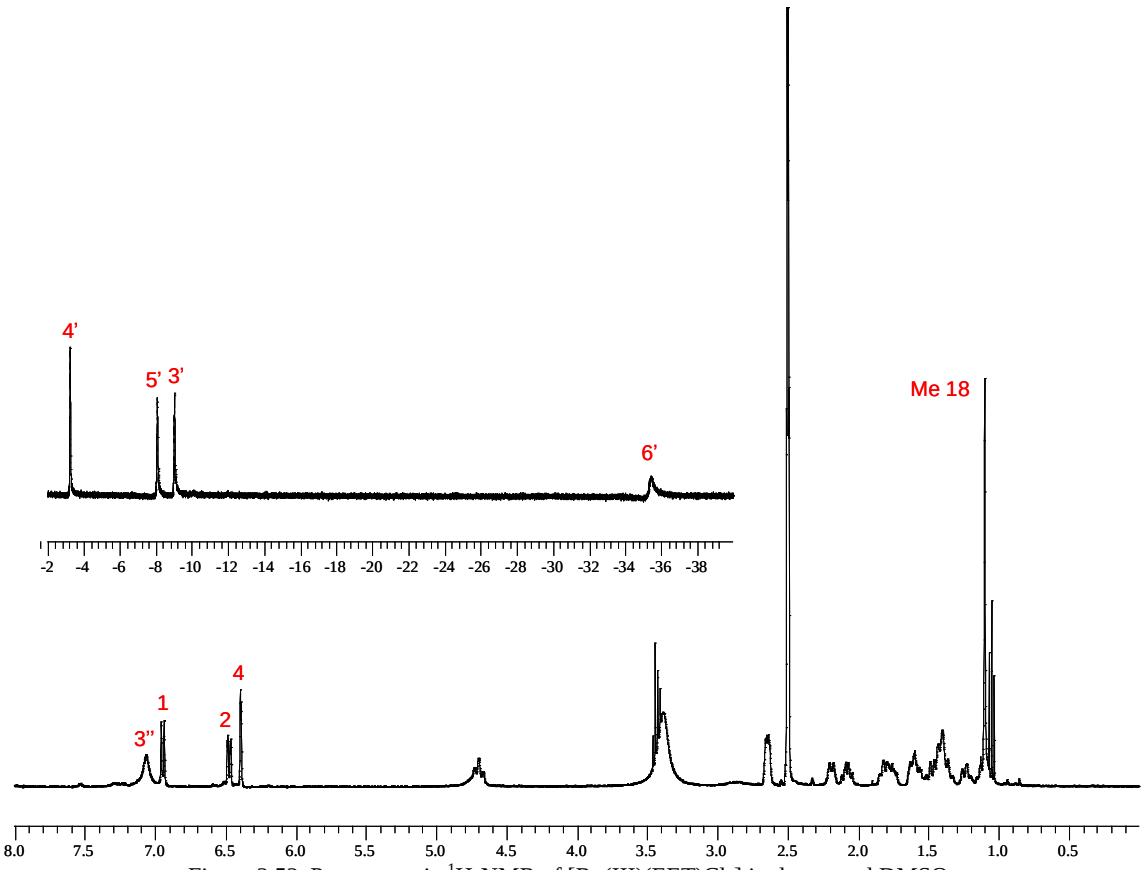

Figure 2.52. Paramagnetic ^{1}H-NMR of $[Ru(III)(EET)Cl_3]$ in deuterated DMSO.

[Ru(ETT)Cl_3]

The synthesis with ETT was analogous. ESI-MS show this time the lost of two chlorides, and elemental analysis confirms the stechiometry. Again ^{1}H-NMR (Fig. 2.53) show the 5 paramagnetic signals at 6.94, -3.33, -8.11, -9.09 and -35.38 ppm, corresponding to the five terpyridine protons close to the Ru(III) centre (with similar assignments to the estradiol complex). These signals are not visible under normal conditions, unlike the steroidal skeleton protons that being far away from the metallic centre does not suffer quenching. H_4 can be seen at 5.58 ppm integrating for a proton and the absence of impurities in the methyl groups (integrating for three protons each at 1.08 and 1.02 ppm) show the purity obtained after the multiple washes.

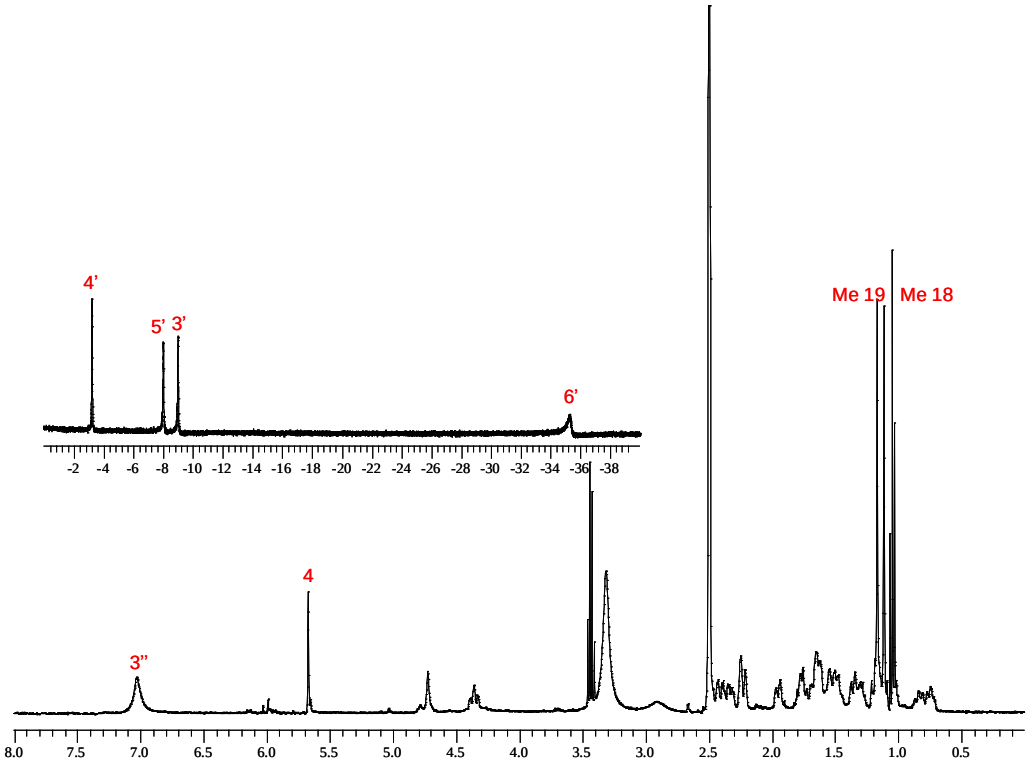

Figure 2.53. Paramagnetic ^{1}H-NMR of [Ru(III)(EET)Cl_3] in deuterated DMSO.

Although these compounds were prepared in order to test their biological activities, their low solubility prevented this, since a high percentage of DMSO in the medium is needed for even low concentration solutions.

2.6 Conclusions

Three different points have been presented in this chapter: the description of new procedures to synthesise and purify steroidal compounds, the interaction of these compounds with cells and the interactions with macrobiomolecules.

First three new pyridine derivates of both estradiol and testosterone linked complexes have been synthesised, and a HPLC procedure optimized for the purification of these and similar compounds. This purification allows us to remove secondary products such as disubstituted Pt molecules or Glaser coupling products, and improves the overall yields as a result of the simplification of the procedures. In addition, removal of the solvents from the complexes allows us to visualize the amino groups from the platinum moiety allowing differentiation between cis and trans isomers through standard ^{1}H-NMR.

The interesting cytotoxicity presented by some metallo-steroid compounds was previously known. For these active compounds we studied their cellular behaviour. As previously seen with testosterone derivatives, toxicity was observed for the estradiol-linked complexes; this showed that functionalisation with an steroid could confer activity to inactive metallic moieties. The possibility that this activity came from a simple hormonal effect forced by the steroid was ruled out: addition of estradiol to the non-steroidal complexes increased the activity (as expected) but did not reach the toxicity of covalently coupled steroidal drug complexes. The steroidal quinoline ligands appear to have some inherent activity, further studies to probe the effects therefore focused on pyridine derivatives (whose ligands have no activity). Since estradiol derivatives show lower toxicity than the testosterone analogues, we focused on the testosterone conjugates. Studies with the cis and trans-$[Pt(2ET)Cl(NH_3)_2]^+$ complexes showed that certain level of specificity towards AR can be achieved. However, this specificity seems to be opposite for cis or trans isomers, with the cis complex more active in AR+ cells and the trans (surprisingly) showing a 2-fold better activity towards

AR- cells. Testosterone derivatives give better activity in cisplatin resistant cell lines than their non-steroidal complexes. Finally, the importance of uptake has been studied using an ICP-MS, showing that although lower uptake is observed for steroidal complexes, better delivery across of the cellular membrane is achieved through linkage of a testosterone. However nuclear or cytoplasmic delivery seems not to be related with cytotoxic values, contrary to previous literature[83] and there seems to be some added steroidal effects that increase the complexes activity. In summary, the conferred activity seems to be not just about delivery but about modulation of the biomolecular binding.

It was observed previously in our group that the presence of an ethynyl-testosterone moiety on a bound aromatic ligand results in complexes substantially altering the structure of DNA[40-41, 46]. Non-steroidal complexes generally produce a much smaller degree of unwinding[40-41, 46] (Section 2.1). This large degree of unwinding cannot simply be obtained by a combination of steroid free metallic centre and steroids. In order to understand this better, the interaction of these agents with mononucleotides was studied. It was found that steroidal platinum(II) complexes are, in certain aspects, similar to those without steroids. All of them bind to the guanine N^7 forming only a monoadduct. This interaction, and its mechanisms, appears to be more related to the particular geometrical isomer than to the presence or not of testosterone. We showed that under low concentrations of Cl^- ions cis isomers do not suffer hydrolysis and bind in a direct way to the Guanine, and trans isomers suffer hydrolysis and bind to Guanine through an aqua intermediate. Cis isomers react more quickly than their trans analogues. Only two small differences between steroidal and non steroidal complexes appear in their interaction with mononucleotides; steroid compounds are slightly quicker to react than the non steroidal ones, and steroidal cis isomers seem to force an interaction between the base and the steroid skeleton.

When interaction with DNA was further studied CD experiments showed that B-DNA conformation is retained when ct-DNA is treated with cis and trans-$[Pt(Py)Cl(NH_3)_2]^+$, but no DNA conformation information could be obtained for testosterone coupled metallic centres, due to the chirality of the steroid. However, the mirror image induced CD signal observed for cis and trans-$[Pt(2ET)Cl(NH_3)_2]^+$ isomers suggest that it is possible that the geometric isomers force a different orientation of the steroid when bound to the DNA. This could be related with the fact that the cis isomers interact differently with mononucleotides bringing the steroid skeleton close to the base

(maybe through a possible intercalation of the A ring). Together with the fact that cis complexes have a different mechanism of binding to nucleobases (being quicker and not suffering hydrolysis), could explain why they are more biologically active than the complexes with trans geometries.

We observed as well that the presence of the metallic moiety is a drawback for interaction with proteins. Our compounds can be a substrate of AKR1Cs enzymes, but are poorly turned over; with a transformation rate 4 times lower than normal substrates. Enzyme inhibition is also observed, although only at high concentrations. That leads us to believe that the target of our complexes is DNA, that the compounds are not significantly metabolized inside the cell, and that the reactive molecule is thus the administered complex.

Finally we reported the synthesis of a reactive intermediate product that had potential to allow easy binding of multitude of metallodrugs to steroids using straightforward chemistry. This intermediate consists in a benzaldehyde linked to a steroid through a normal Sonogashira reaction. The presence of the aldehyde makes possible the connection of different molecules through easy procedures. Picolinamine and thiosemicarbazone derivatives were synthesised as examples, and Pd and Pt complexed with these ligands. This shows the flexibility of this steroidal benzaldehyde as linking moiety. In addition different metals have been introduced and Ru(III) complexes have been created with previously synthesised steroidal tpy ligands. Unfortunately all these types of compounds were neutral and presented very low solubility that made them unsuited for further biological studies. This is an important finding: That a charged (cationic) metal complex is essential to the molecular design of these steroidal metallo-drugs.

2.7 Experimental

Synthesis: All solvents and chemicals were purchased from Sigma-Aldrich. All Sonogashira reaction reagents were fully dried before use and solvents degassed and followed the original protocol with the exception of using THF as a solvent. ^{1}H NMR spectra were recorded on Brucker AC300 or DRX500 spectrometers. ESI mass spectra were recorded on a Micromass LCT Time of flight mass spectrometer. Microanalyses were performed on a CE Instruments EA1110 elemental analyser. UV/VIS was

performed in a Varian Cary 5000 UV/VIS spectrophotometer. HPLC was performed in a Dionex HPLC system with a semi-prep column fitted.

trans-[Pt(1ET)Cl(NH_3)$_2$](NO_3): A solution of $AgNO_3$ (26.1 mg, 0.125 mmol) in DMF (1 ml) was added to a solution of transplatin (40.2 mg, 0.13 mmol) in DMF (2 ml). The mixture was stirred at room temperature with light exclusion for 18 hours. The mixture was cooled to -18ºC using a NaCl-ice bath, and 1ET (48.8 mg, 0.13 mmol) in DMF (2 ml) was added dropwise over 10 minutes. The reaction was then stirred for 3 hours at -18ºC and a further 1 hour at room temperature. The suspension was then filtered through celite to remove any AgCl precipitate, and the filtrate concentrated under reduced pressure. MeOH (10 ml) was added causing precipitation of un-reacted platinum materials, which were removed through filtration. The filtrate was concentrated under reduced pressure and Et_2O (50 ml) was added to precipitate a white solid. This crude solid was collected by filtration, washed with Et_2O, dried under vacuum and purified using semi-prep HPLC (as described in Chapter 2.2.2), resulting in a white solid (47.8 mg, 49%). ^{1}H-NMR (300 MHz, CD_3OD): δ 8.84 (dd, 1H, J = 5.2, 1.5 Hz, $H_{6'}$), 7.94 (ddd, 1H, J = 7.7, 8.1, 1.5 Hz, $H_{4'}$), 7.7 (d, 1H, J = 8.1 Hz, $H_{3'}$), 7.46 (dd, 1H, J = 5.9, 7.7 Hz, $H_{5'}$), 5.67 (s, 1H, H_4), 4.02 (b, 6H, NH_3) 2.60-1.40 (m, 18H, steroid), 1.26 (s, 3H, Me_{19}), 1.15-1.03 (m, 2H, steroid), 0.98 (s, 3H, Me_{18}). IR: υ 3445m, 2945m (C-H str), 2722m (C-H str), 2222m (C≡C str) 1667m (C=O str). Mass spectrum (ESI, +ve): *m/z* = 654 [Pt(1ET)Cl(NH_3)$_2$]$^+$. UV/Vis: λ_{max} (MeOH) 238nm (ε= 15100 $dm^3mol^{-1}cm^{-1}$) and 291 nm (ε= 5010 $dm^3mol^{-1}cm^{-1}$). Elemental analysis: calculated for $C_{26}H_{37}ClN_4O_5Pt.2H_2O$; C, 38.4; H, 4.9; N, 8.6. Found C, 37.9; H, 4.9; N, 9.1.

cis-[Pt(1ET)Cl(NH_3)$_2$](NO_3): A solution of $AgNO_3$ (26.1 mg, 0.125 mmol) in DMF (1 ml) was added to a solution of cisplatin (40.2 mg, 0.13 mmol) in DMF (2 ml). The mixture was stirred at room temperature with light exclusion for 18 hours. The mixture was placed under argon atmosphere, cooled to -18ºC using a NaCl-ice bath, and 1ET (57.4 mg, 0.15 mmol) in DMF (2 ml) was added dropwise over 10 minutes. The reaction was then stirred for 3 hours at -18ºC and a further 1 hour at room temperature. The suspension was then filtered through celite to remove any AgCl precipitate, washed

with MeOH (10 ml) and the colourless filtrate concentrated under reduced pressure. The green solution was concentrated under reduced pressure; dissolved in the minimum amount of MeOH (1ml) and precipitated with Et_2O (100 ml).The light green solid was collected by filtration, washed with Et_2O and dried under vacuum. The crude product was purified using semi-prep HPLC (as described in Chapter 2.2.2), resulting in a green powder (25.1 mg, 26%). ^{1}H-NMR (300 MHz, CD_3OD): δ 8.78 (dd, 1H, J= 5.5, 1.5 Hz, $H_{6'}$), 7.9 (ddd, 1H, J= 7.7, 7.4, 1.5 Hz, $H_{4'}$), 7.62 (d, 1H, J= 7.4 Hz, $H_{3'}$), 7.44 (dd, 1H, J= 7.7, 5.5 Hz, $H_{5'}$), 5.68 (s, 1H, H_4), 4.5(b, 3H, NH_3) 4.1 (b, 3H, NH_3) 2.60-1.40 (m, 18H, steroid), 1.25 (s, 3H, Me_{19}), 1.15-1.03 (m, 2H, steroid), 0.99 (s, 3H, Me_{18}). IR: υ 3278m, 2945m (C-H str), 2861m (C-H str), 2222m (C≡C str) 1667m (C=O str). Mass spectrum (ESI, +ve): *m/z* = 654 $[Pt(1ET)Cl(NH_3)_2]^+$. UV/Vis: λ_{max} (MeOH) 237nm (ε= 16900 $dm^3mol^{-1}cm^{-1}$) and 291 nm (ε= 5500 $dm^3mol^{-1}cm^{-1}$).

cis-[Pt(2EE)Cl(NH$_3$)$_2$](NO$_3$): A solution of $AgNO_3$ (26.1 mg, 0.125 mmol) in DMF (1 ml) was added to a solution of cisplatin (40.9 mg, 0.14 mmol) in DMF (2 ml). The mixture was stirred at room temperature with light exclusion for 18 hours. The mixture was placed under argon atmosphere, cooled to -18ºC using a NaCl-ice bath, and 2EE (56.8 mg, 0.15 mmol) in DMF (2 ml) was added dropwise over 10 minutes. The ratio of platinum group:2EE used was 1:1.1. The reaction was then stirred for 3 hours at -18ºC and a further 1 hour at room temperature under argon atmosphere. The suspension was then filtered through celite to remove any AgCl precipitate, washed with MeOH (10 ml) and the colourless filtrate concentrated under reduced pressure. The concentrated solution was cooled to -4ºC and left for 3 days. Transparent crystals were grown (Glaser coupling). The crude product was purified using semi-prep HPLC (as described in Chapter 2.2.2), resulting in a brown solid (28.4 mg, 30%). ^{1}H-NMR (300 MHz, CD_3OD): δ 8.79 (d, 1H, J= 1.8 Hz, $H_{2'}$), 8.66 (dd, 1H, J = 5.6, 1.5 Hz, $H_{6'}$), 7.99 (dt, 1H, J = 8.1, 1.5, 1.8 Hz, $H_{4'}$), 7.46 (dd, 1H, J = 5.6, 8.1 Hz, $H_{5'}$),7.07 (d, 1H, J= 8.1 Hz, H_1), 6.51 (d, 1H, J= 8.1 Hz, H_2) 6.45 (s, 1H, H_4), 4.58(b, 3H, NH_3) 4.19 (b, 3H, NH_3) 2.60-1.05 (m, 15H, steroid), 0.91 (s, 3H, Me_{18}). IR: υ 3278m, 2917m (C-H str), 2861m (C-H str), 2222m (C≡C str) 1667m (C=O str). Mass spectrum (ESI, +ve): *m/z* = 638 $[Pt(2EE)Cl(NH_3)_2]^+$. UV/Vis: λ_{max} (MeOH) 238nm (ε= 15100 $dm^3mol^{-1}cm^{-1}$) and 291 nm (ε= 5010 $dm^3mol^{-1}cm^{-1}$).

Di-17-α-Ethynyl-Estradiol: 17α-Ethynyl-estradiol (500 mg, 1.69 mmol) was dissolved in 30 ml of dry THF, 0.1 equivalent of CuI (32.3 mg, 0.17 mmol), 0.2 equivalents of bis-(triphenylphospine)dichloropalladium(II) (238.7 mg, 0.34 mmol) and 0.5 ml of dry triethylammine were added. The mixture was left to react in the darkness overnight. Then, the brown solution was filtered and taken to dryness *in vacuo*. The solid was dissolved in the minimum amount of THF and precipitated with hexane, giving a brown crude powder 0.348 g, 70% yield. ^{1}H-NMR (300 MHz, CD_3OD): δ 7.04 (d, 2H, J = 8.5 Hz, H_1), 6.51 (dd, 2H, J = 8.5, 2.6 Hz, H_2), 6.42 (d, 2H, J = 2.6 Hz H_4), 2.75-1.20 (m, 30H, steroid), 0.82 (s, 6H, Me19). Mass spectrum (ESI, +ve): *m/z* = 589 $[(EE)_2\text{-}H^+]^+$.

$[Pt(2ET)_2(NH_3)_2](NO_3)_2$: To a solution of cis-diamminedichloroplatinum(II) (0.300 g, 1 mmol) in DMF (3 ml) was added silver nitrate (0.161 g, 0.95 mmol) in DMF (1 ml) and this mixture was stirred overnight in the absence of light. The silver chloride precipitate was removed by filtration leaving a pale yellow filtrate. To the filtrate was added 17α-pyridin-3-ylethynyl-testosterone (0.390 g, 1 mmol) and the solution stirred overnight. The slow addition of diethylether (200 ml) to the solution yielded a white precipitate which was filtered off. The crude product was purified using the HPLC procedure explained in the section 2.1.3 using a preparative column. Two products were obtained and collected. The first one (retention time 33.6 min; white powder) corresponded to cis-$[Pt(1ET)Cl(NH_3)_2](NO_3)$; 0.318 g, 45% yield. The second peak (retention time 36.7 min; white powder) corresponded to $[Pt(2ET)_2(NH_3)_2](NO_3)_2$; 0.045 g, 4% yield. ^{1}H-NMR (300 MHz, CD_3OD): δ 8.93 (s, 2H, $H_{2'}$), 8.74 (d, 2H, J = 5.9 Hz, $H_{6'}$), 8.02 (d, 2H, J = 8.5 Hz, $H_{4'}$), 7.51 (t, 2H, J= 5.9, 8.5 Hz, $H_{5'}$), 5.68 (s, 2H, H_4), 2.55-1.40 (m, 38H, steroid), 1.24 (s, 6H, Me19), 0.93 (s, 6H, Me18). Mass spectrum (ESI, +ve): *m/z* = 504 $[Pt(NH_3)_2(ET\text{-}3Py)_2]^{2+}$.

17α (4-ethynylbenzaldehyde) testosterone (ETBza): A Schlenk flask was charged with ethistherone (2 g, 6.4 mmol), bis (triphenylphospine)dichloropalladium (II) (0.180 g, 0.256 mmol, 4 mol%) and copper iodide (0.094 g, 0.512 mmol, 8 mol%). THF (50

ml), potassium carbonate (1.325g, 9.6 mmol, 150 mol%) and 4-bromobenzaldehyde (1.2 g, 6.4 mmol) were added resulting in a deep red coloured suspension. The reaction was stirred at 40 ºC for 72 hours under nitrogen atmosphere with light exclusion. The resulting dark brown suspension was filtered and the filtrate reduced *in vacuo* to a crude solid. The final product was purified by column chromatography (silica gel 60, DCM-EtOH 3%, Rx= 0.33) giving a lightly yellow solid. 1.95g, 73% yield. ^{1}H-NMR (300 MHz, $CDCl_3$): δ 10.17 (s, 1H, $H_{5'}$), 7.98 (d, 2H, J = 8.3 Hz, $H_{2'}$), 7.75 (d, 2H, J = 8.3 Hz, $H_{3'}$), 5.92 (s, 1H, H_4), 2.50-1.30 (m, 18H, steroid), 1.38 (s, 3H, Me_{19}), 1.22-1.19 (m, 2H, steroid), 1.14 (s, 3H, Me_{18}). Mass spectrum (ESI, +ve): *m/z* 417.4.

17α (4-ethynylbenzylthiosemicarbazone) testosterone (ETTsc): A round bottom flask was charged with a suspension of thiosemicarbazide (0.49 g, 5.38 mmol) in water with 8% of acetic acid, and the temperature was raised to 40ºC till total solution. Then, ETBza (2.2 g, 5.38 mmol) was added with the minimum amount of ethanol to get a solution. The temperature was raised till reflux, and left during 24h. After that the reaction was stopped and the solvent removed under vacuum to a crude solid. The final product was purified by column chromatography (silica gel 60, DCM-EtOH 3%, R_f= 0.26) giving a slightly yellow solid. 1.9g, 72% yield. ^{1}H-NMR (300 MHz, D^6-Acetone): δ 10.55 (b, 1H, $H_{7'}$), 8,18 (s, 1H, $H_{5'}$), 7.93 (b, 1H, $H_{9''}$), 7.79 (d, 2H, J = 8.3 Hz, $H_{2'}$), 7.58 (b, 1H, $H_{9'}$), 7.45 (d, 2H, J = 8.3 Hz, $H_{3'}$), 5.65 (s, 1H, H_4), 2.50-1.30 (m, 18H, steroid), 1.24 (s, 3H, Me_{19}), 1.15-0.98 (m, 2H, steroid), 0.97 (s, 3H, Me_{18}). Mass spectrum (ESI, +ve): *m/z* 490.3 $[H(ETTsc)]^+$. Elemental analysis: calculated for $C_{29}H_{35}N_3O_2S$-1.5(H_2O); C, 67.4; H, 7.4; N, 8.1. Found C, 67.4; H, 7.1; N, 8.6.

17α ((4-ethynylbenzyl)-pyridin-2-ylmethyl-amine) testosterone (ETPcl): A solution of ETBza (1g, 2.4 mmol) in MeOH is added to a MeOH solution of 2-picolinammine (0.26g, 2.4 mmol). Then 0.8 eq of $NaBH_4$ (0.073 g, 1.92 mmol) were added slowly and the reaction left stirring at room temperature for 4h. After that the reaction is quenched using 6M HCl, driven to almost dryness and 50 ml of water added. This solution is washed three times with chloroform (50 ml). This chloroform is rotated and the crude mixture with ETBza is obtained as a yellow solid (1.1g). All the attempts to purify the product finish in failure. Mass spectrum (ESI, +ve): *m/z* 509 $[H(ETPcl)]^+$.

[Pd(ETTsc)Cl_2]: ETTsc (75 mg, 0.153 mmol) was solved in the minimum amount of Ethanol, after that potassium tetrachloropalladate (50mg, 0.153 mmol) was added. The reaction was heated till reflux and left during 24 hours. After that an orange solid was filtered, and washed with ethanol (10 ml) and ether (10 ml), three times each. The impure final product was obtained as a bright orange solid. 72.52 mg, 71% yield. ^{1}H-NMR (300 MHz, D^6-DMSO): δ 8.24 (s, 1H, $H_{5'}$), 8.06 (d, 2H, J = 8.7 Hz, $H_{2'}$), 7.40 (d, 2H, J = 8.7 Hz, $H_{3'}$), 5.63 (s, 1H, H_4), 2.50-1.30 (m, 18H, steroid), 1.17 (s, 3H, Me_{19}), 1.15-0.98 (m, 2H, steroid), 0.83 (s, 3H, Me_{18}). Mass spectrum (ESI, +ve): *m/z* 666 $[H(Pd(ETTsc)Cl_2)]^+$.

[Pt(ETTsc)Cl_2]: ETTsc (58.5 mg, 0.12 mmol) was solved in the minimum amount of ethanol, after that potassium tetrachloroplatinate (50mg, 0.12 mmol) was added. The reaction was heated to 70ºC for 72 hours. After that an orange solid was filtered, and washed with ethanol (10 ml) and ether (10 ml), three times each. The impure final product was obtained as a pale orange solid. 50.65 mg, 56% yield. ^{1}H-NMR (300 MHz, D^6-DMSO): δ 8,33 (s, 1H, $H_{5'}$), 7.88 (d, 2H, J = 8.9 Hz, $H_{2'}$), 7.46 (d, 2H, J = 8.9 Hz, $H_{3'}$), 5.62 (s, 1H, H_4), 2.50-1.30 (m, 18H, steroid), 1.16 (s, 3H, Me_{19}), 1.15-0.98 (m, 2H, steroid), 0.83 (s, 3H, Me_{18}). Mass spectrum (ESI, +ve): *m z* 756 $[H(Pd(ETTsc)Cl_2)]^+$.

[Pd(ETPcl)Cl_2]: Assuming 50% purity for the crude ETPcl, 1 equivalent of this crude was solved in the minimum amount of methanol (141.4 mg, 0.153 mmol). Then 1 equivalent of potassium tetrachloropalladate was added (50 mg, 0.153 mmol). The reaction was left stirring during 24 hours at room temperature, precipitating a yellow solid. The solid was filtered, and washed three times with water (5 ml), acetone (5 ml), ethanol (5 ml) and ether (5 ml), obtaining the pure expected compound. 47.3 mg, 45% yield. ^{1}H-NMR (300 MHz, D^6-DMSO): δ 8,65 (d, 1H, J= 6.2 Hz, $H_{6''}$), 7.97 (ddd, 1H, J= 7.9, 1.5 Hz, $H_{4''}$), 7.59 (d, 2H, J= 8.5 Hz, $H_{2'}$), 7.52 (d, 1H, J= 7.9 Hz, $H_{3''}$), 7.43 (t, 1H, J= 6.2 Hz, $H_{5''}$) 7.33 (d, 2H, J= 8.5 Hz, $H_{3'}$), 7.01 (bs, 1H, $H_{6'}$), 5.62 (s, 1H, H_4), 4.28-3.93 (bm, 4H, $Met_{5'}$, $Met_{7'}$) 2.50-1.30 (m, 18H, steroid), 1.16 (s, 3H, Me_{19}), 1.15-

0.98 (m, 2H, steroid), 0.82 (s, 3H, Me_{18}). Mass spectrum (ESI, +ve): *m/z* 685 $[H(Pd(ETPcl)Cl_2)]^+$.

[Ru(EET)Cl_3]: 15.8 mg (0.076 mmol) of $RuCl_3$ and 40 mg (0.076 mmol) of EET (synthesised as previously described in Phil Barker's Thesis[50]) were dissolved in 10 ml of ethanol, and the reaction was allowed to reflux overnight. Reaction changed from a really dark brown solution to a dark red suspension, showing an abundant precipitate. This was collected by filtration and washed with abundant ethanol and ether, obtained a bright red solution (di-substituted ruthenium complex, previously synthesised in Phil Barker's Thesis[50]) and a red brick solid corresponding to the target compound (29.2 mg, yield 52 %). ^{1}H-NMR (400 MHz, DMSO): δ 7.06 (b, 2H, $H_{3''}$), 6.95 (d, 1H, J= 8.4 Hz, H_1), 6.46 (ddd, 1H, J= 8.4, 2.4 Hz, H_2), 6.38 (d, 1H, J= 2.4 Hz, H_4), 4.69 (t, 1H, J= 12 Hz, steroid), 2.63 (d, 1H, J= 5.4 Hz, steroid), 2.2-1.15 (m, 13H, steroid), 1.11 (s, 3H, Me_{18}), -3.25 (b, 2H, $H_{4'}$), -8.05 (b, 2H, $H_{5'}$), -9.03 (b, 2H, $H_{3'}$), -35.4 (b, 2H, $H_{6'}$). Mass spectrum (ESI, +ve): *m/z* 738 [Ru(EET)Cl_2]+(K). Elemental analysis: calculated for $C_{35}H_{33}Cl_3N_3O_2Ru$-(H_2O); C, 55.8; H, 4.7; N, 5.6. Found C, 55.1; H, 4.5; N, 5.5.

[Ru(ETT)Cl_3]: 15.3 mg (0.073 mmol) of $RuCl_3$ and 40 mg (0.073 mmol) of ET-Terpy (synthesised as previously described in Phil Barker's Thesis[50]) were dissolved in 10 ml of ethanol, and the reaction set to reflux overnight. Reaction changed from a really dark brown solution to a dark red suspension, showing a big amount of precipitate. This was collected by filtration and washed with abundant ethanol and ether, obtained a bright red solution ($[Ru(ETT)_2]^{2+}$, previously synthesised in Phil Barker's Thesis[50]) and a red brick solid corresponding to our compound (23.5mg, yield 43 %). ^{1}H-NMR (400 MHz, d_6-DMSO): δ 6.94 (b, 2H, $H_{3''}$), 5.58 (s, 1H, H_4), 4.64 (bm, 1H, steroid), 4.27 (t, 1H, J= 13.8, 11.5, steroid), 2.35-0.6 (m, 18H, steroid), 1.08 (s, 3H, Me_{19}), 1.02 (s, 3H, Me_{18}), -3.33 (b, 2H, $H_{4'}$), -8.11 (b, 2H, $H_{5'}$), -9.09 (b, 2H, $H_{3'}$), -35.38 (b, 2H, $H_{6'}$). Mass spectrum (ESI, +ve): *m/z* 758 [Ru(ETT)Cl(DMSO)]+ and 680 [Ru(ETT)Cl]+. Elemental analysis: calculated for $C_{36}H_{37}Cl_3N_3O_2Ru$-1.5(H_2O); C, 55.5; H, 5.1; N, 5.4. Found C, 55.1; H, 5.0; N, 5.2.

Biological Testing: Tissue culture flasks, 96 well plates, RPMI 1640, DMEM, L-glutamine, trypsin-EDTA, HEPES, sodium pyruvate and FBS were obtained from Sigma, UK. Thiazolyl blue tetrazolium bromide (MTT) and DMSO were from Avocado, UK. Cells were grown in RPMI 1640 (T-47D, SK-OV-3) or DMEM (MDA-MB-231, A2780/cr) in 10 % FBS supplemented with 1% L-glutamine, 1% HEPES buffer and 1% sodium pyruvate. The MTT assay[84] was carried out using 96-well plates. Cells were harvested in logarithmic growth, 4,000 (A2780/cr), 10,000 (SK-OV-3, MDA-MB-231) or 25,000 cells (T-47D) were seeded per well and left overnight to attach. The cells were treated, in quadruplicate with 6 difference concentrations of complex dissolved in fresh media; the range of concentrations used is dependent on the complex. The cells were incubated for 72 hours and 20 µl of thaizolyl blue tetrazolium bromide (5mg / ml, 0.2 µm filtered) added. The cells were further incubated for 2 hours. The media was carefully removed by aspiration and 200 µl of DMSO added to dissolve the purple crystals. Absorbance was measured using a 96-well plate reader (Biorad) set at 570 nm. Each cell line was investigated beforehand to determine the correct cell numbers to initially seed and the required amount of time exposed to thiazolyl blue tetrazolium bromide to ensure sensitivity and accuracy.

Cellular Uptake: Two million cells were seeded in a 60mm diameter Petri dishes and left overnight to attach. Next day cells were treated with 30µM of the different compounds for 3 hours. After that time, the medium was removed and cells washed three times with PBS to remove all the platinum complexes not taken up but cells. Cells were collected and two aliquots of one million cells were taken, one of them to see whole cell uptake and the other for Cytoplasm and Nuclei fraction extraction (Nuclear/Cytoplasm extraction kit. BioVision). Two ml of ultrapure concentrated Nitric Acid (Traceselect Ultra, Aldrich) was added to the samples, and digested overnight at 90ºC. Samples were then taken to dryness at 120ºC, resuspended in a 2% solution of Nitric acid and filtered. The amount of Platinum was measured in a Agilent 7500CX ICP-MS (analysis was done with Pt sample cone in He and No-gas mode. Plasma settings: Ar.flow: 15 L/min; Neb gas: 0.8 L/min; RF power 1550W; T of spray chamber: 15 º C).

ESI-MS Nucleotide binding studies: 5'-GMP and 9-ethylguanine were stored at 4°C in a dessicator; they were dissolved freshly in 1mM sodium cacodylate buffer (pH 6.8) before each experiment. Fresh solution of complexes in 1mM sodium cacodylate buffer (pH 6.8) were used and mixed with nucleotides in a 1:1 ratio. The stock solutions of base and complex were both 2 mM. All the solutions were incubated for three days at 37°C in the dark. ESI-MS spectra were taken on a Micromass LCT Time of flight mass spectrometer.

^{1}H-NMR Nucleotide binding studies: 5'-GMP and 9-ethylguanine were stored at 4°C in a dessicator; they were dissolved freshly in 1mM sodium cacodylate buffer in D_2O (pH 6.8) before each experiment. Fresh solution of complexes in 1mM sodium cacodylate buffer in D_2O (pH 6.8) were used and mixed with nucleotides in a 1:1 ratio. The stock solutions of base and complex were both 2 mM. For hydrolysis assays no nucleotide was added, and complex was diluted to 1mM using 1mM sodium cacodylate buffer in D_2O (ph 6.8). H^1-NMR was measured at 0 h, 24 h and 72 h (96 h and 120 h for 9-ethylguanine) in a Bruker MX400 MHz with a BBI 5 mm inverse ^{1}H broadband probe. Between measurements the samples were kept in an incubator at 37ºC in the dark. For kinetic determination samples were prepared as described before and measured in a a Bruker MX400 MHz with a BBI 5 mm inverse ^{1}H broadband probe, at 0 h, 30 min, 1 h and every hour for 24 h at 37ºC. For NOE experiments the samples were prepared as described and measured in a a Bruker DRX500 MHz with a TBI 5 mm inverse Z gradient probe.

Gel electrophoresis unwinding assay: Plasmid pBR322 remained frozen until required for use. It is mixed with varying amounts of complex and steroids (1:1) and incubated for 24 hours. The total solution of 20 µl consists of 1 µl (stock = 1 µg / µl) pBR322, between 1.7 and 17 µl of complex:steroid (stock = 60 µM) and the remainder with ultra-pure water. After an incubation period of 24 h at 37 °C, 10 µl was removed and added to 3 µl of loading buffer and 10 µl loaded onto an agarose gel. The loading buffer consisted of 30 % glycerol, 0.05% bromophenol blue and 0.025 % cyanol xylene in ultra-pure water. 1% agarose gels were used and run using a HE99X Maxi (Amersham Biosciences, UK) submarine gel kit. The gel was loaded with 8 µl of DNA / loading buffer solution and ran using 1x TAE for 250 minutes at 5 V cm $^{-1}$. The gel was

stained after electrophoresis in TAE buffer containing ethidium bromide (0.5 mg ml^{-1}) for 10 minutes. The gel was visualized using an UVIdoc Platinum system (UViDoc, Cambridge, UK) at 312 nm. For gels of non-steroidal complexes with ethysterone a ratio 1:1 was used between the complex and the steroid.

Circular Dichroism: All C*D* spectra were recorded on a Jasco J-810 spectropolarimeter operated with the following parameters: sensitivity, 100 mdeg; start wavelength, 350 nm; end wavelength, 200 nm; data pitch, 0.5 nm; scanning mode, continuous; scanning speed, 200 nm per min; response, 0.1 seconds; bandwidth, 1.0; accumulation, 12. Stock solutions of ct-DNA (500 μM) and complex (500 μM) were mixed in varying proportions, and made up to 1 ml with ultrapure water with 20 mM NaCl and 0.89 mM Sodium Cacodylate pH 6.8, to achieved DNA:complex ratios of 100:1, 60:1, 40:1, 25:1, 15:1, 10:1, and 5:1. The solutions were incubated at 37 °C for 2 days.

HPLC enzymatic substrate assay: All measurements were performed in a Dionex HPLC system with an analytical column and an autosampler fitted operated with the following parameters: injection volume, 75 μl; Solvent A, water 0.05% TFA; Solvent B, methanol 0.05% TFA; method: 0-100% B gradient (0-40 min), 100% B (40-50 min), 100% A (50-60 min). AKR1Cs enzymes remained frozen until required for use. 20 μl (1.5 mg/ml) of recombinant enzyme was treated with 20 μl of cis-$[Pt(2ET)Cl(NH_3)_2](NO_3)$ (5 mM, ethanol) and 100 μl of NADPH (3 mM, Sigma). The final volume was taken to 2 ml with KH_2PO_4 Buffer (50 mM; pH 6.5). The order of addition was Buffer, enzyme, substrate and NADPH. Injections were done every hour for 24 hours. The same experiment was repeated with AKR1C3 for ethisterone and 9,10-phenantrenequinone (4 mM, acetonitrile, Sigma).

Enzymatic substrate assay: All the UV measurements were done in a Varian Cary 5000 UV/VIS spectrophotometer with a Varian 6x6 Multicell Block Beltier and a Varian Cary Temperature Controller attached operated with the following parameters:

sensitivity, 1 nm; wavelength, 340 nm; response, 0.1 seconds; temperature, 35ºC; cicle, 0.5 min; end time, 5 min. And data analysed using the Visual Enzymics program (Softzymics, Princetown, NJ, USA). AKR1Cs enzymes remained frozen until required for use. 10 or 40 µl (1.5 mg/ml) of recombinant enzyme was treated with 20 µl of cis-[Pt(2ET)Cl(NH_3)$_2$](NO_3) (Stock solution: 5mM, ethanol; final concentrations: 40, 20, 10, 5, 2.5, 1.25, 0.625 and 0.3125 µM) and 50 µl of NADPH (3 mM, Sigma). The final volume was taken to 1 ml with KH_2PO_4 Buffer (50m M; pH 6.5) preheated to 35 ºC. The order of addition was Buffer, enzyme, substrate and NADPH. Reaction was placed in a quartz cuvette and measured at 340nm in a prewarmed spectrophotometer.

Enzymatic inhibition assay: All the UV measurements were done in a Varian Cary 5000 UV/VIS spectrophotometer with a Varian 6x6 Multicell Block Beltier and a Varian Cary Temperature Controller attached operated with the following parameters: sensitivity, 1 nm; wavelength, 340 nm; response, 0.1 seconds; temperature, 35ºC; cicle, 0.5 min; end time, 5 min. And data analysed using the Visual Enzymics program (Softzymics, Princetown, NJ, USA). AKR1Cs enzymes remained frozen until required for use. 10 µl (1.5 mg/ml) of recombinant enzyme was treated with 20 µl of 9,10-phenantrenequinone (Stock solution: 4 mM, acetonitrile, Sigma; final concentrations: 20, 10, 5, 2.5, 1.25, 0.625 and 0.3125 µM), 20 µl of cis-[Pt(2ET)Cl(NH_3)$_2$](NO_3) (Stock solution: 5mM, ethanol; final concentrations:100, 20, 4 and 0 µM) and 50 µl of NADPH (3mM, Sigma). The final volume was taken to 1 ml with KH_2PO_4 Buffer (50mM; pH6.5) preheated to 35 ºC. The order of addition was Buffer, enzyme, substrate and NADPH. Reaction was placed in a quartz cuvette and measured at 340nm in a prewarmed spectrophotometer. The same experiment was repeated pretreating the enzymes with the different concentrations of cis-[Pt(2ET)Cl(NH_3)$_2$](NO_3) at 35ºC for 24h.

2.8 References

1 B. Lippert, Cisplatin, Chemistry and Biochemistry of A Leading Anti-Cancer Drug, Wiley-VCH, Weinheim, 1999.

2 J. Reedijk, *Chem. Commun*., 1996, **7**, 801.

3 Z. J. Guo, P. J. Sadler, *Adv. Inorg. Chem.*, 2000, **49**, 183.

4 J. D. Roberts, J. Peroutka, N. Farrell, *J. Inorg. Biochem.*, 1999, **77**, 51.

5 S. J. Lippard, J. M. Berg, *Principles of Bioinorganic Chemistry*; University Science Books, Mill Valley, CA, 1994.

6 M. Galanski, B. K. Keppler, *Anti-Cancer Agents in Medicinal Chemistry*, 2007, **7**, 55.

7 K. Petrak, *Drug Discovery Today*, 2005, **10**, 1667.

8 W. H. Ang, E. Daldini, L. Juillerat-Jeanneret, P. J. Dyson, *Inorg. Chem.*, 2007, **46**, 9048.

9 D. Kirpotin, J. W. Park, K. Hong, S. Zalipsky, W. L. Li, P. Carter, C. C. Benz, D. Papahadjopoulos, *Biochemistry*, 1997, **36**, 66.

10 D. Goren, A. T. Horowitz, D. Tzemach, M. Tarshish, S. Zalipsky, A. Gabizon, *Clin. Cancer Res.*, 2000, **6**, 1949.

11 G. G. Chen, Q. Zeng, G. M. K. Tse, *Med. Res. Rev.*, 2008, **28**, 954.

12 W. Somboonporn, S. R. Davies, *Endocr. Rev.*, 2004, **25**, 374.

13 A. Barqawi, E. D. Carwford, *Int. J. Imp. Res.*, 2006, **18**, 323.

14 S. Borgquist, C. Holm, M. Stendahl, L. Anagnostaki, G. Landberg, K. Jirstrom, *J. Clin. Pathol.*, 2008, **61**, 197.

15 S. Top, H. El Hafa, A. Vessières, J. Quivy, J. Vaissermann, D. W. Hughes, M. J. McGlinchey, J. P. Moron, E. Thoreau and G. Jaouen, *J. Am. Chem. Soc.*, 1995, **117**, 8372.

16 A. Jackson, J. Davis, R.J. Pither, A. Rodger, M.J. Hannon, *Inorg. Chem.*, 2001, **40**, 3964.

17 M. B. Skaddan, F. R. Wust, S. Jonson, R. Syhre, M. J. Welch, H. Spies, J.A. Katzenellenbogen, *Nucl. Med. Biol*., 2000, **27**, 269.

18 R. Devraj, J. F. Barrett, J. A. Fernandez, J.A. Katzenellenbogen, M. Cushman, *J. Med. Chem.*, 1996, **39**, 3367.

19 S. Top, A. Vessières, C. Cabestaing, I. Laios, G. Leclerq, C. Provot, G. Jaouen, *J. Organomet. Chem.*, 2001, **637**, 500.

20 S. Top, E.B. Kaloun, A. Vessieres, G. Leclercq, I. Laios, M. Ourevitch, C. Deuschel, M.J. McGlinchey, G. Jaouen, *ChemBioChem.*, 2003, **4**, 754.

21 M. P. Georgiadis, S. A. Haroutounian, K. P. Chondros, *Inorg. Chim. A-Bioinorg.*, 1987, **138**, 249.

22 D. M. Spyriounis, V. J. Demopoulos, P. N. Kourounakis, D. Kouretas, A. Kortsaris, O. Anronoglou, *Eur. J. Med. Chem.*, 1992, **27**, 301.

23 C. Cassino, E. Gabano, M. Ravera, G. Cravotto, G. Palmisano, A. Vessières, G. Jaouen, S. Mundwiler, R. Alberto, D. Osella, *Inorg. Chim. Acta*, 2004, **357**, 2157.

24 E. Gabano, C. cassino, S. Bonetti, C. Prandi, D. Colangelo, A. L. Ghiglia, D. Osella, *Org. Biomol. Chem.*, 2005, **3**, 3531.

25 V. Gagnon, M. E. St-Germain, C. Descôteaux, J. Provencher-Mandeville, S. Parent, S. K. Mandal, E. Asselin, G. Bérubé, *Bioorg. Med. Chem. Lett.*, 2004, **14**, 5919.

26 V. Perron, D. Rabouin, E. Asselin, S. Parent, R. C. C. Gaudreault, G. Bérubé, *Bioorg. Chem.*, 2005, **33**, 1.

27 Q. He, C. H. Liang, S. J. Lippard, *Proc. Natl. Acad. Sci*, 2000, **97**, 5768.

28 K. R. Barnes, A. Kutikov, S. J. Lippard, *Chemistry and Biology*, 2004, **11**, 557.

29 M.J. Hannon, P.S. Green, D.M. Fisher, P.J. Derrick, J.L. Beck, S.J. Watt, M.M. Sheil, P.R. Barker, N.W. Alcock, R.J. Price, K.J. Sanders, R. Pither, J. Davis, A. Rodger, *Chem. – Eur. J.*, 2006, **12**, 8000.

30 For an example of an androgen targeting a radiopharmaceutical see F. Wust, D. Scheller, H. Spies, B. Johannsen, *Eur. J. Inorg. Chem.*, 1998, 789.

31 J. J. Isola, *J. Pathol*, 1993, **170**, 31.

32 V. Kuenenboumeester, T. H. Vanderkwast, W. L. J. Vanputten, C. Claassen, B. Vanooijen, S.C. Henzenlogmans, *Int. J. Cancer*, 1992, **52**, 581.

33 O. A. Lea, S. Kvinnsland, T. Thorsen, *Cancer Res.*, 1989, **49**, 7162.

34 M. R. Cardillo, E. Petrangeli, N. Aliotta, L. Salvatori, L. Ravenna, C. Chang, G. Castagna, *J. Exp. Clin. Cancer Res.*, 1998, **17**, 231.

35 R. Kuhnel, J. Degraaff, B. R. Rao, J. G. Stolk, *J. Steroid Biochem.*, 1987, **26**, 393.

36 J. V. Ilekis, J. P. Conner, C. S. Prins, K. Ferrer, C. Niederberger, B. Scoccia, *Gynecol. Oncol.*, 1997, **66**, 250.

37 I. Leav, K. M. Lau, J. Y. Adams, J. E. McNeal, M. E. Taplin, J. F. Wang, H. Singh, S. M. Ho, *Am. J. Pathol.*, 2001, **159**, 79.

38 A. Hobisch, Z. Culig, C. Radmayr, G. Bartsch, H. Klocker, A. Hittmair, *Cancer Res.*, 1995, **55**, 3068.

39 J. A. R. Dewinter, P. J. A. Janssen, M. C. T. Verleunmooijman, J. Trapman, A. O. Brinkmann, A. B. Santerse, F. H. Schroder, T. H. Vanderkwast, *Am. J. Pathol.*, 1994, **144**, 735.

40 Martin Huxley, PhD Thesis, University of Warwick, 2006.

41 Michael Browning, PhD Thesis, University of Warwick, 2006.

42 M. Huxley, C. Sanchez-Cano, M. J. Browning, C. Navarro-Ranninger, A. G. Quiroga, A. Rodger, M. J. Hannon, To be submitted.

43 L. S. Hollis, A. R. Amundsen, E. W. Stern, *J. Med. Chem.*, 1989, **32**, 128.

44 L. S. Hollis, W. I. Sundquist, J. N. Burstyn, W. J. Heiger-Bernays, S. F. Bellon, K. J. Ahmed, A. R. Amundsen, E. W. Stern, S. J. Lippard, *Cancer Res.*, 1991, **51**, 1866.

45 Hollis et al. [44] have demonstrated some activity of cis-$[Pt(NH_3)_2(py)Cl]^+$ in sarcoma and murine leukaemia in mice although they noted the agent shows significantly lower potency than cisplatin. In the in-vitro cell-lines studied herein the agent has very low potency (high IC_{50}).

46 M. Huxley, C. Sanchez-Cano, M. J. Browning, C. Navarro-Ranninger, A. G. Quiroga, A. Rodger, M. J. Hannon, *To be submitted*.

47 P. Siemsen, R. C. Livingston, F. Diederich, *Angew. Chem. Intl. Ed.*, 2000, **39**, 2633.

48 G. Berube, D. Rabouina, V. Perron, B. N'Zemba, R. C. Gaudreault, S. Parent, E. Asselin, *Steroids*, 2006, **71**, 911.

49 A. Bajaj, P. Kondaiah, S. Bhattacharya, *J. Med. Chem.*, 2008, **51**, 2533.

50 Phil Barker, PhD Thesis, University of Warwick, 2001.

51 G. Lowe, A. A. Droz, T. Vilaivan, G. W. Weaver, J. J. Park, J. M. Pratt, L. Tweedale, L. R. Kelland, *J. Med. Chem.*, 1999, **42**, 3167.

52 S. Aoki, Y. Watanabe, M. Sanagawa, A. Setiawan, N. Kotoku, M. Kobayashi, *J. Am. Chem. Soc.*, 2006, **128**, 3148.

53 M. Lanzino, F. De Amicis, M. J. McPhaul, S. Marsico, M. L. Panno, S. Ando, *J. Biol. Chem.*, 2005, **21**, 20421.

54 B. C. Behrens, T. C. Hamilton, H. Masuda, K. R. Grotzinger, J. Whang-Peng, K. G. Louie, T. Knutsen, W. M. McKoy, R. C. Young, R. F. Ozols, *Cancer Res.*, 1987, **47**, 414.

55 30 μM was chosen as a good compromise of the activity of cisplatin and the steroidal-complexes through the chosen cell lines.

56 S. F. Bellon, J. H. Colleman, S. J. Lippard, *Biochemistry*, 1991, **30**, 8026.

57 F. J. Ramos-Lima, O. Vrana, A. G. Quiroga, C. Navarro-Ranninger, A. Halamikova, H. Rybnickova, L. Hejmalova, V. Brabec, *J. Med. Chem.*, 2006, **49**, 2640.

58 W. R. Bauer, *Annu. Rev. Biophys. Bioeng.*, 1978, **7**, 287.

59 J. Reedijk, *Proc. Natl. Acad. Sci.*, 2003, **100**, 3611.

60 A. Anzellotti, S. Stefan, D. Gibson, N. Farrell, *Inorg. Chim. Acta*, 2006, **359**, 3014.

61 A. Rodger, B. Nordén, *'Circular Dichroism and Linear Dichroism'* Oxford University Press, 1997.

62 M. Kawata, *Neurosci. Res.*, 1995, **24**, 1.

63 B. M. W. Schmidt, D. Gerdes, M. Feuring, E. Falkenstein, M. Christ, M. Wehling, *Front. Neuroendocrinol.*, 2000, **21**, 57.

64 B. J. Cheskis, J. G. Greger, S. Nagpal, L. P. Freedman, *J. Cell. Physiol.* , 2007, **213**, 610.

65 M. J. Tikkanen, V. Vihma, M. Jauhiainen, A. Höckerstedt, H. Helisten, M. Kaamanen, *Cardiovasc. Res.*, 2002, **56**, 184.

66 D. G. Stocco, *Annu. Rev. Physiol.*, 2001, **63**, 193.

67 D. L. Bain, A. F. Heneghan, K. F. Connaghan-Jones, M. T. Miura, *Annu. Rev. Phisiol.*, 2007, **69**, 201.

68 Y. Jin, T. M. Penning, *Annu. Rev. Pharmacol. Toxicol.*, 2007, **47**, 263.

69 T. M. Penning, J. E. Drury, *Arch. Biochem. Biophys.*, 2007, **464**, 241.

70 Y. Jin, T. M. Penning, *Biochemistry*, 2006, **45**, 13054.

71 T. M. Penning, S. Steckelbroeck, D. Bauman, M. W. Miller, Y. Jin, D. M. Peehl, K.-M. Fung, H.-K. Ling, *Mol. Cel. Endocrinol.*, 2006, **248**, 182.

72 W. Chen, J. A. Kocal, T. A. Brandvold, M. L. Bricker, S. R. Bare, R. W. Broach, N. Greenlay, K. Popp, J. T. Walenga, S. S. Yang, J. J. Low, *Catalysis Today*, 2009, **140**, 157.

73 M. C. Byrns, S. Steckelbroeck, T. M. Penning, *Biochem. Pharmacol.*, 2008, **75**, 484.

74 J. M. Day, H. J. Tutill, A. Purohit, M. J. Reed, *Endocr. Relat. Cancer*, 2008, **15**, 665.

75 K. Sonogashira, Y. Tohda, N. Hagihara, *Tetrahedron Let.*, 1975, **16**, 4467.

76 A. G. Quiroga, C. Navarro-Ranninger, *Coord. Chem. Rev.*, 2004, **248**, 119.

77 J.P. Scovill, D.L Klayman, D.G Franchino, *J. Med. Chem.*, 1982, **25**, 1261.

78 D. X. West, R. E. Kohrman, *J. Inorg. Nucl. Chem.*, 1979, **41**, 477.

79 T. Yajima, M. Okajima, A. Odani, O. Ymauchi, *Inorg. Chim. Acta*, 2002, **339**, 445.

80 P. M. van Vliet, S. M. S. Toekimin, J. S. Haasnoot, J. Reedijk, O. Novakova, O. Vrana, V. Brabec, *Inorg. Chim. Acta*, 1995, **231**, 57.

81 O. Novakova, J. Kasparkova, O. Vrana, P. M. van Vliet, J. Reedijk, V. Brabec, *Biochemistry*, 1995, **34**, 12369.

82 A. H. Velders, PhD Thesis, Leiden, 2001.

83 K. S. Lovejoy, R. C. Todd, S. Zhang, M. S. McCormick, J. A. D'Aquino, J. T. Reardon, A. Sancar, K. M. Giacomini, S. J. Lippard, *Proc. Natl. Acad. Sci.*, 2008, **105**, 8902.

84 T. Mosmann, *J. Inmunol. Meth.*, 1983, **65**, 55.

Chapter 3: Steroidal non-covalent metallodrugs

3.1 Introduction

As explained previously (Section 2.1) sex hormones such as estrogens and testoterone are interesting as delivery vectors because of their importance in reproductive system cancers[1-6]. For that reason active cytotoxic metallo-drugs have been attached to natural or synthetic oestrogens, aiming to target the estradiol receptor (ER; Fig. 3.1 A to D)[7-16]. In the previous chapter (Chapter 2) it was demonstrated that the same strategy can be used to target the androgen receptor (AR). Using a series of testosterone-derived mononufunctional complexes previously synthesised in our group (Fig. 3.1 E)[17-20], it was shown that linkage of the testosterone confered cytotoxic activity to otherwise non toxic compounds. It improved the effectiveness of the uptake of the complexes in cells[20] and the compounds caused big distortions when bound to DNA[21].

Figure 3.1. Recent examples of steroids coordinated to platinum drugs.

All of the previous steroid-drug bioconjugates have focused on DNA "alkylating" agents that form a direct covalent or coordinative bond to the bases (like cisplatin). As explained in Chapter 1.1 small molecules can interact with DNA without binding covalently[21-23]. Non-covalent DNA-binding metallo-drugs (Fig. 3.2) have in general been less extensively studied than cisplatin analogues, but show a broad spectrum of direct activities[24-25]. They represent an interesting alternative to the covalent coordinative DNA-binders, because having a different mode of action they perhaps can circumvent some problems, such as cross-resistance or side effects. For these reasons the conjugation of non-covalent metallo-drug units to steroids was of interest. Synthetic techniques and approaches that allow very easy access to such conjugates are described below, as well as how the presence of the steroid affect the toxicity and behaviour of such drugs in their interaction with both whole cells and macromolecules.

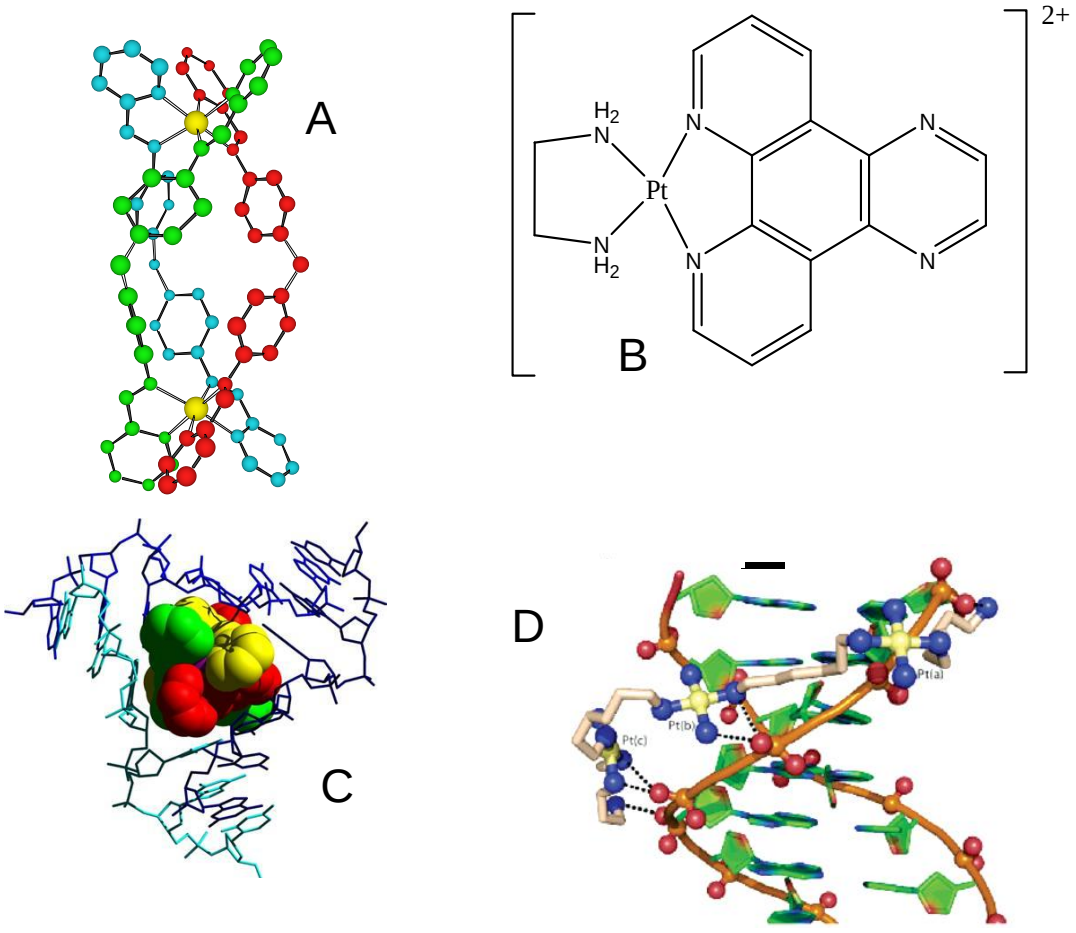

Figure 3.2. Metallodrugs that bind in the major groove (A) or intercalate between DNA bases (B); non-covalent DNA Three Way Junction binding (C, taken from Olesky et al[2]) and Phospate binding (D, TriplatinNC, taken from Komeda et al[3]).

3.2 Design and synthesis of complexes

3.2.1 Design of complexes

There are five commonly accepted kinds of non-covalent DNA binding interactions: minor groove binders, major groove binders, intercalators, phosphate binders and junction binders[21-23] (see Chapter 1 for more details). Normally the molecules binding in these ways are quite big, so the attachment of a steroidal moiety that would make them even bigger can present some challenging syntheses. Furthermore, the bulkiness of these "DNA Binding Domains" could make the final construct too big to target the steroid receptors effectively. The type of non-covalent binder that tends to be smaller, comparable sometimes to covalent binding molecules, are the intercalators. For that reason we decided to focus on these. From the multiple variety of metallo-intercalators[26-29], we chose a Pt(II) metallic centre bound to a terpyridine molecule. This unit has been broadly studied; its DNA binding abilities has been known for a long time (a crystal structure with a short oligomer was published in the late 1970s[30]), a broad spectrum of modified monomers and dimers have been synthesised and showing some of them citotoxicity properties[31-33]. Covalent DNA binders comprising Pt(II) terpyridines linked to steroids have been synthesised previously in our group[16, 34], so this will give us the opportunity to compare the two modes of DNA binding.

Our previous examples of attaching covalent binding terpyridine complexes to steroids, took much effort, and many steps. However, as Ma et al.[35] previously described, platinum terpyridines can be easily coordinated to triple bonds. This procedure allows us to synthesise the new complexes in a much easier way than the covalent binders. A single step would conjugate commercially available 17α-ethynyl-steroids, and terpyridineplatinum(II)chloride, under normal coupling conditions (Fig. 3.3). This is probably the easier way to attach a steroid to a metallodrug, since is a one pot synthesis of a commercially available steroid and a well established metallodrug, without need for prior synthesis of steroidal ligands. Similar strategies can potentially be used for different metals such as gold[36].

Figure 3.3. Synthetic pathway for steroidal and non-steroidal terpyridine intercalators.

Following the same procedure, non-steroidal controls could also be easily synthesised to compare the effect of the steroid on the activity of the complexes. Previously synthesised covalent binding terpyridines steroids could be used as starting material as well (Fig. 3.4); this would show us how the binding mode of the platinum terpy affects the activity of the compounds, and how important the intercalation of the terpyridine is compared with intercalation of smaller aromatic rings.

Figure 3.4. Synthetic pathway for steroidal phenyl intercalators.

3.2.2 Synthesis of complexes

Following the general routes proposed above, we synthesised a series of compounds that satisfied our designs. Starting from commercially available steroids or benzylacetylene and from the chloride salt of $[Pt(tpy)Cl]^+$ (obtained easily following the procedure reported by Buchner et al.[37]) we can obtain our intercalators in a single step using a CuI catalyst. Use of an inert atmosphere (Ar or N_2), was necesary to minimize Glaser[38] coupling (connection of two triple bonds) that occurs when oxygen is present.

Once the complexes have been synthesised, purification is easily achieved through a semipreparative HPLC [40 minutes gradient of water:acetonitrile (0-100%) in presence of 0.05% of TFA] and TFA used in the HPLC replaces the chloride counter ion. Following this procedure the complexes can be obtained in good yields, around 50-70%, and compared with overall yields of previous steroidal complexes their synthesis is extremely effective. Previously reported steroidal terpyridine covalent binders[16, 34] were used as starting material for the steroidal phenyl intercalators (Fig. 3.4). However, while HPLC purification can be achieved following the same protocol and yields are similar, the starting material synthesis means that this complex is obtained in low overall yield. All the complexes are partially soluble in methanol or acetonitrile, but extremely soluble in mixtures of water and acetonitrile.

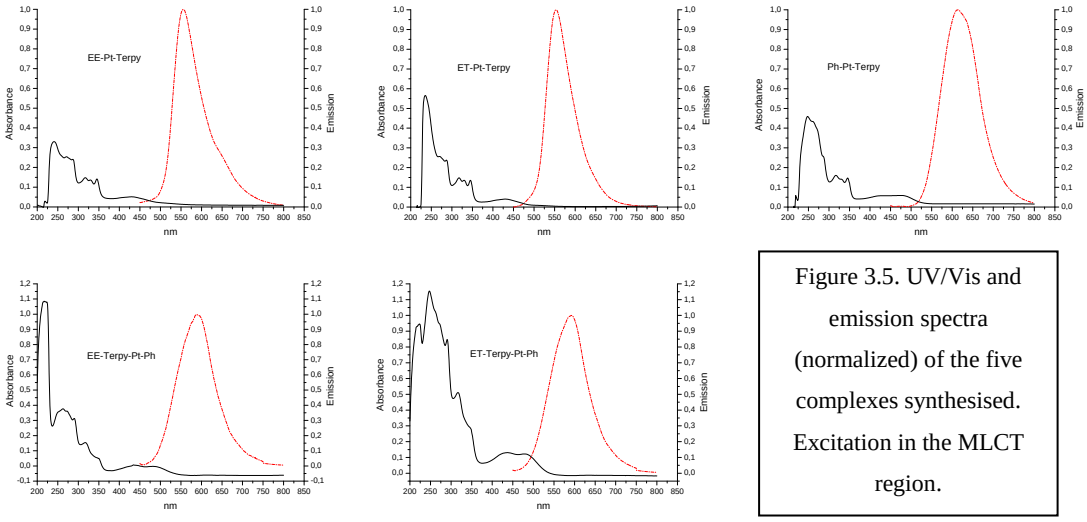

Figure 3.5. UV/Vis and emission spectra (normalized) of the five complexes synthesised. Excitation in the MLCT region.

All five complexes are fluorescent when excited in the MLCT region in dichloromethane and other aprotic solvents. However, this fluorescence is not visible

when the complexes are placed in protic solvents (such as water), because the excited state is quenched by O-H vibrations[39-40] (Fig. 3.5).

(EE-Pt-Terpy)TFA

Using 17α-ethynyl-estradiol we obtained the first of our steroidal intercalator complexes, EE-Pt-Terpy. Analysis by ESI-MS shows the expected +1 cation at 723 m/z. ^{1}H-NMR in mixtures of deuterated water:acetonitrile (Fig. 3.6) show both steroid and terpyridine units in a 1:1 ratio. The steroid protons 1, 2 and 4 can be clearly detected between 7.1 and 6.4 ppm, integrating for one proton each. The methyl group of the estradiol is clearly detected as well at 0.94 ppm, integrating for 3 protons. For the terpyridine there is a doublet at around 9.3 ppm ($H_{6'}$, 2 protons, J_{HH} = 5.5 Hz); a doublet of doublets at 7.78 ppm ($H_{5'}$, 2 protons, J_{HH} = 5.5 and 7.7 Hz) and a multiplet centered around 8.4 ppm integrating for 7 protons. This multiplet corresponds to protons $H_{4'}$, $H_{3'}$, $H_{3''}$ and $H_{4''}$. The expected J_{HH} couplings for the terpyridine protons (around 5 Hz for $H_{6'}$, 5 and 8 Hz for $H_{5'}$, 8 and 8 Hz for $H_{4'}$ and 8 Hz for $H_{3'}$)[33] and the subtle J_{PtH} observed for $H_{6'}$ further prove our assignment, which is consistent with these of ET-Pt-Terpy and Ph-Pt-Terpy (see below), whose assignation was confirmed by 2D-COSY.

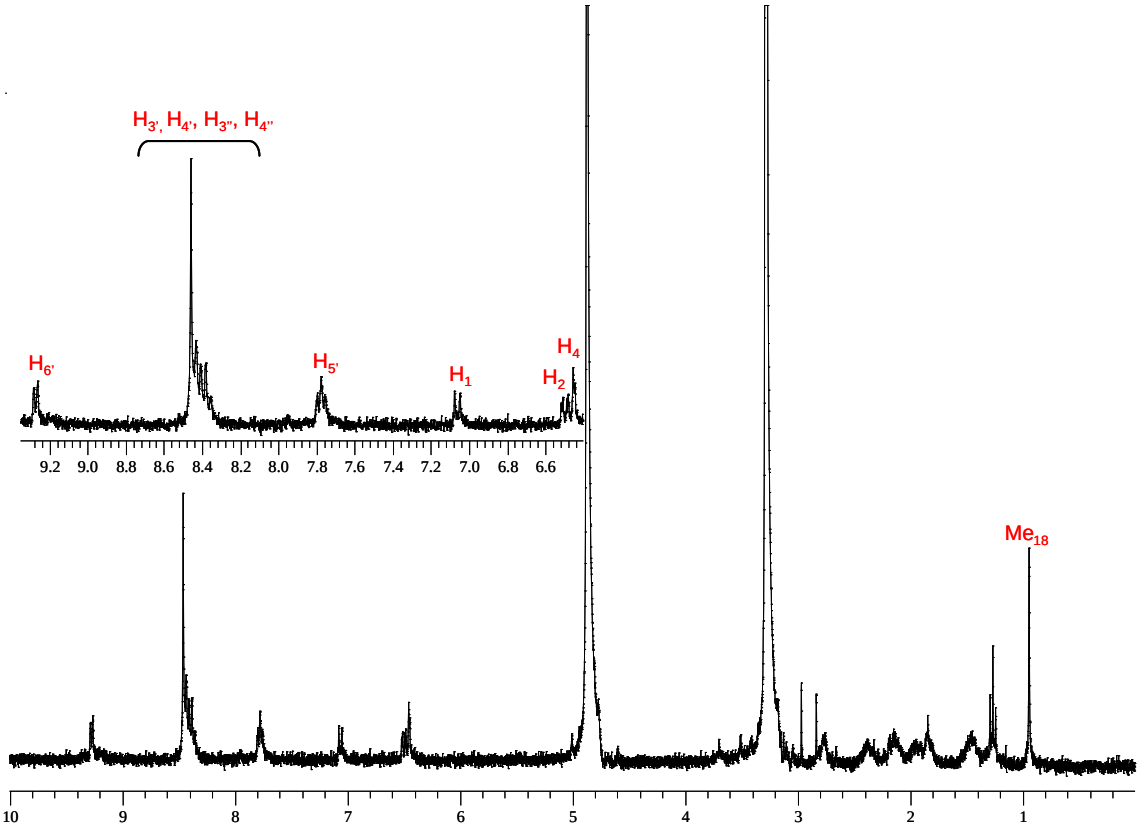

Figure 3.6. ^{1}H-NMR of EE-Pt-Terpy in a mixture of deuterated water:acetonitrile (1:1).

The UV/VIS absorption spectrum was measured in dichloromethane and shows a terpyridine ligand-based band between 300-350 nm and the steroid band, showing the maximum at around 242 nm. The Pt(tpy) region corresponding to the MLCT transitions can be detected between 400-500 nm. The complex can be excited in this MLCT region (around 425 nm), to obtain a fluorescence with a maximum of emission at 540 nm (Fig. 3.7).

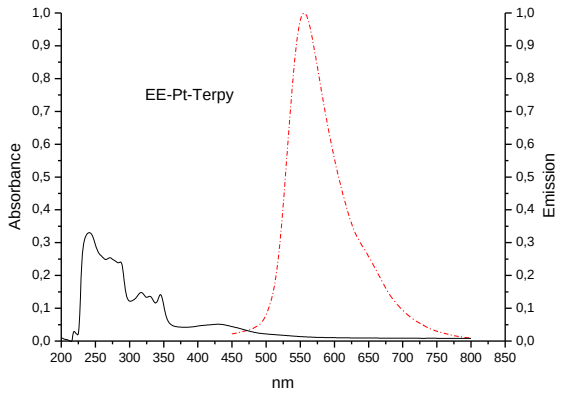

Figure 3.7. UV/Vis and emission spectra (normalized) of EE-Pt-Terpy (25 μM) in dichloromethane. λ_{exc}=425nm.

(ET-Pt-Terpy)TFA

The androgenic version of the previous complex can be synthesised easily if 17α-ethynyl-testosterone (ethisterone) is used. Again analysis by ESI-MS shows the expected +1 cation at 739 m/z, showing that the complex is formed. To prove further this ^{1}H-NMR in mixtures of deuterated water:acetonitrile was performed, showing again steroidal and terpyridine based peaks (Fig. 3.8). The testosterone proton 4 can be detected clearly with an integration of one at 5.7 ppm. Methyl groups of the testosterone, are observed at 1.27 and 0.98 ppm (indicating that only one compound is present). In the terpyridine region, protons integration shows a 1:1 ratio with the testosterone moiety. These terpyridine protons have been assigned through the use of information provided by the observed terpyridine J_{HH} couplings (as explained for EE-Pt-Terpy)[33] and the presence of J_{PtH} couplings, with the help of 2D ^{1}H-NMR (Fig. 3.9). Three peaks and a multiplet can be detected from seven expected peaks, integrating for two (two double doublets and a doublet) and five protons (a multiplet), adding between them the expected 11 protons of the terpyridine molecule. Using the J_{HH} couplings these peaks can be assigned as $H_{6'}$ (d, 9.25 ppm, J_{HH} = 5.5 Hz), $H_{4'}$ (dd, 8.4 ppm, J_{HH} =7.6 and 8.0 Hz) and $H_{5'}$ (dd, 7.78 ppm, J_{HH} = 5.5 and 7.6 Hz), indicating that the multiplet correspond to $H_{3'}$, $H_{3''}$ and $H_{4''}$ protons. This is consistent with the observed satellites produced by the J_{PtH} coupling in the proton assigned as $H_{6'}$ and the information obtained from the 2D-COSY NMR of the molecule (Fig. 8). In this spectrum the resonance signal assigned as $H_{5'}$ is shown to be related to the signal assigned as $H_{6'}$ and $H_{4'}$, showing that these peaks represent correlative protons.

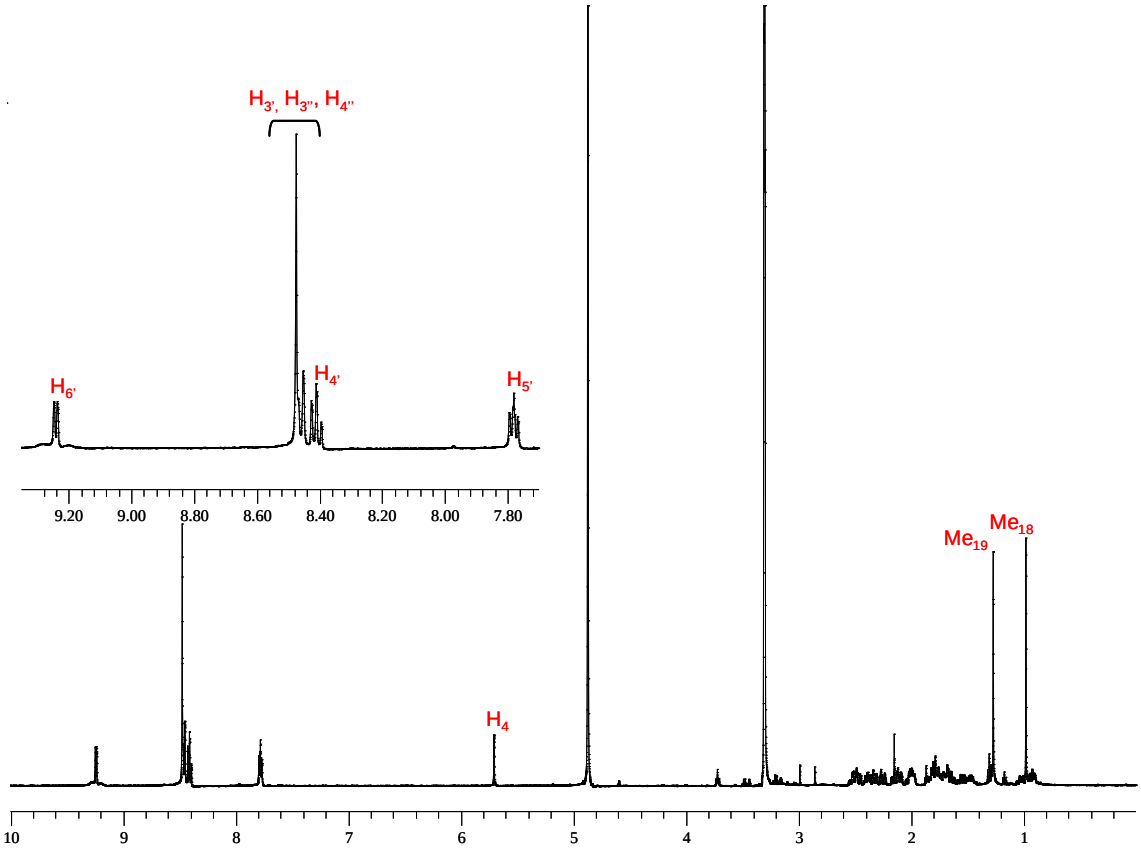

Figure 3.8. ^{1}H-NMR of ET-Pt-Terpy in a mixture of deuterated water:acetonitrile (1:1).

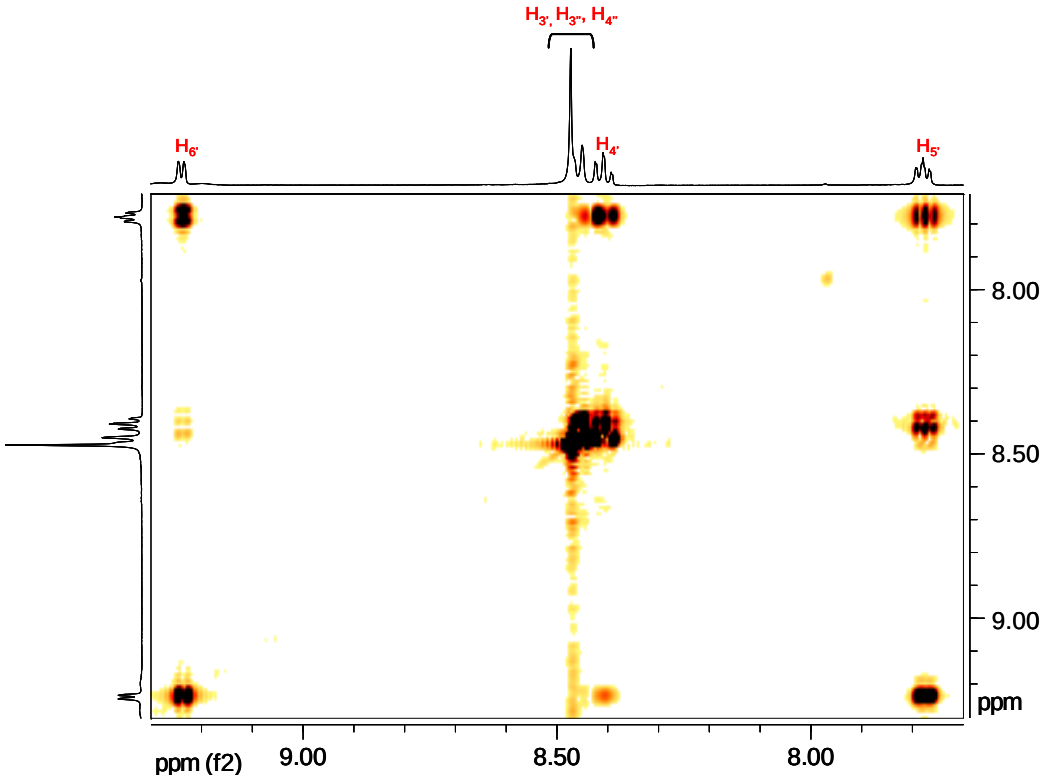

Figure 3.9. 2D-COSY ^{1}H-NMR of ET-Pt-Terpy (aromatic region) in a mixture of deuterated water:acetonitrile (1:1).

The UV/VIS spectrum in dichlorometane shows similar pattern that the estradiol complex, with the terpyridine-based region between 300-350 nm, and the steroidal with a maximum at 248 nm. However this testosterone band is more intense showing an absortion of almost twice the intensity of the oestrogenic compound. The MLCT area can be detected between 400-500 nm and is the place were the complex can be excited (around 425 nm), to obtain a fluorescence with a maximum of emission at 540 nm (Fig. 3.10).

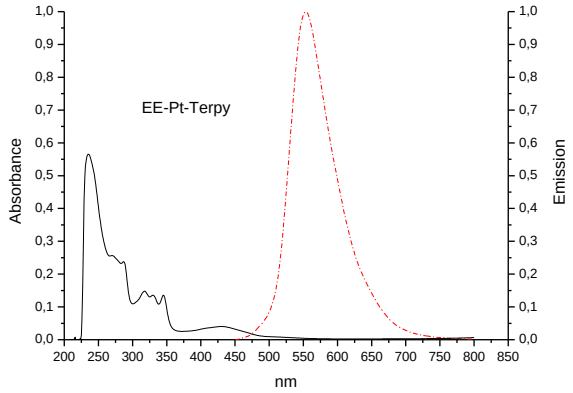

Figure 3.10. UV/Vis and emission spectra (normalized) of ET-Pt-Terpy (25 μM) in dichloromethane. λ_{exc}=425 nm.

(Ph-Pt-Terpy)TFA

Following the same procedure that the steroidal versions, with the use of the commercially available benzylacetylene, Ph-Pt-Terpy can be obtained. Analysis by ESI-MS shows the expected +1 cation at 529 m/z. Again ^{1}H-NMR (deuterated water:acetonitrile) allow us to confirm the data from ESI-MS showing that we obtained the desired compound (Fig. 3.12). A benzyl molecule is seen, in the aromatic region. Five protons can be clearly detected, with the correct integration, showing two doublets integrating for two protons (H_1 and H_2) and a doublet doublet for one (H_3), between 7.2 and 7.3 ppm. The terpyridine signals maintain a 1:1 ratio with the phenyl group and can be assigned using a similar reasoning to the one used for EE and ET-Pt-Terpy. $H_{6'}$ (d,

8.7 ppm, J_{HH} = 5. 4 Hz), $H_{4'}$ (dd, 8.15 ppm, J_{HH} = 7. 7, 7.8 Hz, visible J_{PtH} coupling), $H_{3'}$ (d, 8.09 ppm, J_{HH} = 7.7 Hz) and $H_{5'}$ (dd, 7.59 ppm, J_{HH} = 5.5 and 7.6 Hz) can be assigned following the standard patterns of the J_{HH} couplings presented by the terpyridine molecule[33]. $H_{3''}$ and $H_{4''}$ then, can be assigned as the multiplet visible at 8.2 ppm. 2D-COSY ^{1}H-NMR (Fig. 3.11) confirms the assignment showing close relation between the signals assigned to $H_{5'}$-$H_{6'}$, $H_{5'}$-$H_{4'}$ and $H_{4'}$-$H_{3'}$ and weak interactions between $H_{6'}$-$H_{4'}$ and $H_{5'}$-$H_{3'}$.

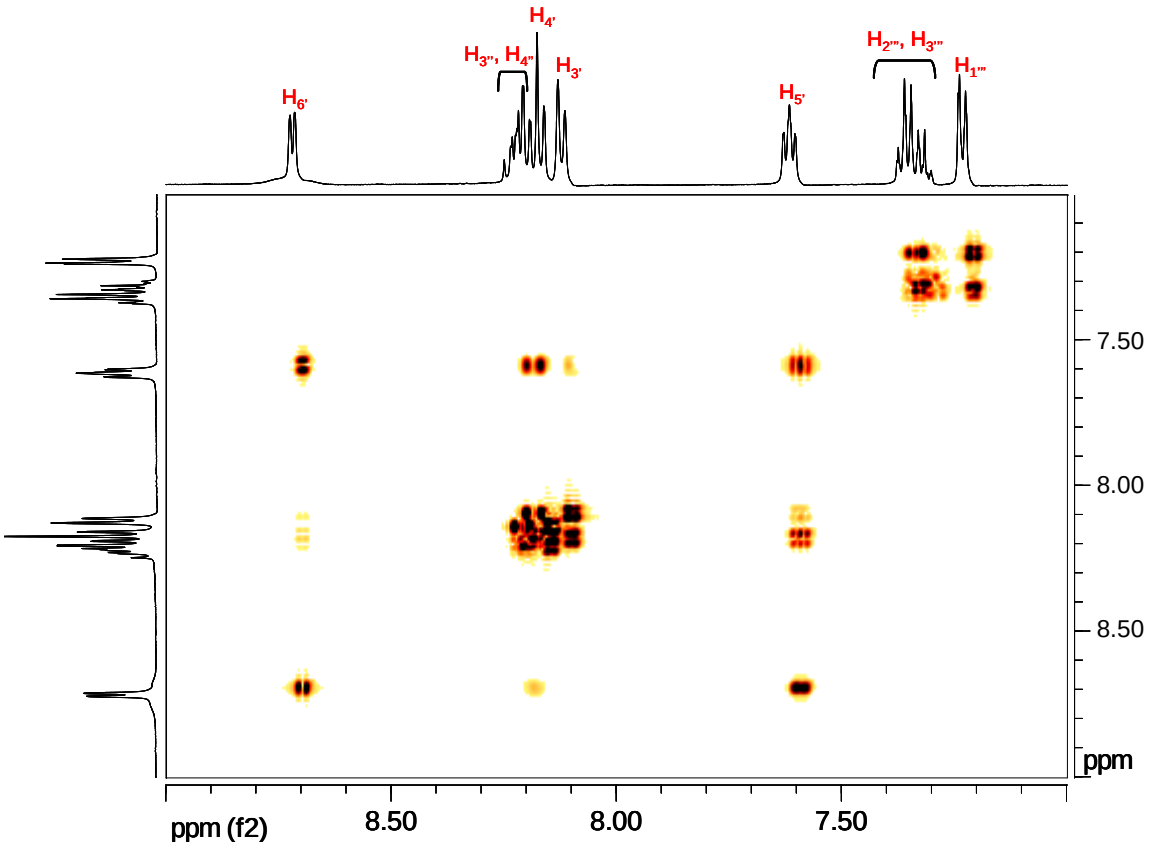

Figure 3.11. 2D-COSY ^{1}H-NMR of Ph-Pt-Terpy in a mixture of deuterated water:acetonitrile (1:1).

UV/VIS shows the same tpy-based band and a maximum at 248 nm with intensity between the two previous complexes. The MLCT region can be detected between 400-500 nm, being broader than the steroidal compounds. If this transition is excited (around 480 nm), fluorescence emission is obtained with a maximum at 650 nm. However, for this complex the area of excitation is bigger than for the steroidal ones, showing the same emission when excited all the way through the MLCT region (Fig. 3.13).

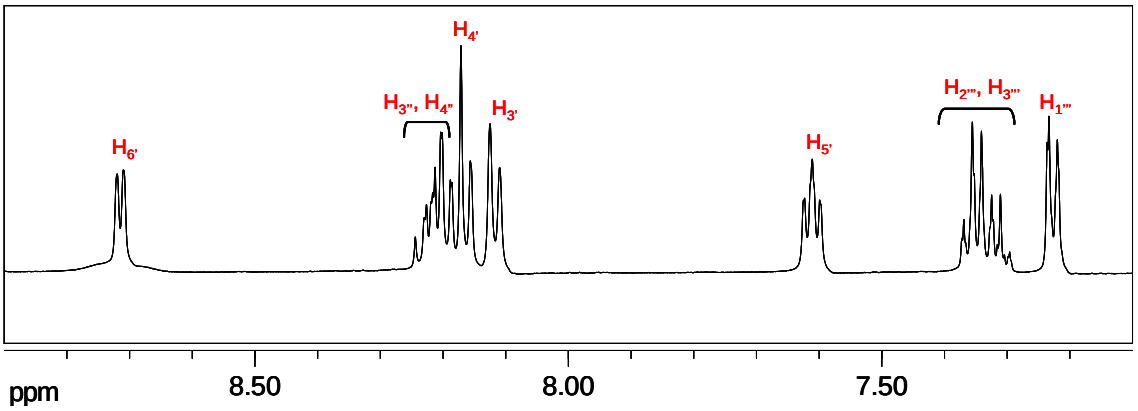

Figure 3.12. ^{1}H-NMR of Ph-Pt-Terpy in a mixture of deuterated water:acetonitrile (1:1).

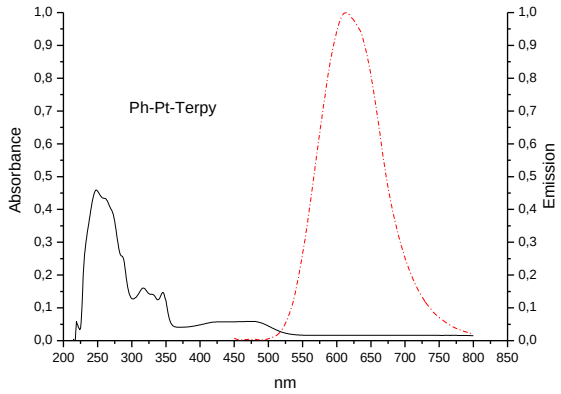

Figure 3.13. UV/Vis and emission spectra (normalized) of Ph-Pt-Terpy (25 μM) in dichloromethane. λ_{exc}=480 nm..

(EE-Terpy-Pt-Ph)TFA

EE-Terpy-Pt-Ph is created through the coupling of benzylacetylene and EETPt[16, 34]. The increased complexity of the molecule make the ^{1}H-NMR (mixtures of deuterated water:acetonitrile) more complicated than usual (Fig. 3.14). The addition of the benzyl unit, adds (theoretically) 3 new peaks to the aromatic region, making it more crowded. As observed in Figure 3.15, the coupling of this phenyl acetylene group produces a broadening of the signals close to the metallic centre (maybe due to a possible different stacking between the molecules to the one presented by previously explained

complexes). This makes it impossible to assign the peaks by following the terpyridine J_{HH} coupling pattern. A possible assignment of these terpyridines proton signals can be done using the EETPt[16, 34] parent complex as a guide. Using this as a template, $H_{6'}$ (8.11 ppm), $H_{4'}$ (7.95 ppm, seen as a broad triplet), $H_{3'}$ (7.67 ppm, seen as a broad doublet), and $H_{3''}$ (7.56 ppm) can be assigned. $H_{5'}$ resonance is found to be close to the ones belonging to the phenyl group. This combination of signals ($H_{5'}$ and phenyl protons) produces a multiplet integrating for 5 protons at 7.21 ppm and a broad peak at 6.85 ppm integrating for 2 protons. Again, using EETPt as a template, $H_{5'}$ can be assigned in the multiplet (because chemical shift difference with other protons is similar to the one observed in EETPt) togheter with two signals from the phenyl ring probably $H_{2'''}$ and $H_{3'''}$ (by comparison with Ph-Pt-Terpy), allowing to assign $H_{1'''}$ as the broad signal at 6.85 ppm. Since the steroid is far away from the platinum centre, it is not affected by broadening problems. That makes assignment easier; protons H_1, H_2 and H_4 are assigned to the doublets at 7.14 and 6.60 ppm and to the singlet at 6.56 ppm respectively, showing integration for a proton each. The methyl group appears at 0.89 ppm as a single peak giving an initial confirmation about purity of the complex. Analysis by ESI-MS shows the expected +1 cation at 823 m/z.

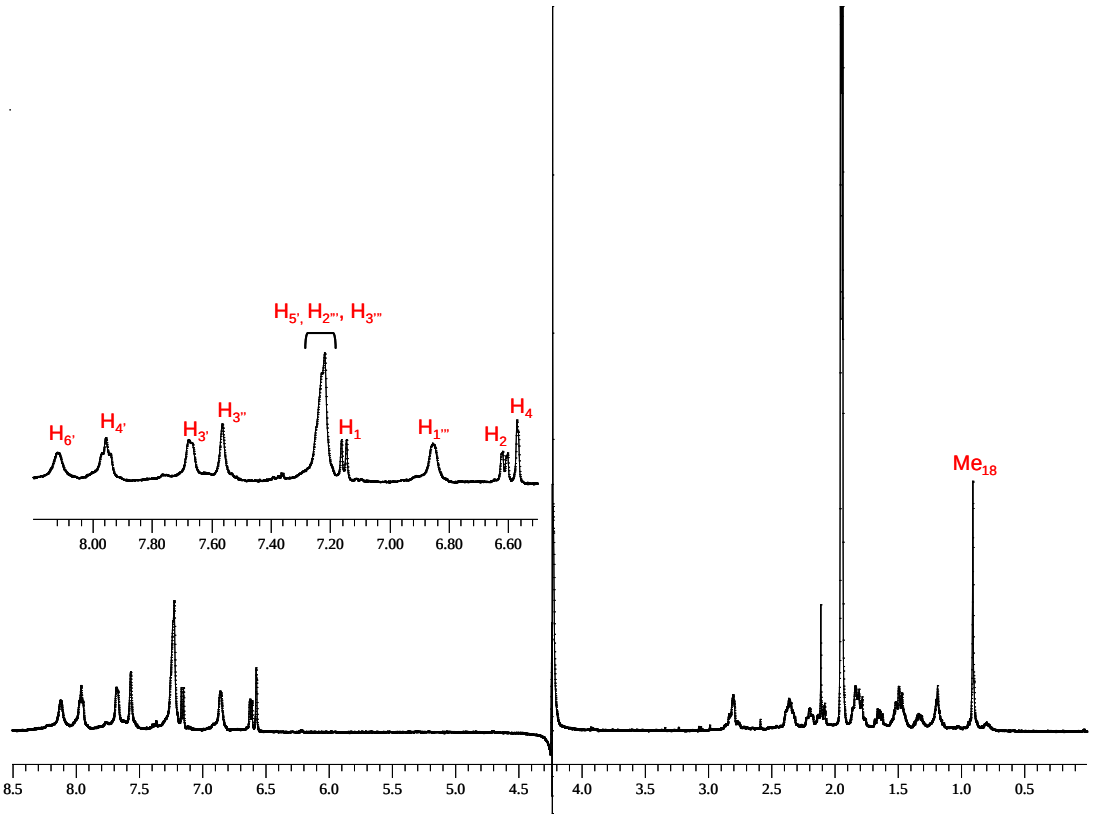

Figure 3.14. ^{1}H-NMR of EE-Terpy-Pt-Ph in a mixture of deuterated water:acetonitrile (1:1).

The UV/VIS was measured in dichloromethane and shows terpyridine-based (300-350 nm), benzyl (200-220 nm) and estradiol (250-300 nm) bands. A MLCT signal can be detected between 400-500 nm. This MLTC band is broader when the phenyl is attached. When excited in the MLCT (maximum around 480 nm), fluorescence is obtained with a maximum of emission at 600 nm (Fig. 3.15).

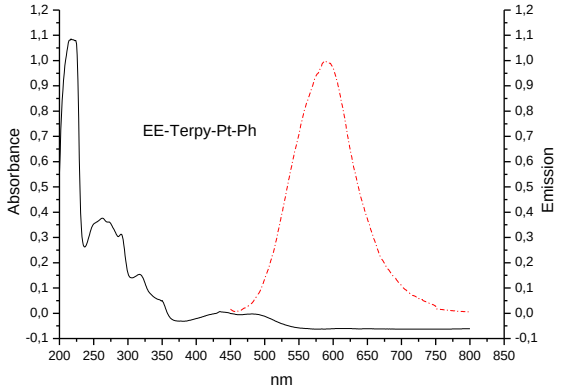

Figure 3.15. UV/Vis and emission spectra (normalized) of EE-Terpy-Pt-Ph (25 μM) in dichloromethane. λ_{exc}=480 nm.

(ET-Terpy-Pt-Ph)TFA

The androgenic phenyl intercalator can be easily synthesised when benzylacetylene and ETTPt[34] are used. ESI-MS shows the expected +1 cation at 839 m/z, without signals corresponding to complex breakdown. ^{1}H-NMR in mixtures of deuterated water:acetonitrile show similar behaviour to these of the oestrogen derivative, showing the broadening of peaks close to platinum (preventing the assignment through the expected terpyridine J_{HH} couplings; maybe due to a possible stacking between the molecules) and the form of multiplets with the signal of the phenyl ring (Fig. 3.16). Again, using ETTPt as a template, $H_{6'}$, $H_{4'}$, $H_{3'}$, and $H_{3''}$ terpyridine proton resonances can be assigned as the peaks observed at 8.13, 7.99, 7.69 and 7.55 ppm respectively. $H_{5'}$

(assigned following the similar chemical shift difference with other terpyridine protons compared with ETTPt[34]) is found forming a broad multiplet at 7.25 ppm with protons $H_{2'''}$ and $H_{3'''}$ of the phenyl ring (assigned by comparison with Ph-Pt-Terpy). Proton $H_{1'''}$ of the same ring can be detected as a broad signal at 6.84 ppm. Finally testosterone signals again do not suffer the broadening seen for the aromatic peaks, showing a 1:1 ratio steroid:metallo-moiety. H_4 is detected at 5.73 ppm and the methyl groups (1.21 and 0.90 ppm) give us a first idea about the purity of the complex.

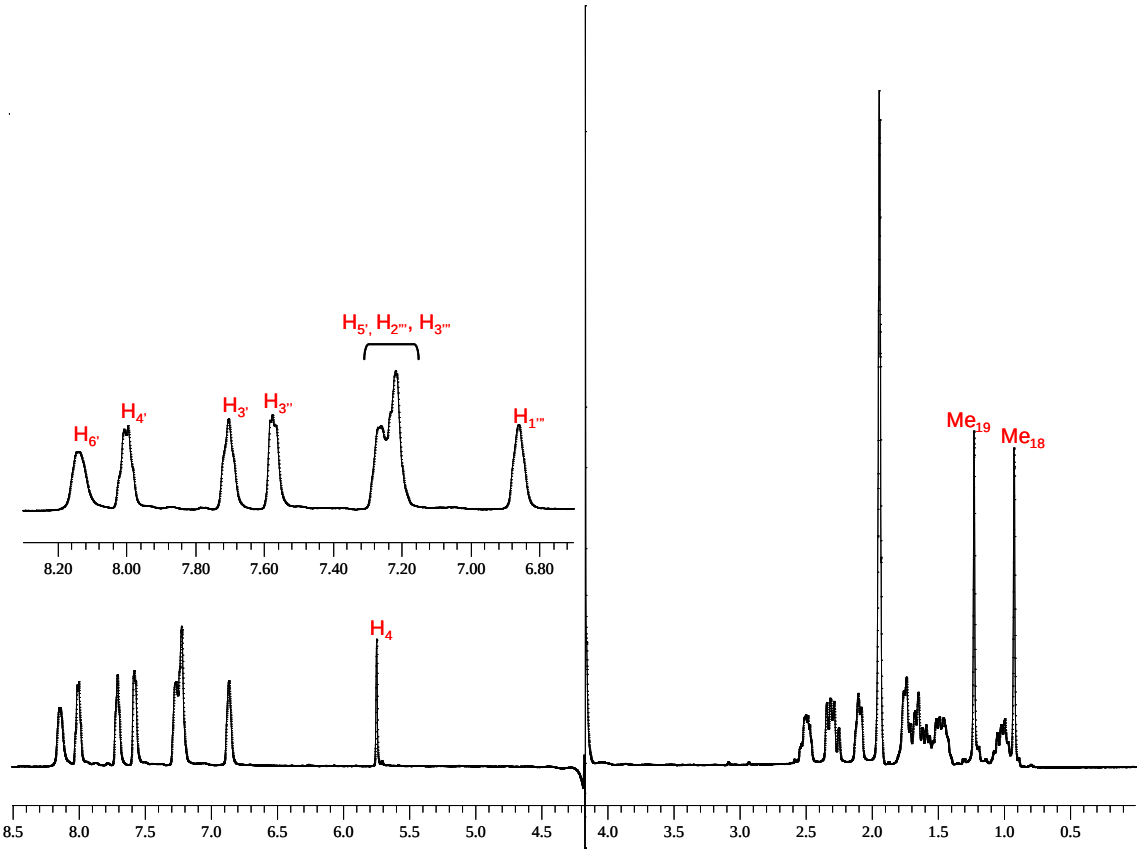

Figure 3.16. ^{1}H-NMR of ET-Terpy-Pt-Ph in a mixture of deuterated water:acetonitrile (1:1).

The UV/VIS (dichloromethane) shows similar bands to the oestrogenic compound. However, the maximum this time is present at 248 nm, in the region of testosterone, not in the phenyl. The MLCT area can be detected between 400-500 nm, and again is broader that for steroidal terpyridine intercalators. Exciting in the MLCT (maximum around 480 nm) again leads to a broad fluorescence, with a maximum of emission at 600 nm (Fig. 3.17).

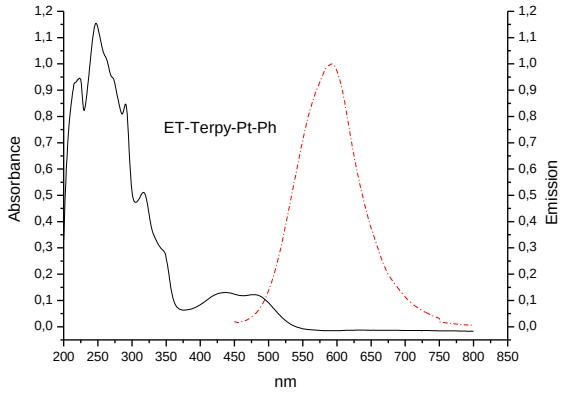

Figure 3.17. UV/Vis and emission spectra (normalized) of Et-Terpy-Pt-Ph (25 μM) in dichloromethane. λ_{exc}=480 nm.

3.3 Biological activity

3.3.1 Cytotoxic activity

To study their potential anti-cancer properties, EE, ET and Ph-Pt-Terpy were subject to *in vitro* testing in three cancer cell lines, ovarian line SK-OV-3 (AR-, ERα+, ERβ+), and breast lines T-47D (AR+, ERα+, ERβ+) and MDA-MB-231 (AR-, ERα-, ERβ+). The results are shown in Figure 3.18. The complexes are more active than cisplatin for the breast cancer cell lines (between 3 and 10 fold) and less active in the ovarian cell line. The non-steroidal compound is, as expected, quite active (as previously reported[35], similar activity has been observed for complexes with smaller ligands compared with the phenylacetylene[33]), but surprisingly it is even more active than the steroidal derivatives. This is different from examples of covalent binders discussed in the previous chapter, where there was always an increase in the activity of the complexes when a steroidal unit was bound[17, 19]. Especially dramatic is the case with T-47D cells, where the non-steroidal complex is 6 times more active than the testosterone derivative and 7 time more than the estradiol. For the other cell lines, however, the difference is smaller.

In order to measure the possible influence of the phenyl moiety on the toxicity, the activity of EE-Pt-Terpy and ET-Terpy-Pt-Ph (the second kind of steroidal complexes) was measured in the same cell lines (Fig. 3.18). The results show a drastic difference in the activity between the steroidal compounds with intercalative phenyl and terpyridine molecules. This effect is specially pronounced for estradiol complexes, where a 6 fold reduction can be observed in the T-47D cell line. If activity comes from intercalating

the platinum (II) terpyridine unit, the difficulty of access to this when the steroid is directly linked to it could explain the drop in the activity.

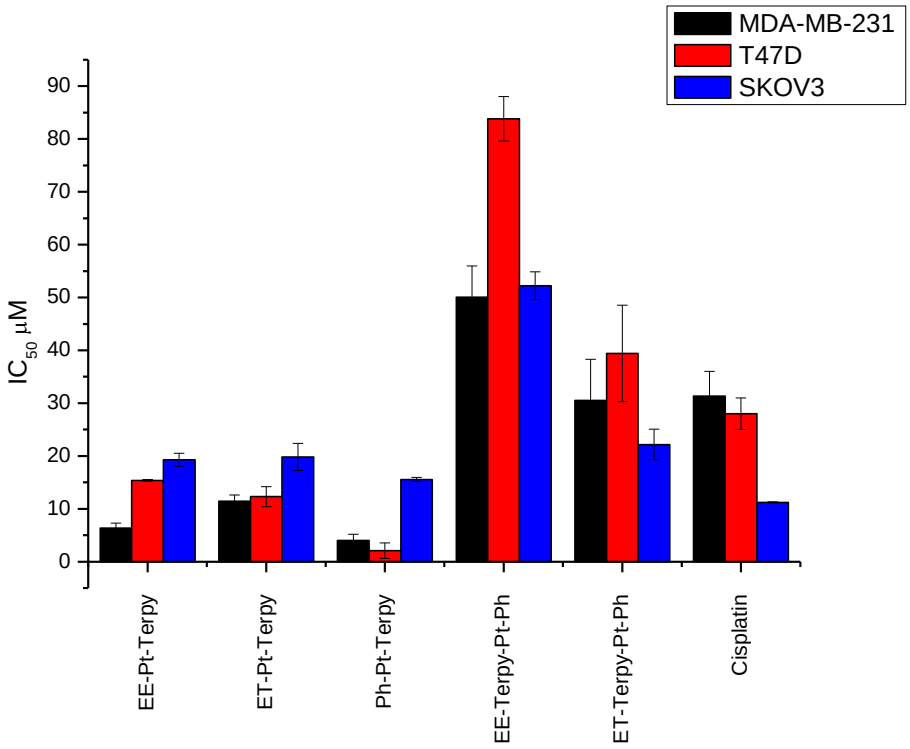

Figure 3.18. Toxicity of steroidal and non-steroidal platinum(II) compounds (IC_{50} µM) in breast and ovarian cell lines.

There seems not to be a big dependence on the status of receptors in the activity. This is particularly true for the testosterone derivatives, where activity for MDA-MB-231 (AR-) and T-47D (AR+) is almost the same. However, for the estradiol derivatives some effect is noticed in breast cancer cell lines (though not that expected). The oestrogenic complexes show better activity (2.5 fold) for MDA-MB-231 (ERα-, ERβ+) than for T-47D (ERα+, ERβ+), although the ER status might have been expected to favour the former. The fact that the non-steroidal complex shows the opposite trend (IC_{50} is lower in T-47D than in MDA-MB-231) removes the possibility that the difference of the activity comes from a better response from any of the cell lines to the mode of action of the complexes. So this difference of activity may come from the interaction of the oestrogenic complexes with the receptors.

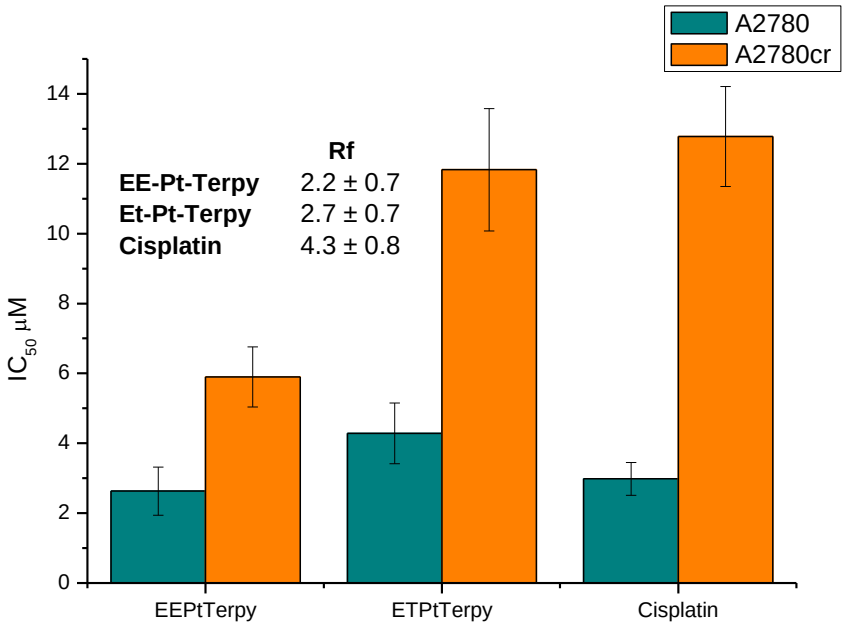

Figure 3.19. Toxicity of EE and ET-Pt-Terpy (IC_{50} µM) in ovarian cell lines. Effect of cisplatin resistance.

As highlighted previously, non-covalent DNA binders can be useful for overcoming cisplatin resistance, as their mode of action is different. Ovarian cell line A2780 (AR-, ERα- and ERβ +) and its cisplatin resistant strain A2780cr were chosen to study this possibility (Fig. 3.19). Major resistance mechanisms found in A2780cisR are reduced uptake of platinum(II) drugs and elevated levels of the tri-peptide glutathione whose cysteine residue detoxifies platinum(II) drugs via rapid binding[41]. The stability of this kind of terpyridine complex (without leaving groups) makes it possible for us to exclude glutathione coordination as a factor. As observed in previous experiments in ovarian cell line, the complexes show a similar activity to cisplatin. However, a better response to the resistant cell line is observed, with a 2 fold increase in the capacity to overcome platinum resistance mechanisms. These results confirm that by using a non-covalent drug we can achieve different activity to cisplatin-like molecules (as seen with breast and cisplatin resistant cell lines).

3.3.2 Cellular uptake

In order to explore how the presence of the steroid affects cellular uptake, MDA-MB-231, T-47D and SK-OV-3 cells were treated with platinum drugs and uptake determined using ICP-MS. A single concentration for all compounds (30 µM)[42] was chosen in order to determinate speed and efficiency, under the same conditions. Short time of exposure (3

h) was used because it has been previously shown that platinum terpyridine-like compounds can enter in the cell very quickly, sometimes entering in large quantities in times as short as five minutes[43]. Both testosterone and estradiol complexes were tested and non-steroidal analogues and cisplatin were used as controls. EE and ET-Terpy-Pt-Ph were not used due to their low toxicity. Whole cell, cytoplasm and nuclear fractions were obtained from the same experiment to observe distribution through the cell. In Figure 3.20 we can see the results. As expected, the delivery is very quick, with a large amount of compound entering the cell after only 3 hours. If compared with cisplatin, the difference is at least of an order of magnitude in each fraction (also observed when compared with the steroidal DNA-covalent-binding complexes from previous chapter; Section 2.3.5). It is noticeable that linking to the steroids can lower the delivery in MDA-MB-231 and SK-OV-3 cell lines (2 or 3 fold). There is no noticeable co-relation between platinum uptake and cytotoxicity across the different cell lines: there is not a larger uptake in cells with lower IC_{50} (Appendix B).

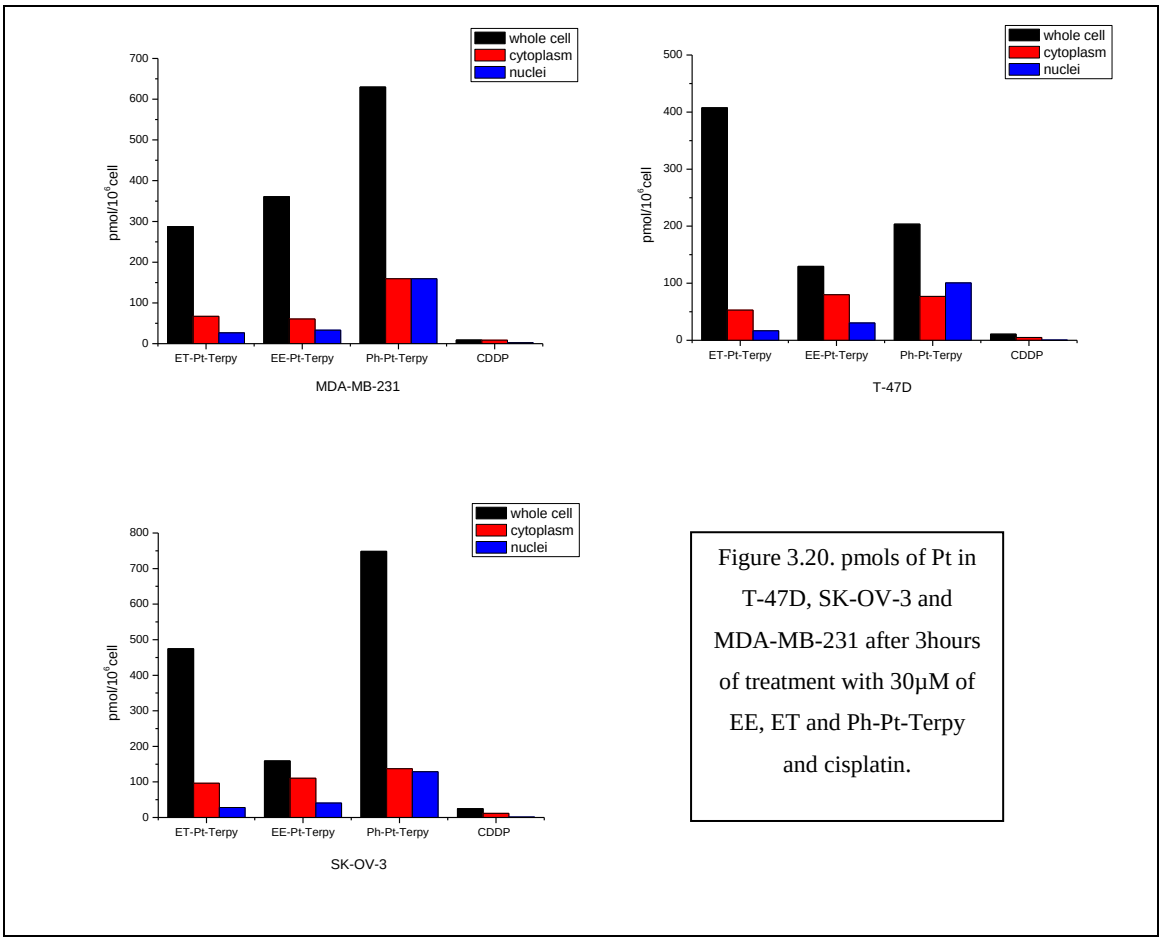

Figure 3.20. pmols of Pt in T-47D, SK-OV-3 and MDA-MB-231 after 3hours of treatment with 30μM of EE, ET and Ph-Pt-Terpy and cisplatin.

In previous chapter it was shown that for covalent DNA-binders, even though non-steroidal complexes were taken up more, the steroidal ones were more effective at

crossing the membrane and arriving in the cytoplasm (Section 2.3.5)[16, 19]. When steroids are coupled to non-covalent DNA-binders, this effect is only evident for estradiol derivatives in ERα+ cell lines (Table 3.1), where between 80-100% of the compound taken up crosses the membrane. When an ERα- cell line is studied, this percentage drops to 25%. The non-steroidal analogues show between 30-80% in the different cell lines and there is a clear co-relation between the cytotoxicity and percentage of complex that cross the membrane. The testosterone compound is the least effective at crossing the membrane (around 20%). However, the uptake of the testosterone compound is increased for AR+ T-47D cell line (in whole cell), compared with the non-steroidal control. So in this case (unlike in the toxicity assay) a dependence on the receptor status can be traced.

	ET-Pt-Tpy			*EE-Pt-Tpy*			*Ph-Pt-Tpy*		
	MDA-MB-231	T-47D	SK-OV-3	MDA-MB-231	T-47D	SK-OV-3	MDA-MB-231	T-47D	SK-OV-3
% across the membrane	33	17	26	26	85	95	51	87	35
% cytoplasm	23	13	20	17	62	69	25	38	18
% nuclei	9	4	6	9	23	26	25	49	17

Table 3.1. % of compound found crossing the membrane (related to compound taken up by whole cell) and in nuclear or cytoplasm fractions after 3 h.

When intracellular fractions are investigated, we observed that the non-steroidal complex shows a 1:1 ratio between cytoplasm and nuclei (nuclear transport doesn't depend on cytoplasmic proteins), while the steroidal complexes show a 3:1 ratio. These data are consistent with the presence of steroid affecting the interaction with macromolecules in the cytoplasm and that influencing the cellular distribution of the complexes (as seen previously in Section 2.3.5). The non-steroidal complex is always delivered to the nucleus in larger amounts and this may be the reason why complexes with an attached steroid show lower activity. To study how this might affect the toxicity, studies of the interaction with nucleic acids are needed.

3.4 DNA interaction

3.4.1 Stability of complexes

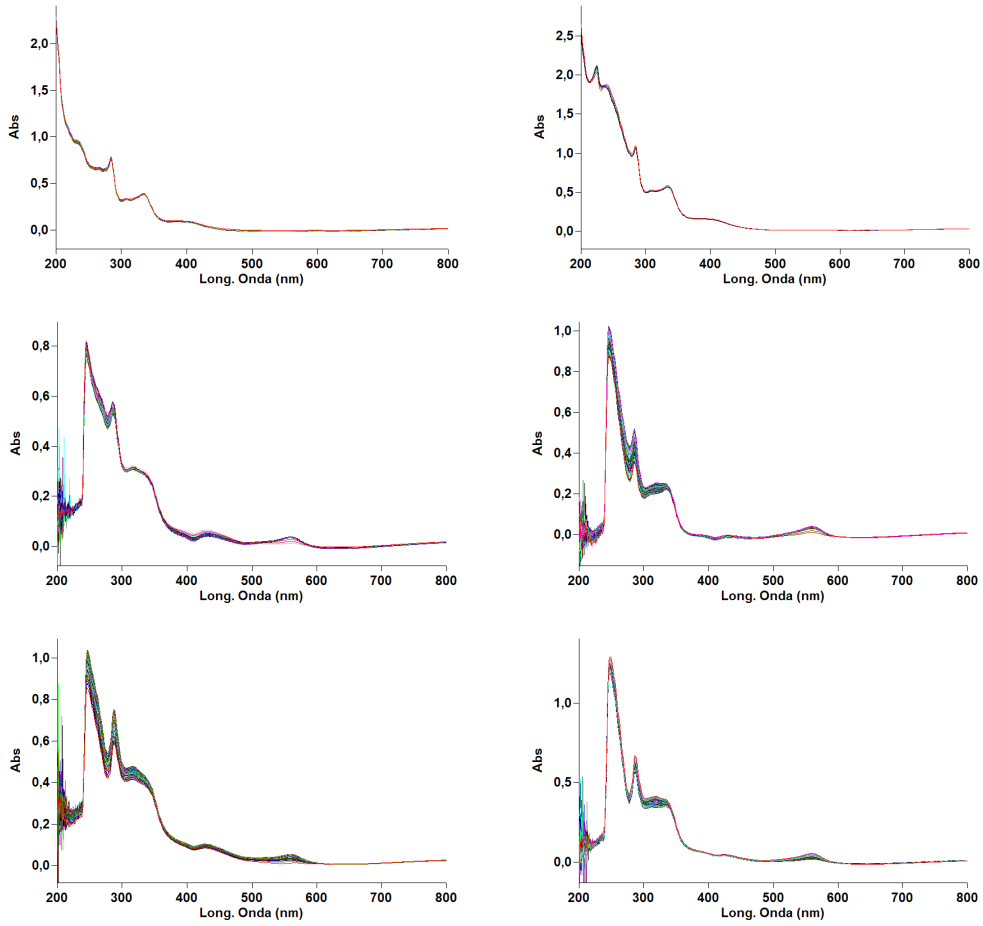

Figure 3.21. UV/Vis of EE-Pt-Terpy (left) and ET-Pt-Terpy (right) (50 μM) during 72h in water (top), RPMI 1640 (middle) and DMEM medium (bottom).

In order to see how the presence of the steroid affects the interaction with DNA, different techniques have been used. By exploring possible interactions with nucleobases we confirm that coordinative binding did not take place. First, stability in water and media of the complexes alone was measured over a 72 h period[44] by UV/VIS (Fig. 3.21). The complexes are very stable in water and only small changes appear in DMEM medium, probably as result of interaction with proteins present in the medium (Foetal Bovine Serum is added to the medium and serum albumin in known to bind to steroids[16]). This indicates that the reactive species are the provided complexes and not degradation products. The compounds were then incubated with 5'GMP for 72 h[44] and measured with ESI-MS. No adducts were observed, only the initial complex, suggesting that the hypothetical interaction with DNA would indeed be in a non-covalent non-coordinative mode.

Once it was determined that no covalent interaction was detected with nucleobases, and that the compounds were stable under experimental conditions, studies of the interaction with polymeric DNA were performed. Gel electrophoresis was uninformative: being an intercalator, no retardation was observed (Fig. 3.22)[45]. However, other techniques proved more successful.

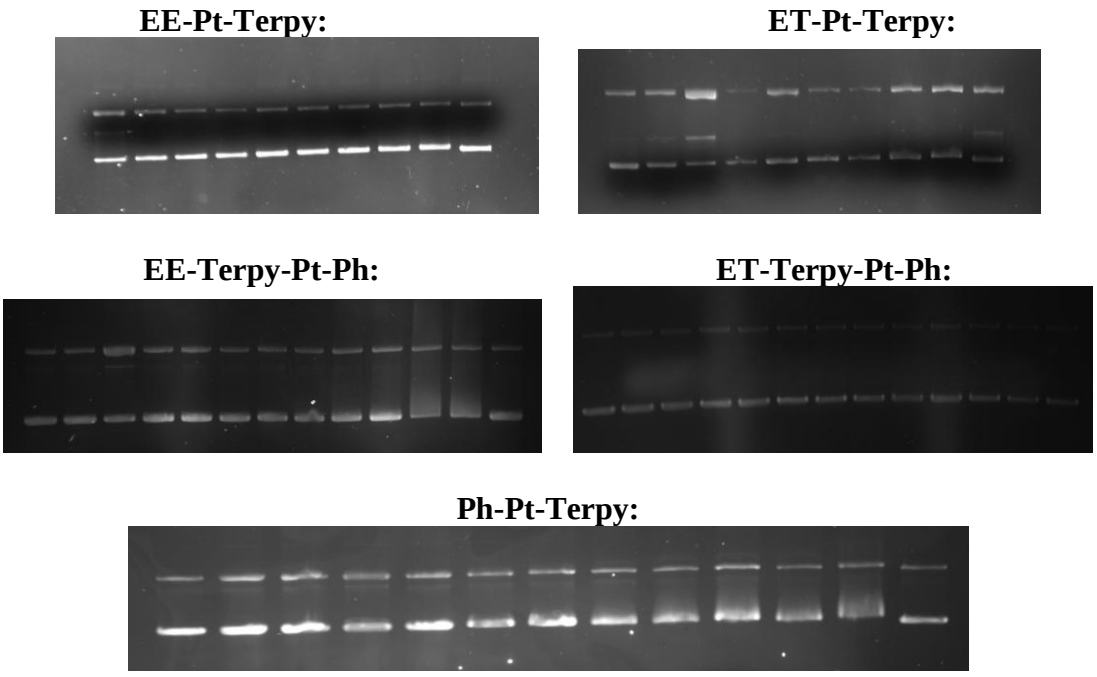

Figure 3.22. Gel electrophoresis of the complexes with circular plasmid pBR322 after 1 hour incubation. Lanes indicate (left to right in bp:complex ratio): plasmid, 15:1, 10:1, 8:1, 6:1, 5:1, 4:1, 3:1, 2:1 and plasmid (EE and ET-Pt-Terpy); plasmid, 40:1, 30:1, 20:1, 15:1, 10:1, 8:1, 6:1, 5:1, 4:1, 3:1, 2:1 and plasmid (EE and ET-Terpy-Pt-Ph and Ph-Pt-Terpy). The small bands observed in some of the lanes correspond to different supercoiling states of the plasmid and they can be observed as well for the plasmid control lanes. Possible DNA cleavage abilities where tested in presence of H_2O_2 with negative results.

3.4.2 Ethidium bromide displacement

In order to see if our compounds interact with DNA, a simple Ethidium Bromide (EB) displacement assay was performed. This assay is based in the fact that, when bound to DNA, EB show an increase in its fluorescent capacities[46]. So, molecules of DNA are loaded with EB measuring the fluorescence, and then, we titrate this EB loaded DNA with an expected DNA binding compound. If the intensity of the fluorescence signal observed decrease as result of the titration, this can be interpreted as a signal that EB is being displaced from DNA by our compound. The effectiveness of this displacement is co-related to the binding affinity of the compound to DNA[46].

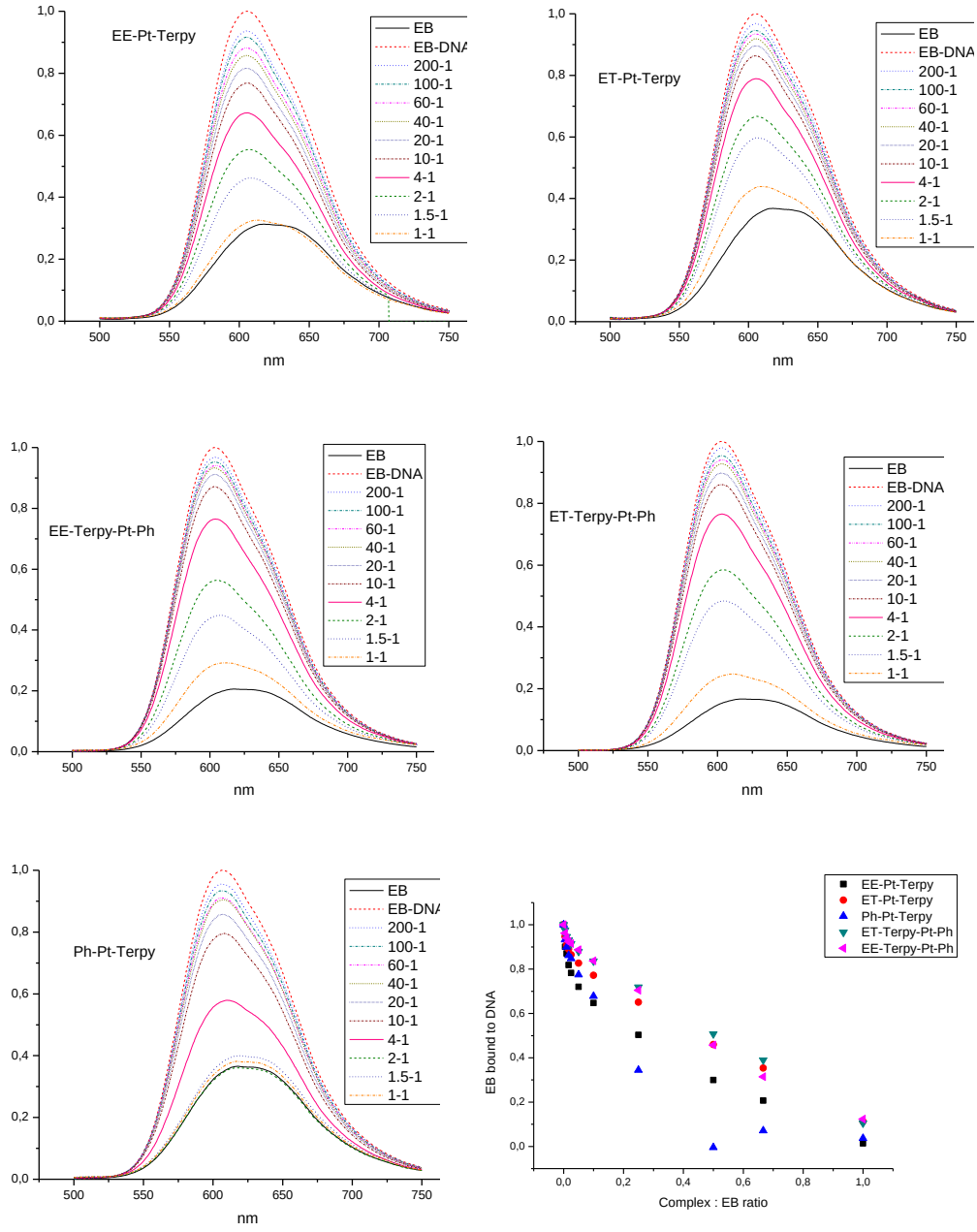

Figure 3.23. Displacement of ethidium bromide (15 μM) from ct-DNA (12 μM) by the synthesized Pt complexes. Mixing ratios EB/complex are shown in the caption. λ_{exc}=480nm. Decreasing ratios of emission (bottom right). (Normalized to the maximum of emission of EB-DNA)

We expected our compounds to be able to displace EB from DNA, since they were designed to be intercalators. All of them displace EB (Fig. 3.23), however not all with the same efficiency. The non-steroidal control compound has a greater ability to displace EB compared to the steroidal derivatives, indicating a decrease in DNA binding affinity upon conjugation. Between the steroidal complexes, we observed that terpyridine intercalators show higher binding affinities, than the phenyl intercalators, with estradiol derivatives being better binders than testosterone derivatives (Fig. 3.23). These data show

correspondence with the cytotoxicity data previously presented, indicating that maybe the presence of steroid decrease the ability of the complexes to intercalate into DNA, and this brings the lose of biological activity.

3.4.3 Hoechst displacement

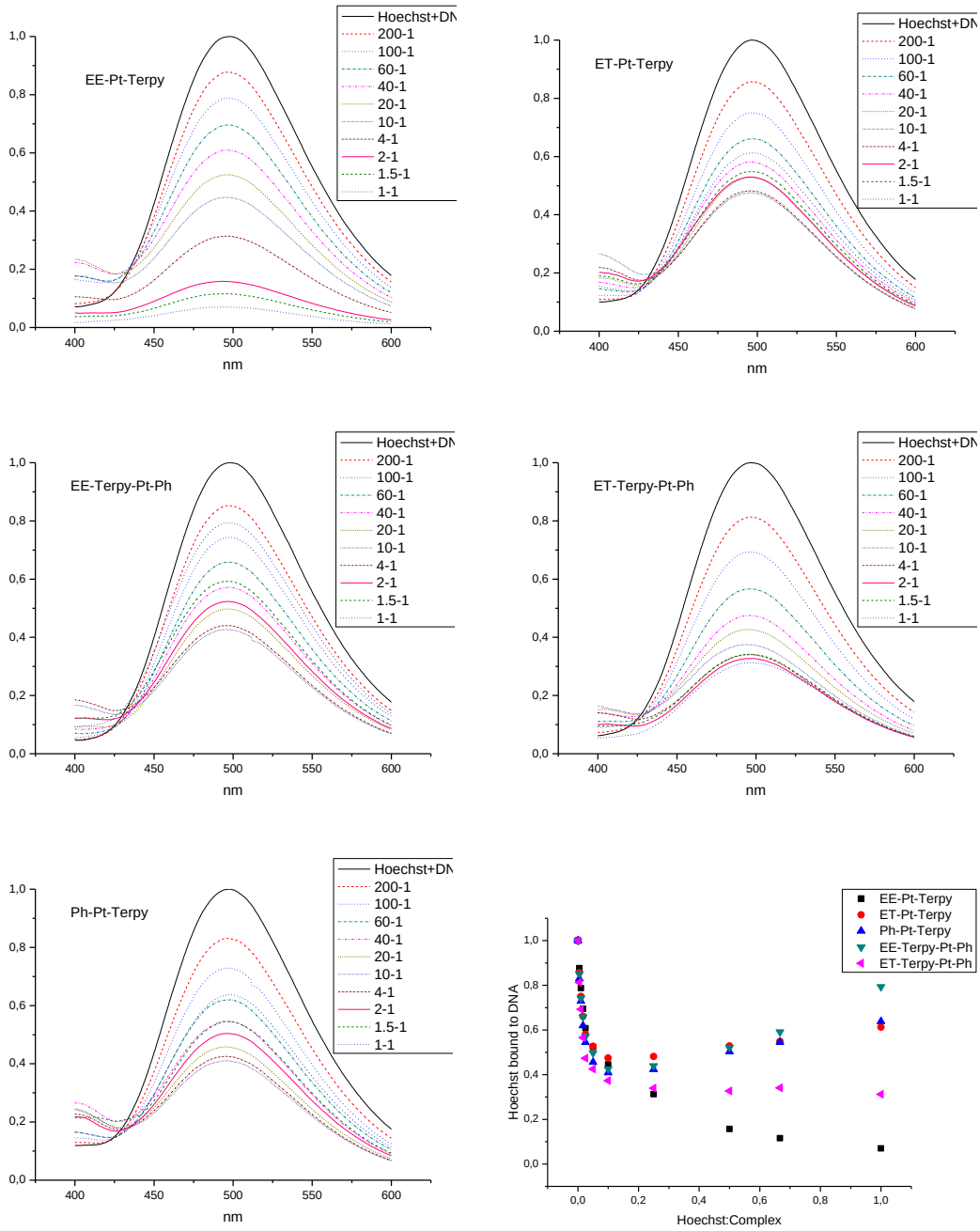

Figure 3.24. Displacement of Hoechst 33258 (1.5 μM) from ct-DNA (12 μM) by synthesized complexes. Mixing ratios EB/complex are shown in the caption. λ_{exc}=350nm. Decreasing ratios of emission (bottom right). (Normalized to the maximum of emission Hoechst-DNA)

A similar experiment was performed with Hoechst 33258[47-49], a minor groove binder. The results are a little different. All the complexes again seem to be able to displace the pre-loaded molecule (Fig. 3.24). But, contrary to previous experiment, all show the same

efficiency in removing Hoechst from DNA up to a 15:1 ratio (Hoechst:complex). After that all of them show different behaviour. The estradiol terpyridine intercalator is the most effective at displacing Hoechst, followed by the testosterone phenyl intercalator. The other three remaining complexes rebind Hoechst at high concentrations. This could be binding of Hoechst to the DNA after structural changes forced by the complexes, or result of an interaction between the complexes and Hoechst 33258. The EB results, being displacement of an intercalator, may be more pertinent.

3.4.4 Circular and linear Dichroism

In order to detect possible DNA structural changes, circular and linear dichroism (CD and LD) were performed with the complexes and ct-DNA[50]. CD measures the difference of absorption of left and right circularly polarised light, and when performed on macromolecules can be used to report changes in the conformation of the macromolecule itself, and to prove interaction with small molecules, especially if an induced CD (ICD) signal is observed in the small molecule spectroscopy[50]. When a titration of ct-DNA with our complexes was investigated by CD, the first thing observed was that the B-DNA conformation (evidenced by a characteristic positive CD band centred at 275 nm, and a negative band at 240 nm, with the zero being around 260 nm) is retained with all the complexes, except ET-Terpy-Pt-Ph (Table 3.2). For EE-Terpy-Pt-Ph, EE, ET and Ph-Pt-Terpy distortions to the DNA structure are quite small and an ICD signal was observed in all the complexes spectroscopy around 300 nm. The observation of such ICD signals for these complexes confirms the binding to DNA consistent with the findings from EB displacement.

When ct-DNA is titrated with ET-Terpy-Pt-Ph, changes in the B-DNA conformation are bigger compared with the other complexes (Fig. 3.25), although only when the CD absorbance of the complex is subtracted (Fig. 3.25 C). Free ET-Terpy-Pt-Ph presents a surprising CD absorbance spectrum: very high compared with the other steroidal complexes (Fig. 3.25 A). An explanation for this difference in CD absorbance might be different solution behaviours due to the stacking of the planar aromatic units present in the molecule. In this case, on interaction with DNA the CD absorbance would be lost; explaining why small modifications are observed in the ct-DNA titration (Fig. 3.25 B) and why the ICD is a mirror image of the original CD absorbance spectrum of the free

complex (Fig. 3.25 D). However, this is only a hypothesis and no information on the B-DNA conformation can be obtained.

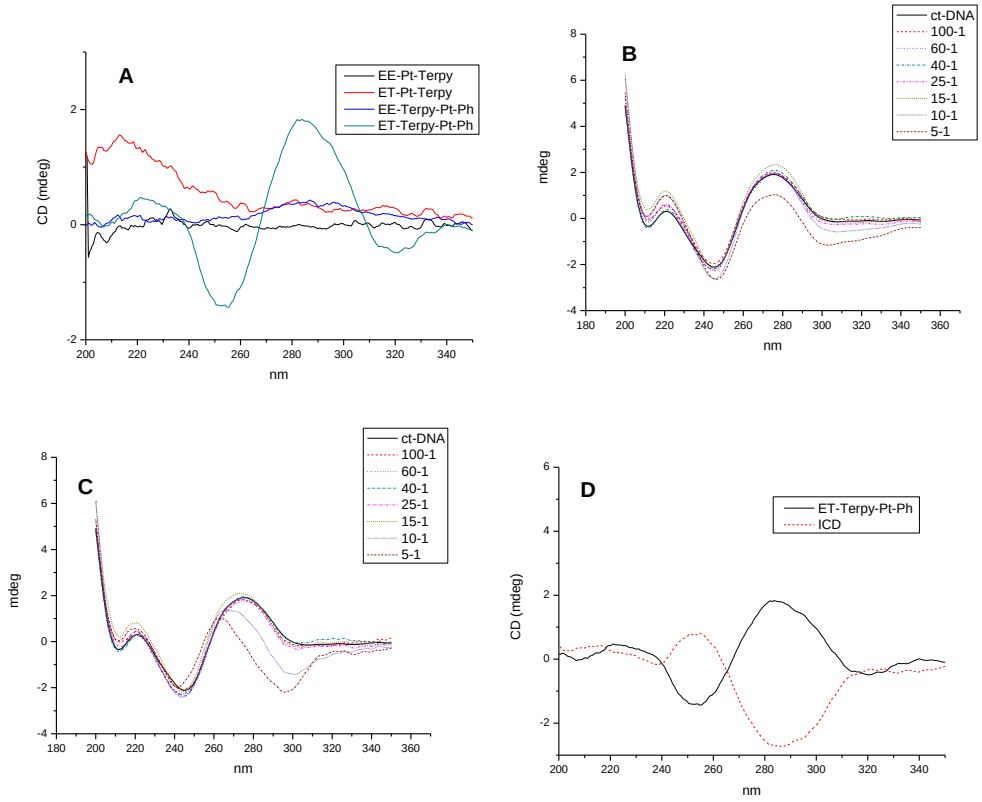

Figure 3.25. CD absorbance of the complexes at equivalent concentration to the 5-1 (DNA(bp):complex) titration point (A); ct-DNA titration with ET-Terpy-Pt-Ph (B); ct-DNA titration with ET-Terpy-Pt-Ph after subtraction of the CD absorbance of the free complex (C); CD absorbance spectrum and ICD signal at the 5-1 DNA(bp):complex point (D).

Modification of the DNA structure was further studied using flow linear dichroism (LD)[51]. In this experiment long polymeric ct-DNA is orientated by viscous drag in a couvette cell and the extent of orientation may be assessed by the difference in absorption of light linearly polarised parallel and perpendicular to the orientation direction. B-DNA produces a characteristic negative band between 220 nm and 300 nm (arising from π - π^* transitions) as the base pairs are orientated at almost 90° to the orientation axis. The magnitude of this LD signal is dependent on the degree to which DNA is orientated, being reduced by effects such as DNA-bending, and increased by intercalation of aromatic rings between the bases of the DNA ("stiffening").

	CD		LD
	200-350nm	280-750nm	200-700nm
EE-Pt-Terpy	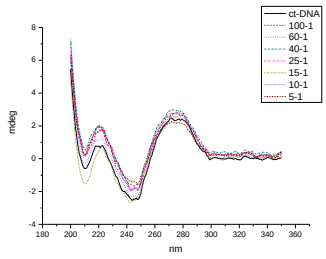	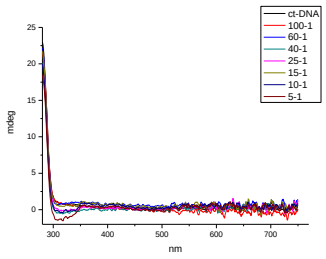	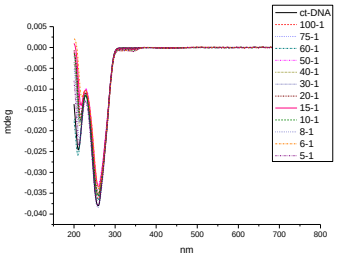
ET-Pt-Terpy	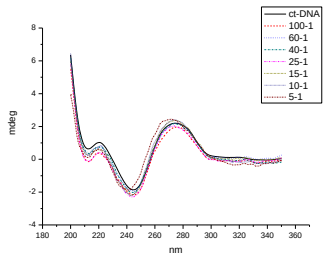	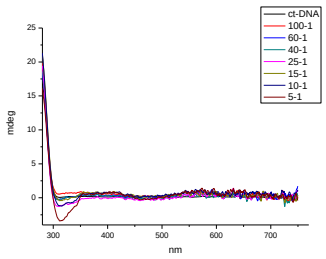	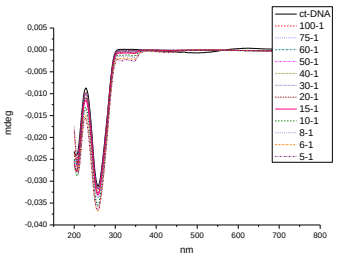
Ph-Pt-Terpy	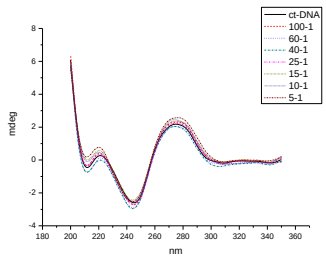	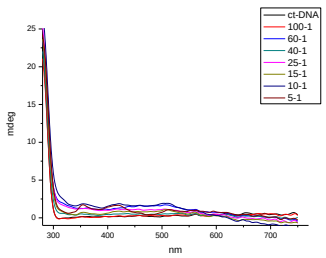	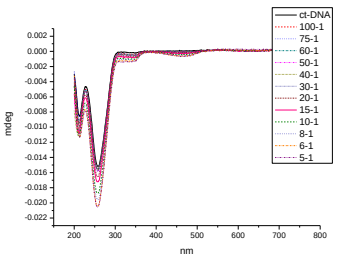
EE-Terpy-Pt-Ph	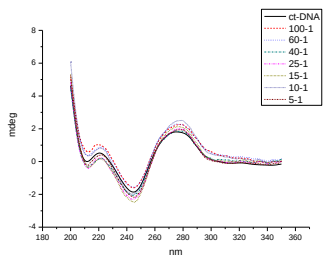	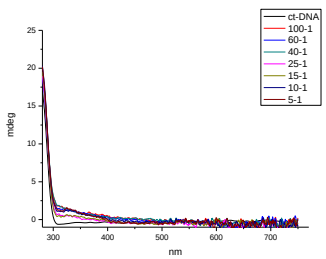	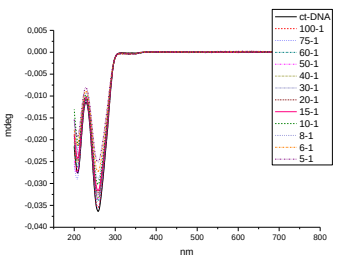
ET-Terpy-Pt-Ph	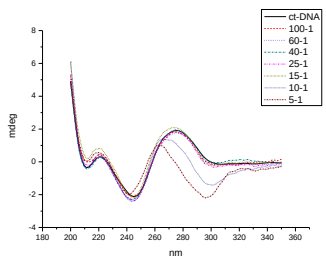	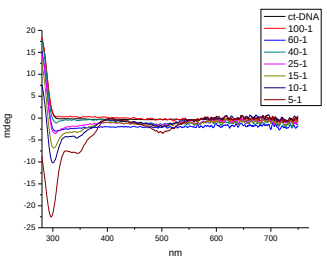	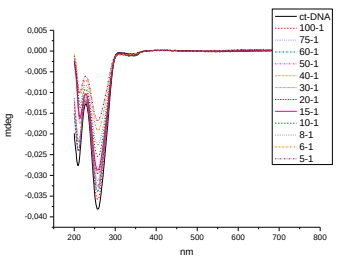

Table 3.2. CD and LD spectra of titration of ct-DNA(300 μM in 20 mM NaCl and 0.89 mM Sodium Cacodylate pH 6.8) with EE-Pt-Terpy, ET-Pt-Terpy, Ph-Pt-Terpy (third), EE-Terpy-Pt-Ph and ET-Terpy-Pt-Ph. Corrected substracting CD absorbance of the complexes.

When the complexes are titrated into oriented ct-DNA we observed different effects (Table 3.2). The first thing observed, as in previous CD experiment, is the appearance of induced LD (ILD) signals around 300 and 400nm, (the second of which is weaker). This again confirms that the binding to DNA is happening. The second thing observed is that

for all the terpyridine intercalators (steroidal and non-steroidal; although EE-Pt-Terpy appear to be mantained) the signal at 260nm is increased consistent with the "stiffening" characteristic of intercalation. This "stiffening" is quite visible for the non-steroidal complex, less so for the steroidal ones, maybe as result of the presence of the bulky steroid, that make the DNA loose some orientation to accommodate the big molecule (as seen previously for alkylating examples). Nevertheless an overall intercalation is detected (Fig. 3.26). When the steroidal complexes with phenyl moieties are studied, another effect is observed. These compounds do not show any signal of intercalation into the DNA. Rather, big loses of orientation are observed, especially for the testosterone complex, indicating that the complexes somehow bend the DNA double helix (Fig. 3.26). This implies that terpyridines and phenyl complexes interact with DNA in different ways. This difference in interaction could be responsible for the lower biological activity of the phenyl derivatives.

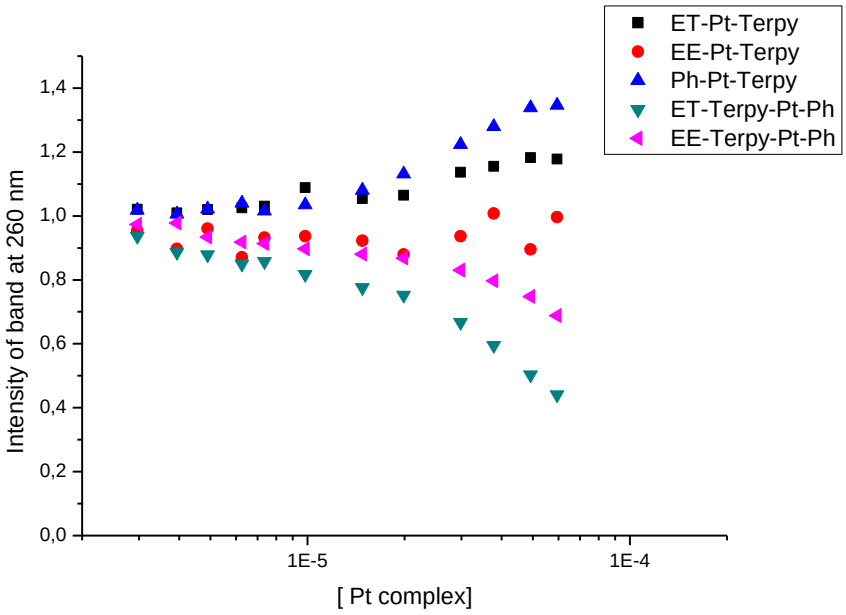

Figure 3.26. Effect in the orientation of ct-DNA when complexes were added.

3.4.5 DNA Fluorescence tritation

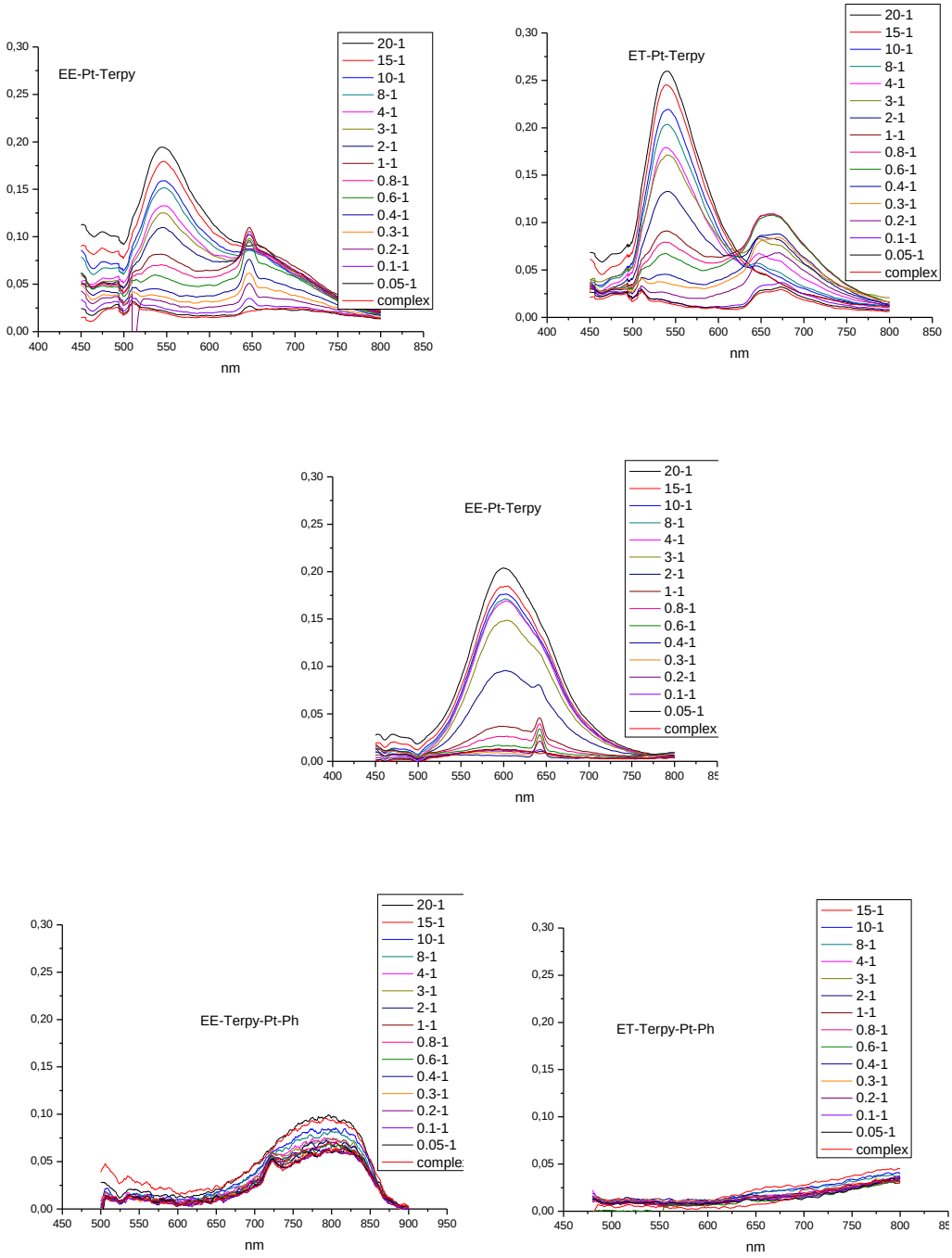

Figure 3.27. Titration of the complexes (25 μM) with ct-DNA, in 50 mM NaCl and 1mM sodium cacodylate buffer (pH 6.8). Mixing ratios DNA (bp)/complexes are shown in the caption. λ_{exc}=450 (EE and ET-Pt-Ph) or 480nm (Ph-Pt-Ph, EE and ET-Terpy-Pt-Ph). The graphs were normalized to the emission of the complexes (25 μM) in DCM.

In order to probe further this difference of DNA interaction between the terpyridine and phenyl terminated complexes, another experiment was undertaken. As explained before, the complexes are fluorescent in aprotic solvents, but in protic solvents this fluorescence is quenched. Our hypothesis was that if the platinum(II) terpyridine unit bound in an

intercalative way between the bases of DNA, the complex would be again in a hydrophobic environment and its fluorescence would be unquenched. Thus, terpyridine intercalators would show a fluorescence response on interaction with DNA, while if the phenyl ring is intercalated or a complete intercalation of the terpyridine is avoided they would not. All the complexes were titrated against ct-DNA and the fluorescence recorded (Fig. 3.27). As predicted, for EE, ET-Pt-Terpy and Ph-Pt-Terpy complexes fluorescence is observed, being visible starting at a 1:1 ratio (DNA (bp):complex). However, for EE and ET-Terpy-Pt-Ph (where the phenyl group and the position of the steroid can make the intercalation of the terpyridine difficult) this fluorescence is not observed (Fig. 3.27), indicating that the interaction with DNA does not occur through intercalation of the platinum(II) terpyridine moiety (or that this intercalation is only partial and the complex remains exposed to the solvent).

When the fluorescence is plotted against the ratio DNA (bp):complex we see that all the terpyridine intercalators (EE, ET and Ph-Pt-Terpy) present similar rates in the increase of their fluorescence (Fig. 3.28). However, it is noticeable that the non-steroidal complex arrives at a possible saturation point before the other two. This could imply more effective intercalation by the smaller non-steroidal complex.

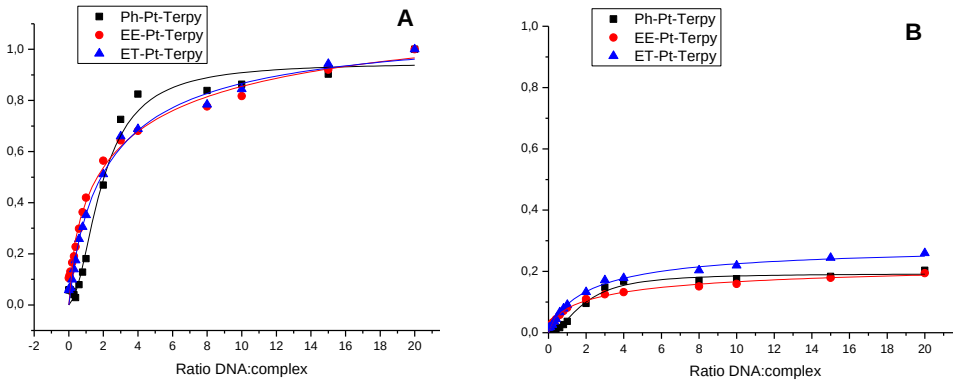

Figure 3.28. Fluorescence response of the complexes at their maximum of emission (540 nm for EE-Pt-Terpy and ET-Pt-Terpy and 625 nm for Ph-Pt-Terpy) observed on addition of DNA (bp): normalized to maximun of fluorescence observed upon addition of DNA at 20:1 (A); related to maximun of fluorescence of the complexes at 25 μM in dichloromethane (B).

The fact that only DNA bound complex would produce a fluorescence response was used to attempt to follow cellular uptake and localisation. Adherent ovarian cell line SK-OV-3 (AR-, ERα+, ERβ+), and breast lines T-47D (AR+, ERα+, ERβ+) and MDA-

MB-231 (AR-, ERα-, ERβ+) were treated with the complexes. Similar conditions to the ICPMS uptake experiment (15 μM for 3 hours) were used, knowing that in this time the complexes are internalized and arrive in different quantities to the nuclei. Treated cells were then visualized under a confocal microscope, exciting the cells with an Argon laser (λ_{ex}=488 nm; Ph-Pt-Terpy, EE and ET-Terpy-Pt-Ph) or a Blue Diode laser (λ_{ex}=405 nm; EE and ET-Pt-Terpy). Unfortunately, no fluorescence response was obtained.

3.4.6 Interaction with proteins

Figure 3.29. Induced CD spectrum for various mixtures of chiral components. DNA+complex , HSA+complex and HSA+complex+DNA. The order of the component denotes the order of mixing.

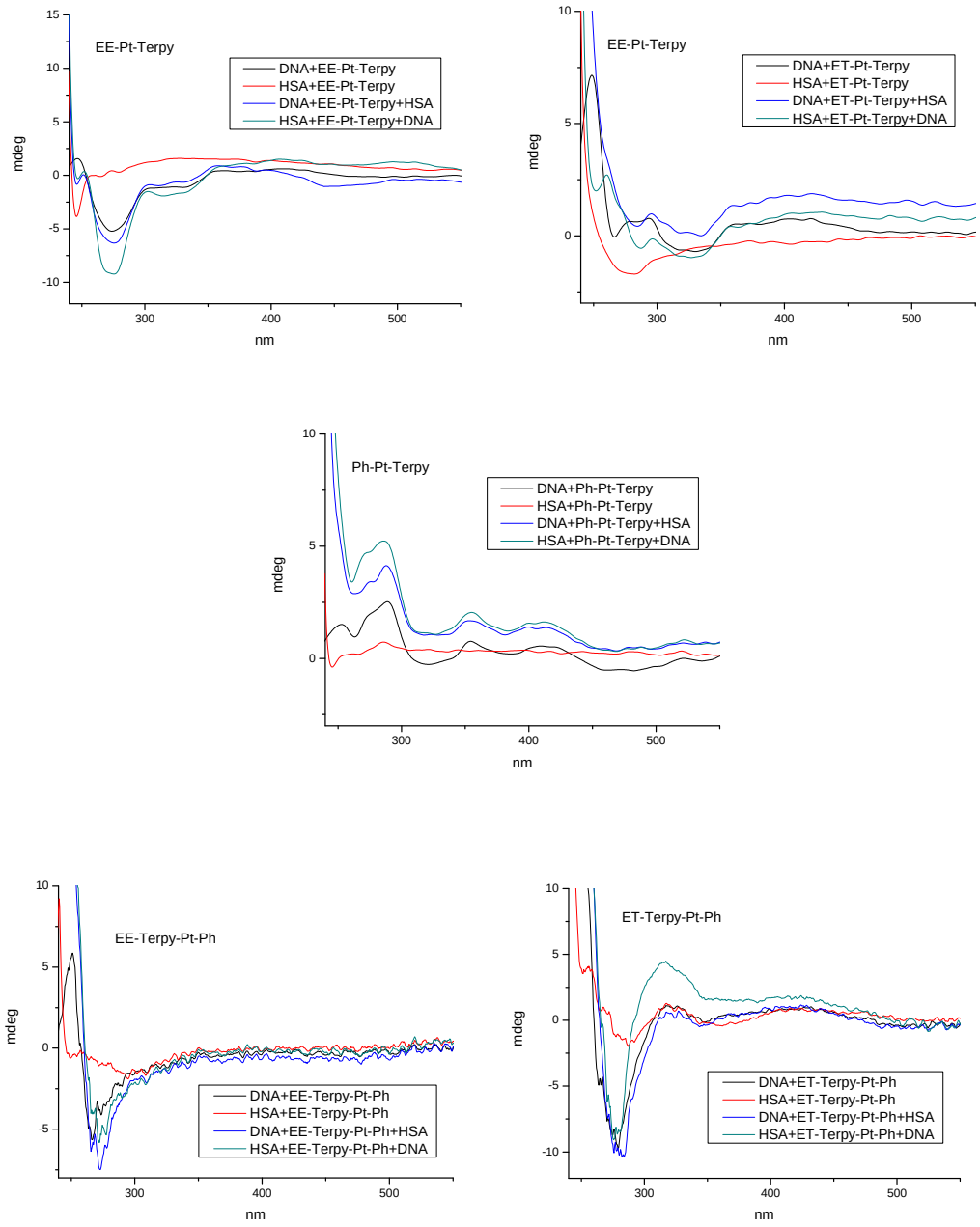

The previous steroidal terpyridine (covalent binding) complexes interacted with proteins as well as with DNA[16, 34]. This interaction varied depending of the order of addition of the macromolecules. To ascertain if these new complexes also had the same ability to bind proteins, interaction with Human Serum Albumin (used as a model of protein interaction), DNA, and both in concert, were measured through CD and Fluorescence (not shown). Observed ICD signals (Fig. 3.29), indicate that all the steroidal complexes have the ability to interact with HSA, while the non-steroidal analogue does not. As expected all the complexes (steroidal and non-steroidal) interact with DNA. When both of the macromolecules are added to the complexes, the results are independent of the order of addition of the macromolecules, with no significative differences between ICDs. This indicates that each macromolecule interacts with a different unit of the complexes (intercalator with DNA, and steroid with HSA). This is reinforced by fluorescence experiments (not shown) that show that fluorescence is only observed when DNA (not HSA) is added.

3.5 Conclusions

Steroidal intercalators have been synthesised in a simple way that allows good yields and flexibility of starting materials. The same procedures could potentially be used for different steroids and different metals allowing the rapid formation of a library of compounds. Controls without a steroid and with a different intercalative moiety have been prepared and allowed us to determine the importance of both of the components in the activity of the complexes. The complexes were tested against breast and ovarian cell lines. These tests showed that coupling of steroids has a negative effect on the biological activity of the intercalative terpyridines. The attachment of steroids did not seem to increase the uptake into the cells either (however, compared to covalent binders, intercalators show much better abilities to enter into the cell). When the amount of complex that arrives to the nuclei is compared we see that greater amounts of the non-steroid complexes is localised there, while the steroidal complexes are concentrated in the cytoplasm. However, this effect does not seem big enough difference to explain the loss of activity.

The stability of the complexes and their ability to bind to DNA were also studied. The compounds proved to be stable in the reaction conditions over 72 h, excluding the

possibility of a covalent interaction with DNA. Ethidium bromide displacement experiments showed the same order in possible DNA affinity as in toxicity potency, a circumstantial indication that the DNA binding affinity is co-related to toxicity. This, together with the fact that the presence of steroid does not produce major distortions in the DNA double helix (as seen for covalent binders) can explain why in this system steroid conjugation does not enhance activity. Indeed when the conjugation locks the ability of the terpyridine to intercalate, the affinity drops even more, and the intercalation is replaced by a mode that includes bending of the double helix. This seems to reinforce the hypothesis that the active factor is the intercalation of the terpyridine. Finally, steroidal complexes showed the ability to interact with proteins, probably through the steroidal moiety. This can explain the difference in distribution inside the cells of the complexes (more in cytoplasm when the steroid is conjugated).

As a result of all of this we could say that coupling of a steroidal moiety to a intercalative unit, unlike in the case of covalent binders, appears to be a drawback in the potency and activity of the complex (at least within the confines of the molecular design explored herein). This is mainly a result of the impediments that the steroidal molecule has to intercalation, but may also be because of the possible interactions inside the cell that distract the complex from its DNA target.

3.6 Experimental

Synthesis: All solvents and chemicals were purchased from Sigma-Aldrich. [Pt(terpyridine)Cl] and EE and [ET(terpyridine)Cl] were synthesised following previous procedures[16, 34, 37]. ^{1}H NMR spectra were recorded on Brucker AC300 or DRX500 spectrometers. ESI mass spectra were recorded on a Micromass LCT time-of-flight mass spectrometer. Microanalyses were performed on a CE Instruments EA1110 elemental analyser. UV/VIS was performed in a Varian Cary 5000 UV/VIS spectrophotometer. HPLC was performed in a Dionex HPLC system with a semi-prep column fitted. Fluorescence spectra were recorded using a Shimadzu RF-5301 PC Fluorescence Spectrophotometer (resolution = 0.4nm; Speed medium; Excitation split = 5; Emmision split = 1.5)

(EE-Pt-Terpy)TFA: The chloride salt of Pt(terpyridine)Cl (50 mg, 0.1 mmol) was dissolved in 50 ml of dry DMF. To that, 1.1 equivalent of 17α-ethynylestradiol (32.6 mg, 0.11 mmol), 8% w/w of CuI (1.68 mg, 8 µmol) and a couple of drops of dry triethylamine were added. The reaction was left overnight under Argon atmosphere and at room temperature. Then 10 ml of dry methanol was added, and the reaction left for another 24 h in the same conditions. After that the solution was filtered and the solvent removed under vacuum, yielding a dark solid containing the chloride salt of the wanted product. This solid was purified by HPLC using a 40 minutes gradient of water/acetonitrile (0-100% acetonitrile) with TFA (0.05%), during which the Chloride salt was exchanged to the TFA salt. After removing the solvent we obtained a bright orange solid (54.8 mg, yield 65.6%). ^{1}H-NMR (300 MHz, CD_3OD): δ 9.26 (d, 2H, J = 5.5 Hz, $H_{6'}$), 8,43 (m, 7H, $H_{4'}$,$H_{3'}$,$H_{3''}$,$H_{4''}$), 7.78 (dd, 2H, J = 5.5, 7.7 Hz, $H_{5'}$), 7.06 (d, 1H, J = 8.8 Hz, H_1), 6.49 (d, 1H, J= 8.8, H_2), 6.45 (s, 1H, H_4), 2.9-1.2 (m, 18H, steroid), 0.94 (s, 3H, Me_{18}). UV / Visible (Dichloromethane): 242nm (ε = 14600 mol^{-1} dm^3 cm^{-1}). Mass spectrum (ESI, +ve): *m/z* 723 [(17α-Ethinylestradiol)Pt(Terpy)]$^+$. Elemental analysis: calculated for $C_{37}H_{34}N_3F_3O_4Pt$- (H_2O); C, 52.0; H, 4.3; N, 5.0. Found C, 52.2; H, 4.6; N, 5.3.

(ET-Pt-Terpy)TFA: The chloride salt of Pt(terpyridine)Cl **(**20 mg, 0.04 mmol) was dissolved in 20 ml of dry DMF. To that, 1.1 equivalent of ethisterone (13.8 mg, 0.044 mmol), 8% w/w of CuI (0.61 mg, 3.2 µmol) and a couple of drops of dry triethylamine were added. The reaction was left overnight under Argon atmosphere and at room temperature. Then 10 ml of dry methanol was added, and the reaction left for another 24 h in the same conditions. After that the solution was filtered and the solvent removed under vacuum, yielding a dark solid containing the chloride salt of the wanted product. This solid was purified by HPLC using a 40 minutes gradient of water/acetonitrile (0-100% acetonitrile) with TFA (0.05%), during which the chloride salt was exchanged to the TFA salt. After removing the solvent we obtained a bright orange solid (24.9 mg, yield 73.1%). ^{1}H-NMR (500 MHz, CD_3OD): δ 9.25 (d, 2H, J = 5.5 Hz, $H_{6'}$), 8.47 (m, 5H, $H_{3'}$,$H_{3''}$,$H_{4''}$), 8.40 (dd, 2H, J = 8.0, 7.6 Hz, $H_{4'}$), 7.78 (dd, 2H, J = 5.5, 7.6 Hz, $H_{5'}$), 5.71 (s, 1H, H_4), 2.5-0.89 (m, 20H, steroid), 1.27 (s, 3H, Me_{19}), 0.98 (s, 3H, Me_{18}). UV / Visible (Dichloromethane): 242nm (ε = 26800 mol^{-1} dm^3 cm^{-1}). Mass spectrum (ESI, +ve): *m/z* 739 [(Ethisterone)Pt(Terpy)]$^+$. Elemental analysis: calculated for $C_{38}H_{38}N_3F_3O_4Pt$-2/3(TFA); C, 50.9; H, 4.1; N, 4.5. Found C, 51.1; H, 3.9; N, 4.1.

(Ph-Pt-Terpy)TFA: The chloride salt of Pt(terpyridine)Cl **(**20 mg, 0.04 mmol) was dissolved in 20 ml of dry DMF. To that, 1.1 equivalent of benzylacetinele (4.5 mg, 0.044 mmol), 8% w/w of CuI (0.61 mg, 3.2 µmol) and a couple of drops of dry triethylamine were added. The reaction was left overnight under Argon atmosphere and at room temperature. Then 10 ml of dry methanol was added, and the reaction left for another 24 h in the same conditions. After that the solution was filtered and the solvent removed under vacuum, yielding a dark solid containing the chloride salt of the wanted product. This solid was purified by HPLC using a 40 minutes gradient of water/acetonitrile (0-100% acetonitrile) with TFA (0.05%), during which the chloride salt was exchanged to the TFA salt. After removing the solvent we obtained a dark brown solid (16 mg, yield 64.6%). ^{1}H-NMR (500 MHz, CD_3OD): δ 8.70 (d, 2H, J = 5.4 Hz, $H_{6'}$), 8.2 (m, 3H, $H_{3''}$,$H_{4''}$), 8.15 (dd, 2H, J= 7.7, 7.8 Hz, $H_{4'}$), 8.09 (d, 2H, J= 7.7 Hz, $H_{3'}$), 7.59 (dd, 2H, J= 5.5, 7.6 Hz, $H_{5'}$), 7.33 (m, 3H,H_2, H_3), 7.21 (d, 2H, J= 6.6 Hz, H_1). UV / Visible (Dichloromethane): 248nm (ε = 18400 mol^{-1} dm^3 cm^{-1}). Mass spectrum (ESI, +ve): *m/z* 529 [(benzylacetylen)Pt(Terpy)]$^{+}$. Elemental analysis: calculated for $C_{25}H_{16}F_3N_3O_2Pt$-1.5(TFA); C, 41.4; H, 2.0; N, 5.2. Found C, 41.7; H, 2.2; N, 5.5.

(EE-Terpy-Pt-Ph)TFA: The chloride salt of estradiol(terpyridine)PtCl (15 mg, 0.019 mmol) was dissolved in 15 ml of dry DMF. To that, 1.1 equivalent of benzylacetilene (2.2 mg, 0.021 mmol), 8% w/w of CuI (0.3 mg, 1.5 µmol) and a couple of drops of dry triethylamine were added. The reaction was left overnight under Argon atmosphere and at room temperature. Then 10 ml of dry methanol was added, and the reaction left for another 24 h in the same conditions. After that the solution was filtered and the solvent removed under vacuum, yielding a dark solid containing the chloride salt of the wanted product. This solid was purified by HPLC using a 40 minutes gradient of water/acetonitrile (0-100% acetonitrile) with TFA (0.05%), during which the chloride salt was exchanged to the TFA salt. After removing the solvent we obtained a brown solid (10 mg, yield 56.5%). ^{1}H-NMR (500 MHz, D_2O/CD_3CN): δ 8. (b, 2H,$H_{6'}$), 7.95 (bt, 2H, $H_{4'}$), 7.67 (bd, 2H, H_3'), 7.56 (bs, 2H, $H_{3''}$), 7.21 (m, 5H, $H_{5'}$,$H_{2'''}$,$H_{3'''}$), 7.14 (d, 1H, J= 8.4 Hz, H_1), 6.85 (b, 1H, $H_{1'''}$), 6.60 (dd, 1H, J= 8.4, 2.2 Hz, H_2), 6.56 (d, 1H, J= 2.2 Hz, H_4), 2.79-1.17 (m, 18H, steroid), 0.89 (s, 3H, Me_{18}). UV / Visible (Dichloromethane): 219nm

(ε = 43200 mol^{-1} dm^3 cm^{-1}). Mass spectrum (ESI, +ve): *m/z* 823 $[ET(Terpy)Pt(benzylacetylen)]^+$. Elemental analysis: calculated for $C_{45}H_{38}N_3F_3O_4Pt$; C, 57.7; H, 4.1; N, 4.5. Found C, 58.1; H, 3.9; N, 4.9.

(ET-Terpy-Pt-Ph)TFA: The chloride salt of testosterone(terpyridine)PtCl (15 mg, 0.018 mmol) was dissolved in 15 ml of dry DMF. To that, 1.1 equivalent of benzylacetilene (2 mg, 0.02 mmol), 8% w/w of CuI (0.3 mg, 1.5 μmol) and a couple of drops of dry triethylamine were added. The reaction was left overnight under Argon atmosphere and at room temperature. Then 10 ml of dry methanol was added, and the reaction left for another 24 h in the same conditions. After that the solution was filtered and the solvent removed under vacuum, yielding a dark solid containing the chloride salt of the wanted product. This solid was purified by HPLC using a 40 minutes gradient of water/acetonitrile (0-100% acetonitrile) with TFA (0.05%), during which the chloride salt was exchanged to the TFA salt. After removing the solvent we obtained a brown solid (9.5 mg, yield 53.9 %). ^{1}H-NMR (300 MHz, D_2O/CD_3CN): δ 8.13 (b, 2H, $H_{6'}$), 7.99 (b, 2H, $H_{4'}$), 7.69 (b, 2H, $H_{3'}$), 7.55 (b, 2H, $H_{3''}$), 7.25 (bm, 5H, $H_{5'}$,$H_{2'''}$,$H_{3'''}$), 6.84 (b, 2H, $H_{1'''}$), 5.73 (s, 1H, H4) 2.48-0.98 (m, 20H, steroid), 1.21 (s, 3H, Me_{19}), 0.90 (s, 3H, Me_{18}). UV / Visible (Dichloromethane): 248nm (ε = 46100 mol^{-1} dm^3 cm^{-1}). Mass spectrum (ESI, +ve): *m/z* 839 $[ET(Terpy)Pt(benzylacetylen)]^+$. Elemental analysis: calculated for $C_{46}H_{42}N_3F_3O_4Pt$-2.25(TFA); C, 50.2; H, 3.5; N, 3.5. Found C, 50.5; H, 3.0; N, 3.3.

Cell test: Tissue culture flasks, 96 well plates, RPMI 1640, DMEM, L-glutamine, trypsin-EDTA, HEPES, sodium pyruvate and FBS were obtained from Invitrogen. Thiazolyl blue tetrazolium bromide (MTT) and DMSO were from Sigma, UK. Tissue culture flasks, 96-well plates, RPMI 1640, DMEM, L-glutamine, trypsin-EDTA, HEPES, sodium pyruvate and FBS were obtained from Sigma, UK. Thiazolyl blue tetrazolium bromide (MTT) and DMSO were from Avocado, UK. Cells were grown in RPMI 1640 (T-47D, SK-OV-3) or DMEM (MDA-MB-231, A2780/cr) in 10 % FBS supplemented with 1% L-glutamine, 1% HEPES buffer and 1% sodium pyruvate. The MTT assay[52] was carried out using 96 well plates. Cells were harvested in logarithmic growth, 4,000 (A2780/cr), 10,000 (SK-OV-3, MDA-MB-231) or 25,000 cells (T-47D) were seeded per well and left overnight to attach. The cells were treated, in quadruplicate with 6

difference concentrations of complex dissolved in fresh media; the range of concentrations used is dependent on the complex. The cells were incubated for 72 hours and 20 µl of thaizolyl blue tetrazolium bromide (5mg / ml, 0.2 µm filtered) added. The cells were further incubated for 2 hours. The media was carefully removed by aspiration and 200 µl of DMSO added to dissolve the purple crystals. Absorbance was measured using a 96-well plate reader (BioRad) set at 590 nm. Each cell line was investigated beforehand to determine the correct cell numbers to initially seed and the required amount of time exposed to thiazolyl blue tetrazolium bromide to ensure sensitivity and accuracy.

Cellular Uptake: Two million cells (T-47D, SK-OV-3 and MDA-MB-231) were seeded in a 60mm diameter Petri dishes and left overnight to attach. Next day cells were treated with 30 µM of the different compounds for 3 hours. After that time, the medium was removed and cells washed three times with PBS to remove all the unwanted (non uptaked) Platinum complexes. Cells were collected and two aliquots of one million cells were taken, one of them to see whole cell uptake and the other for Cytoplasm and Nuclei fraction extraction (Nuclear/Cytoplasm extraction kit. BioVision). Two ml of ultrapure concentrated nitric acid (Traceselect Ultra, Aldrich) was added to the samples, and digested overnight at 90ºC. Samples were then taken to dryness at 120ºC, resuspended in 3ml of a 2% solution of nitric acid and filtered. The amount of platinum was measured in a Agilent 7500CX ICP-MS (analysis was done with Pt sample cone in He and No-gas mode. Plasma settings: Ar.flow: 15 L/min; Neb gas: 0.8 L/min; RF power 1550W; T of spray chamber: 15 º C).

Stability: RPMI 1640, DMEM, L-glutamine, trypsin-EDTA, HEPES, sodium pyruvate and FBS were obtained from Invitrogen, ultrapure water was obtained from Sigma. Samples were prepared as follow: Solutions of the complexes were dissolved in water and RPMI and DMEM medium in 10 % FBS supplemented with 1% L-glutamine, 1% HEPES buffer and 1% sodium pyruvate, to a final complex concentration of 50µM. Stability was measured during 72 h at 37ºC, measuring a UV spectrum every hour, using a Varian Cary 5000 UV/VIS spectrophotometer with a Varian 6x6 Multicell Block Beltier and a Varian Cary Temperature Controller attached.

Gel electrophoresis: Plasmid pBR322 (New England Biolabs, UK) and varying amount of complex were mixed and incubated for 1 h or 24 h. The total solution of 16 µl consists of 1 µl (stock = 1 µg / µl) pBR322, between 0.5 and 12.8 µl of complex (stock = 60 µM) and the rest with ultra-pure water. After the incubation period, 4 µl of loading buffer were added and 16 µl loaded onto an agarose gel. The loading buffer consisted of 30 % glycerol and 0.05% bromophenol blue in ultra-pure water. The agarose (Fisher, UK) gel was prepared from 200 ml of 1x TAE buffer and 0.20 g of agarose (1%) the gel cast and run using a HE99X Maxi (Amersham Biosciences, UK) submarine gel kit. The gel was ran using 1x TAE for 250 minutes at 5 V cm^{-1}. The gel was stained after electrophoresis in TAE buffer containing ethidium bromide (0.5 µg ml^{-1}) for 40 minutes. The gel was visualized using an UVIdoc Platinum system (UViDoc, Cambridge, UK) at 312 nm.

ESI-MS Nucleotide binding studies: 5'-GMP and 9-ethylguanine were stored at 4°C in a dessicator; they were dissolved freshly in 1mM sodium cacodylate buffer (pH 6.8) before each experiment. Fresh solution of complexes in 1mM sodium cacodylate buffer (pH 6.8) were used and mixed with nucleotides in a 1:1 ratio. The stock solutions of base and complex were both 2 mM. All the solutions were incubated for three days at 37°C in the dark. ESI-MS spectra were taken on a a Micromass LCT time-of-flight mass spectrometer.

Circular Dichroism: All C*D* spectra were recorded on a Jasco J-810 spectropolarimeter operated with the following parameters: sensitivity, 100 mdeg; start wavelength, 350 or 700 nm; end wavelength, 200 or 280 nm; data pitch, 0.5 nm; scanning mode, continuous; scanning speed, 200 nm per min; response, 0.1 seconds; bandwidth, 1.0; accumulation, 12. Stock solutions of ct-DNA (300 µM) with 20 mM NaCl and 0.89 mM Sodium Cacodylate pH 6.8 was tritated with complex (500 µM), maintaining the concentrations. DNA:complex ratios 100:1, 60:1, 40:1, 25:1, 15:1, 10:1, and 5:1.

Linear Dichroism: All L*D* spectra were recorded on a Jasco J-810 spectropolarimeter modified for *LD* spectroscopic measurement. The spectropolarimeter was operated in *LD* mode with the following parameters: sensitivity, 100 mdeg; start wavelength, 750 nm; end wavelength, 200; data pitch, 0.5 nm; scanning mode, continuous; scanning speed, 500 nm per min; response, 0.25 seconds; bandwidth, 2.0; accumulation, 8. Stock solutions of ct-DNA (300 μM) with 20mM NaCl and 0.89 mM sodium cacodylate pH 6.8 was tritated with complex (500 μM), maintaining the concentrations. DNA:complex ratios 100:1, 75:1, 60:1, 50:1, 40:1, 30:1, 20:1, 15:1, 10:1, 8:1, 6:1 and 5:1.

Ethidium Bromide displacement: The fluorescence spectra for the ethidium bromide displacement experiment were recorded in a Shimadzu RF-5301 PC Fluorescence Spectrophotometer (λ_{exc} = 480 nm; Range emission = 500-750 nm; resolution = 0.4nm; Speed medium; Excitation split = 5; Emmision split = 1.5). Solutions of ethidium bromide (15 μM), ct-DNA (12 μM), NaCl (50 mM) and sodium cacodylate buffer (1 mM) were prepared, measured and titrated with the different complexes from ratios EB:complex 200-1 to 1-1, keeping the concentration of ethidium bromide and ct-DNA constant.

Hoechst 33258 displacement: The fluorescence spectra for the hoechst 33258 (Hoechst) displacement experiment were recorded in a Shimadzu RF-5301 PC Fluorescence Spectrophotometer (λ_{exc} = 350 nm; Range emission = 400-600 nm; resolution = 0.4nm; Speed medium; Excitation split = 5; Emmision split = 1.5). Solutions of hoechst (1.5 μM), ct-DNA (12 μM), NaCl (50 mM) and sodium cacodylate buffer (1 mM) were prepared, measured and titrated with the different complexes from ratios hoechst:complex 200-1 to 4-1, keeping the concentration of hoechst and ct-DNA constant.

ct-DNA fluorescence: The fluorescence spectra tritation of the complexes with ct-DNA were recorded in a Shimadzu RF-5301 PC Fluorescence Spectrophotometer (λ_{exc} = 425 or 480 nm; Range emission = 450-800 or 500-850 nm; resolution = 0.4nm; Speed medium; Excitation split = 5; Emmision split = 1.5). Solutions of the different complexes

(25 μM) in water with NaCl (50 mM) and sodium cacodylate buffer (1 mM) were prepared, measured and titrated with ct-DNA (2 mM) mantaining the concentrations constant. DNA:complex ratios 0.05:1, 0.1:1, 0.2:1, 0.3:1, 0.4:1, 0.6:1, 0.8:1, 1:1, 2:1,3:1, 4:1, 8:1, 10:1, 15:1 and 20:1.

Cellular Imaging: 500000 cells (T-47D, SK-OV-3 and MDA-MB-231) were seeded in 30 mm diameter Petri dishes with glass bottom and left overnight to attach. The cells were treated then with 15μM of the complexes for 3hours. After that time, the medium was removed and the cells washed three times with PBS to remove all the unwanted (non uptaked) complexes. The resulting cells were observed through a Leica DMIRE2 system with an Argon laser (operated at 405 or 488 nm) and a temperature control chamber (operated at 37 ºC) attached.

HSA-DNA interaction: Solutions of ct-DNA (300 μM) and HSA (16 μM) in NaCl (50mM) and sodium cacodylate buffer (1mM), were treated with the different complexes (30 μM). Solutions of ct-DNA, HSA and complexes were created, adding the macromolecules in different order. CD spectra and fluorescence of all solutions was measured. All fluorescence and CD spectra were measured as previously described. Induced CD (ICD) spectra were obtained by subtracting the baseline corrected spectrum of all chiral components of any mixture from the baseline corrected spectrum of the mixture of the components.

3.7 References

1 W. H. Ang, E. Daldini, L. Juillerat-Jeanneret, P. J. Dyson, *Inorg. Chem.*, 2007, **46**, 9048.

2 D. Kirpotin, J. W. Park, K. Hong, S. Zalipsky, W. L. Li, P. Carter, C. C. Benz, D. Papahadjopoulos, *Biochemistry*, 1997, **36**, 66.

3 D. Goren, A. T. Horowitz, D. Tzemach, M. Tarshish, S. Zalipsky, A. Gabizon, *Clin. Cancer Res.*, 2000, **6**, 1949.

4 M. Galansky, B. K. Keppler, *Anti Canc. Agents Med. Chem.*, 2007, **7**, 55.

5 G. G. Chen, Q. Zeng, G. M. K. Tse, *Med. Res. Rev.*, 2008, **28**, 954.

6 (a) W. Somboonporn, S. R. Davies, *Endocr. Rev.*, 2004, **25**, 374; (b) A. Barqawi, E. D. Carwford, *Int. J. Imp. Res.*, 2006, **18**, 323.

7 S. Top, A. Vessières, C. Cabestaing, I. Laios, G. Leclerq, C. Provot, G. Jaouen, *J. Organomet. Chem.*, 2001, **637**, 500.

8 S. Top, E.B. Kaloun, A. Vessieres, G. Leclercq, I. Laios, M. Ourevitch, C. Deuschel, M.J. McGlinchey, G. Jaouen, *ChemBioChem.*, 2003, **4**, 754.

9 M. P. Georgiadis, S. A. Haroutounian, K. P. Chondros, *Inorg. Chim. A-Bioinorg.*, 1987 **138**, 249.

10 D. M. Spyriounis, V. J. Demopoulos, P. N. Kourounakis, D. Kouretas, A. Kortsaris, O. Anronoglou, *Eur. J. Med. Chem.*, 1992, **27**, 301.

11 C. Cassino, E. Gabano, M. Ravera, G. Cravotto, G. Palmisano, A. Vessières, G. Jaouen, S. Mundwiler, R. Alberto, D. Osella, *Inorg. Chim. Acta*, 2004, **357**, 2157.

12 E. Gabano, C. cassino, S. Bonetti, C. Prandi, D. Colangelo, A. L. Ghiglia, D. Osella, *Org. Biomol. Chem.*, 2005, **3**, 3531.

13 A. V. Gagnon, M. E. St-Germain, C. Descôteaux, J. Provencher-Mandeville, S. Parent, S. K. Mandal, E. Asselin, G. Bérubé, *Bioorg. Med. Chem. Lett.*, 2004, **14**, 5919.

14 V. Perron, D. Rabouin, E. Asselin, S. Parent, R. C. C. Gaudreault, G. Bérubé, *Bioorg. Chem.*, 2005, **33**, 1.

15 K. R. Barnes, A. Kutikov, S. J. Lippard, *Chemistry & Biology*, 2004, **11**, 557.

16 M.J. Hannon, P.S. Green, D.M. Fisher, P.J. Derrick, J.L. Beck, S.J. Watt, M.M. Sheil, P.R. Barker, N.W. Alcock, R.J. Price, K.J. Sanders, R. Pither, J. Davis, A. Rodger, *Chem. – Eur. J.*, 2006, **12**, 8000.

17 Martin Huxley, PhD Thesis, University of Warwick, 2006.

18 Michael Browning, PhD Thesis, University of Warwick, 2006.

19 M. Huxley, C. Sanchez-Cano, M. J. Browning, C. Navarro-Ranninger, A. G. Quiroga, A. Rodger, M. J. Hannon, *To be submitted*.

20 M. Huxley, C. Sanchez-Cano, M. J. Browning, C. Navarro-Ranninger, A. G. Quiroga, A. Rodger, M. J. Hannon, *To be submitted*.

21 M. J. Hannon, *Chem. Soc. Rev.*, 2007, **36**, 280.

22 A. Oleksy, A.G. Blanco, R. Boer, I. Usón, J. Aymami, A. Rodger, M.J. Hannon and M. Coll, *Angew. Chem., Intl. Ed.*, 2006, **45**, 1227.

23 S. Komeda, T. Moulaei, K. K. Woods, M. Chimuka, N. P. Farrell, L. D. Williams , *J. Am. Chem. Soc*., 2006, **128(50)**, 16092.

24 G. I. Pascu, A. C. G. Hotze, C. Sanchez Cano, B. M. Kariuki, M. J. Hannon, *Angew. Chem., Intl. Ed.*, 2007, **46**, 4374.

25 A.C.G. Hotze, N.J. Hodges, R.E. Hayden, C. Sanchez-Cano, C. Paines, N. Male, M.-K. Tse, C.M. Bunce, J.K. Chipman, and M.J. Hannon, *Chemistry & Biology*, 2008, **15**, 1258.

26 S. Kemp, N. J. Wheate, D. P. Buck, M. Nikac, J. G. Collins, J. R. Aldrich-Wright, *J. Inorg. Biochem.*, 2007, **101**, 1049.

27 J. R. Choudhury, R. Guddneppanavar, G. Saluta, G. L. Kucera, U. Bierbach, *J. Med. Chem.*, 2008, **51**, 3069.

28 C. A. Puckett, J. K. Barton, *Biochemistry*, 2008, **47**, 11711.

29 T. Biver, F. Secco, M. Venturini, *Coord. Chem. Rev.*, 2008, **252**, 1163.

30 A. H. Wang, J. Nathans, M. G. van der, J. H. van Boom, A. Rich, *Nature*, 1978, **276**, 471.

31 I. Eryazici, C. N. Moorefield, G. R. Newkome, *Chem. Rev*. 2008**, 108**, 1834.

32 P. B. Glover, P. R. Ashton, L. J. Childs, A. Rodger, M. Kercher, R. M. Williams, L. De Cola, Z. Pikramenou, *J. Am. Chem. Soc.*, 2003, **125**, 9918.

33 G. Lowe, A. A. Droz, T. Vilaivan, G. W. Weaver, J. J. Park, J. M. Pratt, L. Tweedale, L. R. Kelland, *J. Med. Chem.*, 1999, **42**, 3167.

34 Phil Barker, PhD Thesis, University of Warwick, 2001.

35 D. Ma, T.Y. Shum, F. Zhang, C. Che, M. Yang, *Chem. Commun.*, 2005, **37**, 4675.

36 R. A. Stockland, M. C. Kohler, I. A. Guzei, M. E. Kastner, J. A. Bawiec, D. C. Labaree, R. B. Hochberg, *Organometallics*, 2006, **25**, 2475.

37 R. Buchner, C. T. Cunningham, J. S. Field, R. J. Haines, D. R. McMillin, G. C. Summerton, *Dalton Trans.*, **1999**, 711.

38 P. Siemsen, R. C. Livingston, F. Diederich, *Angew. Chem., Intl. Ed*, 2000,**39**, 2633.

39 C. S. Peyratout, T. K. Aldridge, D. K. Crites, D. R. McMillin, *Inorg. Chem.*, 1995, **34**, 4484.

40 D. R. McMillin, J. J. Moore, *Coord. Chem. Rev.*, 2002, **229**, 113.

41 B. C. Behrens, T. C. Hamilton, H. Masuda, K. R. Grotzinger, J. Whang-Peng, K. G. Louie, T. Knutsen, W. M. McKoy, R. C. Young, R. F. Ozols, *Cancer Res.*, 1987, **47**, 414.

42 This concentration was used as a compromise with the toxicity of cisplatin in the cell lines, and in order to be able to compare with previous experiments.

43 S. W. Botchway, M. Charnley, J. W. Haycock, A. W. Parker, D. L. Rochester, J. A. Weinstein, J. A. Gareth Williams, *Proc. Natl. Acad. Sci.*, 2008, **105**, 16071.

44 The period of incubation was chosen as a result of the protocol used to determinate the cytotoxicity that runs for that period of time.

45 To determinate the DNA unwinding angle through gel electrophoresis techniques is necessary the use of topoisomerases, as explained in: S. M. Zeeman, K. M. Depew, S. J. Danishefsky, D. M. Crothers, *Proc. Natl. Acad. Sci*, 1998, **95**, 4327.

46 J. C. Peberdy, J. Malina, S. Khalid, M. J. Hannon, A. Rodger, *J.Inorg. Biochem.,* 2007, **101**, 1937.

47 H.R. Mahler, B. Kline, B.D. Mehrota, *J. Mol. Biol.*, 1964, **9**, 801.

48 P.E. Pjura, K. Grzeskowlak, D.E. Dickerson, *J. Mol. Biol.*, 1987, **197**, 257.

49 M.J. Waring, *J. Mol. Biol.*, 1965, **13**, 269.

50 A. Rodger, B. Nordén, *Circular Dichroism and Linear Dichroism* Oxford University Press, **1997**.

51 M. J. Hannon, V. Moreno, M. J. Prieto, E. Molderheim, E. Sletten, I. Meistermann, C. J. Isaac, K. J. Sanders, A. Rodger, *Angew. Chem. Int. Ed.*, 2001, **40**, 880.

52 T. Mosmann, *J. Inmunol. Meth.*, 1983, **65**, 55.

Chapter 4: Metallosupramolecular cylinders

The importance of specific DNA binding in nature is well known. Synthetic agents with less specific DNA binding abilities are of importance in the clinical field. A good example is the molecule cisplatin that binds coordinatively, principally to two neighbouring guanine bases of DNA (i.e. not particularly specific), and is broadly used to treat diverse cancers[1-3]. Non-covalent DNA interactions are commonly used in nature for multiple functions. For this reason metallodrugs aimed at binding to DNA in a non-coordinative manner have recently started to receive attention[4-6]. In our lab we have developed metallo-supramolecular agents with similar size and shape to DNA recognition protein domains. They are positively charged, dimetallic iron(II) triple-stranded helicates ($[Fe_2L_3]^{4+}$) with cylindrical structure and a size of approximately 2 nm in length and 1 nm in diameter (Fig. 4.1). Their synthesis is relatively simple (and cheap) and they present the correct size and shape to fit into the major groove, occupying a space corresponding to around five base pairs[7-12].

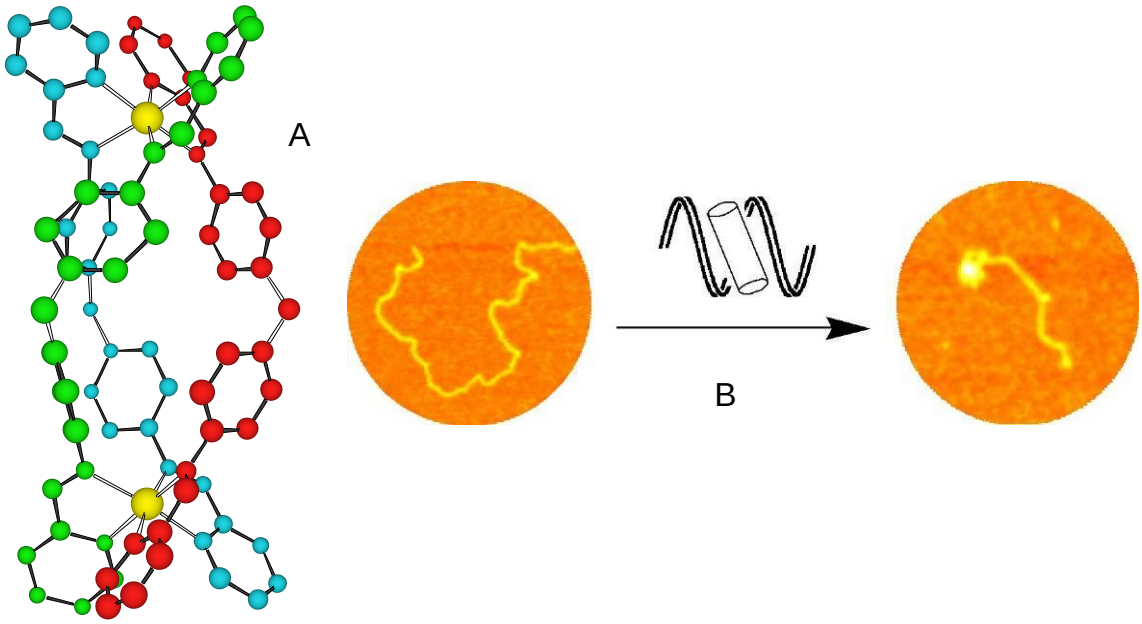

Figure 4.1. Structure of the triple stranded iron helicate (A, taken from Hotze et al[24]) and AFM image of the intramolecular coiling effect induced by the helicate (B, taken from Hannon et al[7]).

These molecules bind strongly, non-covalently to the major groove of DNA, inducing unexpected and dramatic intramolecular DNA coiling (Fig. 4.1)[7, 8, 13] and producing bending of around 45º per ligand[7]. Also, they unwind the double helix by

around 27º and show certain specificity for alternating purine-pyrimidine sequences[14]. These abilities seem to come as a result of their shape: similar but bulkier structures have less structural effects on DNA[13, 15]. Although all these structural changes seem to be a result of binding in the major groove, recently it was discovered that the complex can bind at the heart of a Y-shaped three way junction (Fig. 4.2)[16-18]. This is an unprecedented mode of DNA binding and opens the possibility of accessing new targets such us replication or RNA secondary structures.

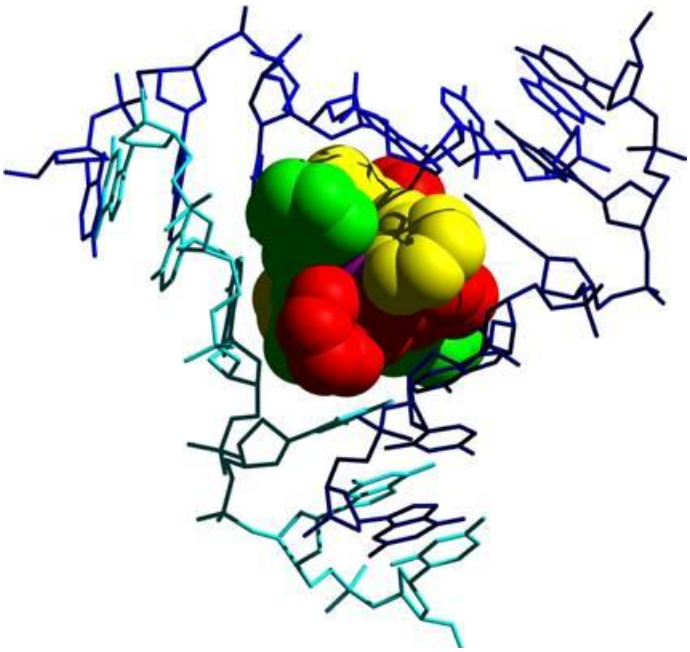

Figure 4.2. Image of the interaction between an iron triple helicate molecule and a DNA three way junction structure. Taken from Oleksy et al[16].

Similar double and triple stranded complexes with different metal centres have been synthesised. Copper(I) double-stranded complexes show weaker binding to DNA, but they present the ability to act as a nuclease[19]. Double-stranded ruthenium(II) structures have high cytotoxicity, although their low solubility did not allow detailed study of the DNA binding abilities[20]. Ruthenium(II) triple-stranded helicates ($Ru_2L_3^{4+}$) present an analogous structure to the iron helicate (Fig. 4.3) and have similar DNA binding affinity, specificity and coiling properties[21-22]. This is a strong indication that most of the effects observed upon interaction with DNA are produced by the structural shape of the complex and not by the properties of the metallic centre. However, the metallic centre can be an important factor in this interaction: the ruthenium cylinder produces a much lower unwinding of the double helix (13º), can cleave the DNA when irradiated

with UV/VIS light, usually at a guanine base, and show fluorescent emission when excited in the MLCT[22]. None of these effects are observed for the iron cylinder.

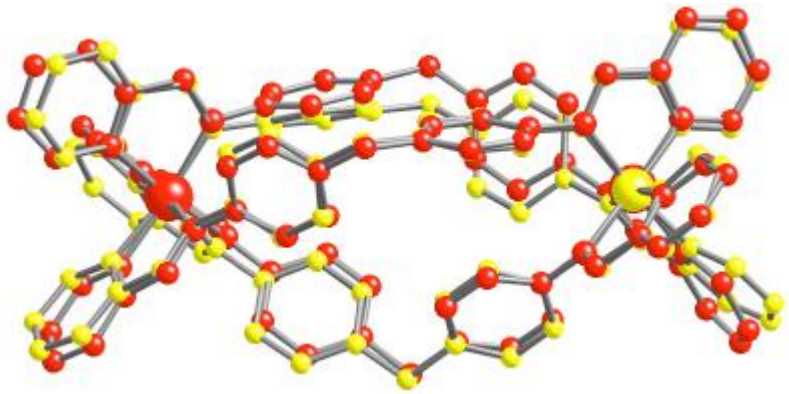

Figure 4.3. Overlay of the X-Ray structures of iron (yellow) and ruthenium (red) triple stranded helicates. Taken from Pascu et al[21].

Recent experiments have shown that the iron triple helicate has antimicrobial activity, showing *in vivo* binding to the bacterial DNA[23]. Studies in human cells show that our metallo-supramolecular complex inhibits proliferation in a panel of tumour cells and induces cytostasis and apoptosis in myeloid leukaemia cell line HL-60. More importantly, this activity is observed without the presence of unwanted genotoxic effects[24]. All of this is thought to be arising from the binding of the complex to cellular DNA. However, even if strong evidence suggests this to be the case (bacterial data), no proof of *in vivo* DNA interactions or evidence of uptake into human cells had been observed. For this reason, studies about the uptake and cellular distribution of the triple stranded helicates were performed and are presented in this chapter. In addition, the relationship between DNA binding and cytotoxicity was probed by exploring the cytotoxicity of cylinders with surface modifications that will influence the DNA binding.

4.1 Cellular toxicity

The DNA binding capacities of our metallo-supramolecular complexes are related to the triple helicate ($[Fe_2L_3]^{4+}$) structure. If the ability to inhibit the proliferation in cancer cells[24] is linked to the interaction with the DNA we could reason that modification of this structure, since it affects the DNA binding, would lead to a change in cytotoxic

properties. Complexes retaining similar shapes and structure, on the other hand, should maintain similar cytotoxicity. To examine this, the ruthenium (II) triple helicate ($[Ru_2L_3]^{4+}$) was tested against cell lines used previously for the iron derivative. In addition, the free ligand and $FeCl_2$ were tested as well, to rule out the possibility that extra or intracellular degradation of the original iron complex could be the cause of the toxicity.

Table 4.1. IC_{50} μM of iron and ruthenium cylinders against Breast and ovarian cancer cell lines.

	HBL-100	*T-47D*	*SK-OV-3*	*A2780*	*A2780cr*	*Rf*[a]
Ru Cylinder	**22±2**	**53±5**	**Not active**	**72±3.3**	**152±4.3**	**2.1±0.1**
Fe Cylinder	**27±5***	**52±10***	**35±5***	**≈10[&]**	**≈12[&]**	**≈1.2[&]**
$FeCl_2$(100 μM)	**100% grow**	**90-95% grow**	**95-100 grow**			
Parent ligand	**>300**	**>700**	**>400**			
cisplatin	**4.9±0.3**	**28±1.7**	**6±0.3**	**3±0.5**	**12.8±1.4**	**4.3±0.8**

* Data taken from A. C. G. Hozte, ref. 24. [&]Data taken from A. J. Pope, ref. 25. [a]*Rf* is increase in IC_{50} observed for a compound when tested in the cisplatin-resistant A2780cisR compared to A2780.

Table 4.1 shows the results of these experiments. Immediately we can observe that the ruthenium cylinder possesses almost exactly the same activity as the iron cylinder in breast cancer cell lines (HBL-100 and T-47D). The inactivity of the free ligand and $FeCl_2$, also rule out the possibility that the action is produced by the toxicity of the subproducts of the degradation of the complex. However, for the ovarian SK-OV-3 line, the ruthenium(II) derivative is not toxic, while the iron(II) compound is. This is probably the only difference between the two cylinders, and tells us that at certain levels (as seen for the DNA unwinding) the two complexes can show different actions (independent of its almost identical structure). To further study this, the ruthenium cylinder was tested against another ovarian cell line A2780, and its cisplatin resistant strand. Again low activity was observed for ruthenium while similar activity to cisplatin was observed for the iron cylinder.

To explore whether other small modifications in the structure of the iron complex could produce big changes of activity in ovarian cell lines, surface-modified iron cylinders with small structural modifications (Fig. 4.4) were tested in the same A2780 cell lines[26]. These complexes showed DNA binding abilities comparable with the non-NH equivalent compounds ($[Fe_2(LNHD)_3]^{4+}$ similar binding properties to the $[Fe_2L_3]^{4+}$

with addition of methyl groups producing decrease in DNA binding affinities)[27]. The results (Table 4.2) showed that the three complexes presented much higher toxicity than the $[Ru_2L_3]^{4+}$ complex, with IC_{50} values similar to cisplatin and were more effective at overcoming resistance. Even more interestingly, the complex $[Fe_2(LNHD)_3]^{4+}$, which has the most similar structure to the parent complex, showed identical activity.

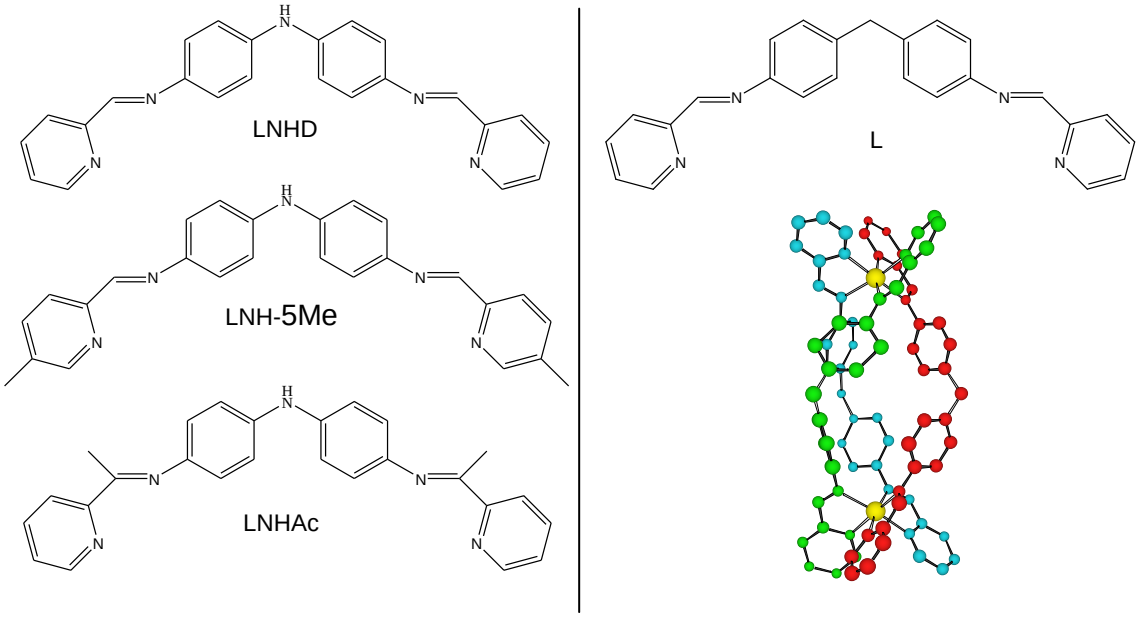

Figure 4.4. Structure of the ligands forming the different iron triple helicates (left) compared with the parent ligand (right).

Table 4.2. Cell growth inhibition values (MTT assay) IC_{50} (μM) values of different iron triple stranded helicates against A2780 and A2780cr ovarian cancer cell lines. [&]Data taken from A. J. Pope, ref. 25.

	A2780	*A2780cr*	*Rf*
$[Fe_2(LNHD)_3]^{4+}$	**9.9±0.6**	**12.6±2.6**	**1.3±0.3**
$[Fe_2(LNH\text{-}5Me)_3]^{4+}$	**3.3±0.6**	**5±1**	**1.5±0.4**
$[Fe_2(LNHAc)_3]^{4+}$	**6.9±0.8**	**11±1**	**1.6±0.2**
Fe Cylinder	**≈10[&]**	**≈12[&]**	**≈1.2[&]**
cisplatin	**3±0.5**	**12.8±1.4**	**4.3±0.8**

In breast cancer cell lines, on the other hand, both ruthenium and iron triple helicates showed similar toxicity. This could indicate that in these cell lines the activity was

mainly due to structural features. To study this, the activity of tetra-stranded palladium dinuclear ($[Pd_2L_4]^{4+}$) (Fig. 4.5) complexes[28] in breast cancer cell line T-47D was studied. These compounds are bigger than the $[Fe_2L_3]^{4+}$ cylinder, and their DNA binding properties are totally different[28]. Data in Table 4.3 show that they presented high activity in this cell line. Unfortunately one of them ($[Pd_2(LST)_4]^{4+}$) was not sufficiently soluble in the required concentrations. However, for the other two complexes, a 6 fold improvement compared with cisplatin was observed, while the triple helicates were an order of magnitude less toxic.

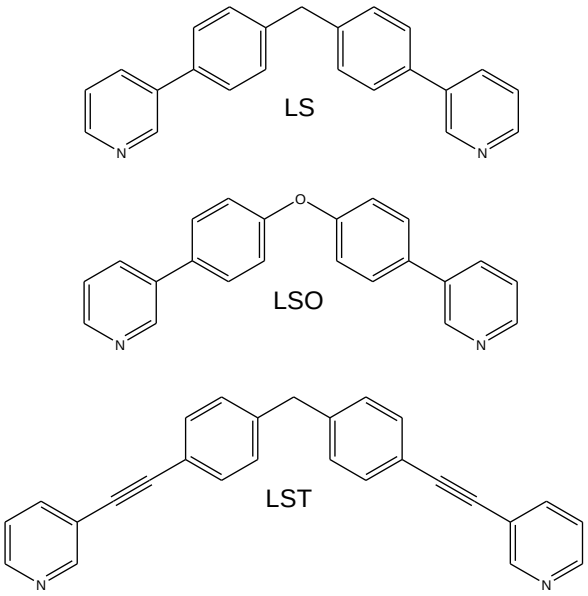

Table 4.3.	*T-47D*
$[Pd_2(LS)_4]^{4+}$	**5.6±0.5**
$[Pd_2(LSO)_4]^{4+}$	**4.8±1.1**
$[Pd_2(LST)_4]^{4+}$	**Not soluble enough**
cisplatin	**28±1.7**

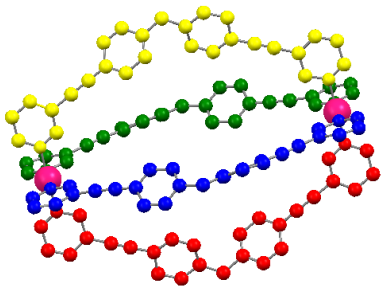

Figure 4.5. Structure of the ligands forming the different Pd tetrastranded complexes (left), crystal structure of $[Pd_2(LST)_4]^{4+}$ [28] and cell growth inhibition values (MTT assay) IC_{50} (μM) values against breast cancer cell line T-47D.

4.2 Cellular distribution

While our working hypothesis is that cellular activity is related to the DNA binding, which will be dependent of the structure the complex, similar effects might be produced if the cylinder affects other macromolecules or organelles. To probe and understand this, it is important to know if the cylinders are taken up into the cell and where they are distributed once inside.

4.2.1 Propidium iodide displacement

Previous Flow Cytometer analysis showed an increase in the number of apoptotic cells after treatment with the iron triple helicate[24]. When this was further investigated with dual propidium iodide (PI) and annexin-V (AV) staining (a technique that differenciates between early apoptotic and post-apoptotic cells), a decrease in the PI staining was observed in apoptotic cells treated with the complex[24]. PI is a fluorescent dye that increases its emission when bound to DNA. A decrease in PI DNA staining could suggest that it cannot bind to cellular DNA when the complex is present. The observed decrease could therefore indicate the desired complex-DNA interaction on nuclear DNA. In order to see if this could be possible, a PI displacement assay was undertaken with free ct-DNA (Fig. 4.6).

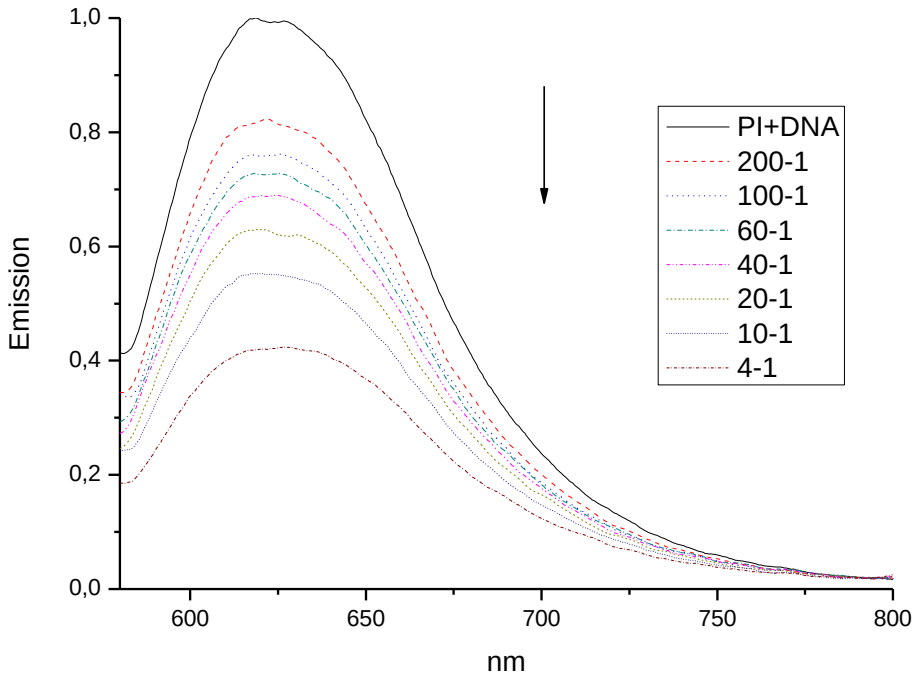

Figure 4.6. Displacement of propidium iodide (1.5 μM) from ct-DNA (6 μM) by iron cylinder $[Fe_2L_3]^{4+}$. Mixing ratios Pi/cylinder are shown in the caption. λ_{exc}=535nm. (Normalized to the maximum of emission PI-DNA).

Ct-DNA was loaded with PI, then aliquots of $[Fe_2L_3]^{4+}$ added and the change in PI fluorescence monitored. As observed in Figure 4.6, the iron triple helicate can displace PI at very low concentrations (200-1 PI:complex). Such displacement has been observed before with other dyes (e.g. ethidium bromide)[13], and indicates that the lower PI staining observed in the flow cytometry could indeed be due to our complex interacting with the

cellular DNA. Unfortunately, PI is not membrane permeable and can only enter apoptotic cells, which have big pores in their membrane. For that reason the observation does not inform on whether our helicate might have reached cellular DNA in healthy cells (causing apoptosis), or caused the apoptosis by a different mechanism and subsequently bound to the DNA of dead cells as the PI.

4.2.2 Hoechst 33258 displacement

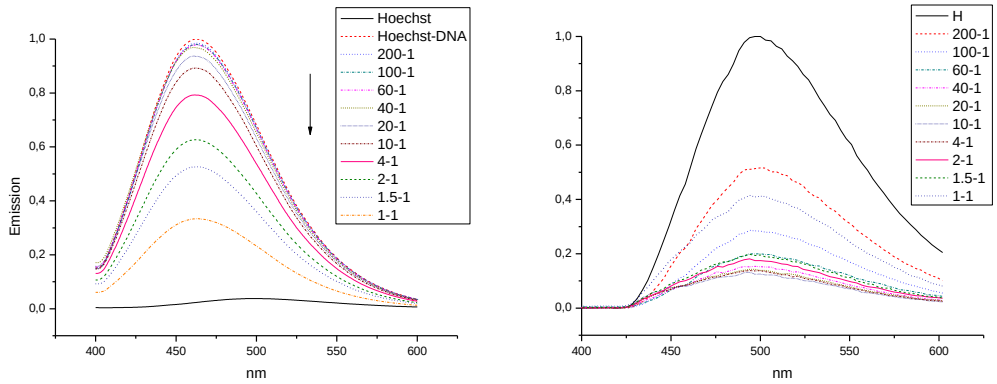

Figure 4.7. Displacement of Hoechst 33258 (1.5 μM) from ct-DNA (12 μM) by iron cylinder $[Fe_2L_3]^{4+}$(Left). Quenching of Hoechst 33258 by iron cylinder $[Fe_2L_3]^{4+}$(right). Mixing ratios Hoechst/cylinder are shown in the caption. λ_{exc}=350 nm. (Normalized to the maximum of emission Hoechst-DNA or Hoechst alone).

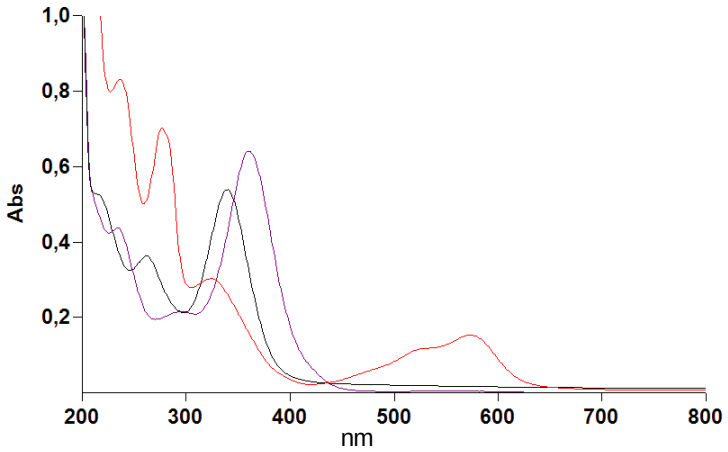

Figure 4.8. UV spectra of iron cylinder 15 μM (red), and Hoechst 33258 (black) and Hoechst 34580 (purple) 25 μM.

Hoechst 33258 is a nuclear staining agent that binds to the minor groove of the DNA and can penetrate the membrane and stain the nuclei of *live* cells[29-31]. When excited at 350 nm it produces a fluorescent emission with the maximum at around 500 nm. This emission is increased upon binding to DNA, shifting the maximum approximately to

450 nm. Previous work showed that the iron cylinder could displace this molecule from naked DNA *in vitro*[13]. For that reason it looked like an interesting tool to see if our complexes could arrive at and bind to the nuclear DNA of *live* cells. When the experiment was repeated with the same conditions used for PI, displacement was observed as expected (Fig. 4.7). However, when the same experiment was measured in absence of DNA as a control, quenching of the Hoechst fluorescence was observed as well (Fig. 4.7).

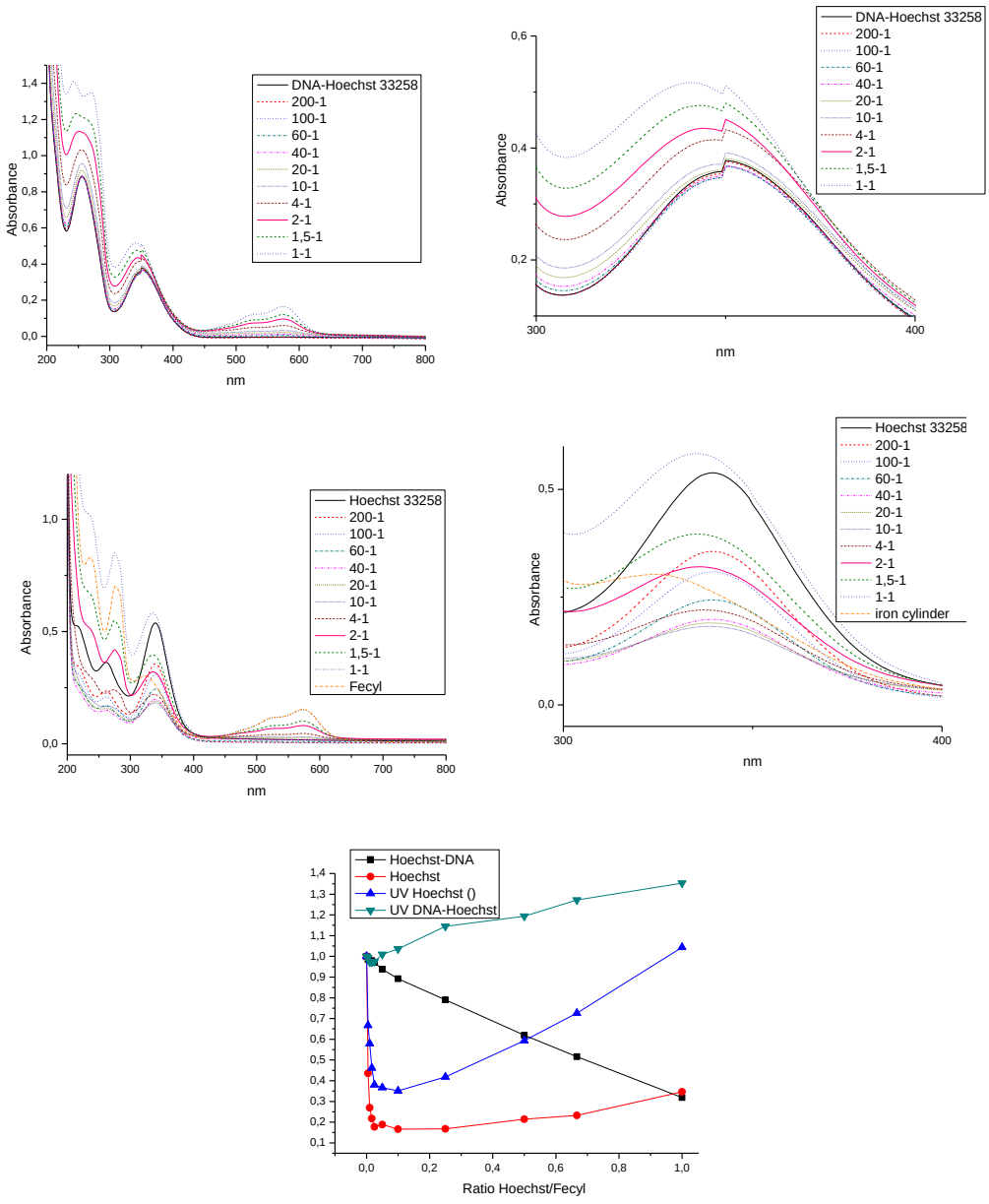

Figure 4.9. UV titration of Hoechst 33258 (15 µM) with iron cylinder in presence (top) or absence (middle) of DNA (120 µM) and decreasing ratios of emission at 450 nm and absorbance at 350 nm (bottom). Mixing ratios Hoechst/cylinder are shown in the caption.

This decrease in intensity was much bigger than the decrease observed when DNA was present (Fig. 4.7). We first thought that the fluorescence was quenched as a result of the iron cylinder band with maximum at 325 nm (Fig. 4.8) absorbing the energy provided for the excitation of the Hoechst molecules. However, when the same titration was followed by UV/VIS spectroscopy, we could observe a decrease in the absorbance band produced by the transition responsible of the fluorescence emmision (and others) similar to the decrease in fluorescence intensity observed previously (Fig. 4.9). Again this was stronger in the absence of DNA, but not visible in its presence. This indicated that somehow the DNA was protecting Hoechst 33258 from the quenching effect caused by the iron cylinder and the loss of fluorescence in this case was probably due to removal of the Hoechst from DNA.

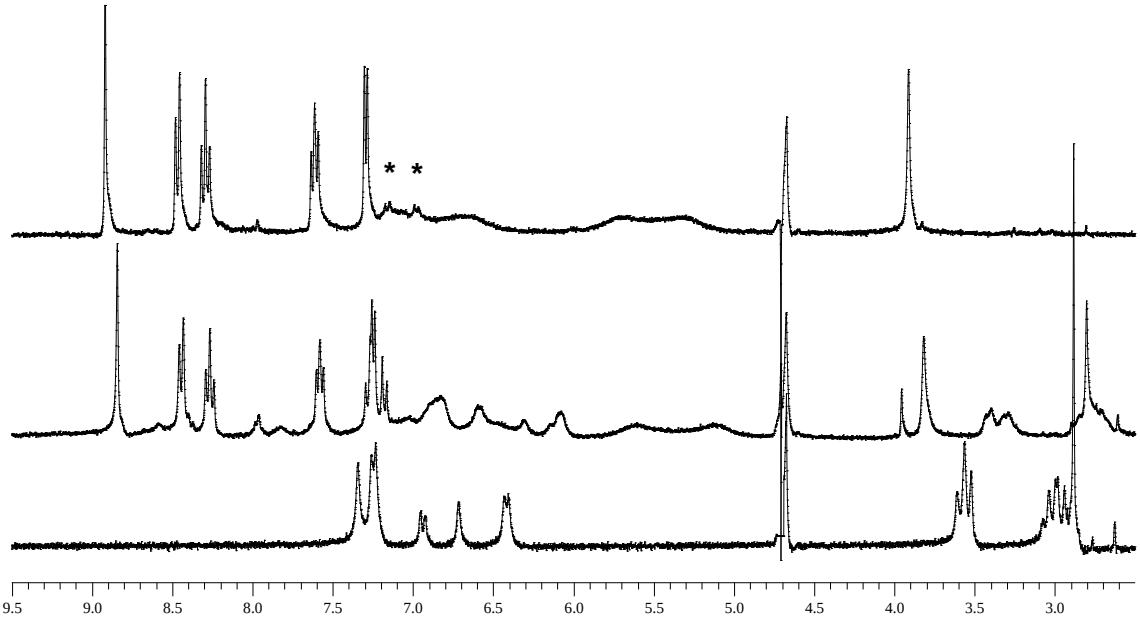

Figure 4.10. ^{1}H NMR spectrum of iron cylinder (top), Hoechst 33258 (bottom) and mixture 1:1 of both (middle) in deuterated water (4.5 mM). * indicates a small percentage of complex hydrolysis.

The fact that absorbance due to the Hoechst 33258 was disappearing during the titration was uncommon. Stranger was the observed reappearance of the bands belonging to the staining agent when a certain cylinder concentration was reached. This could only be explained if somehow there was a (weak?) chemical interaction between our iron cylinder and the Hoechst 33258, that would be stopped when enough cylinder to interact with themselves or the DNA were present. To explore this hypothesis, the NMR spectra of iron cylinder, Hoechst 33258 and of a 1:1 mixture of both were recorded (Fig. 4.10). Immediately we could see that the mixture produces a small shift

towards higher field in the signals from the free iron cylinder, and a big shift in the Hoechst protons. This indicated that there was interaction between both compounds and that the quenching was more due to chemical interaction than physical interferences (at least in absence of DNA).

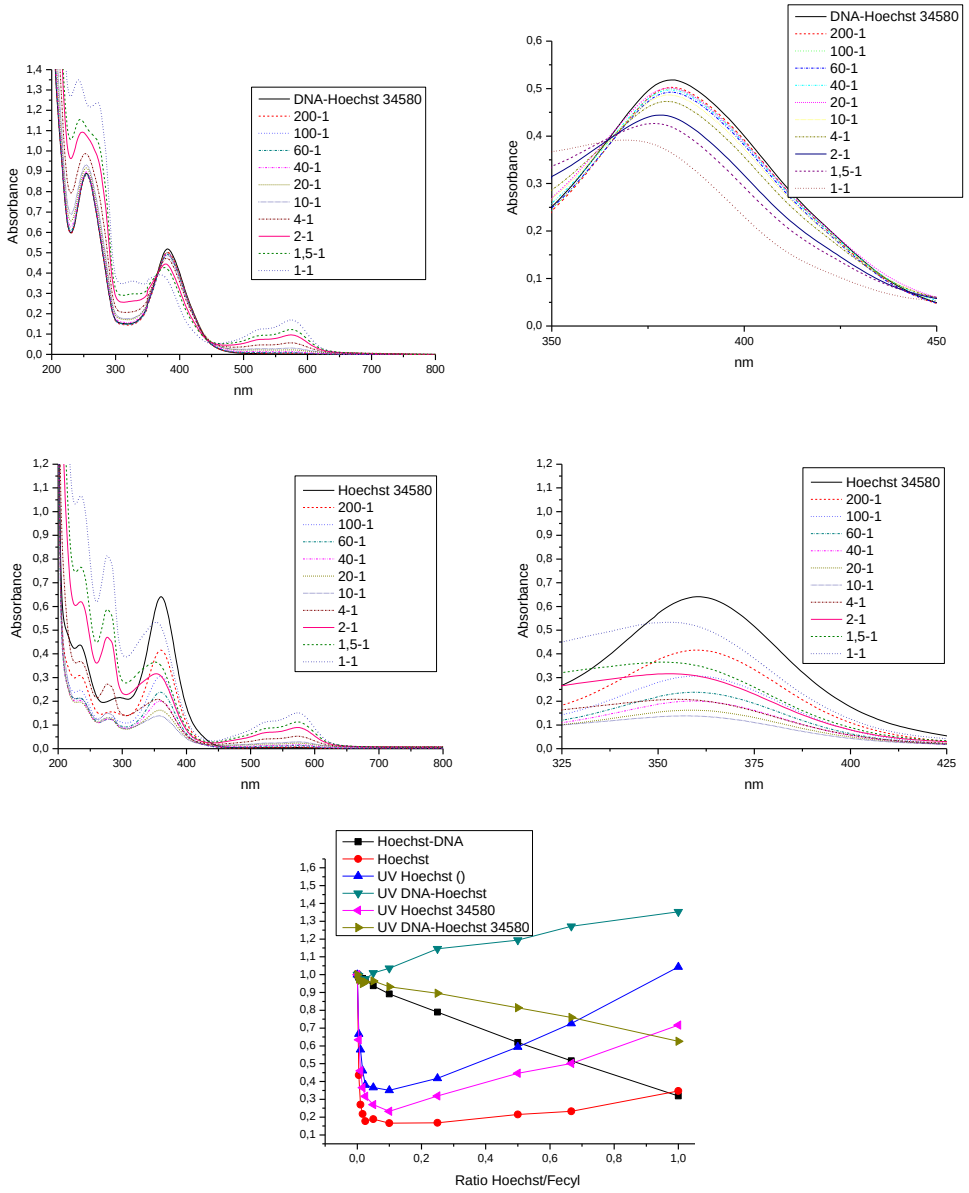

Figure 4.11. UV titration of Hoechst 34580 (15 µM) with iron cylinder in presence (top) or absence (middle) of DNA (120 µM) and decreasing ratios of emission at 450 nm (Hoechst 33258) and absorbance at 350 (Hoechst 33258) or 392 nm(Hoechst 34580) (bottom). Mixing ratios Hoechst/cylinder are shown in the caption.

This was reinforced when a different nuclear dye from the same Hoechst family (Hoechst 34580, normally excited at 392 nm, a region were the iron cylinder have a window with low absorbance, between 390 and 410 nm; Fig. 4.8) suffered a similar UV absorbance quenching process (Fig. 4.11).

4.2.3 In vivo Hoechst 33258 displacement

Despite these problems, we chose to continue to try and follow Hoechst displacement from cells. Matsuda et al have used Hoechst displacement to detect if a DNA binder could target nuclear DNA *in vivo*[32]. Cells were incubated with Hoechst 33258 for a time long enough to stain the cellular DNA. Then they were treated with the DNA binder for some time. If a decrease in the emission was observed, that meant that Hoechst was displaced and the compound could interact with cellular DNA. In our case, although cylinder can displace the dye from the DNA, this will be difficult to quantify due to the simultaneous quenching of free Hoechst molecules. For that reason the experiment will not tell us if our cylinder displaces Hoechst 33258 from cellular DNA, however, it can be used to observe uptake inside the cell. If, after treatment with our cylinder, the Hoechst emission decreases, it will tell us that the Hoechst emission is quenched or displaced, and our compound is therefore inside the cell. The cells used here were HL-60, a myeloid leukemia cell line that grows in suspension. They were chosen because suspension growth makes easier the treatment and posterior recollection of the cells compared with adherent cell lines.

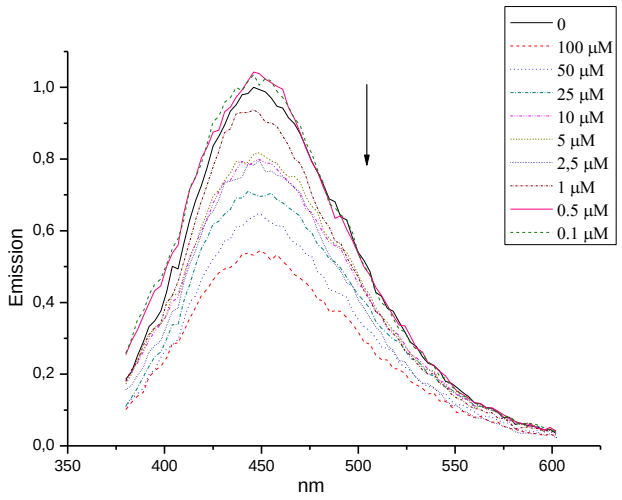

Figure 4.12. Fluorescence displacement assay for HL60 cells loaded with 10 µM Hoechst 33258 and then treated with varying concentrations of cylinder (concentrations indicated in the figure). λ_{exc}=350nm. (Normalized to the maximum of emission of cells untreated with cylinder)

Figure 4.12 show the emission of Hoechst 33258 stained cells after treatment with different concentrations of iron cylinder. Immediately we can observe that the fluorescence coming from Hoechst decrease with the addition of cylinder and the

quenching of this emission seems to be dependent of the concentration of iron cylinder added (Fig. 4.13). As explained before, this means that the intracellular dye is been quenched by our complex, indicating that our compound is been taken up and that this uptake depends on the concentration of cylinder present in the medium.

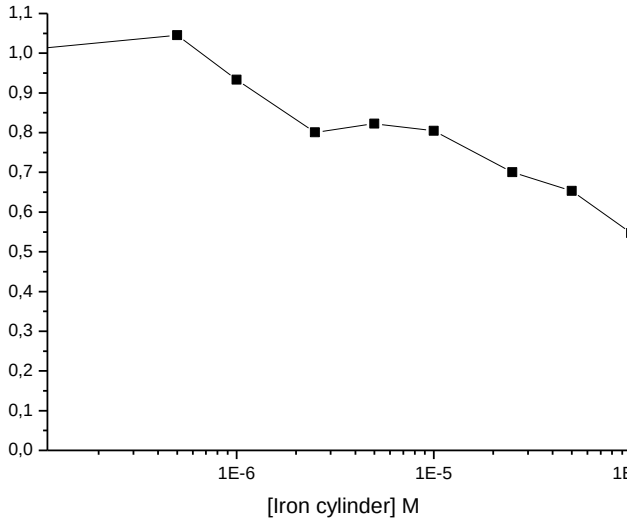

Figure 4.13. Ratios of decreasing Hoechst 33258 fluorescence upon treatment with different concentrations of iron cylinder.

4.2.4 Cellular uptake

In order to explore uptake in a more rigorous manner, HL-60 cells were treated with drugs and uptake determined using ICP-MS. The iron cylinder, as the most interesting compound, and its ruthenium derivative (due to its similitude in structure and activity) were chosen, and cisplatin was used as a control. A short time of exposure (3 h) and a single concentration (50 μM)[33] was used in order to determinate speed and efficiency of cell uptake for all the compounds, under the same conditions. Whole cell, cytoplasm (including mitochondria and the other organelles) and nucleic fractions were obtained from the same experiment to observe distribution through the cell. Uptake could be immediately observed by eye since the different fractions were coloured with the colour of the compound (red-brown for ruthenium cylinder; purple for iron cylinder. Fig. 4.14).

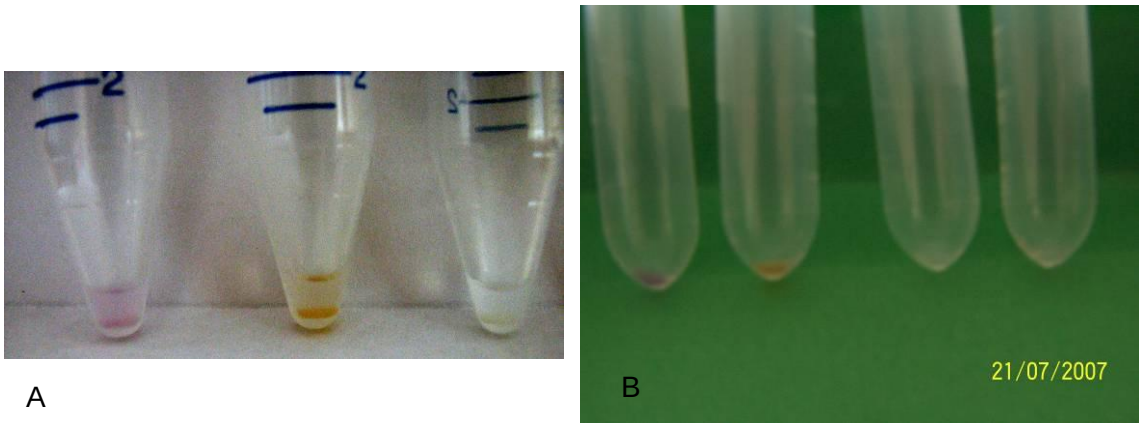

Figure 4.14. HL-60 whole cells (A) and nuclear fractions (B) after 3 h treatment with iron cylinder (purple), ruthenium cylinder (red-brown) and cisplatin (white)

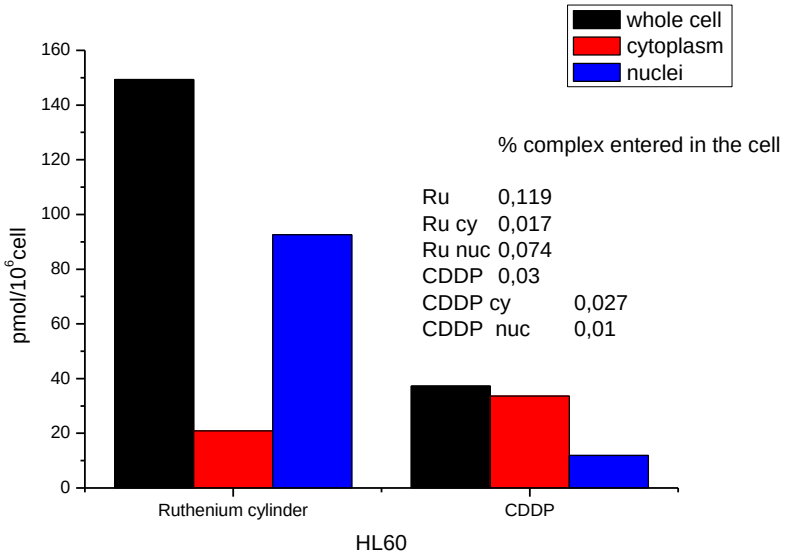

Figure 4.15. pmols of Pt and Ru (as dinuclear) in HL-60 after 3hours of treatment with 50μM of the complexes. Iron cylinder (nmol/10^6 cells): 1.93 whole cells, 0.2 cytoplasm, 0.68 nuclei.

Unfortunately the high background of iron in the cell did not allow us to get reliable data from the iron cylinder (see Fig. 4.15 caption for an example value). However, uptake data of ruthenium and platinum were obtained for cells treated with cisplatin and ruthenium cylinder (Fig. 4.15). Cisplatin was found in similar concentrations to these observed previously[34] (and chapters 2.2.5 and 3.3.2), showing that most of the drug stays in the cytoplasm, and just one third of the platinum arrives at the nuclei (at this time point). However, the ruthenium cylinder was taken up 4 times more than cisplatin. The compound does not get stuck in the membrane as more than 80% of the compound is found in the cytoplasm or nucleus, and only 15% stays in the cytoplasm (against the

two thirds of cisplatin). Over 60% of the ruthenium cylinder taken up into the cell is found to be in the nuclei (much higher than for cisplatin).

If cellular volume is known, intracellular concentration can be calculated. This data is interesting because it can give us preliminary information about how our compound is taken up. If the compound is found in higher concentration than the original treatment solution, it can be indicative of an active uptake mechanism or binding to a cellular target. Lower or similar concentrations to the initial medium could indicate passive transport or not equilibrium reached. Two different volume values are found in the literature for HL-60 cells, 0.7 pl/cell[35] (2005) or 0.05 pl/cell[36] (1983). When the second value is used, internal concentrations of 3 mM and 0.75 mM for the ruthenium cylinder and cisplatin respectively are found. These high values would mean that in times as short as 3 hours our cylinder is concentrated inside the cell 60 times and cisplatin 15, making the calculations hard to believe. Using 0.7 pl/cell concentrations of 213.3 µM for the ruthenium cylinder (4 times more concentrated than the 50 µM of the treatment medium) and 53.4 µM for cisplatin are found. These values are more understandable (and similar to previous data presented for ruthenium(II) polypyridyl complexes in HeLa cells[37]) and could indicate that the cylinder is concentrated inside the cell (maybe due to active transport) while cisplatin is not (probably due to its passive transport). These experiments prove that the cylinders enter the cell, and arrive in contact with or close to cellular DNA (a similar conclusion could be reached for the iron derivative. Figure caption from Fig. 4.15).

4.2.5 Single cell electrophoresis for detection of DNA strand breaks (Comet assay)

As previously described, the ruthenium cylinder has the ability to act as a nuclease when irradiated with UV or Vis light[22]. In order to reinforce the previous experiment and establish whether this cylinder can interact with the nuclear DNA, HL-60 cells were treated with the ruthenium helicate for one hour (at the same concentration used for uptake experiments: 50µM). Then, some of the cells were illuminated with visible light using a 250 W halogen lamp giving out white light for 10 minutes, to see if our ruthenium cylinder could cleave the DNA under cellular conditions. Cisplatin was used as a control. To detect strand breaks we used the comet assay. The cells were collected and the nuclei isolated. These nuclei were studied with normal electrophoretic techniques; this will show any damaged DNA as a tail flowing out of the nuclei and

allow us to quantify the damage produced to the cellular DNA (as % of DNA in the tail)[38]. This is an increasingly used (and recognised) assay for genotoxicity. The results can be observed in Table 4.4 and Fig. 4.16.

Table 4.4. % tail-DNA indicative of DNA strand breaks after 1h treatment with 50 μM of the complexes. With and without light irradiation.

	No-Light	*Light*
Ruthenium cylinder	**2.9±2**	**47.2±4.9**
Cisplatin	**0.7±0.5**	**24±1**
Untreated	**0.5±0.1**	**28±3.3**

Cisplatin did not affect the DNA more after radiation with light than seen in the untreated cells. However, when the cells were treated with ruthenium cylinder and irradiated doubled the amount of DNA damaged compared with the illuminated controls. In times as short as 1 hour the ruthenium cylinder can be taken up into the nuclei and interact with DNA and in the presence of light cleave it.

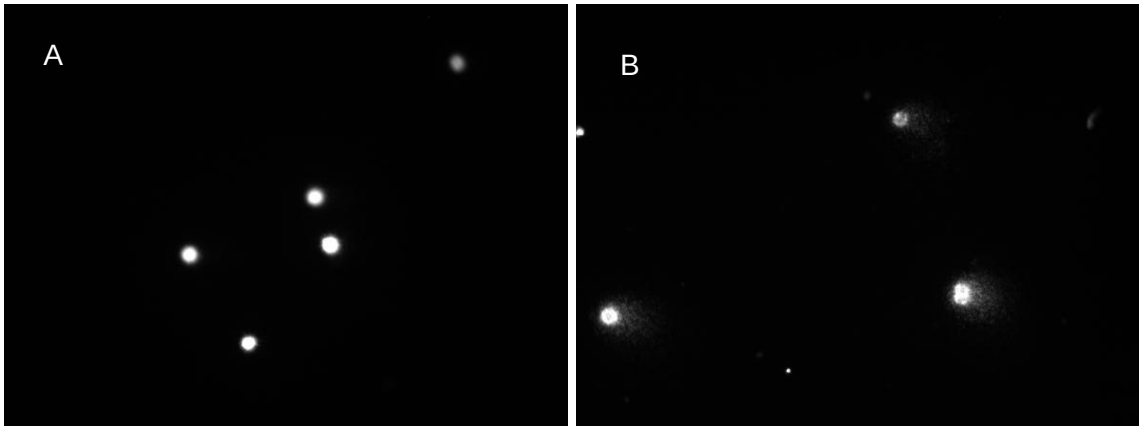

Figure 4.16. Image of HL-60 nuclei treated with 50μM ruthenium cylinder for 1h with (B) and without light irradiation (A).

4.2.6 Microscopy cell distribution

Another property of the ruthenium cylinder is that it produces a fluorescence emission when excited in the MLCT region. The maximum wavelength for this excitation is at 480 nm producing a broad emission band between 600 and 800 nm with a maximum at around 700 nm[21]. We decided to use this property to follow cellular uptake and localisation. Adherent cell line T-47D (breast) was treated with the ruthenium complex under the same conditions used for the ICPMS uptake experiment

(50 μM for 3 hours), knowing that in this time the complex is internalized and arrives in large quantities to the nuclei. Treated cells were then visualized under a confocal microscope, exciting the cells with an Argon laser (λ_{ex}=488 nm). The first question was whether our compound could be detected, as its emission is not very strong. Beyond that we were interested to see where the ruthenium cylinder would be concentrated or observed in *live* cells. Fig. 4.17 shows some of the images taken from this experiment.

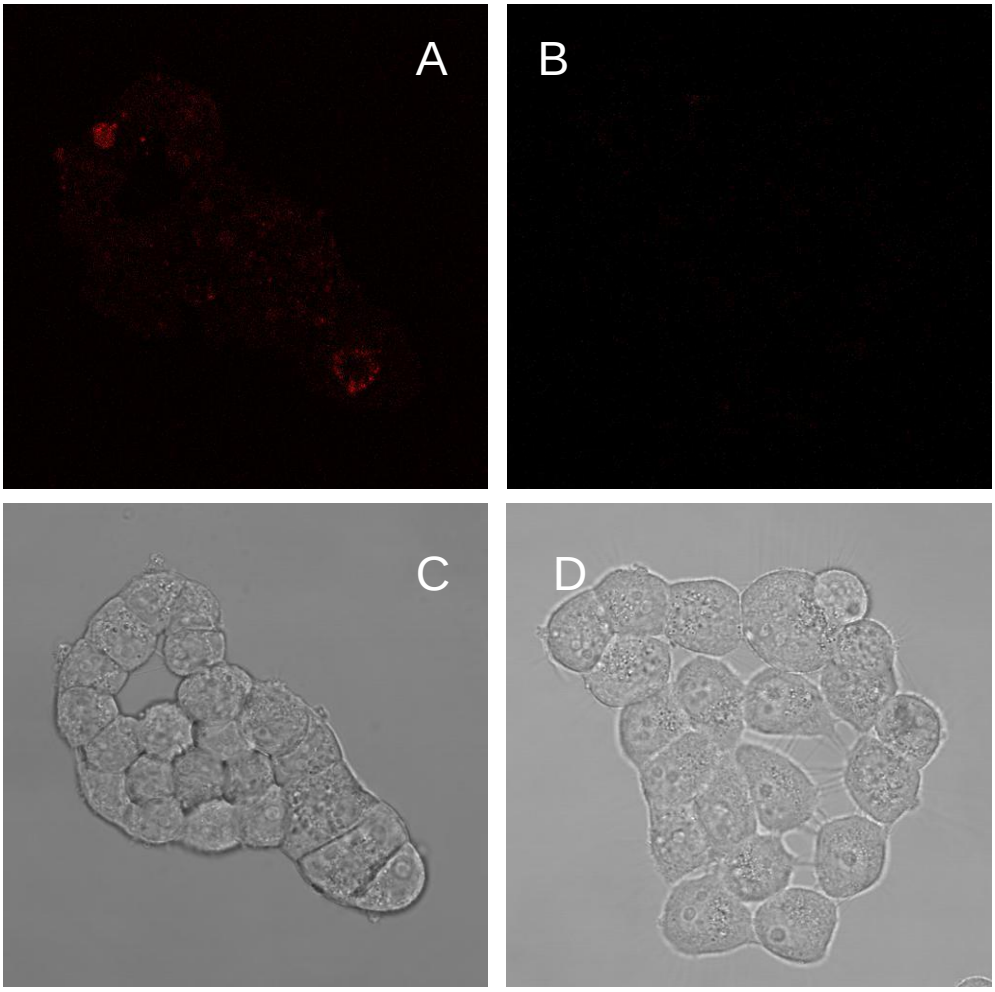

Figure 4.17. Confocal microscopy image under Argon laser (488 nm) or with light of cells treated (A or C) and untreated (B or D) with 50 μM ruthenium cylinder.

In the pictures (Fig. 4.17A) the ruthenium cylinder can be observed in the cells. When a control without complex was studied under the same conditions no comparable (auto)fluorescence was observed (Fig. 4.17B). The confocal images allow us to confirm that the compound is in the cell, not merely on the membrane. We can see that the complex is distributed through the whole cell at this time point, but is more concentrated in some circular corpuscles. Small really intense dots can be observed as

well. We can speculate that the big circular corpuscles are nuclei and the small dots endosomes, but further studies are required using nuclear, endocytosis or other markers to confirm this.

4.3 Conclusions

As observed previously the iron cylinder has cytotoxic activity[24]. This is not unique to this compound but a feature of the class and the structurally similar iron and ruthenium compounds show similar toxicities. However, size and shape are not the only factors involved in their anticancer properties, as observed by the fact that the ruthenium cylinder doesn't show activity in ovarian cell lines and the iron one does. Since the size and shape are important for DNA binding[13, 15, 21-22], the possible relation between the toxicity and the structure of the complexes could indicate that their cytotoxic properties could depend of the interaction between the metallo-cylinders and the DNA.

To probe the potential link between DNA binding and toxicity, uptake and cellular distribution of the cylinders were studied. The complexes showed the ability to quench Hoechst 33258 emission inside cells, suggesting that they could be taken up. ICP-MS studies showed that the cylinders can cross the membrane arriving in relative short times at the nuclei. The amount of compound that arrives there is very high compared with cisplatin, showing that more than 60% of uptaken cylinders arrive at the nuclei compared to less than 30% of cisplatin. Remarkably our compound was concentrated in the nuclei, arriving in large quantities close to the cellular DNA. When cells preloaded with ruthenium cylinder were irradiated with visible light, they presented a high percentage of DNA strand breaks compared with untreated and cisplatin controls. This could be considered as the *in vivo* equivalent of the *in vitro* DNA photocleavage activity observed for the same complex[22], showing that the same or similar effects observed *in vitro* could be present *in vivo*. Finally, confocal microscopy showed us that the fluorescent emission of the ruthenium cylinder can be observed inside *live* cells. Although no detailed information was obtained, it can be an important tool for the study of accumulation and transport process in the future.

Summarizing, our metallo-supramolecular cylinders can be taken up in *live* cells, being accumulated in the nuclei. There, the complexes can interact with DNA, being the probable cause of their final cytotoxic activity.

4.4 Experimental

Cell test: Tissue culture flasks, 96-well plates, RPMI 1640, DMEM, L-glutamine, trypsin-EDTA, HEPES, sodium pyruvate and FBS were obtained from Invitrogen. Thiazolyl blue tetrazolium bromide (MTT) and DMSO were from Sigma, UK. Tissue culture flasks, 96 well plates, RPMI 1640, DMEM, L-glutamine, trypsin-EDTA, HEPES, sodium pyruvate and FBS were obtained from Sigma, UK. Thiazolyl blue tetrazolium bromide (MTT) and DMSO were from Avocado, UK. Cells were grown in RPMI 1640 (HBL-100, T-47D, SK-OV-3) or DMEM (A2780/cr) in 10 % FBS supplemented with 1% L-glutamine, 1% HEPES buffer and 1% sodium pyruvate. The MTT assay[39] was carried out using 96 well plates. Cells were harvested in logarithmic growth, 4,000 (A2780/cr), 10,000 (SK-OV-3, HBL-100) or 25,000 cells (T-47D) were seeded per well and left overnight to attach. The cells were treated, in quadruplicate with 6 difference concentrations of complex dissolved in fresh media; the range of concentrations used is dependent on the complex. The cells were incubated for 72 hours and 20 μl of thaizolyl blue tetrazolium bromide (5mg / ml, 0.2 μm filtered) added. The cells were further incubated for 2 hours. The media was carefully removed by aspiration and 200 μl of DMSO added to dissolve the purple crystals. Absorbance was measured using a 96-well plate reader (BioRad) set at 590 nm. Each cell line was investigated beforehand to determine the correct cell numbers to initially seed and the required amount of time exposed to thiazolyl blue tetrazolium bromide to ensure sensitivity and accuracy.

Propidium Iodide displacement: The fluorescence spectra for the propidium iodide (PI) displacement experiment were recorded in a Shimadzu RF-5301 PC Fluorescence Spectrophotometer (λ_{exc} = 535 nm; Range emission = 580-800 nm; resolution = 0.4 nm; Speed medium; Excitation split = 10; Emmision split = 1.5). Solutions of PI (15 or 1.5 μM), ct-DNA (12, 1.2 or 6 μM), NaCl (50 mM) and sodium cacodylate buffer (1 mM)

were prepared, measured and tritiated with iron parent cylinder from ratios PI:iron cylinder 200-1 to 4-1, keeping the concentration of PI and ct-DNA constant.

Hoechst 33258 displacement: The fluorescence spectra for the Hoechst 33258 (Hoechst) displacement experiment were recorded in a Shimadzu RF-5301 PC Fluorescence Spectrophotometer (λ_{exc} = 350 nm; Range emission = 400-600 nm; resolution = 0.4 nm; Speed medium; Excitation split = 5; Emmision split = 1.5). Solutions of Hoechst (1.5 µM), ct-DNA (12 µM), NaCl (50 mM) and sodium cacodylate buffer (1 mM) were prepared, measured and tritated with the different complexes from ratios Hoechst:complex 200-1 to 4-1, keeping the concentration of Hoechst and ct-DNA constant.

Hoechst 33258 cellular displacement assay: The cellular displacement assay of Hoechst 33258 was done following the procedure described in Matsuba et al[31]. Fluorescence spectra were recorded in a PTIA fluorescence system. The illumination source was a PTI L-201M source using a 75W Xenon arc lamp. The detection system a Shimadzu R298 PMT in a PTI model analogue/photon-counting photomultiplier (λ_{exc} = 350 nm; Range emission = 380-600 nm; speed = 3nm/s; Excitation split = 5; Emission split = 1.5). 50000 HL-60 cells were preincubated with 10 µM Hoechst 33258 in 0.5 ml culture medium RPMI 1640 (supplemented as explained before) at 37ºC for 20 min. The iron cylinder was then added (concentrations between 0.1 and 100 µM) followed by a further 20 min incubation at 37ºC. Cells were then collected, washed once with chilled PBS, resuspended in chilled PBS and the fluorescence measured.

Cellular Uptake: Four million HL-60 cells were seeded in 100 mm diameter Petri dishes (medium used RPMI 1640 supplemented as explained before) and treated with 50 µM of the different compounds for 3 hours. After that time, the medium was removed and cells washed three times with PBS to remove all the unwanted (non uptaked) complexes. Cells were collected and two aliquots of two million cells were taken, one of them to see whole cell uptake and the other for cytoplasm and nuclei fraction extraction (Nuclear/Cytoplasm extraction kit. BioVision). Two ml of ultrapure concentrated Nitric

Acid (Traceselect Ultra, Aldrich) was added to the samples, and digested overnight at 90ºC. Samples were then taken to dryness at 120ºC, resuspended in 3ml of a 2% solution of Nitric acid and filtered. The amount of Platinum was measured in a Agilent 7500CX ICP-MS (analysis was done with Pt sample cone in He and No-gas mode. Plasma settings: Ar.flow: 15 L/min; Neb gas: 0.8 L/min; RF power 1550W; T of spray chamber: 15 º C).

Comet Assay for DNA strand breaks: This method was based on that of Singh et al[40], as modified in Prof. Chipman's laboratory[41]. 100000 HL-60 cells were incubated with 50 µM Hoechst 33258 in 1 ml in supplemented phenol red-free RPMI 1640 culture medium for 1 hour in the dark (wrapped in silver foil). Pre-treated cells were placed on ice and exposed to visible light from a 250 W halogen lamp (Philips, U.K.), at a distance of 19 cm. 10 minutes of illumination corresponded to 111 kJ/m^2 between 400 and 800 nm, equivalent to 9.3 kJ/m^2 between 400 and 500 nm. Cells were collected and washed in cold PBS. Then, cells were centrifuged (200 x g, 5 min) and pellets re-suspended in PBS (150 µl). An aliquot of re-suspended cells (15 µl) was placed into a sterile tube containing low melting point agarose (150 µl) and this cell suspension transferred to a glass microscope slide (150 µl per slide, BDH, U.K.), pre-coated with 0.5 % normal melting point agarose. Glass coverslips (BDH, U.K.) were added and slides placed on a metal tray over ice for 10 min. Coverslips were removed and slides incubated for 1 h at 4 °C in lysis buffer (2.5 M NaCl, 0.1 M Na_2EDTA, 10 mM Tris base, 1 % sodium N - lauryl sarcosinate, 10 % DMSO and1 % Triton X-100). Following lysis slides were transferred to a horizontal electrophoresis tank (Pharmacia Biotech, U.S.A.) containing electrophoresis buffer (75 mM NaOH and 1 mM Na_2EDTA, pH approximately12.8) and DNA allowed to unwind for 10 min. DNA was subjected to electrophoresis (25 V, 0.8 Vcm^{-1}, 10 min) and slides neutralised by washing (3 x 5 min) with neutralisation buffer (0.4 M Tris, adjusted to pH 7.5). Slides were subsequently stained with Sybr Gold 50 µl (Invitrogen, 10 x solution). The slides were examined at 320 x magnification using a fluorescence microscope (Zeiss Axiovert 10, Germany), fitted with a 515 - 560 nm excitation filter and a barrier filter of 590 nm. A USB digital camera (Merlin, Allied Vision Technologies) received the images, which were analysed using a personal computer-based image analysis system Comet assay IV (Perceptive instruments). Images of one hundred randomly selected nuclei were analyzed per slide.

Measurement of percent tail DNA (TD %) was chosen to assess the extent of DNA damage as this has been shown to suffer much less from inter-run variation than other comet parameters because it is independent of electrophoresis voltage and run time[38]. Median values of three separate experiments were analysed using ANOVA and post-hoc Student's t-test, as recommended by Duez *et al*[42].

Cellular Imaging: 500000 T-47D cells were seeded in 30 mm diameter Petri dishes with glass bottom and left overnight to attach. The cells were treated then with 50 μM of the ruthenium cylinder for 3 hours. After that time, the medium was removed and the cells washed three times with PBS to remove all the unwanted (non uptaked) complexes. The resulting cells were observed through a Leica DMIRE2 system with an Argon laser (operated at 488 nm) and a temperature control chamber (operated at 37 ºC) attached.

4.5 References

1 B. Lippert, Cisplatin, Chemistry and Biochemistry of A Leading Anti-Cancer Drug, Wiley-VCH, Weinheim, 1999.

2 Z. Guo, P.J. Sadler, *Angew. Chem. Intl. Ed.*, 1999, **38**, 1512.

3 M.J. Hannon, *Pure and Applied Chemistry*, 2007, **79**, 2243.

4 M. J. Hannon, *Chem. Soc. Rev.*, 2007, **36**, 280.

5 S. Kemp, N. J. Wheate, D. P. Buck, M. Nikac, J. G. Collins, J. R. Aldrich-Wright, *J. Inorg. Biochem.*, 2007, **101**, 1049.

6 S. Komeda, T. Moulaei, K. K. Woods, M. Chimuka, N. P. Farrell, L. D. Williams, *J. Am. Chem. Soc*., 2006, **128**, 16092.

7 M. J. Hannon, V. Moreno, M. J. Prieto, E. Molderheim, E. Sletten, I. Meistermann, C. J. Isaac, K. J. Sanders, A. Rodger, *Angew. Chem. Int. Ed.*, 2001, **40**, 879.

8 M. J. Hannon, I. Meistermann, C. J. Isaac, C. Blomme, A. Rodger, J. R. Aldrich-Wright, *Chem. Commun.*, 2001, 1078.

9 I. Meistermann, V. Moreno, M. J. Prieto, E. Moldrheim, E. Sletten, S. Khalid, P. M. Rodger, J. C. Peberdy, C. J. Isaac, A. Rodger, M. J. Hannon, *Proc. Natl. Acad. Sci.*, 2002, **99**, 5069.

10 J. M. C. A. Kerckhoffs, J. C. Peberdy, I. Meistermann, L. J. Childs, C. J. Isaac, C. R. Pearmund, V. Reudegger, S. Khalid, N. W. Alcock, M. J. Hannon, A. Rodger, *Dalton Trans.*, 2007, 734.

11 S. Khalid, M. J. Hannon, A. Rodger, P. M. Rodger, *Chem. Eur. J.*, 2006, **12**, 3493.

12 E. Moldrheim, M. J. Hannon, I. Meistermann, A. Rodger, E. Sletten, *J. Biol. Inorg. Chem.*, 2002, **7**, 770.

13 C. Uerpmann, J. Malina, M. Pascu, G. J. Clarkson, V. Moreno, A. Rodger, A. Grandas, M. J. Hannon, *Chem. Eur. J.*, 2005, **11**, 1750.

14 J. Malina, M. J. Hannon, V. Brabec, *Nucleic Acids Res.*, 2008, **38**, 3630.

15 J. C. Peberdy, J. Malina, S. Khalid, M. J. Hannon, A. Rodger, *J.Inorg. Biochem.,* 2007, **101**, 1937.

16 A. Oleksy, A.G. Blanco, R. Boer, I. Usón, J. Aymami, A. Rodger, M.J. Hannon and M. Coll, *Angew. Chem., Intl. Ed.*, 2006, **45**, 1227.

17 L. Cerasino, M. J. Hannon, E. Sletten, *Inorg. Chem.*, 2007, **46**, 6245.

18 J. Malina, M. J. Hannon, V. Brabec, *Chem. Eur. J.*, 2007, **13**, 3871.

19 L. J. Childs, J. Malina, B. E. Rolfsnes, M. Pascu, M. J. Prieto, M. J. Broome, P. M. Rodger, E. Sletten, V. Moreno, A. Rodger, M. J. Hannon, *Chem. Eur. J.*, 2006, **12**, 4919.

20 A. C. G. Hotze, B. M. Kariuki, M. J. Hannon, *Angew. Chem., Intl. Ed.*, 2006, **45**, 4839.

21 G. I. Pascu, A. C. G. Hotze, C. Sanchez Cano, B. M. Kariuki, M. J. Hannon, *Angew. Chem. Intl. Ed.*, 2007, **46**, 4374.

22 J. Malina, M. J. Hannon, V. Brabec, *Chem Eur J.*, 2008, **14**, 10408.

23 A. D. Richards, A. Rodger, M. J. Hannon, A. Bolhuis, *Int. J. Antimicrob. Agents*, 2009, *in press,* DOI 10.1016/j.ijantimicag.2008.10.031.

24 A. C. G. Hotze, N. J. Hodges, R. E. Hayden, C. Sanchez-Cano, C. Paines, N. Male, M.-K. Tse, C. M. Bunce, J. K. Chipman, M. J. Hannon, *Chemistry & Biology*, 2008, **15**, 1258.

25 Unpublished Preliminary data from A. Pope.

26 Unpublished data. Complexes synthesised and provided by Dr. D. Drahonovsky and Dr. R. M. Pedrido-Castiñeira.

27 Unpublished data. DNA binding data provided by Dr. R. M. Pedrido-Castiñeira.

28 Unpublished data. Complexes synthesised and provided by S. Kaur.

29 H.R. Mahler, B. Kline, B.D. Mehrota, *J. Mol. Biol.*, 1964, **9**, 801.

30 P.E. Pjura, K. Grzeskowlak, D.E. Dickerson, *J. Mol. Biol.*, 1987, **197**, 257.

31 M.J. Waring, *J. Mol. Biol.*, 1965, **13**, 269.

32 Y. Matsuba, H. Edatsugi, I. Mita, A. Matsunaga, O. Nakanishi, *Cancer Chemother. Pharmacol.*, 2000, **46**, 1.

33 50μM was chosen as a compromise of the activity of cisplatin and the cylinders in some cell lines (T47D).

34 A. E. Egger, C. Rappel, M. A. Japukec, C. G. Hartinger, P. Heffeter, B. K. Keppler, *J. Anal. At. Spectrom.*, 2009, **24**, 51.

35 A. Ghosh, P. C. Keng, P. A. Knauf, *Apoptosis*, 2007, **12**, 1281.

36 R. M. Zucker, K. Whittington, B. J. Price, *Cytometry*, 1983, **3**, 414.

37 C. A. Puckett, J. K. Barton, *Biochemistry*, 2008, **47**, 11711.

38 P. L. Olive, R. E. Durand, *Cytometry A*, 2005, **66**, 1.

39 T. Mosmann, *J. Inmunol. Meth.*, 1983, **65**, 55.

40 N. P. Singh, M. T. McCoy, R. R. Tice, E. L. Schneider, *Exp. Cell Res.*, 1998, **175**, 184.

41 A. J. Lee, N. J. Hodges, J. K. Chipman, *Cancer Epidemiol. Biomarkers Prev.*, 2005, **14**, 497.

42 P. Duez, G. Dehon, A. Kumps, J. Dubois, *Mutagenesis*, 2003, **18**, 159.

Chapter 5: Conclusions and Future Work

5.1 Conclusions

The work described in this thesis has been directed by two questions: how the use of steroids as delivery vectors affects the anticancer properties of different metallodrugs, and whether active anticancer metallosupramolecular cylinders previously synthesised (and which present interesting DNA interaction properties) could act through structural interaction with cellular DNA. Herein we showed experiments that tried to address these questions.

In Chapters 2 and 3 the use of improved and new synthesis and purification routes allowed us to obtain in good yields a series of new and previously reported steroidal (estradiol and testosterone) metallodrugs (both DNA covalent and non-covalent binders), aiming to target their receptors (ER or AR). The procedures were quick and simple with standardised purification through HPLC techniques.

Chapter 2 focused on the study of the steroidal covalent DNA-binders. The cytotoxicity assays of these complexes showed that the coupling of a steroid to a DNA covalent-binding complex conferred activity to the otherwise non-active non-steroidal analogues. This activity was not the result of the known cell sensitisation to platinum drugs that steroids induce (as shown by Lippard[1]) or the biological activity of the steroidal ligands used, as the performed cytotoxicity assays showed. Increase of the cellular uptake of the complexes upon steroid coupling was not the origin of this new activity either; ICP-MS experiments showed that the attachment of the steroid decreased the amount of complex taken up by the cells in short times. However, coupling to the steroid helped the complexes to cross the cellular membrane (compared with the non-steroidal equivalents) and modified the cellular distribution; concentrating the complexes in the cytoplasm (showing a cytoplasm:nuclei ratio of 3:1 against 1:1 distribution for the non-steroidal analogues).

More remarkably, steroidal coupled compounds produced a dramatic modification of the mode of binding to DNA, as demonstrated by the CD (performed with ct-DNA) and MS and NMR (performed with mononucleotides, and that could explain the observed

difference in activity between cis and trans isomers) experiments herein presented and some previous experiments[2-5].

Chapter 3 studied the steroidal non-covalent metallodrugs, showing that the coupling of a steroidal moiety to intercalative metallodrugs produced a decrease of the anticancer properties of the complexes (compared with active non-steroidal analogues). This difference in activity was not the result of the effect on the cellular uptake; the steroidal complexes were not taken up by cells less when compared with the non-steroidal analogues, as ICP-MS experiments showed. As seen for the steroidal DNA covalent-binding metallodrugs, the steroids again concentrated the complexes in the cytoplasm, showing a cytoplasm:nuclei ratio of 3:1 against a 1:1 distribution for the non-steroidal analogues. The ability to intercalate between the bases of ct-DNA was found to be of high importance for activity, as the cytoxicity decreased dramatically in complexes where the access to the intercalating terpyridine was hindered. LD and DNA fluorescence titrations proved that these hindered complexes did not show intercalating properties, while the compounds showing anticancer activity did (both steroidal and non-steroidal). The fact that the anticancer activity was produced by the intercalation of the platinum(II) terpyridine moiety would explain the decrease in activity when a steroid is coupled, as Ethidium Bromide (EB) displacement assays showed lower binding affinities for steroidal complexes compared with the non-steroidal analogue.

Concluding, we can say that the unprecedented effects observed in the anticancer activity (decrease or dramatic increase) upon attachment of steroid moieties to metallodrugs are related to the changes that this steroid molecule produce in their DNA-binding properties. Steroidal covalent DNA-binders produce dramatic structural changes in the double helix as a result of the necessity to accommodate the bulk of the steroid (improving the cytotoxic properties of the non-steroidal complexes), while DNA-intercalating metallodrugs suffer a decrease in their DNA binding affinity when a steroid is attached (being a drawback for their anticancer abilities).

In Chapter 4 the biological activity of iron(II) and ruthenium(II) metallosupramolecular cylinders were studied[24]. Both are known to show similar DNA-binding properties, due to their almost identical size and structural shape[6-7]. When their cytotoxicity was studied, they presented almost identical activity against breast cancer cell lines, perhaps suggesting that the compounds could act through DNA interaction.

However, size and shape proved to be not the only factors involved in their anticancer properties, as observed by the fact that the ruthenium cylinder did not show activity in ovarian cell lines and the iron one did. Both complexes showed, also, the ability to go across the cellular membrane. Iron cylinders quenched the emission of intracellular Hoechst 33258 in HL-60 leukaemia cells, while the presence of the ruthenium complex inside the cell was proved by confocal fluorescence microscopy in T-47D breast cancer cell line. ICP-MS uptake experiments of the performed in HL-60 cell line also showed that surprisingly, the ruthenium cylinders were not only taken up but concentrated inside the cells, being mainly found in the nuclei. Once in the nuclei, the ruthenium compound could interact with cellular DNA; cells pre-treated with ruthenium cylinder showed an increase in the DNA breaks after irradiation with white light.

In summary, the metallo-supramolecular cylinders can be taken up in *live* cells, and are accumulated in the nuclei. There, the complexes can interact with DNA, and this is the probable cause of their ultimate cytotoxic activity.

5.2 Future work

Although the work in this thesis much has been learnt about the design principles and activities through, this new knowledge brings new possibilities and raises new questions to be addressed. Further experiments should be taken in consideration to better understand how the complexes presented in this thesis work and behave in full organisms. For steroidal complexes information about cytoxicity in prostate and testicular cancers would be interesting, since testosterone and its receptor play an important role in these types of cancers. Work in more ordered systems presenting cells both with and without high quantity of steroidal receptors is desired as well, to know if they are really capable to fulfil their target (specificity for reproductive cancer cells over-expressing ER or AR). The initial studies herein showed that they do not posses significantly different cytotoxicity towards isolated cell lines over-expressing or not their receptors. However, uptake experiments show that although they are not more active for steroid dependent cancer types, they can be internalized better in those cells (compared to the ones not over-expressing their receptors).

Steroidal complexes can interact with proteins, although the presence of the metallic centre alters this ability. This should be further studied and interaction with their receptors and other steroid-related proteins (such metabolic and transport proteins) would be needed to better understand how the complexes would behave inside the body.

Finally, the different distribution, uptake and mechanism of action of metallosupramolecular cylinders in different cell lines would need to be further studied. This could confirm if they are taken up through an active transport process, where they accumulate and why they show different anticancer activity against certain cell lines.

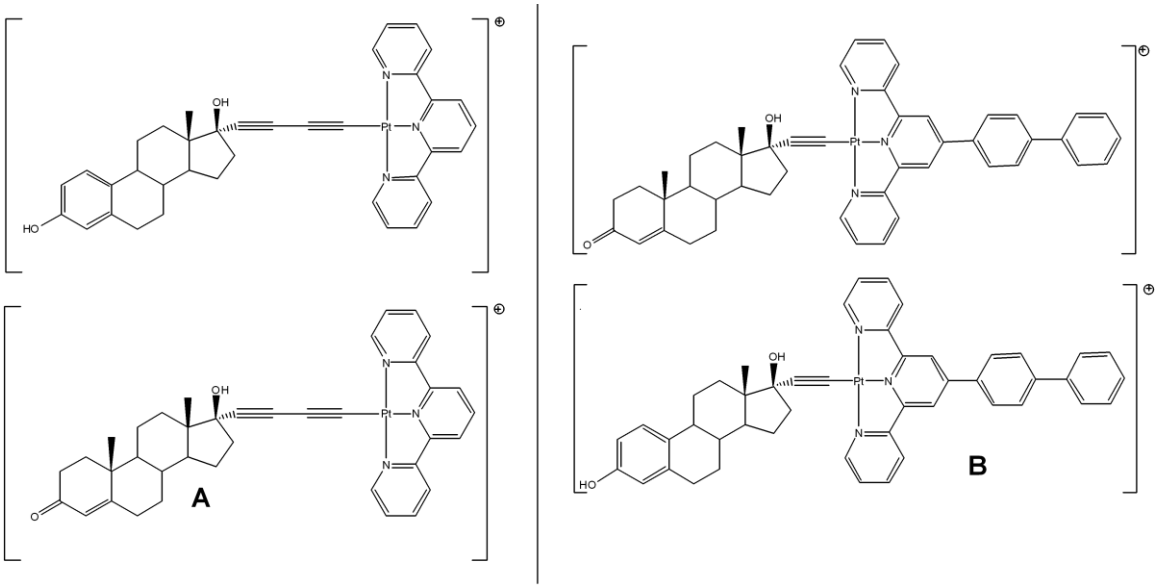

Figure 5.1. New Non-covalent steroidal designs for a farther DNA-steroid interaction(A) and aiming telomeric G-quadruplexes (B).

The coupling of steroids to coordination complexes has proven to be a very interesting mode of targeting metallodrugs, showing unexpected effects in their cytotoxicity and mode of action (both positives and negatives). This makes the design of new complexes that further explore targeting through steroidal coupling desired. For non-covalent DNA-binding metallodrugs, steroids proved to be a drawback in their cytotoxicity and DNA-binding abilities, probably because the steroid hindered the intercalation of the terpyridine moiety between the DNA bases. To overcome this negative effect one could synthesise complexes where the steroid is further away from the terpyridine unit, maybe allowing an easier intercalation with the DNA (Fig. 5.1 A). A different approach would be the use of extended planar terpyridines aiming not for intercalation between the bases of the DNA but the interaction with telomeric G-quadruplexes[8] (Fig. 5.1 B).

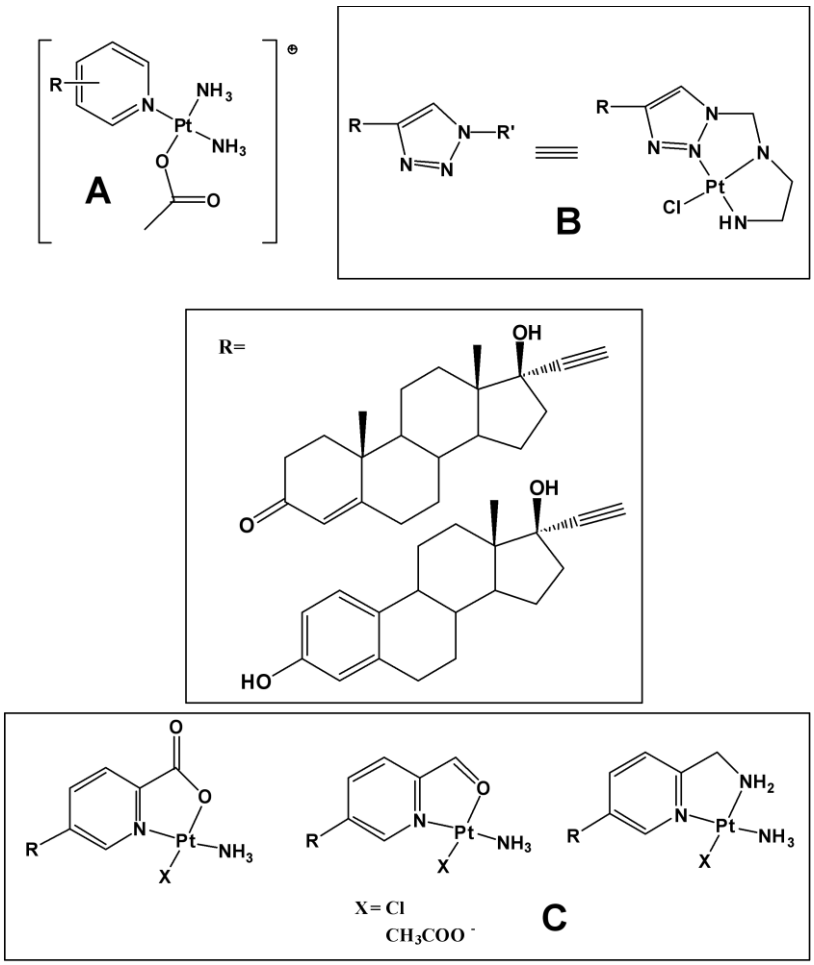

Figure 5.2. New covalent steroidal designs with acetate leaving groups for higher solubility (A), using Click chemistry (B) and using bidentate ligands (C).

New designs of DNA-covalent binders could help to address the low solubility of the steroidal complexes, to explore structures with different orientations or create bifunctional complexes (Fig. 5.2). Substitution of the Cl for an acetate leaving group should increase the water solubility, as observed previously for non-steroidal platinum(II) complexes[9] (Fig. 5.2 A). Bidentate ligands could provide an easier possibility to produce bifunctional complexes (as cisplatin, transplatin and analogues) compared with other failed approaches tried previously[2-3] (Fig. 5.2 C). Use of tools as the "Click" chemistry could help to produce easily steroidal ligands and complexes that would bind to DNA with different orientations, compared with the ethynyl derived compounds used herein.

All these would be exciting possibilities to drive this work forward to create more compounds that could be specifically delivered directly to the location of a selected tumour.

5.3 References

1 Q. He, C. H. Liang, S. J. Lippard, *Proc. Natl. Acad. Sci*, 2000, **97**, 5768.

2 Martin Huxley, PhD Thesis, University of Warwick, 2006.

3 Michael Browning, PhD Thesis, University of Warwick, 2006.

4 M. Huxley, C. Sanchez-Cano, M. J. Browning, C. Navarro-Ranninger, A. G. Quiroga, A. Rodger, M. J. Hannon, *To be submitted*.

5 M. Huxley, C. Sanchez-Cano, M. J. Browning, C. Navarro-Ranninger, A. G. Quiroga, A. Rodger, M. J. Hannon, *To be submitted*.

6 G. I. Pascu, A. C. G. Hotze, C. Sanchez Cano, B. M. Kariuki, M. J. Hannon, *Angew. Chem. Intl. Ed.*, 2007, **46**, 4374.

7 M. J. Hannon, V. Moreno, M. J. Prieto, E. Molderheim, E. Sletten, I. Meistermann, C. J. Isaac, K. J. Sanders, A. Rodger, *Angew. Chem. Int. Ed.*, 2001, **40**, 879.

8 D.-L. Ma, C.-M. Che, S-C. Yan, *J. Am. Chem. Soc.*, 2009, **131**, 1835.

9 A. G. Quiroga, J. M. Perez, C. Alonso, C. Navarro-Ranninger, N. Farrell, *J. Med. Chem.*, 2006, **49**, 224.

Appendix A

Table 1. Crystal data and structure refinement for Di-17-α-Ethynyl-Estradiol.

Empirical formula	C52 H74 N4 O8	
Formula weight	883.15	
Temperature	296(2) K	
Wavelength	1.54178 Å	
Crystal system, space group	Orthorhombic, P212121	
Unit cell dimensions	a = 7.0012(16) Å	alpha = 90 deg.
	b = 22.481(5) Å	beta = 90 deg.
	c = 31.946(7) Å	gamma = 90 deg.
Volume	5028(2) $Å^3$	
Z, Calculated density	4,	1.167 Mg/m^3
Absorption coefficient	0.624 mm^{-1}	
F(000)	1912	
Crystal size	0.50 x 0.40 x 0.40 mm	
Theta range for data collection	2.40 to 66.01 deg.	
Limiting indices	-8<=h<=8, -25<=k<=25, -37<=l<=35	
Reflections collected / unique	32263 / 8345 [R(int) = 0.0962]	
Completeness to theta = 66.01	97.9 %	
Max. and min. transmission	0.7883 and 0.7454	
Refinement method	Full-matrix least-squares on F^2	
Data / restraints / parameters	8345 / 3 / 577	
Goodness-of-fit on F^2	1.072	
Final R indices [I>2sigma(I)]	R1 = 0.0913,	wR2 = 0.2362
R indices (all data)	R1 = 0.1252,	wR2 = 0.2650
Absolute structure parameter	-0.2(5)	
Largest diff. peak and hole	0.578 and -0.273 e. $Å^{-3}$	

Table 2. Atomic coordinates (x 10^4) and equivalent isotropic displacement parameters (A^2 x 10^3) for Di-17-α-Ethynyl-Estradiol. U(eq) is defined as one third of the trace of the orthogonalized Uij tensor.

	x	y	z	U(eq)
C(1)	10647(9)	3885(3)	3728(2)	60(1)
C(2)	8934(9)	3614(2)	3669(2)	58(1)
C(3)	7928(7)	3667(2)	3294(2)	50(1)
C(4)	8634(7)	4016(2)	2966(1)	44(1)
C(5)	10391(8)	4295(2)	3040(2)	57(1)
C(6)	11374(8)	4241(3)	3414(2)	60(1)
C(7)	5997(7)	3348(2)	3252(2)	53(1)
C(8)	4938(7)	3465(2)	2849(2)	52(1)
C(9)	6269(6)	3539(2)	2480(1)	41(1)
C(10)	7573(7)	4082(2)	2553(2)	42(1)
C(11)	8864(7)	4208(2)	2175(2)	48(1)

C(12)	7743(7)	4267(2)	1770(2)	45(1)
C(13)	6461(6)	3729(2)	1687(1)	38(1)
C(14)	5190(6)	3632(2)	2073(1)	39(1)
C(15)	3737(7)	3159(2)	1931(2)	52(1)
C(16)	3474(7)	3291(2)	1459(2)	50(1)
C(17)	4890(7)	3806(2)	1346(1)	42(1)
C(18)	7690(7)	3178(2)	1581(2)	55(1)
C(19)	-5830(8)	6212(3)	3739(2)	59(1)
C(20)	-4153(8)	6512(2)	3688(2)	54(1)
C(21)	-3041(7)	6462(2)	3328(2)	46(1)
C(22)	-3665(7)	6093(2)	3001(1)	44(1)
C(23)	-5405(8)	5784(2)	3070(2)	52(1)
C(24)	-6435(8)	5826(3)	3426(2)	58(1)
C(25)	-1143(7)	6788(2)	3306(2)	49(1)
C(26)	-28(7)	6681(2)	2905(2)	53(1)
C(27)	-1316(7)	6599(2)	2528(1)	41(1)
C(28)	-2560(7)	6040(2)	2597(1)	43(1)
C(29)	-3805(7)	5901(2)	2213(2)	50(1)
C(30)	-2663(7)	5872(2)	1810(2)	47(1)
C(31)	-1458(6)	6428(2)	1743(1)	38(1)
C(32)	-196(6)	6532(2)	2126(1)	38(1)
C(33)	1208(7)	7019(2)	1985(2)	49(1)
C(34)	1444(7)	6914(2)	1512(2)	48(1)
C(35)	88(7)	6396(2)	1396(1)	41(1)
C(36)	-2761(8)	6954(2)	1645(2)	56(1)
C(37)	1134(7)	5829(2)	1409(1)	44(1)
C(38)	2054(7)	5370(2)	1410(1)	43(1)
C(39)	3057(7)	4844(2)	1395(1)	45(1)
C(40)	3901(7)	4382(2)	1374(1)	43(1)
O(1)	11524(7)	3812(2)	4110(1)	87(1)
O(2)	5530(5)	3706(2)	927(1)	53(1)
O(3)	-696(6)	6445(2)	989(1)	59(1)
O(4)	-6940(7)	6260(2)	4092(1)	88(1)
C(41)	8920(16)	5303(3)	4026(3)	119(3)
C(42)	8033(18)	4726(6)	4654(3)	165(5)
C(43)	6052(14)	4706(4)	4058(3)	98(2)
C(44)	1905(16)	5421(4)	319(3)	115(3)
C(45)	1800(30)	4384(5)	164(5)	242(10)
C(46)	-776(16)	4869(5)	572(2)	125(4)
C(47)	5430(20)	6725(5)	271(5)	217(8)
C(48)	5530(20)	7680(5)	540(4)	164(5)
C(49)	5314(18)	7404(4)	-209(2)	291(13)
C(50)	5819(12)	3390(3)	-191(3)	95(2)
C(51)	5570(14)	2384(4)	-503(2)	99(2)
C(52)	5642(10)	2507(3)	248(2)	74(2)
N(1)	7532(8)	4907(3)	4250(2)	84(2)
N(2)	802(10)	4880(2)	356(2)	87(2)
N(3)	5451(9)	7342(3)	200(2)	90(2)
N(4)	5622(8)	2736(2)	-134(2)	69(1)
O(5)	4862(11)	4378(4)	4226(2)	137(2)
O(6)	-1753(18)	4409(6)	607(2)	278(8)
O(7)	5683(12)	7862(5)	-392(2)	205(5)
O(8)	5565(9)	1972(2)	313(2)	98(2)

Table 3. Bond lengths [A] and angles [deg] for Di-17-α-Ethynyl-Estradiol.

C(1)-C(2)	1.358(8)
C(1)-O(1)	1.376(7)
C(1)-C(6)	1.379(8)
C(2)-C(3)	1.394(7)
C(3)-C(4)	1.398(7)
C(3)-C(7)	1.537(7)
C(4)-C(5)	1.402(7)
C(4)-C(10)	1.521(7)
C(5)-C(6)	1.385(8)
C(7)-C(8)	1.509(7)
C(8)-C(9)	1.510(7)
C(9)-C(14)	1.518(6)
C(9)-C(10)	1.541(6)
C(10)-C(11)	1.535(7)
C(11)-C(12)	1.520(7)
C(12)-C(13)	1.528(6)
C(13)-C(14)	1.537(6)
C(13)-C(18)	1.546(6)
C(13)-C(17)	1.558(7)
C(14)-C(15)	1.540(6)
C(15)-C(16)	1.547(7)
C(16)-C(17)	1.565(7)
C(17)-O(2)	1.430(5)
C(17)-C(40)	1.471(6)
C(19)-C(20)	1.364(8)
C(19)-O(4)	1.374(7)
C(19)-C(24)	1.392(8)
C(20)-C(21)	1.394(7)
C(21)-C(22)	1.404(7)
C(21)-C(25)	1.519(7)
C(22)-C(23)	1.419(7)
C(22)-C(28)	1.509(7)
C(23)-C(24)	1.349(7)
C(25)-C(26)	1.521(7)
C(26)-C(27)	1.514(7)
C(27)-C(32)	1.512(6)
C(27)-C(28)	1.544(7)
C(28)-C(29)	1.538(7)
C(29)-C(30)	1.517(7)
C(30)-C(31)	1.523(6)
C(31)-C(36)	1.525(6)
C(31)-C(32)	1.529(6)
C(31)-C(35)	1.549(6)
C(32)-C(33)	1.539(6)
C(33)-C(34)	1.536(7)
C(34)-C(35)	1.547(6)
C(35)-O(3)	1.417(5)
C(35)-C(37)	1.471(6)
C(37)-C(38)	1.215(6)
C(38)-C(39)	1.377(7)
C(39)-C(40)	1.197(6)
C(41)-N(1)	1.499(10)
C(42)-N(1)	1.397(12)
C(43)-O(5)	1.236(10)
C(43)-N(1)	1.286(10)
C(44)-N(2)	1.445(9)
C(45)-N(2)	1.453(11)
C(46)-O(6)	1.245(11)

C(46)-N(2)	1.302(11)
C(47)-N(3)	1.406(12)
C(48)-N(3)	1.324(11)
C(49)-O(7)	1.2097(11)
C(49)-N(3)	1.3193(11)
C(50)-N(4)	1.488(8)
C(51)-N(4)	1.419(8)
C(52)-O(8)	1.222(7)
C(52)-N(4)	1.325(7)

C(2)-C(1)-O(1)	117.6(6)
C(2)-C(1)-C(6)	119.0(5)
O(1)-C(1)-C(6)	123.3(6)
C(1)-C(2)-C(3)	121.8(5)
C(2)-C(3)-C(4)	120.8(5)
C(2)-C(3)-C(7)	118.7(5)
C(4)-C(3)-C(7)	120.5(5)
C(3)-C(4)-C(5)	115.9(5)
C(3)-C(4)-C(10)	122.1(4)
C(5)-C(4)-C(10)	122.0(4)
C(6)-C(5)-C(4)	122.8(5)
C(1)-C(6)-C(5)	119.7(5)
C(8)-C(7)-C(3)	115.2(4)
C(7)-C(8)-C(9)	112.4(4)
C(8)-C(9)-C(14)	112.0(4)
C(8)-C(9)-C(10)	109.6(4)
C(14)-C(9)-C(10)	108.5(4)
C(4)-C(10)-C(11)	114.4(4)
C(4)-C(10)-C(9)	110.1(4)
C(11)-C(10)-C(9)	112.1(4)
C(12)-C(11)-C(10)	112.5(4)
C(11)-C(12)-C(13)	112.4(4)
C(12)-C(13)-C(14)	108.3(4)
C(12)-C(13)-C(18)	110.2(4)
C(14)-C(13)-C(18)	112.6(4)
C(12)-C(13)-C(17)	116.6(4)
C(14)-C(13)-C(17)	99.7(3)
C(18)-C(13)-C(17)	109.1(4)
C(9)-C(14)-C(13)	114.7(3)
C(9)-C(14)-C(15)	119.2(4)
C(13)-C(14)-C(15)	104.1(4)
C(14)-C(15)-C(16)	103.5(4)
C(15)-C(16)-C(17)	106.9(4)
O(2)-C(17)-C(40)	110.0(4)
O(2)-C(17)-C(13)	114.6(4)
C(40)-C(17)-C(13)	112.8(4)
O(2)-C(17)-C(16)	107.3(3)
C(40)-C(17)-C(16)	109.8(4)
C(13)-C(17)-C(16)	101.8(4)
C(20)-C(19)-O(4)	123.1(5)
C(20)-C(19)-C(24)	119.0(5)
O(4)-C(19)-C(24)	117.8(5)
C(19)-C(20)-C(21)	122.6(5)
C(20)-C(21)-C(22)	119.3(5)
C(20)-C(21)-C(25)	119.2(4)
C(22)-C(21)-C(25)	121.5(4)
C(21)-C(22)-C(23)	116.1(4)
C(21)-C(22)-C(28)	121.6(4)
C(23)-C(22)-C(28)	122.3(4)
C(24)-C(23)-C(22)	123.8(5)

C(23)-C(24)-C(19)	119.1(5)
C(21)-C(25)-C(26)	114.3(4)
C(27)-C(26)-C(25)	112.5(4)
C(32)-C(27)-C(26)	112.2(4)
C(32)-C(27)-C(28)	109.4(4)
C(26)-C(27)-C(28)	108.8(4)
C(22)-C(28)-C(29)	114.1(4)
C(22)-C(28)-C(27)	110.3(4)
C(29)-C(28)-C(27)	111.8(4)
C(30)-C(29)-C(28)	112.8(4)
C(29)-C(30)-C(31)	112.1(4)
C(30)-C(31)-C(36)	109.5(4)
C(30)-C(31)-C(32)	109.4(4)
C(36)-C(31)-C(32)	113.0(4)
C(30)-C(31)-C(35)	116.7(4)
C(36)-C(31)-C(35)	108.0(4)
C(32)-C(31)-C(35)	100.1(3)
C(27)-C(32)-C(31)	113.4(4)
C(27)-C(32)-C(33)	120.7(4)
C(31)-C(32)-C(33)	104.0(4)
C(34)-C(33)-C(32)	104.3(4)
C(33)-C(34)-C(35)	106.6(4)
O(3)-C(35)-C(37)	106.7(4)
O(3)-C(35)-C(34)	113.5(4)
C(37)-C(35)-C(34)	109.9(4)
O(3)-C(35)-C(31)	112.4(4)
C(37)-C(35)-C(31)	111.6(4)
C(34)-C(35)-C(31)	102.8(3)
C(38)-C(37)-C(35)	177.4(5)
C(37)-C(38)-C(39)	177.5(5)
C(40)-C(39)-C(38)	178.4(5)
C(39)-C(40)-C(17)	178.5(5)
O(5)-C(43)-N(1)	123.0(8)
O(6)-C(46)-N(2)	122.0(11)
O(7)-C(49)-N(3)	123.62(16)
O(8)-C(52)-N(4)	122.6(6)
C(43)-N(1)-C(42)	122.8(8)
C(43)-N(1)-C(41)	120.2(8)
C(42)-N(1)-C(41)	116.7(8)
C(46)-N(2)-C(44)	120.9(7)
C(46)-N(2)-C(45)	128.2(9)
C(44)-N(2)-C(45)	110.7(8)
C(49)-N(3)-C(48)	138.9(8)
C(49)-N(3)-C(47)	105.3(8)
C(48)-N(3)-C(47)	115.8(9)
C(52)-N(4)-C(51)	123.2(6)
C(52)-N(4)-C(50)	119.8(6)
C(51)-N(4)-C(50)	116.8(6)

Symmetry transformations used to generate equivalent atoms

Table 4. Anisotropic displacement parameters (A^2 x 10^3) for Di-17-α-Ethynyl-Estradiol. The anisotropic displacement factor exponent takes the form: -2 pi^2 [h^2 a^{*2} U11 + ... + 2 h k a* b* U12]

	U11	U22	U33	U23	U13	U12
C(1)	61(3)	66(3)	53(3)	-10(3)	-16(3)	11(3)
C(2)	70(4)	59(3)	45(3)	2(2)	-6(3)	2(3)
C(3)	50(3)	43(3)	57(3)	-8(2)	2(3)	3(2)
C(4)	48(3)	46(3)	38(3)	-6(2)	-1(2)	3(2)
C(5)	53(3)	63(3)	55(3)	-3(3)	-1(3)	-2(3)
C(6)	49(3)	76(4)	56(3)	-14(3)	-12(3)	0(3)
C(7)	49(3)	53(3)	57(3)	4(2)	2(3)	-1(2)
C(8)	41(3)	65(3)	51(3)	7(2)	2(2)	-3(2)
C(9)	36(2)	36(2)	52(3)	3(2)	3(2)	0(2)
C(10)	41(2)	34(2)	51(3)	0(2)	-5(2)	-2(2)
C(11)	42(3)	49(3)	53(3)	6(2)	-2(2)	-12(2)
C(12)	45(3)	41(2)	48(3)	2(2)	-5(2)	-11(2)
C(13)	31(2)	33(2)	52(3)	-4(2)	6(2)	1(2)
C(14)	31(2)	39(2)	48(3)	-1(2)	6(2)	0(2)
C(15)	38(2)	54(3)	63(3)	3(2)	4(2)	-12(2)
C(16)	44(3)	46(3)	61(3)	-5(2)	-1(2)	-8(2)
C(17)	45(3)	40(2)	40(2)	-6(2)	1(2)	1(2)
C(18)	47(3)	54(3)	63(3)	-8(2)	6(3)	14(2)
C(19)	56(3)	74(4)	47(3)	11(3)	14(3)	10(3)
C(20)	63(3)	60(3)	40(3)	-1(2)	7(3)	2(3)
C(21)	48(3)	47(3)	44(3)	4(2)	0(2)	3(2)
C(22)	50(3)	44(2)	37(2)	4(2)	0(2)	2(2)
C(23)	52(3)	57(3)	48(3)	1(2)	3(3)	1(3)
C(24)	53(3)	68(3)	52(3)	6(3)	10(3)	-6(3)
C(25)	45(3)	54(3)	48(3)	-1(2)	-3(2)	-5(2)
C(26)	47(3)	60(3)	51(3)	-5(2)	-5(2)	-2(2)
C(27)	38(2)	41(2)	45(3)	-2(2)	-4(2)	3(2)
C(28)	46(3)	40(2)	43(3)	0(2)	1(2)	0(2)
C(29)	47(3)	53(3)	50(3)	-5(2)	0(2)	-10(2)
C(30)	45(3)	50(3)	47(3)	-7(2)	1(2)	-8(2)
C(31)	37(2)	33(2)	43(2)	-1(2)	-3(2)	3(2)
C(32)	35(2)	33(2)	45(3)	-4(2)	-6(2)	-1(2)
C(33)	43(3)	45(3)	57(3)	-4(2)	0(2)	-7(2)
C(34)	45(3)	43(3)	58(3)	0(2)	-1(2)	-5(2)
C(35)	47(3)	39(2)	36(2)	3(2)	-5(2)	3(2)
C(36)	51(3)	54(3)	63(3)	3(2)	-3(3)	16(3)
C(37)	48(3)	46(3)	37(2)	-2(2)	4(2)	2(2)
C(38)	49(3)	41(2)	39(3)	-1(2)	2(2)	13(2)
C(39)	53(3)	45(3)	36(2)	-9(2)	-8(2)	9(2)
C(40)	46(3)	42(3)	42(3)	-7(2)	-8(2)	3(2)
O(1)	98(3)	104(3)	58(3)	-3(2)	-28(3)	9(3)
O(2)	63(2)	54(2)	40(2)	-12(1)	7(2)	-5(2)
O(3)	70(2)	67(2)	41(2)	7(2)	-10(2)	4(2)
O(4)	97(3)	112(4)	57(3)	-6(2)	30(3)	-5(3)
C(41)	149(8)	76(5)	131(7)	10(5)	50(7)	4(6)
C(42)	138(9)	268(15)	90(7)	6(8)	-6(7)	-9(10)
C(43)	98(6)	112(6)	85(5)	-3(5)	-26(5)	0(5)
C(44)	152(9)	112(6)	81(5)	-1(4)	18(5)	-48(6)
C(45)	330(20)	99(8)	300(19)	-53(10)	177(18)	20(11)
C(46)	137(8)	181(9)	58(4)	-6(5)	12(5)	-85(8)
C(47)	188(14)	97(8)	370(20)	-4(11)	-79(15)	12(9)
C(48)	185(12)	151(9)	157(10)	-53(8)	-55(10)	17(9)
C(49)	156(11)	610(40)	113(9)	204(16)	51(8)	162(18)

C(50)	94(5)	69(4)	123(6)	16(4)	-4(5)	11(4)
C(51)	123(6)	107(6)	65(4)	-27(4)	-2(4)	-17(5)
C(52)	85(5)	82(5)	54(4)	2(3)	8(3)	-5(4)
N(1)	79(4)	105(4)	67(4)	-22(3)	-9(3)	17(4)
N(2)	117(5)	65(3)	78(4)	-8(3)	11(4)	-9(3)
N(3)	92(4)	106(5)	73(4)	7(3)	-10(3)	-15(4)
N(4)	74(3)	77(3)	57(3)	-1(2)	10(3)	11(3)
O(5)	112(5)	174(7)	124(5)	-27(5)	-30(4)	-16(5)
O(6)	354(16)	366(15)	113(6)	-12(7)	45(7)	-295(14)
O(7)	128(6)	290(11)	197(8)	152(8)	-12(6)	28(7)
O(8)	129(4)	85(3)	80(3)	12(2)	14(3)	-14(3)

Table 5. Hydrogen coordinates (x 10^4) and isotropic displacement parameters (A^2 x 10^3) for Di-17-α-Ethynyl-Estradiol.

	x	y	z	U(eq)
H(2)	8418	3387	3884	70
H(5)	10920	4527	2829	69
H(6)	12519	4443	3454	72
H(7A)	6213	2923	3276	64
H(7B)	5189	3467	3484	64
H(8A)	4174	3822	2880	63
H(8B)	4075	3136	2794	63
H(9)	7063	3182	2455	49
H(10)	6731	4427	2584	51
H(11A)	9568	4573	2225	58
H(11B)	9784	3888	2147	58
H(12A)	8630	4312	1539	54
H(12B)	6961	4622	1783	54
H(14)	4461	4001	2109	47
H(15A)	2539	3201	2081	62
H(15B)	4230	2761	1975	62
H(16A)	2169	3411	1403	61
H(16B)	3758	2940	1295	61
H(18A)	8363	3246	1324	82
H(18B)	6878	2837	1551	82
H(18C)	8591	3109	1802	82
H(20)	-3736	6761	3902	65
H(23)	-5861	5539	2858	63
H(24)	-7535	5599	3461	69
H(25A)	-362	6666	3542	59
H(25B)	-1380	7211	3334	59
H(26A)	815	7016	2855	63
H(26B)	759	6329	2938	63
H(27)	-2154	6946	2504	50
H(28)	-1681	5704	2631	52
H(29A)	-4445	5523	2256	60
H(29B)	-4779	6206	2186	60
H(30A)	-3532	5825	1576	57
H(30B)	-1834	5527	1817	57
H(32)	568	6170	2159	45
H(33A)	690	7412	2039	58
H(33B)	2422	6980	2128	58
H(34A)	2756	6810	1448	58
H(34B)	1107	7269	1357	58

H(36A)	-3584	7027	1880	84
H(36B)	-3519	6865	1403	84
H(36C)	-1999	7301	1592	84
H(1)	12539	3994	4111	130
H(2A)	6275	3970	859	79
H(3)	168	6441	816	89
H(4)	-6427	6487	4258	133
H(41A)	9007	5184	3738	178
H(41B)	10154	5270	4155	178
H(41C)	8487	5707	4042	178
H(42A)	7783	5043	4847	248
H(42B)	9367	4627	4661	248
H(42C)	7295	4383	4730	248
H(43)	5869	4814	3780	118
H(44A)	1422	5712	511	173
H(44B)	1806	5570	38	173
H(44C)	3219	5339	382	173
H(45A)	3021	4333	296	363
H(45B)	1984	4463	-129	363
H(45C)	1060	4028	197	363
H(46)	-1185	5216	703	150
H(47A)	5425	6520	7	326
H(47B)	4298	6621	425	326
H(47C)	6537	6613	428	326
H(48A)	6819	7700	638	246
H(48B)	4728	7511	753	246
H(48C)	5083	8073	473	246
H(49)	4913	7079	-366	349
H(50A)	6076	3574	74	143
H(50B)	4654	3548	-305	143
H(50C)	6853	3470	-381	143
H(51A)	6851	2308	-596	148
H(51B)	4885	2594	-717	148
H(51C)	4940	2014	-444	148
H(52)	5717	2763	476	88

Appendix B

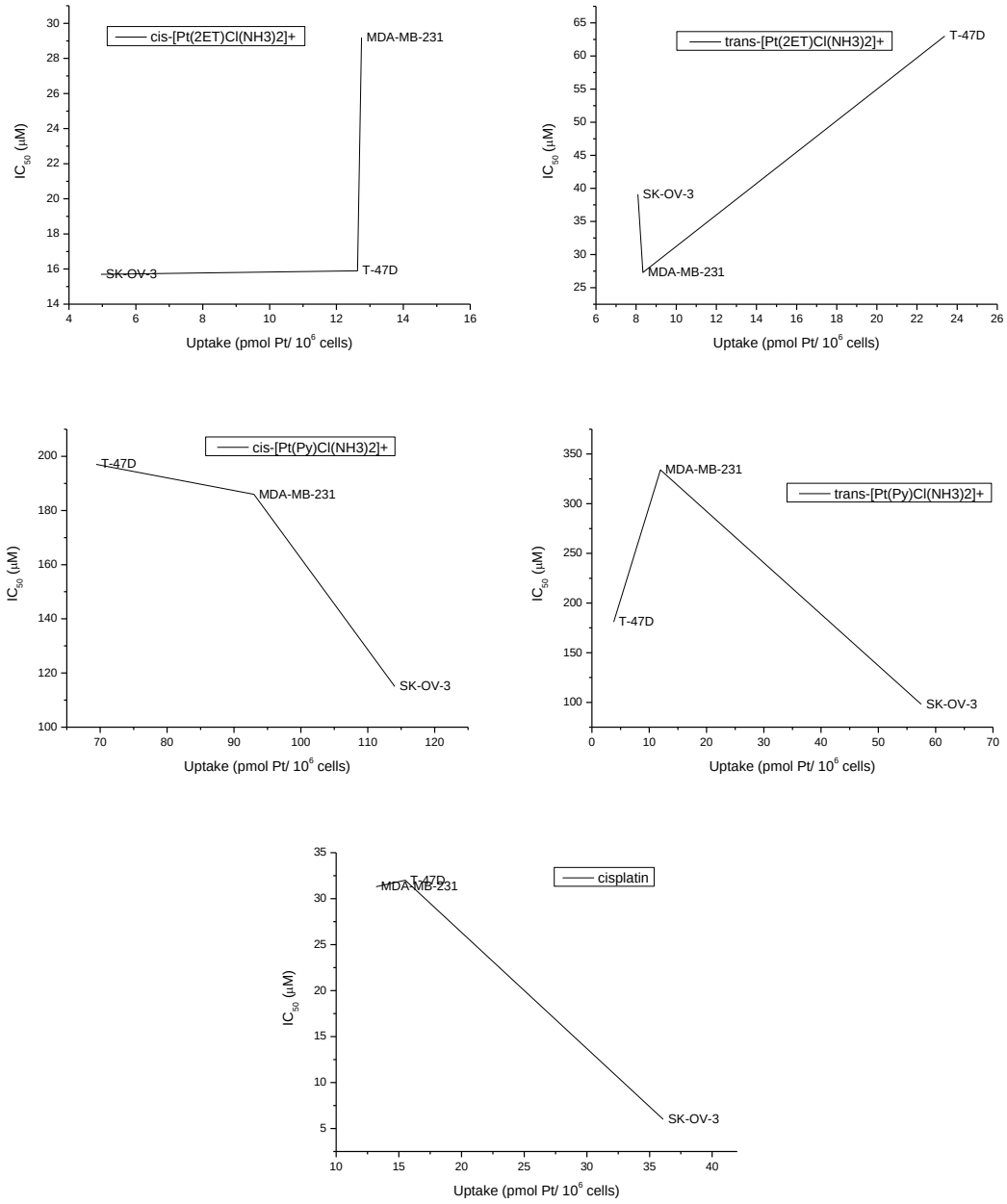

Figure B.1. Relation between pmols of Pt uptaked and cytotoxicity in T-47D, SK-OV-3 and MDA-MB-231 of cis and trans-$[Pt(2ET)Cl(NH_3)_2]^+$, cis and trans-$[Pt(Py)Cl(NH_3)_2]^+$ and cisplatin.

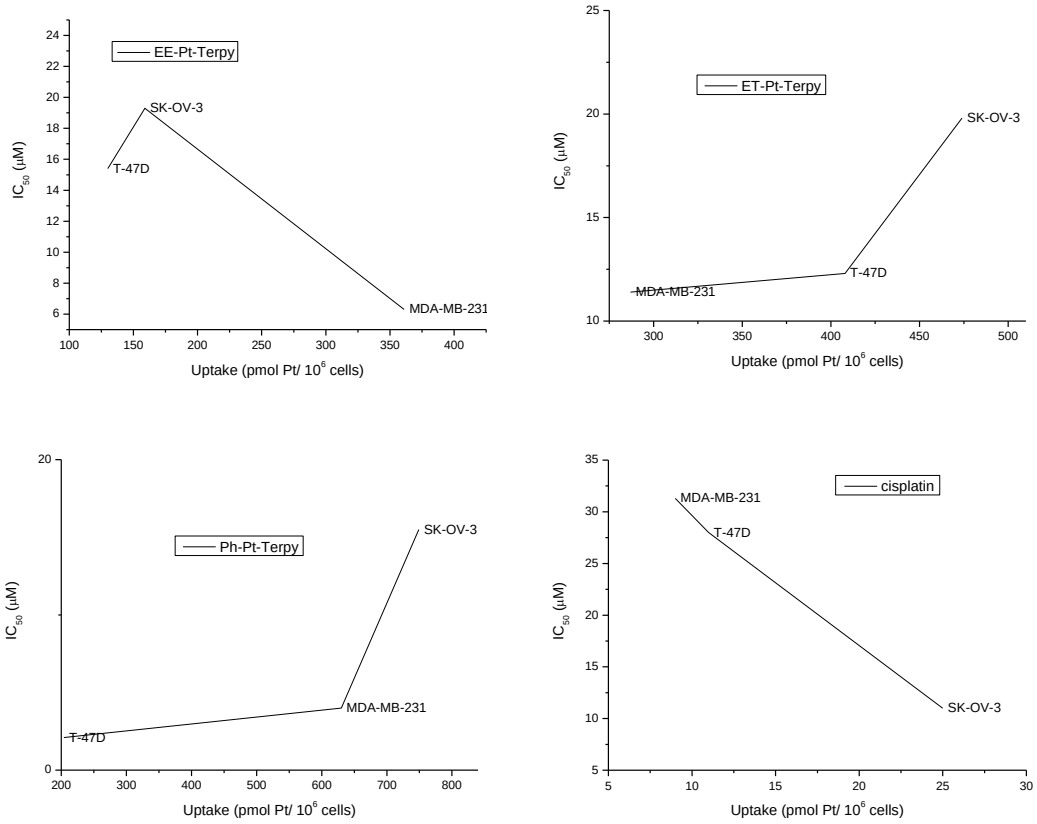

Figure B.2. Relation between pmols of Pt uptaked and cytotoxicity in T-47D, SK-OV-3 and MDA-MB-231 of EE, ET and Ph-Pt-Terpy and cisplatin.

Appendix C

Data sheet for Nuclear/Cytosol Fractionation Kit
http://www.biovision.com/pdf/K266.pdf